DOCTOR OF PHILOSOPHY

The role of mRNA splicing factor B52 in regulating Choline Acetyltransferase and larval locomotion in Drosiphila

Liu, Boyin

Award date:
2014

Awarding institution:
Bangor University

PRIFYSGOL
BANGOR
UNIVERSITY

The role of mRNA splicing factor B52 in regulating Choline Acetyltransferase and larval locomotion in *Drosophila*

Ph.D. Thesis

By

Boyin Liu

School of Biological Sciences

Bangor University

14th June 2014

Summary

This work investigates how two daughter cells, which arise from the same progenitor cell, can mature in two distinct neurons. Single cell transcriptome analysis of the two sibling cells vMP2 and dMP2 in the *Drosophila* central nervous system revealed that the expression level of the mRNA splicing factor B52 is around 45 times higher in dMP2 than that in vMP2 in stage 17 embryos. Given that the axons of vMP2 and dMP2 project in opposite directions, the up-regulation of *B52* in the dMP2 cell suggests that B52 might play a role in the selection of synaptic partners before synaptogenesis takes place. This process involves the selection of neurotransmitter expression, which subsequently contributes to control of locomotion in late stage embryos and larvae.

Using mutants created in this study, which are devoid of *B52* RNA in larval stages, I first discovered that the expression level of choline acetyltransferase (ChAT) is elevated as a result of reduced B52 activity. This increase in ChAT correlates with the presence of an aberrantly spliced *ChAT* mRNA in embryos and mutant larvae with reduced B52 levels. In addition to this, abnormal behaviours were observed in hatching embryos with reduced B52 levels as well as in 36hrs post hatching larvae devoid of B52 mRNA. Given the upregulation of ChAT, the resulting high levels of acetylcholine may interfere with hatching by triggering paralysis of the larval muscle through its highly sensitive and abundant receptors thereby rendering the larvae unable to move.

Interestingly, the behaviour and physical appearance of 36hrs post hatching larvae devoid of *B52* RNA highly resemble that seen in mutants defective in the ecdysone receptor (EcR), especially the lack of motion and reduced larval body size. This nuclear hormone receptor is closely linked with growth and development. More importantly, genomic studies have identified *EcR* as a potential splicing target of B52.

These results suggest that the synthesis of acetylcholine by ChAT is critical for the differentiation of the dMP2 sibling cells and normal movement of larvae in a B52-dependent manner.

Acknowledgments

I would like to thank Dr. Torsten Bossing and Dr. Claudia Barros for their guidance and help throughout my PhD. Thanks to Dr. Natalia Mikhaleva-Harrison for her support, both technically and morally, in the lab. Thanks to Ellie Gonzaga and Karolina Jaworek for keeping me entertained especially during those endless dissection sessions in the last year of my PhD.

Also thanks to Dr. Thomas Caspari for his advice and suggestions on completing my PhD, and as a part of my committee members. Thanks to Karim Ashour Garrido, Alessa Jaendling and Rolf Kraehenbuehl for their generous supply of equipment and materials, and experience shared with me on molecular biology techniques.

Thanks to Catia Antunes for her support and encouragement during my PhD, especially during the time of my thesis writing.

Finally, special thanks to my parents for providing the environment and support for me to pursue my dream as a scientist.

Table of Contents

Abbreviations

5-HT: 5-hydroxytryptamine

AC: anterior commissures

ACh: acetylcholine

AChE: acetylcholine esterase

AL: antennal lobe

Bax: Bcl-2-associated X protein

BBS: B52 Binding Sites

BDNF: brain-derived neurotrophic factor

bp: base pair

BP: basal progenitors

CAM: cell adhesion molecule

CaMK: Ca2+/calmodulin-dependent kinase

cGMP: cyclic guanosine monophosphate

ChAT: choline acetyltransferase

CNS: central nervous system

CNTs: carbon nanotubes

CPT: camptothecin

da: dendritic arborisation

DEPC: Diethylpyrocarbonate

DLM: dorsal longitudinal muscle

dMP2: dorsal MP2

DRG: dorsal root ganglion

DSB: double strand break

EcR: ecdysone receptor

EDTA: ethylenediaminetetraacetic acid

EGTA: ethylene glycol tetraacetic aci

ER: endoplasmic reticulum

FasII: Fasciclin II

FGF: fibroblast growth factor

GABA: gamma-Aminobutyric acid

GF: Giant Fibre

GFP: green fluorescent protein

GMC: ganglion mother cell

GWR: Gill Withdrawal Reflex

LGB: longitudinal glioblast

mAChR: muscarinic acetylcholine receptors

mRNA: messenger RNA

nAChR: nicotine acetylcholine receptors

NB: neuroblast

NBCS: Newborn Calf Serum

NEC: neuralepithelial cell

NGF: nerve growth factor

NMDA: N-methyl-D-aspartate

NSC: neural stem cell

ORF: open reading frame

PBS: phosphate buffered saline

PC: posterior commissures

PCR: polymerase chain reaction

PSD: postsynaptic density

PSI: peripherally synapsing interneuron

RFP: red fluorescent protein

PN: projection neuron

RG: radial glial cell

RGC: retinal ganglion cell

SDS: sodium dodecyl sulphate

TH: tyrosine hydroxylase

TTM: tergotrochanteral muscle

TTMn: tergotrochanteral motor neuron

UTR: untranslated region

vGlut: vesicular glutamate transporters

vMP2: ventral MP2

VNC: ventral nerve cord

YFP: yellow fluorescent protein

List of Figures

List of Tables

CHAPTER 1: Introduction

1.1. Neural Circuits

Neural circuits are the functional units mediating animal behaviour. Activities such as reading, exercising and sleeping are all executed in response to signals passed along the neural circuits. Formation of neural circuits during embryogenesis is largely dependent on the genetic information passed on by the parents which is translated into different kinds of molecular mechanisms directing interactions among neurons. After this initial stage, environmental factors are also introduced to the fate determination processes, which allow modifications of both existing links among neurons and new neuronal connections. Typical examples include the replacement of injured neurons, rewiring of damaged nervous system after axonal injury, and memory consolidation and recall.

While synaptogenesis is the ultimate key step for the establishment of functional neuronal circuits, it is well known that the formation of networks involves several other developmental and selection processes before synaptogenesis takes place. The highly adventurous axon and comparatively less active dendrites first go through a series of exploratory events, interacting with and rejecting potential partners, based on whether the signalling molecules and the receptors possessed by each side make a perfect match. Potential targets are narrowed down from hundreds to tens, and sometimes even to a single individual neuron, with which a stable connection is made. Nevertheless, this is not the end. Additional neurotransmitters and proteins are constantly needed to ensure a permanent bonding between the two sides. It is remarkable that, despite having to go through these complicated selection processes, both the presynaptic axon and postsynaptic dendrites will faithfully choose the specific target they are programmed to.

Moreover, recent genome-wide gene expression analysis added another layer of complexity by revealing that local activity of cells also affects this target selection process by inducing gene expression, which in turn alters the fate of the whole neuronal circuits.

Before going into details of the molecular mechanisms underlying the operational function of neuronal circuits, it is worth going through how neuronal circuits, the actual physical building block of the nervous system, are formed from nothing but a cluster of cells.

1.2. Neural Development

Formation of neuronal circuits starts with the development of single cells, and the pattern follows what is seen in most biological processes: from seemingly simple construct to extremely complicated system. The central nervous system (CNS) in *Drosophila* originates from precursor cells with stem cell-like properties known as neuroblasts (NBs). NBs of the ventral neurogenic region delaminate from the neuroectodermal epithelium into the interior of the embryo, and later give rise to the ventral nerve cord (VNC). While NBs divide asymmetrically for several times to generate another NB and a ganglion mother cell (GMC), the GMC produced from each division only divides once more to give a pair of neurons or glia [1].

The primary cause of this asymmetric division is the establishment of apical-basal cell polarity. Upon delamination, an apical stalk connects the newly formed NB with the neuroectodermal cells. The PAR/aPKC protein complex [2, 3], which is localised in the apical cortex of the neuroectodermal epithelium remains in the apical stalk [4-7]. This apical-basal polarity in the apical stalk is passed on to the NB. During mitosis the spindle undergoes a 90 degrees rotation creating an equatorial plane perpendicular to the apical-basal axis of the cell [8]. This leads to an uneven distribution and separation of cell fate determinants during cytokinesis which later contributes to the distinct properties of the two daughter cells (Fig. 1.1).

Mutations in genes encoding the PAR/aPKC complex lead to loss of apical-basal polarity in neuroectodermal epithelial cells and NBs [4-7, 9]. Distribution of primary basal cell fate determinants such as Pros, Numb, and their adaptor proteins Miranda and Partner of Numb (Pon) is completely disrupted, and so is the orientation of the mitotic spindle [4-7, 9, 10]. A similar situation is also seen in mutants of the apical cell fate determinant Insc and its binding partners, Partner of Insc (Pins) and Gαi [8, 11-15]. In addition, tumour suppressor genes including *lethal giant larvae*, *discs large* and *scribble* have also been shown to be involved in basal localisation of cell fate [16-18].

Now that the fundamental units of the nervous system, individual neurons and glial cells, have emerged, linking up of these neurons which are scattered in different locations is about to take place. While network connections are built up in a rather programmed manner, certain degree of flexibility is still maintained during this process which allows systemic function to be established from these neuronal circuits in the most appropriate way.

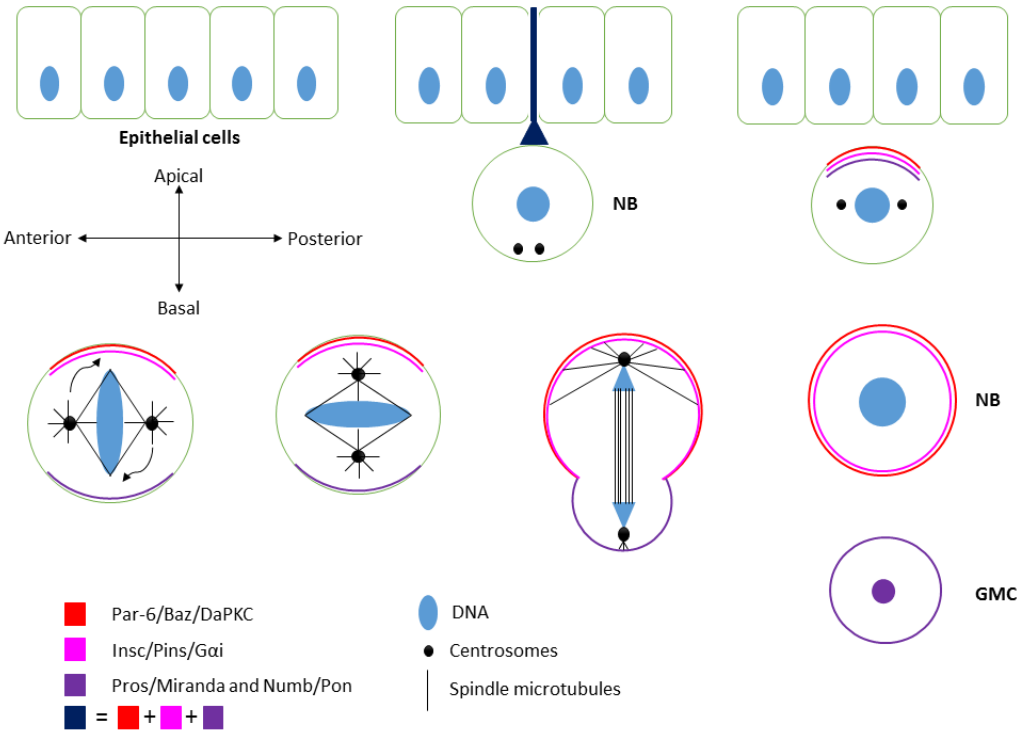

Figure 1.1 Asymmetric division of NB.

NB first delaminates from neuroectodermal epithelial cells, followed by the establishment of apical-basal polarity as a result of separation of cell fate determinants. Par-6/Baz/DaPKC and Insc/Pins/Gαi are localised in the apical side of the cell, whereas Pros/Miranda and Numb/Pon are localised in the basal side of the cell. A 90 degrees rotation of mitotic spindle takes place during this process. Separation of cellular constituents is completed upon cytokinesis, which results in formation of one NB and one GMC.

1.3. Neuronal Targeting and Neuronal Network Formation

As soon as most neuronal cells are in place, the process of target seeking and building up connections among them takes place. The completion of this stage will provide the ultimate infrastructure of the nervous system – the neuronal network (Fig. 1.2). It takes a series of events before an individual neuron can find its right partner. A single neuron A first needs to explore the neighbourhood by extending filopodia. Various road signs (signalling molecules) will then guide neuron A to its preferred place through the big traffic made up of axons extended simultaneously from adjacent neurons. After several turnings and circling around the destination area, neuron A finally arrives at the party. This is followed by examining and

interacting with a moderate number of potential partners. Only then, can neuron A commit itself to a permanent bonding with, in most cases, its lifelong partner, through synaptogenesis. Nevertheless, the whole journey is not completed yet. Constant maintenance of the synaptic connection has to be provided for stabilising the newly formed neuronal network. On the other side, neuron B, which is picked up by the axon of neuron A, will also undergo a series of selections via regulating its dendrites and soma, so as to ensure the right target is chosen.

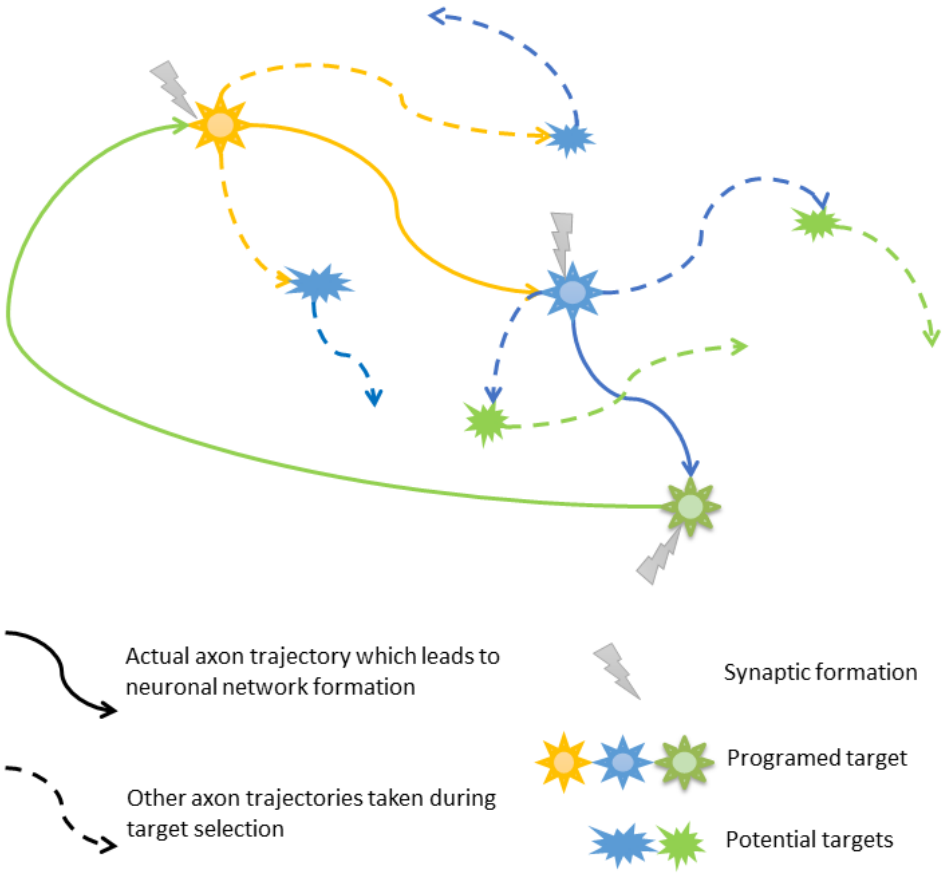

Figure 1.2 Neuronal targeting and neuronal network formation.

Axon is sent out by neuron A to different locations where target selection takes place. Dotted curves represent axon projections made before the final target is chosen. Solid curve represents the final axon projection which leads to synaptogenesis between partner neurons. Connections made among several neurons eventually leads to formation of a closed neuronal circuit.

To put it in a simple way, at least three steps, which often take place simultaneously, make up the processes of neuronal network formation. Namely, axonal elongation, axonal and dendritic targeting, and synaptogenesis. A lot of research has been done to address questions arisen from the first stage: what guides the axon towards its destination?

1.3.1. Axonal elongation

The growth cone, the mobile tip of a growing axon, plays the leading role in driving and directing the elongation process of an axon, by generating forward tension force [19] during the initial stage of neuronal network formation.

A growth cone consists primarily of three domains: the peripheral domain, the transition zone and the central domain. Actin filaments are first assembled in the peripheral domain, which is the edge of the growth cone, leading to extension of F-actin-based lamellipodia and filopodia, and at the same time stretching the membrane of the growth cone towards the direction of elongation. On the other end sits the microtubule-based central domain, where actin filaments advanced to the distal tips are dragged back by myosin-like molecular motors and are depolymerised [20-22]. This retrograde flow functions as a controlling mechanism which limits the rate of axon elongation and prevents microtubules from entering the peripheral domain. Thus, the balance between anterograde flow and retrograde flow determines whether the axon is elongating or retracting. Extracellular signals play the determining role in setting the balance. Typically, once cell-adhesion molecules come into contact with the growth cone, an increasingly strong connection, which is enough to overcome the force generated from retrograde flow, is built up between the growth cone and the extracellular matrix. In situations where close contact has been made, a force between the growth cone of the approaching axon and the target neuron is established. Depending on which domain of the axon is reached by the extracellular molecules, different responses may be generated [23]. Eventually, polymerisation of microtubules will promote their entrance into the peripheral domain. As a result, microtubules move one step

forward, causing elongation and thickening of the filopodium which now becomes part of the axon [24].

In reality, a single axon can be surrounded by countless number of signalling molecules. Therefore, specific patterns have to be matched for the correct transduction of signals to the cytoskeleton during axon development, and this process is mediated by various receptors spanning the membrane. One of the important receptors that have been identified are integrin heterodimers. These transmembrane receptors link up the extracellular matrix and the cytoskeleton inside a cell. Upon binding to a ligand, such as fibronectin and type I collagen, in the matrix, the cytoplasmic tail of the integrin subunit binds to actin via anchor proteins such as talin, a-actinin and filamin, initiating clustering of more integrins and generating a strong adhesive force between the cell and the extracellular matrix.

Immediately downstream the surface receptors are the Rho-GTPases. Intensive studies have linked this receptor family to growth cone mobility, axon elongation and guidance [25-27]. Among family members, Rho inhibits growth cone polymerisation when it is activated upon binding to GTP, while activated Rac and Cdc42 promote the assembly of actin filaments of filopodia and lamellipodia. Activators and repressors such as guanine nucleotide exchange factors (GEFs) and GTPase activating proteins (GAPs), respectively, along with other effector kinases act upon the GTPases to regulate their action state through GTP metabolism [28].

These GTPases in turn control the activities of numerous actin binding proteins, such as Profilin, which is recruited to enhance actin polymerisation in the growth cone [29]. The balance between polymerisation and disassemble of the actin filaments also involves Gelsolin [30] and AFF/Cofilin [31].

While actin filaments are busy with gathering themselves to the right place in response to extracellular signals, immediately adjacent to them are the microtubules, the core elements for

axonal lengthening [32-34], ready to be called up for action. Experiments have demonstrated that in addition to a decrease in retrograde actin flow, polymerisation of microtubules can be directly induced by CAMs [35]. Destabilisation of microtubules then takes place to allow the insertion of new membrane in the growth cone [36]. Microtubule-associated proteins are key players in regulating the stability of microtubules since they bind and thus interact directly with microtubules during polymerisation. For example, CRMP-2 binds tubulin dimers and is involved in axonal growth and branching in hippocampal neurons in culture [37]. Down-regulation of microtubule associated protein Tau has been shown to cause inhibition of axon outgrowth and reduction in size of motility of the growth cone [38]. Transportation of microtubules is mediated by dynein which facilitates microtubule invasion during axon elongation [39]. On the other hand, the lack of dendritic microtubule associated protein 2 (MAP2) leads to decreased dendritic growth [40].

In addition to the transport of actin and microtubules, the supply of cellular constituents for biosynthesis is also needed for the rapid axon growth. Experiments carried out by Shaw and Bray in 1977 demonstrated that adult sensory axons separated from their cell bodies were able to grow further in culture [41], indicating the synthesis of corresponding proteins, lipid and other molecules was carried out within the axon itself. Since then, several experiments have shown that smooth endoplasmice reticulum (ER) is distributed along the axon, and by using radioactive lipid precursors, synthesis of lipid has also been observed in axons *in vivo* [42-48]. Accompanying experiments have shown that both the cell body and axons are able to transform lipoproteins into cholesterol, so as to keep up with the demand of plasma membrane synthesis [47-49]. Therefore, it seems that although the cell body plays a major role in synthesising basic building blocks for the axonal elongation process, secretion of essential materials to supply to the growth cone also relies on the organelles within the extending axon. Consistently, the presence of ribosomes and mRNAs also suggests the possibility of translational process taking place in axons, as demonstrated by studies of other laboratories [50-52].

1.3.2. Axonal targeting

1.3.2.1. Axon guidance

In order to build up functional neuronal circuits, simply sending out neuronal processes to reach to one another randomly is certainly not a good and efficient strategy. Thus, in addition to factors stimulating axonal elongation, guidance molecules also play an essential part in steering axons, as well as dendrites. These molecules ensure the right links among neuronal cells to be established.

During this passive hiding and active seeking process, an axon projected from a single neuron tends to get in contact with all sorts of cues which in general fall into two categories, attractants and repellents. In *Drosophila*, the elongating direction of the axon bundle is diverted after reaching the vicinity of the midline. Axons which are more sensitive to repellent cues secreted by midline cells such as Slit, will remain ipsilateral (on the side where they emerge from). The main function of Slit is to repel longitudinal axons from crossing the midline in the CNS. Other axons which are more sensitive to midline secreted attractants such as Netrins will cross the midline and thus become commissural axons. Netrin has the opposing function of Slit in guiding longitudinal axons in this case, acting as an attractant and facilitates midline crossing.

It has been shown in embryos devoid of either Slit or its receptor Robo1, that all the axons grow towards the midline and stay there [53-55]. In embryos lacking Netrins, some axons failed to orient normally towards midline but most axons still form commissures [56]. It has been suggested that commissural axons can overcome the repulsive force generated by Slit-Robo near the midline, and thus cross over the midline. Previous studies demonstrated that Commissureless is essential to help axons to overcome Slit repulsion, and the lack of Commissureless results in nearly complete loss of axon commissures. [53, 57-60]. On the contrary, loss of *robo1* leads to abnormal midline crossing [53].

It has been shown later that Commissureless acts on Robo1 possibly by regulating the intracellular movement of the latter, deviating it from reaching the growth cone and thus numbing the sensitivity of the axons to Slit [61]. This insensitivity for the repellent Slit, allows Netrins to be in the lead and hence axons are attracted towards the midline.

It is thought that all the members of the Robo family, the receptors for Slit, would have a rather conserved role in midline repulsion. However, research on locating the functionally related counterpart of Commissureless in vertebrates unexpectedly found that deletion of robo3 did not result in the supposed loss of midline repulsion, but instead inducing the axons to remain ipsilateral [62], similar to the phenotype observed in the Commisureless mutant of *Drosophila*. Further research shows that rather than having a completely opposite function as the *Drosophila* Robo3, the vertebrate Robo3 can be spliced into another isoform, Robo3.1, which antagonises Slit/Robo possibly by inhibiting the transduction of repulsive signal from Slit to the growth cones [62, 63]. Inspired by the above findings, mutation of the *Drosophila robo2* gene, which is most closely related to vertebrate *robo3*, has been performed. Yet, compared to the deletion of *robo3* in vertebrates, *Drosophila robo2* mutants only exhibit minor axonal pathfinding defects. In a different experiment, mutation of *robo2* in a *netrin* or *fra* mutant background, loss of commissures is observed, suggesting that Robo2 does have a positive role in commissure formation [56].

In vertebrates, midline crossing is also mediated by factors regulating both gain and loss of axon attraction/repulsion. For example, in the hindbrain of vertebrates, commissural axons formed from neurons in the dorsal cerebellar plate no longer respond to Netrin-1 after midline crossing [64], and a similar phenotype is observed in the spinal cord where commissural axons are not attracted by Netrin-1 and Shh after midline crossing [65]. On the other hand, factors such as Slit, Sema3B and Sema3F, which have no effect on axonal guidance before midline crossing, start to become influential after crossing [66]. A possible explanation provided by Stein and Tessier-

Lavigne is that Slit-1 can neutralise the attractive effect of Netrin-1 by cutting off Deleted in Colorectal Cancer (DCC), the Netrin receptor, and thus isolating axons from the attractive forces [66]. The gain of repulsion from Sema3B and Sema3F after midline crossing is thought to be regulated by Shh in a similar manner – the axonal contact of these two Semaphorins seems to be prevented before midline crossing [67]. As soon as Sema3B and Sema3F are free from the restriction induced by Shh, repulsion becomes the principal force that prevents commissural axons from turning back.

However, the same mechanism does not seem to exist in *Drosophila*. Instead it is thought that c*ommissureless* and *robo1* are down- and up-regulated, respectively, to elevate the repulsion of commissural axons after midline crossing [68]. After the safe arrival on the other side of the midline, axons are now facing the choice of which direction to go – anterior or posterior (A-P)? In fact, the direction has already been set by the time axons cross either through the anterior commissure (AC) or the posterior commissure (PC) . This step is thought to be partly influenced by the initial position of the cell bodies from where the axons originate, since they tend to cross through the nearest commissures. Nevertheless, experimental evidence indicates that accumulation of Wnt5 on PC is required to keep the anterior axons away from PC and thus maintain their own characters, and AC fails to form when Wnt5 is ectopically expressed along the midline [69]. This process requires the presence of a second factor, which is Derailed, the receptor of Wnt5, on the anterior axons, to respond to the repellent signal generated by Wnt5 at the PC. In consistence, the lack of Derailed has been shown to result in anterior axons crossing through the PC [69, 70].

On the other hand, things are quite reversed in vertebrates. Instead of acting as a repellent signal, Wnt attracts axons that have already crossed the midline. It has been shown there is a Wnt gradient built up along the spinal cord with high concentration in the anterior and low concentration in the posterior. As a result, axons which become sensitive to the Wnt signals

after midline crossing tend to turn to the anterior. It has been shown that disruption of this Wnt gradient caused by introducing soluble Frizzled-related proteins, which are the membrane bound receptors of Wnt, leads to defects in anterior-posterior growth, and mutation in Frizzled3 results in disorientation of axons along the anterior-posterior axis [65]. A second factor which is thought to be involved in the A-P orientation is Shh, which act as repellents to the commissural axons, and is distributed in an anterior-low and posterior-high manner. Loss of Shh function in chicken caused by RNAi has been shown to induce A-P guidance defects [71].

The turning of commissural axons, either anteriorly or posteriorly, is large affected by Slit/Robo and Netrin/Frazzled. For example, in *robo* mutants, while MP1 axon projects as in wildtype (WT) posteriorly, the axon of dMP2 is somehow guided towards the commissures, and eventually ends up in crossing the midline. In addition, the dMP2 axon in *robo* mutant never reaches to the next segment [72]. Although initially the axon of dMP2 is still fasciculated with that of MP1 in the *robo* mutant, this does not prevent the dMP2 axon from choosing the wrong path regardless of the adhesion force generated by the other MP1 pioneer neuron. Further to this observation of dMP2 misprojection, the authors isolated the causing factor by expressing *commisuresless* specifically in dMP2 neuron to remove Robo from the cell membrane. In this way, axons of dMP2 neuron project contralaterally. Also, in *robo* mutant background, induced expression of *robo* in dMP2 brings its axon back to track, regardless of the surrounding misprojected axons [72]. In an attempt to rescue the misprojection of dMP2 axons in *robo* mutant, the authors reduced the level of attractants located near the lateral region of the commissure by, in one case removing *NetrinA* and *NetrinB*, and in another inducing mutation in *frazzled*, where a reduction of misprojection to 61% and 24% were observed, respectively [72].

It is first thought that the Netrin/Frazzled affects the dMP2 trajectory in a way similar to that of Slit/Robo, i.e. autonomously. However, in the *robo* mutant, dMP2 axons only transverse as they approaching the commissure at the end. Also, antibody staining has revealed that Frazzled is

completely absent in dMP2 cell. These suggest Netrin/Frazzled is regulated in a different manner from that of Slit/Robo. In *frazzled* and *robo* double mutant, where misprojection of dMP2 was greatly reduced as compared to *robo* mutant, expression of *UAS-Frz-ΔC* (truncated Frazzled protein which lost its intracellular domain) in cells found along the normal dMP2 projection pathway, but excluding dMP2 cells, rendered the axons exhibiting roundabout-like trajectory. In contrast to it, induction of *UAS-Frz-ΔC* in dMP2 did not change the trajectory of dMP2 axon. These indicate Frazzled controls the projection of dMP2 axon in a non-cell-autonomous fashion [72].

On the other hand, misprojection of ascending neurons was also observed in *robo* mutant, where vMP2 and pCC extended their axons towards the midline instead of following their longitudinal path. This abnormal phenotype was once again rescued by the removal of either Netrin or Frazzled. In *robo* and *frazzled* double mutant, expression of *UAS-Frz-ΔC* restored the midline crossing defects of the ascending neurons. All these together indicate the misprojection of dMP2 axons in *robo* mutant is caused by dMP2 axons failing to overcome the force barrier created by Netrin/Frazzled in the commissures due to the absence of Robo, and therefore unable to cross the segment boundary [72].

1.3.2.2. Axon branching

Given the complicated interactions established within the nervous system, surely a one to one connection made between a pair of neurons is not sufficient to serve the purpose of communication among the huge neuron population. A regional neuronal network must somehow link to a different one via more than one route.

The application of functional magnetic resonance imaging (fMRI), which is based on monitoring regional changes of blood oxygenation resulting from neural activity [73, 74], has demonstrated that in the presence of stimuli, for example, 16-bit digitally synthesised tones, human subjects

always respond first by processing the information in more than one area of the brain, which in this case include cerebral hemispheres, cerebellum bilaterally, bilateral deep nuclei, and brainstem [75].

The only way to allow a single neuron to have multiple targets is achieved through axon branching. Axon branching is a process that defines the morphology and connections of each neuronal cell type. It is also a higher controlling mechanism for target selection and structural plasticity [76, 77].

The involvement of multiple factors in axon branching enables a high flexibility in terms of shape-shifting in space and time. One kind of branching is known as arborisation, where branches are formed in a tree-like fashion at axon terminals in the target region. A rather simplified version of arborisation is called bifurcation, where a pair of branches are generated which often grow into separate ways. A third type is collateral branches, where branches extend either orthogonally or obliquely from the axon, and usually end up at different targets to that of the main axon.

Despite these seemingly simple forms of branching, recent studies have highlighted the underlying mechanisms by which a rather complicated intermediate branching map is often involved in the formation process. In general, the ultimate form of axonal branches in mature neural circuits may not reflect how these branches are formed during development, and multiple steps regulated by different extracellular signals are present. A typical example is the RGC axons, which first overshoot their target, and then form branches in the target region. The whole branching process is completed by retracting the overshot axons to the target region [78, 79]. The formation of the daughter branch has been linked to the C-type natriuretic peptide pathway. The C-type natriuretic peptide binds to the membrane-associated guanylate cyclase natriuretic peptide receptor 2, which activates the production of cGMP. Any disruption induced along the pathway, including genetic ablation of the cGMP target Prkg1, would lead to failure in

the generation of a second branch [80, 81]. As soon as the daughter branch is formed, guidance molecules Slit1 and Slit2 come into play, interacting with their corresponding Robo1 and Robo2 receptors. Mutants in either ligands or receptors result in disorientation of the bifurcation fork [82].

Axon branching can take place essentially everywhere along the axon. Recent studies have shed light on several mechanisms that specify the location of branching. Whilst some of the axons form branches in a relative early stage, such as those of dMP2, in most other cases, branches are formed at axon terminals, i.e. the target regions, such as those of peripheral and central axons of sensory neurons in the DRG. These terminal branches are generated in response to a group of target-derived factors. A typical factor is the nerve growth factor (NGF), which induces the branching of sensory axons in the peripheral tissue as soon as they approach the skin [83]. In mice lacking the low-affinity NGF receptor p75, arborisation of sensory neurons in the peripheral tissue is reduced [84]. In a different study where double deletions of *Ngf* and *Bcl-2-associated X protein (Bax)* is examined in mice, axons of the sensory neurons are able to reach their skin targets, but fail to innervate them and initiate arborisation [85]. The close relation between NGF and arborisation has been further demonstrated in neurons from the sympathetic ganglion, where deletion of NGF in *Bax* null mutation background results in reduced innervation of multiple sympathetic targets due to defective arborisation [86]. Interestingly, not all of the targets lose innervations, suggesting there has to be a second axon branching factor, which acts on the same pathway. This factor has later been found to be a Wnt family protein. Wnt3 has been found to be expressed in motor neurons in the ventral spinal cord where axon terminals of sensory neurons are located [87]. Artificial induction of Wnt3 signal in cultured embryonic mouse DRG neurons leads to increase in formation of secondary and higher order branches, indicating Wnt3 functions as a signal to specify the location for terminal arborisation.

In addition to the above mentioned growth factors, other diffusible factors secreted around the

terminal tissue also promotes branch formation [88, 89]. During early spinal cord development, collateral branching takes place 2 days after the sensory afferents bifurcate [90, 91]. This suggests an accumulation of local regulatory factors might be needed to function as a secondary stimulus to trigger formation of collateral branches [92].

Guidance molecules like Netrin 1 has also been found to affect branch formation in cultured hamster cortical axons, as introducing Netrin 1 to these axons leads to filopodial extension towards the stimuli [93]. The presence of Netrin 1 coincides spatiotemporally with Ca^{2+} transients [94] and new branch formation [95].

On the other hand, factors inhibiting branch formation are also involved. It has been shown that cultured chick RGCs derived from the temporal side of the retina form branches exclusively on membrane stripes derived from the anterior tectum, their endogenous terminal zone, whereas axons of nasal RGCs show no preference. However, after adding soluble EphA3 receptors to the culture to block the ephrin A pathway, the biased branch formation is resolved, suggesting ephrin A functions as an inhibitor for axon branching [96].

1.3.2.3. Axon retraction

Axonal branches formed during development are not necessarily retained by mature neuronal circuits [97]. During early mammalian cortical development, multiple collateral branches are generated from axons projected from the motor and visual cortex [98]. Many of them are eliminated in later stages through a process known as pruning. The retraction of overshooting axons and redundant interstitial branches during RGC development also employs the same pruning strategy [99]. Once again, guidance molecules are involved [100], which coordinate with other cellular factors to regulate branch degeneration [97].

Several factors, such as branch number, length and order, will influence the function and capacity of the terminal arbours during synaptogenesis. Guidance molecules of the Slit family

and their Robo receptors are associated with these properties of the terminal arbour. In general, both mutations in *Slit* (*Slit2*; *Slit3* or *Slit1*; *Slit2*; *Slit3*) and the lack of Robo (Robo1; Robo2), can cause reduction in size of branching or missing of the entire arbour of the trigeminal ganglion in mice [82], whereas overexpression of *slit2* leads to increased branching in peripheral sensory neurons [101]. Just like every coin has its two sides, Sema acts in the opposite way of Slit. Loss of Sema 3A function leads to overgrowth of peripheral axon and branching in both DRG and trigeminal ganglion [102, 103]. Similar defects have also been found in mice devoid of Semaphorins receptors, neuropilin 1 or plexin A3/A4 [104, 105]. The inhibitory role of Sema 3A is further verified by its effect on limiting axon branching of cortical neurons in culture [93].

Inhibitory cues also contribute to self-avoidance and tiling. *In vivo* imaging of sensory axons in zebrafish has shown that the removal of an existing arbour allows the neighbouring neurons to take over the terminal region [106], indicating repulsion is needed even after synaptogenesis to maintain the correct neural network status.

Several studies have demonstrated that developing synapses participate in stabilising specific branches, and neural activity can regulate axon branching. More details will be discussed in the synaptogenesis section.

1.3.3. Dendritic formation and targeting

Compared to axons, dendrites play a relatively less active role in neuronal network formation since their travel distance is limited to the vicinity of the neuronal cell body. However, the importance of dendritic formation and targeting cannot be neglected.

Dendrites are the neurites that serve as the receiver of synaptic input in a neuronal circuit. Dendritic development has everything in common with axon in terms of development. Processes such as outgrowth, guidance, targeting and arbour remodelling are also seen during dendritic development.

The cytoskeleton of dendrites is slightly different from that of axons, consisting of relatively more microtubules than actin filaments, and rougher ER and polyribosomes. In contrast to axonal microtubules whose plus-ends pointing distally, the ends of dendritic microtubules consists of both plus- and minus-ends. In addition to the above features, the distinctive functions of axons and dendrites are mainly attributed to the localisation of different types of proteins. The specific shapes of both axons and dendrites are crucial in neuronal function and circuit assembly, as well as in processing and integration of electrical signals.

During the initial formation stage, incorporation of membrane and proteins is in high demand for dendritic growth and branching. Golgi compartments have been found in dendrites, suggesting a local secretion of cellular constituents in dendrites [107-109]. This is further confirmed by defects observed in dendritic growth and maintenance in cultured rat hippocampal neurons, where Golgi trafficking, including that from ER to Golgi and cargo budding from the trans-Golgi network have been blocked [108]. Screening for genes shaping formation using *Drosophila* class IV da sensory neurons identified several genes involved in the ER to Golgi transport pathway, such as *sar1*, *sec23* and *Rab1* [109]. Among them, mutation in *sar1* causes reduced dendrite growth and diffuse Golgi outposts, while axons are not strongly affected, indicating there are independent pathways mediating the growth of axons and dendrites [109].

It has been shown that the lineage and identity of neurons are the primary factors affecting the targets of dendrites [110-113]. Studies of *Drosophila* antenna lobe (AL) have shown that the information stored in the olfactory receptor neurons is transmitted to second-order olfactory neurons, the projection neurons (PNs). There are mainly three lineages of PN: anterodorsal PN, lateral PN and ventral PN lineages. Each PN targets one out of 50 AL glomeruli in its lineage. This is achieved by recognising specific patterns of its targets, and also via self-avoidance. Both processes are mediated by the dendrites formed on the AL. Transcription factors, such as Acj6 and Drifter, are found to be essential for the correct targeting of glomeruli on DL1 anterodorsal

PN dendrites and ventral PN dendrites, respectively [112, 113]. These transcription factors show target specificity, since misexpression of drifter in acj6 anterodorsal PN mutant results in mistargeting the more anterior glomeruli, and if *cut* is also expressed in this anterodorsal PN mutant, the target will shift almost entirely to the glomeruli of lateral PN [113]. This indicates lineage-specificity of PN targeting is imprinted by the combination of different transcription factors.

Although having non-overlapping pathways to that of axon growth, several guidance molecules have been found to be shared by both dendritic and axonal targeting, including Semaphorins, Robo/Slit, and Netrin/DDC.

Recent studies of the cues involved in early dendritic targeting of *Drosophila* AL revealed an important role of Semaphorins. Sema-1 belongs to the Semaphorin family which mediates axon guidance via regulation of transmembrane receptors including Neuropilins and Plexin. Sema-1a is found to be expressed in a graded level across different PN dendrites, and targeting of PN to specific regions in *Drosophila* AL is related to the concentration of Sema-1a. For example, PNs that express the highest level of Sema-1a form protoglomeruli at the most dorsolateral regions of the AL, whereas those expressing lower levels of Sema-1a target to the more ventromedial regions. Sema-1a acts more like a receptor rather than a ligand in this case, suggesting the existence of a yet unknown ligand involved in dendritic targeting [114].

Deletion of Slit leads to complete loss of dendrites in the aCC motor neuron in the VNC of *Drosophila* embryo. In addition, in *robo* null mutant embryos, the size of aCC dendrites is reduced to 26% compared to that in wild type [115]. In an earlier study conducted by the same group, null mutation of *frazzled*, *netrin* and *commissureless* caused guidance defects in dendrites of certain neurons in the embryonic CNS, including RP3 and aCC. The dendrites of these neurons failed to cross the midline [116]. This result is consistent with the study of contralateral dendrites of zebrafish octavolateralis efferent neurons, where blocking of *dcc* and *netrin1* expression by

injecting their antisense morpholino oligonucleotides prevented the dendrites from crossing the midline [117].

In addition to attractive cues, cell-cell repulsion also plays an important part in dendritic guidance. This repulsive interaction between dendrites is required to maintain dendrites within the specific territories so as to avoid unwanted tangling of dendrites, and thus allowing, for example, the PN in *Drosophila* to target to the corresponding glomeruli in the AL without interfering with the activity of other PNs [118]. This repulsive force also ensures an even growth and distribution of neuronal cells. This self-avoidance strategy applied by neurons based on cell-cell repulsion guarantees that dendritic branches originated from the same neuron will not cross or fasciculate with each other, so that connections between branches of the same neuron are avoided.

1.3.4. Synaptogenesis

As soon as axons and dendrites find their perfect matches, synaptogenesis occurs, integrating the many individual neuronal cells into a complete new network that grants them the property of communication.

As mentioned above, neurons reach for one another by extending single axons whose path are determined by various guidance cues encountered during the targeting process. Upon reaching the right target, synaptic contact is made between the presynaptic sites and postsynaptic sites (Fig. 1.3). In most cases, this synaptic contact is maintained and reinforced throughout life. Several properties have emerged along with the neuronal circuit.

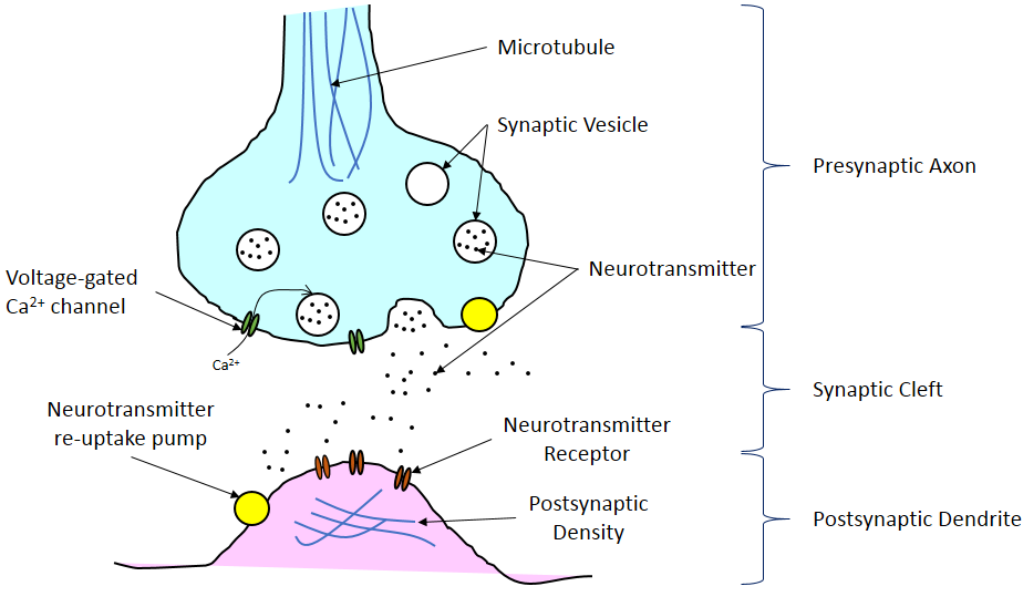

Figure 1.3.: Synaptogenesis.

Synaptogenesis requires the presynaptic axon (blue) and postsynaptic dendrite (pink) to make contact with each other. Upon completion of synaptic formation, both electrical and chemical signals can be passed from one neuron via its axon to another neuron through its dendrite. In this case, neurotransmitters kept in the synaptic vesicles in the presynaptic axon are released into the synaptic cleft as a result of Ca^{2+} influx. The released neurotransmitter binds to receptors localised to the postsynaptic membrane.

First of all, electric and chemical signals can now be passed from one neuronal cell to another in a unidirectional manner via the newly established bridge – the synapse or synaptic junction. A synaptic junction consists of three parts: presynaptic bouton, synaptic cleft and the postsynaptic reception apparatus [119]. Presynaptic boutons are found along the axons, but mainly in the axon terminals, and filled with synaptic vesicles that carry neurotransmitters. These neurotransmitters are released in the synaptic cleft in regions called active zones, characterised by the presence of protein matrix known as the presynaptic web [119, 120]. Immediately adjacent to the active zones is the postsynaptic plasma membrane where receptors and ion channels are anchored. Another protein rich structure named postsynaptic density (PSD) links the active zones and the cytoplasm of the postsynaptic cells together [121, 122]. Variations in

size and organisation of presynaptic active zones and also the thickness of PSD have been attributed to the difference in synaptic type, function and efficacy.

The transfer of electric signal is mediated by channels called gap junctions which allow the passing of electric current that causes voltage changes in presynaptic and subsequently postsynaptic cells in a rapid way [123, 124]. On the other hand, chemical synapse decrypts the electric code into a message that triggers the release of chemical compounds known as neurotransmitters, which then bind to the receptors in the postsynaptic sites that can lead to complex effects, either causing direct changes in membrane potential via opened ion channels or inducing the activation of excitatory, inhibitory or modulatory signalling pathways [125]. Among the three different pathways, the vast majority is excitatory where glutamate plays the leading role. Inhibitory pathways are mediated by glycine or GABA. Modulatory pathways are regulated mainly by 5-HT, dopamine, Ach, noradrenaline and neuropeptides [125]. In general, neurotransmitters released by a single neuron are limited to one specific type, whereas postsynaptic sites have to deal with multiple forms of input which requires the placement of the right receptors from.

Apart from genetic contributions towards temporal regulation of the process, local interactions and molecules generated by target neurons also take part in synaptogenesis, as well as neuronal differentiation [126, 127]. Extensive studies have identified both the internal genetic components and the external target derived factors involved in regulating synaptogenesis. While mapping of individual genes in the giant network is a complicated process, several target derived factors have been well studied.

The first category of molecules that regulate synaptogenic activity is characterised by their diffusible properties. These molecules are generally needed for axonal guidance, arborisation, promoting neuronal differentiation and maturation, and facilitating axo-dendritic contact. As previously mentioned, molecules such as Netrins, Semaphorins and EphrinA are essential in

axonal guidance. When it comes to axon arborisation and regulation of synaptic vesicles, a second group of members including the Wnt and FGF families become the core players [128]. For example, Wnt-3 and Wnt-7a induce arborisation of innervating sensory axons in the spinal cord [87] and innervating mossy fibre terminals in cerebellar granule cells [129], respectively. In addition, FGF22 secreted by cerebellar granule cells also promotes the formation of active zones in innvervating mossy fibre axons [127]. Recent studies have shed light on glial-derived factors which might also play a part in regulating synapse formation. This has been found out initially due to the correlation between synaptogenesis in the CNS and the birth of astrocytes and their enhancing effects in synapse formation [126, 130-133]. Two glial-derived factors, cholesterol bound to apolipoprotein E [134] and TSP1 [126] have been identified in promoting synapse formation by facilitating maturation of the neuronal cells which are about to undergo synaptogenesis.

In the meantime, CAMs also join in the forces that guide the connection of presynaptic and postsynaptic parts. Among them, classical cadherins have been intensively studied. Different members of this cadherin family have been found and named after their locations, including E-cadherin (epithelial), N-cadherin (neural) and P-cadherin (placental). Individual cadherins can be found on both presynaptic and postsynaptic plasma membranes [135, 136], and also axon-dendritic contact sites [137]. Several experiments have demonstrated the primary role of cadherins in guiding instead of inducing synapse formation. Blocking N-cadherin with antibodies in the developing chick optic tectum leads to overshooting of retinal ganglion cell axons, which consequently causes synapse formation at the wrong site, as opposed to failure in initiating synapse formation [138]. Also in *Drosophila*, the lack of N-cadherin leads to mistargeting of axons from the photoreceptor cells, but deos not affect synapse formation [139].

A second group of the CAMs, which are known for their highly diverse functions due to the ability to undergo alternative splicing of RNAs that make up the extracellular domains [140, 141], is the

protocadherin. They share common features with classical cadherins in a way that they are more essential in targeting recognition rather than synapse formation [142]. Studies of protocadherin gamma knockout mice indicate these CAMs are not required for neuronal differentiation [143].

On the other hand, CAMs such as Narp, Ephrin B1, SynCAM and neuroligin have also been largely examined for their direct involvement in synapse specification, adhesion and signalling [144-147].

Narp belongs to the pentraxin family of secreted proteins. Narp is secreted at synapses, and binds to the extracellular domains of AMPA-type glutamate receptor. The increase in synaptic clustering of AMPA receptors is correlated with overexpression of Narp in spinal cord neurons [146]. In cell cultures, overexpression of Narp in human embryonic kidney 293 cells shows more aggressive clustering of AMPA receptors on co-cultured spinal cord neurons [148]. Clustering of NMDA on glutamatergic synapses formed on inhibitory interneurons is also affected by Narp [149].

EphrinB is a member of the Ephrin family, a major player in axonal guidance. The primary target of EphrinB is the NMDA type of glutamate receptor [145]. Ephrins and Eph receptors are found to be involved in dendritic spine development [150, 151]. Triple knockout of EphB1, EphB2 and EphB3 results in abnormal hippocampal spine morphology in mice [152].

Compared to Narp and EphrinB, SynCAM and neuroligin have a more direct involvement in synapse formation by inducing presynaptic differentiation through axo-dendritic contact. It has been shown that the postsynaptic membrane protein neuroligin is capable of inducing presynaptic differentiation when expressed in human embryonic kidney 293 cells [147]. This is achieved by interacting with its presynaptic receptor β–neuroxin [153]. Interestingly, the interaction domains of neuroligin and β–neuroxin are laminin-G and AChE-like domains. The laminin-G domain has also been found in laminin and agrin [154], both of which are ligands for

Integrins and involved in differentiation of neuromuscular junction [155]. However, the AChE-like domains have been shown to be catalytically inactive [153]. Recent evidences have demonstrated that bi-directional signalling between neuroligin and β–neuroxin also contributes to the shaping of synapses. While neuroligin induces presynaptic differentiation in aonxs, its matching receptor β–neuroxin induces postsynaptic differentiation in dendrites [156].

SynCAM is a member of the Ig superfamily of adhesion molecules. It is expressed on both sides of the synapse and able to induce presynaptic differentiation [128, 144]. Overexpression of SynCAM1 in cultured neurons promotes synapse formation, whereas in other neurons it leads to formation of functional presynaptic active zones in the connecting axons [144]. Three other SynCAM encoding genes have been found which contribute to the generation of various SynCAM isoforms [157]. It is unclear whether this diversity contribute to the synaptic specification. Although most of the observations favour the above model, it has been reported that the active zones can exist independent of postsynaptic partners [158].

From the regulation point of view, whilst it is reasonable to think that CAMs such as neuroligin and SynCAM are the first group of regulator factors present on the site of synaptogenesis, it is unclear whether they are located within the plasma membrane well in advance of synaptogenesis, or if they are delivered to the site only upon synapse formation. Shortly after the first group of CAMs has been delivered and inserted into synaptic membranes, the arrival of 80nm dense core vesicles takes place. This is thought to be necessary for the rapid establishment of docking and fusion sites for synaptic vesicles [159].

In contrast to presynaptic active zones whose foundation requires transportation of materials by synaptic vesicles, postsynaptic differentiation is induced by gradual accumulation of molecules [159, 160]. A typical example is the recruitment of scaffolding proteins of the PSD-95 family. These molecules are first found 2 days after the formation of hippocampus [161], and accumulation starts 20 minutes after axon-dendritic contact in culture [162-164]. Although

gradual accumulation of PSD-95 is achieved mainly by local trapping of diffuse plasma membrane [162, 165], active transport of recombinant PSD-95 clusters by vesicles has also been observed [166]. The next group of molecules recruited to the postsynaptic sites are the NMDA-type and AMPA-type glutamate receptors, where similar synaptic delivery mechanism to that of PSD-95 are used [160, 167-169]. Accumulation of other postsynaptic components is more straightforward, involving only on-site regulation. For example, CaMKII is gathered by trapping of local pools instead of active transport [170]. Scaffolding proteins Homer 1C and Shank2/3 are also recruited from the cytosolic pool [160, 164]. Local synthesis of proteins such as CaMKIIα, Shank, NR1 and GluR1/2 in the mRNA rich dendrites might also contribute to the synaptogenesis [171-173].

Maturation is an important phase of synaptic development, where synapses expand in size, which is correlated with the increase in bouton volume and number of total synaptic vesicles, area of active zones and PSD [174-176] This suggests cell adhesion molecules and associated factors work in a highly coordinated manner to determine the area of extracellular matrix and synapse volume. Changes in postsynaptic morphology is another distinctive feature of synaptogenesis. Filopodia found on dendrites, which are initially targeted by most synapses, later develop into dendritic spines of various shapes, including mushroom, branched and stubby [164, 176]. It has been shown that CAMs, Rho and Ras family GTPase, actin-binding proteins and calcium regulator mechanisms are involved in regulating dendritic spine morphogenesis [177, 178].

Structural changes of synapses always lead to functional changes. Mature hippocampal synapses tend to reduce the release of neurotransmitters [179, 180]. Also, the shifting of receptors would now trigger different level or type of responses when exposed to the same pool of signalling molecules. For example, the lack of surface AMPA receptors causes “silent synapse” in some

developing brain regions [181-183]. A second explanation for the silent AMPA receptors is that alteration in vesicle fusion failed to activate AMPA receptors [184, 185].

While synaptogenesis is a process occurring largely during early developmental stages, synapses can also form or get eliminated in mature brain in response to neuronal activities [186-189]. For example, by following fluorescently labelled synaptobrevin II to visualise synapses in optic axons of *Xenopus* tadpoles, there are synapses formed and eliminated during axon branch remodelling [190]. In fact, there are many more synapses formed during development than those retained in the end [191, 192]. Aactivity-dependent synapse elimination becomes more essential during remodelling of neuronal circuits. It has been shown that while about 50% of dendritic spines remain stable for at least a month in pyramidal neurons in the mouse barrel cortex, the rest are only present for a few days. Sprouting and retraction of these spines correlate with synapse formation and elimination, and turnover of synapse can be up-regulated as a result of decreasing sensory input, in this case, whisker trimming [187]. In another research using the same model, stimulation applied to the whisker led to an increase of 35% synapse density and 25% spine density. Moreover, these synapses faded as the stimulation ceased after several days [193].

Synaptic plasticity has been associated with memory consolidation, the storage of information. It has been shown that synthesis of several proteins, including Per, CaMKII and Cry, takes place in DAL neurons (two neurons located at the dorsal-anterior-lateral region of protocerebrum) during long-term memory formation. In addition, blocking of neuronal output in DAL neurons leads to impairment of memory retention, and disruption of neurotransmission in *per* neurons causes defects in retrieving of 1-day memory after spaced training [194].

1.3.5 Neuronal circuits and animal behaviour

The final physical products of the above mentioned pathways are neuronal circuits, the media by which living creatures of the animal kingdom use to conduct movement, communicate with one another and interact with the environment. So how are the signals transduced from one

end to another, and what are the outcomes? To tackle these questions, large amount of research have been done by close examination of specific neuronal circuits, such as those mediating reflexes, the involuntary movement generated in response to stimuli.

Three particular cases have been well studied, namely, the jump reflex in *Drosophila*, gill withdrawal reflex in *Aplysia*, and the patellar reflex in humans.

1.3.5.1. Jump Reflex

The Giant Fibre (GF) escape response (also known as the jump reflex) in *Drosophila* can be triggered by three different stimuli: intracellular, extracellular and visual. This process is mediated by a pair of GFs (Fig. 1.4), which are aligned bilaterally symmetrical in the region connecting the head and the thorax of *Drosophila*. These GFs relay signals from brain to the thoracic ganglia by forming electrochemical synapses with tergotrochanteral motor neuron (TTMn) and peripherally synapsing interneuron (PSI). Both synapses are needed to complete the action of jump reflex. Firstly, signals sent through TTMn lead to contraction of the tergotrochanteral muscle (TTM), and consequently initiates the escape jump. Secondly, signals sent through PSI trigger chemical synapses of PSI to the motor neurons, via five motor axons, innervating the dorsal longitudinal muscle (DLM), which then initiates flight [195].

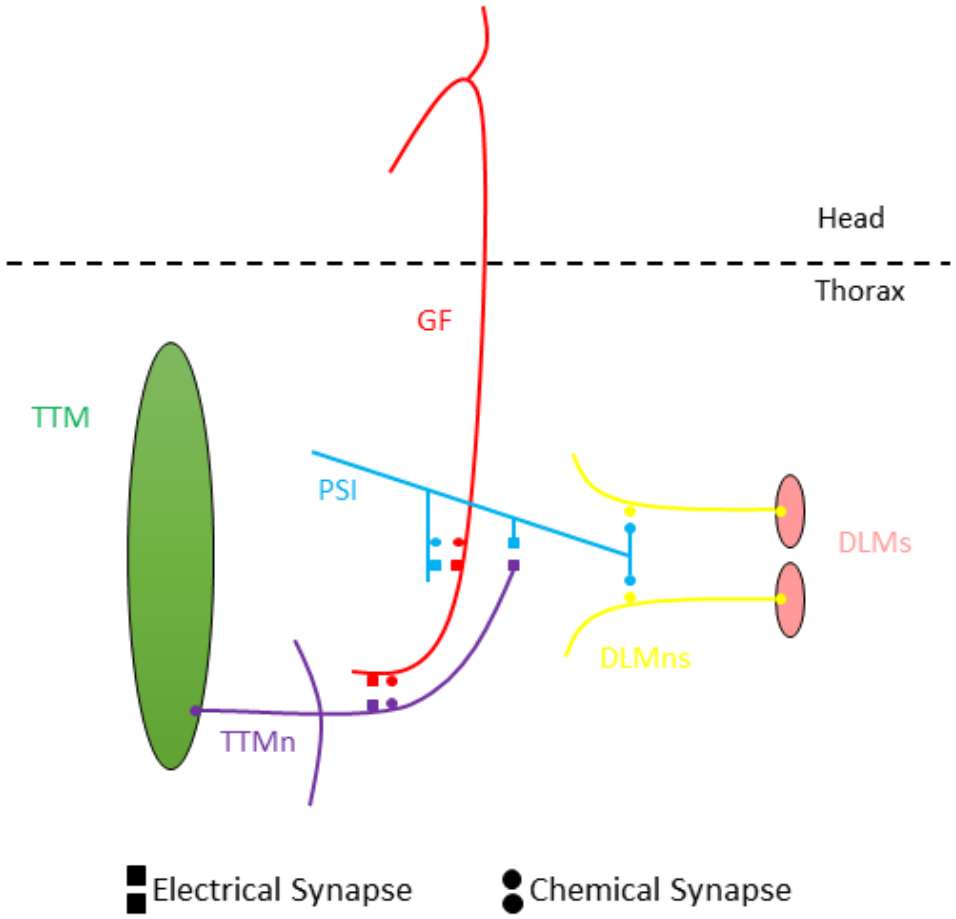

Figure 1.4 The giant fibre system of Drosophila.

The escape response is mediated by a pair of Giant Fibres (GFs, red), which are aligned bilaterally symmetrical between head and thorax. For simplicity, only one side of the GFs is shown. The GFs relay signals from brain to the thoracic ganglia by forming electrochemical synapses with tergotrochanteral motor neuron (TTMn, purple) and peripherally synapsing interneuron (PSI, blue). The synapse with TTMn leads to the contraction of the tergotrochanteral muscle (TTM, green), and consequently initiates the escape jump. The synapse with the PSI triggers chemical synapses of PSI to the dorsal longitudinal motor neurons (DLMns, yellow), and thus innervates the dorsal longitudinal muscle (DLM, pink) to initiate flight.

The connections involved in this process were elucidated by performing several electrophysiological experiments, where insulated tungsten electrodes and glass micropipettes were inserted into the muscles on the dorsal side of *Drosophila*, including the TTM and DLM. The aim was to record any electric potential generated in these locations after applying electrical stimuli to the brain, so as to find out neurons that are involved in the circuit.

Intracellular microelectrode recording of the GF showed that after electric stimulation to the brain, a potential threshold was detected first in the TTM and then in the DLM, with a latency of 1.25ms on average [195]. These observations indicate that the escape response is mediated by the GF pathway. In addition, it has been shown that mutations of *bendless* and *gfA* result in disruption of the motor output in the GF-TTM and GF-DLM pathways, respectively. Also, mutations in *passover* leads to disruption of both pathways. The disruption in each case was caused mainly by synaptic failure due to dysfunction of both pre- and post-synaptic neurons and/or morphological changes in the neuronal branches of TTMn, which can cause them to miss their postsynaptic targets (as in the case of *passover* mutants) [196, 197]. Anatomic study of the GF in *bendless* mutants has also illustrated that GF synapses only to PSI but not TTM [196].

1.3.5.2. Gill Withdrawal Reflex

Gill Withdrawal Reflex (GWR) is an involuntary, defensive response of *Aplysia* which leads to retraction of its gill. Coincidentally, the study of GWR in *Aplysia* has always been associated with the study of short-term learning processes, including habituation, sensitisation and classical conditioning. Habituation refers to a decrease in behavioural response after repetitive stimulations with no adverse effect. In contrast to it, sensitisation is an increase in behavioural response to a stimulus that does have an adverse effect. Classical conditioning is a form of associative learning by which the animal recognises and responds to a single stimulus which usually does not trigger significant responses (conditioned stimulus), after it has been paired with another stimulus which usually has a noxious effect (unconditioned stimulus) and causes significant response of the animal.

When a stimulus (gentle touch of the siphon) is applied, the action potential is first built up in the siphon sensory neurons, and then conducted to the motor neurons via a chemical synapse, which triggers Ca^{2+} and the subsequent Na^{+} influx into the motor neurons. As soon as the plasma membrane of the motor neuron is depolarised, the action potential is relayed to the cells of the

gill muscle, leading to the contraction of the gill. A gill withdrawal can become habituated (less strong) in response to repeated stimulation, and eventually, there will be no gill withdrawal after the sea slug is being touched. This habitual response is caused by a progressive decrease in the amount of neurotransmitter, glutamate, released by the siphon sensory neurons at their synapses with the motor neurons. Eventually, the magnitude of the excitatory postsynaptic potential becomes insignificant, and is thus unable to trigger gill muscle contraction.

When unconditioned stimulus such as an electric shock to the tail is applied, another group of neurons come into play. These neurons are termed facilitator neurons due to their enhancement effect of the gill withdrawal response. Anatomically, the axon of the facilitator neuron makes synaptic contact with the terminal of a siphon sensory neuron, on top of the synapse formed between the sensory and motor neurons. This results in the release of more glutamate at the synaptic regions and, as a consequence, the generation of a stronger action potential which leads to a vigorous contraction of the gill. If a weak stimulus, such as a touch of the siphon, is introduced after that, a strong and rapid withdrawal of the gill will still be triggered, and this effect is known as sensitisation.

Classical conditioning is more or less the same as sensitisation, despite that the unconditioned stimulus is applied few seconds after the conditioned stimulus, whereas sensitisation is triggered solely by unconditioned stimulus. The former process requires the presence of coincidence detectors, which are adenylate cyclase and NMDA glutamate receptors in sensory neuron and motor neuron, respectively, to make them more sensitive to the stimulus. In this way, the animal learns to associate the conditioned stimulus with the unconditioned stimulus, and thus responds to the former stimulus more significantly.

1.3.5.3. Patellar Reflex

A patellar response can be defined as the tendency of the knee to jerk involuntarily when hit sharply. In a knee-jerk test (Fig. 1.5), an action potential is first built up in the sensory neurons located in the tendon of the quadriceps muscle upon being tapped by a hammer. The sensory neurons in turn excite the motor neurons in the spinal cord as well as the spinal interneuron by travelling through the afferent axons. From then on, the action potential is conducted via two different pathways. Excitation of the motor neuron causes contraction of the quadriceps muscle (extensor). On the other hand, the interneuron inserted between the sensory and the motor neuron which innervates the biceps muscle (flexor), prevents the action potential from transferring to the motor neuron, and thus results in relaxation of the biceps. Contraction of the extensor muscle and relaxation of the flexor muscle together cause the sudden extension of the leg at the knee joint.

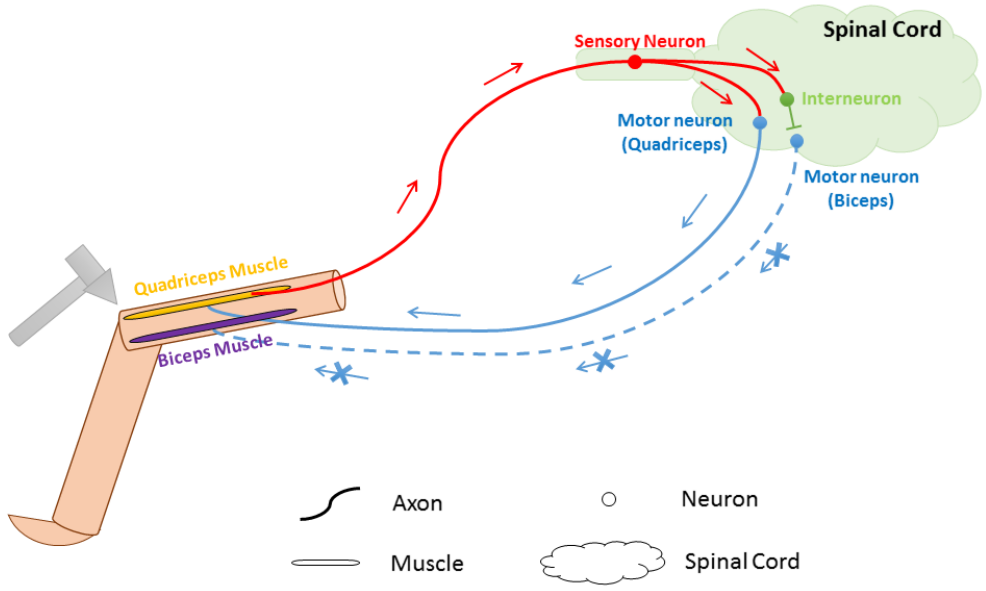

Figure 1.5 Patellar Reflex.

Upon tapping on the tendon, an action potential is established in the quadriceps muscle. This action potential then travels along the afferent axon (red), passing through the sensory neuron. The sensory input is then received by the motor neuron and interneuron located in the spinal cord. The signal relayed directly to the (quadriceps) motor neuron continues to travel along the efferent axon (blue) and

subsequently causes contraction of the quadriceps muscle, while the single "intercepted" by the interneuron prevents the signal from reaching the (biceps) motor neuron, and thus causing relaxation of the biceps muscle. These altogether result in the sudden extension of the leg.

1.4. Aim of the Work

Genetic codes transform cells into neural stem cells which give rise to individual neurons which eventually become part of complicated networks. This, as a result, leads to the establishment of the fundamental building blocks, neural circuits, which endows the animal with the ability to mediate the power of another dimension – behaviour. The molecular mechanisms involved to regulate and control the above processes are certainly intriguing, and therefore have been attracting considerable attentions in the field of neuroscience.

In one way, the "apparent randomness" of the spatial-temporal regulation of each individual units within the whole process of neuronal network formation is believed to contribute to the distinct features observed in different creatures. In the other way, current knowledge and technology have allowed people to understand how these individual units are regulated based on specific behaviour patterns, may it be during early development or after maturation. For example, the causes of associated symptoms displayed in neurological diseases can now be tracked down to specific pathways, combinations of altered gene expression or chemical components. To fully understand and be able to exploit the great power of nature, study of behaviour correlated genotype, and prediction of genetically induced behaviour is necessary in order to reveal the molecular connections between the two ends: genotypes and behaviour.

The aim of my experimental work is to identify regulatory factors which determine the identity and function of the sibling vMP2 and dMP2 neurons which are produced by the same progenitor cell but adopt later different neuronal activities. While vMP2 is an interneuron, dMP2 is a motor

neuron. Their axons project to different direction in the CNS and they express different neurotransmitters. These differences suggest the likelihood of vMP2 and dMP2 innervating different targets. Intriguingly, our transcriptome analysis revealed a striking difference in the levels of the splicing factor B52, the levels of which are 45 times higher in dMP2 than that in vMP2.

B52 belongs to the SR (serine-arginine rich) protein family. Its human orthologue is SRp55. It has been shown in humans that DNA damage can cause up-regulation of SRp55 in p53-deficient cells (p53 is the well know tumour suppressor protein) [198] leading to the alternative splicing of the gene encoding the CD44 receptor, a cell surface molecule involved in cell adhesion and migration in humans [199]. Also in p53-deficient U2OS cells, DNA damage induced by mitomycin C alters the splicing activity of SRp55, which leads to the enrichment of Fas, a key proapoptotic p53-inducible death receptor in its soluble form [200]. In addition to this, reduction of SRp55 activity affects the splicing of two genes *KSR1* and *ZAK*. For example, upon depletion of SRp55, exon 21 of *KSR1* becomes truncated and also the ratio between *ZAK*-α and *ZAK-β* mRNAs is changed [200]. *KSR1* encodes the Kinase Suppressor of Ras1, and *ZAK* encodes a member of the MAPKKK family of single transaction kinases [200]. In a different study, SRp55 was shown to be involved in the tissue-specific splicing of calcitonin/calcitonin gene-related peptide (CGRP) [201]. This *calcitonin/CGRP* gene is the template of two different mRNAs products. In thyroid c cells, more than 98% of the splicing products of *calcitonin/CGRP* gene becomes calcitonin, a hormone involved in Ca^{2+} regulation [202]. In neurons, 99% of the splicing products turns into CGRP [203], which is involved in the transmission of pain [204].

B52 or SRp55 in humans is referred to as serine/arginine-rich splicing factor 6 (SRSF6) in the database of NCBI. The domain structure of *Drosophila* B52 isoform A (the longest isoform), isoform D (the shortest isoform), and human SRp55/SRSF6 is shown in Figure 1.6. Both B52 isoform A and SRp55 contain two RNA recognition motifs (RRMs). The obvious difference

between the B52 isoform A and isoform D is the lack of one RRM domain in isoform D suggesting a difference in RNA binding capacity among different B52 isoforms. While all of the RRMs present in *Drosophila* B52 share similarity with SRSF4 in humans, SRSF6 from humans consists of one unique RRM, and one SRSF4_like motif.

Figure 1.6 Protein structures of Drosophila B52 and humans SRp55/SRSF6

Protein blast of *Drosophila* B52 indicates both of the RRMs in isoform A and the single RRM in isoform D are SRSF4 like. On the other hand, in Srp55 of humans, the RRM in its N-terminus is unique, and the second RRM is SRSF4 like.

https://blast.ncbi.nlm.nih.gov/Blast.cgi?PROGRAM=blastp&PAGE_TYPE=BlastSearch&LINK_LOC=blasthome

Within the RRM of *Drosophila*, two regions have been found to be highly conserved among over 200 RNA-binding proteins. The primary function of B52 is pre-mRNA splicing [205, 206]. B52 has 10 splicing isoforms (data from flybase.org), suggesting the gene of B52 itself is regulated by a splicing factor. The longest isoform is 350 amino acid (aa) in length, and the shortest two isoforms are 135aa and 147aa long, respectively. The rest of the isoforms are all around 330aa or longer (see Fig. A1 in the Appendix for B52 protein sequence alignment).

In *Drosophila*, B52 is ubiquitously expressed throughout all developmental stages [207] (also see FlyBase High Throughput Expression Pattern Data). Deletion of B52 mutants are homozygous lethal at the second-instar larval stage [208], and overexpression of B52 leads to lethality and

various defects such as reduced salivary glands and curled wings depending on the tissue where B52 is overexpressed [209]. B52 shares a high degree of similarity with *Drosophila* dASF, which is one of the many other splicing factors, and therefore may be able to functionally replace B52 [210]. Western blot analysis determining the level of B52 has identified a sudden decrease of B52 through the first instar, after which the level of B52 is only about 15%-20% compared to that in the embryo. The level of B52 remains more or less constant for the rest of the later development [209]. The expression level of B52 is tissue specific, with the highest expression in adult ovaries and lowest in larval intestine [209]. Other body parts including the imaginal disc, the brain and ventral ganglion all have very high B52 levels [209]. Several targets and potential targets of B52 mRNA splicing factor have been identified, this will be discussed with more detail in Chapter 4.

My results suggest that B52 is involved in splicing the mRNAs of Choline Acetyltransferase (ChAT) and vesicular Glutamate uptake protein (vGlut). ChAT is the enzyme that catalyses the biosynthesis of acetylcholine, and vGlut is responsible for the uptake and transportation of glutamate within the synapse. Both proteins are involved in the regulation of neurotransmitters whose functions are critical to functional neuronal circuits.

CHAPTER 2: Materials and Methods

2.1. Fly Stocks

Flies were maintained on standard fly food at 25°C and egg lays were collected on agar juice plate. The following mutant and transgenic fly strains were used:

Table 2.1 Mutant and Transgenic lines used

Name	Reference	Expression pattern / function
elav-Gal4 on X	[211]	All differentiated neurons
elav-Gal4 on III	[212]	All differentiated neurons
Gal4^{Cy27} on III	[213]	dMP2 cells
eagle-Gal4 on III	[214]	NB2-4, NB3-3, NB6-4 and NB7-3 and progenies, including serotonergic neurons
19H09-Gal4 on III	[215]	Subsets of type II neuroblasts and their progenies
Gal4^{V2h}	[216]	Maternal expression
UAS-mCD8-GFP on III	[217]	Tagging cell membrane with GFP
UAS-myr-mRFP on III	[218]	Tagging cell membrane with RFP
UAS-GFP-B52 on III	[219]	B52 overexpression
UAS-Denmark	[220]	Tagging dendrites with mCherry (RFP)
UAS-BBS	[221]	B52 binding sites – antagonising B52 activity
UAS-B52-RNAi (101740)	[208]	Knocking down B52 RNA level
UAS-B52-TRiP-RNAi	TRiP* Bloomington	Knocking down B52 RNA level
UASp-GFP-pav	[222]	Tagging mitotic spindle and interphase nuclei with GFP
UAS-His-YFP	[223]	Tagging Histone with YFP

Jupiter	[224]	Tagging Microtubules with GFP, protein trap strain into the Jupiter gene
p{lacW}B52^{S2249}	[225]	lacW insertion into the open reading frame of *B52* gene
B52*L24	This Study	Deletion of 800bp sequence in the open reading frame of *B52* gene

TRiP – Transgenic RNAi Project Fly Stocks

2.2. Embryos and Larval brain preparation

Fly embryos were collected from agar juice plates by first washing in bleach for 2 minutes, and then rinsed extensively with distilled H_2O into a nylon tissue fixed over the end of a funnel. The embryos were then transferred into a mixture of 100µl of 37% formaldehyde, 400µL of PBS and 500µL heptane for fixation for 20 minutes on shaker. After that, the lower phase of the solution was removed. 1ml of methanol was added and samples were vortexed for 1 minute, followed by washing with methanol 3 times. Samples were stored at -20°C in methanol overnight before further application.

Fly larvae were dissected in 1X PBS and larval brains were fixed in a mixture containing 889µL of 1XPBS, 1µL of 0.5M EGTA, 10µL of 1M $MgCl_2$ and 100µL of 37% formaldehyde for 20 minutes on shaker. After that, the fixation solution was removed and brains were washed 3 times with methanol. Samples were stored at -20°C in methanol overnight before further application.

2.3. RNA extraction and reverse transcription to cDNA

A minimum of 50 fly embryos or 20 larvae were collected without fixation, and frozen at -80°C overnight. RNA was extracted from these samples using the GenElute™ Mammalian Total RNA Miniprep Kit following the protocol provided. 500ul of lysis solution (10µL 2-ME/1ml Lysis Solution) was added to the samples. Samples were fully disrupted with a small pestle, which had

been treated with 70% ethanol and RNaseZap before procedure. The mixture was transferred to a Filtration Column (blue insert) and spun at 12000rpm for 2 minutes to obtain the filtrate. 500µL of 70% ethanol was added to the filtrate, mixed by vortex, and transferred to binding column and spun at 12000rpm for 15 seconds. The flow-through was discarded. 500µL of Wash Solution 1 was added to the column, followed by spinning at 12000rpm for 15 seconds. The column was transferred to a new collection tube. 500µL of Wash Solution 2 was added to the column, followed by spinning at 12000rpm for 15 seconds. The flow-through was discarded. The last step was repeated with an additional spinning at 12000rpm for 2 minutes. The column was transferred to a new collection tube. 50µL of elution solution was added to the column, followed by spinning at 12000rpm for 1 minute. The resulting solution contained the RNA and was stored at -80°C .

The RNA was reverse transcribed to cDNA first by mixing 4µL of RNA sample with 7µL of 3' SMART CDS Primer IIA (12µM) and 7µL of SMART IIA oligonucleotide (12µM) in 46µL of DEPC H_2O, and incubated at 65°C for 2 minutes for annealing. A second mixture containing 20µL of 5X First-Strand Buffer, 2µL of DDT (100mM), 10µL of dNTP (10mM), 2µL of SUPERase In RNase Inhibitors (20 units/µL) and 2µL of SuperScript II Reverse Transcriptase, was added immediately to the previous mixture and incubated at 42°C for 90 minutes. In this way, 1^{st} strand cDNA was created. 2µL of 0.5M EDTA was added in the end to stop the reaction and samples were stored at -20°C . Up to 20µL of samples could be used as template to run a PCR, where 5' PCR Primer II A was used, to generate double-stranded cDNA template for further PCR reactions.

2.4. Genomic DNA extraction

A minimum of 50 fly embryos/20 larvae were collected and frozen at -80°C overnight. Samples were first smashed in 200µL of Buffer A, with an addition of another 200µL of Buffer A. Samples were incubated at 65°C for 30 minutes and then 800µL of Solution B was added and samples

were incubated on ice for at least 10 minutes. Next samples were centrifuged at maximum speed for 15 minutes at 4°C. The supernatant was taken and transferred to a new centrifuge tube. For every 1ml of supernatant transferred, 600µL of isopropanol was added. After mixing, samples were centrifuged at maximum speed for 15 minutes at 4°C. The resulting sample was washed with 70% ethanol and left to air dry for 1 hour. 100µL of distilled H_2O was added to the tube to re-suspend the DNA. An amount between 2µL and 20µL of the resulting DNA was usually used as the genomic DNA template for PCR reaction.

Buffer A
100mM Tris-HCl, pH7.5
100mM EDTA
100mM NaCl
0.5% SDS

Solution B
1 part 5M KAc
2 parts 6M LiCl

2.5. PCR and Primers

The standard PCR reaction and primers used are listed below:

For Expand Long Template PCR system:

a) PCR mixture: 39.5µL of distilled H_2O, 5µL of Buffer No.1, 2µL dNTP(10mM), 1µL of cDNA template, 1µL of forward primer, 1µL of reverse primer, 0.5µL of Expand Long Template Enzyme mix

b) PCR cycle: 94°C for 2 minutes, 35 cycles of[94°C for 10 seconds, 50°C for 30 seconds and 68°C for 0.5kb/min], 68°C for 10 minutes, and Hold at 4°C

All PCR products were run on agarose gel and purified using GenElute™ Gel Extraction Kit (Sigma).

Table 2.2 Primers used

Primer Name	Sequence (5'-3')	Description
B52-SP6	ATTTAGGTGACACTATAGAAGTG GGCTGGCGAGGTCACCTATGC Underlined sequence is SP6	Forward Primer for partial amplification of all *B52* transcripts
B52-T7	TAATACGACTCACTATAGGGAGA CAAATCGGCACATTCAGC Underlined sequence is T7	Reverse Primer for partial amplification of all *B52* transcripts
CG7433-SP6	ATTTAGGTGACACTATAGAAGTG GGTACTCCACCAACGTTGAGC Underlined sequence is SP6	Forward Primer for partial amplification of *CG7433-RA* and *-RB* transcripts
CG7433-T7	TAATACGACTCACTATAGGGAGA CCAAGAAGGTTCCACGACCGC Underlined sequence is T7	Reverse Primer for partial amplification of *CG7433-RA* and *-RB* transcripts
Fwd-Cha Intron 2	CCAAAGAAATGGCTCTCAACG	Forward primer starting from the middle region of Exon 2 of *Cha*
Rev-Cha Intron 2	CAGCAGATACTGATGCAGCCG	Reverse primer ending at the middle region of Exon 3 of *Cha*
Fwd-Cha Intron 4-7	GCAGGACTCGCAGTTCCTGCC	Forward primer starting from the middle region of Exon 4 of *Cha*

Rev-Cha Intron 4-7	CGGATGCGGATTGTAGGAGCA	Reverse primer ending at the middle region of Exon 8 of *Cha*
U400-B52-start	CTTGTAAATTATTTTGTATTGAATTGTATATTTGTAA	Forward primer located 400bp upstream the start of *B52* gene
D400-B52-start	GAGCAGGTGCTATAAAATAGTGAAGTATATATATATAT	Reverse primer located 400bp downstream the start of *B52* gene
Fwd-B52-genomic	TTCACCATCGTCGTAGTTTCC	Forward primer starting from 967bp upstream of the start of *B52* gene (the end of *Hrb87F* is 780bp upstream of *B52* in the genome)
Rev-B52-genomic	CGGCTAGACAAATTCTCCACA	Reverse primer ending at the 1728bp of *B52* gene
Plac 1	CACCCAAGGCTCTGCTCCCACAAT	Forward primer for amplifying *lacW* from 5' terminal region
Pry 2	CTTGCCGACGGGACCACCTTATGTTAT	Forward primer for amplifying *lacW* from 3' terminal region
SMART CDS Primer IIA	AAGCAGTGGTATCAACGCAGAGTACT$_{(30)}$VN (N = A, C, G, or T; V = A, G, or C)	For hybridising with the poly-A tail found on the 3' end of all mature mRNAs

		(1st DNA strand is synthesised downstream this primer)
SMART IIA oligonucleotide	AAGCAGTGGTATCAACGCAGAGTACXXXXX X = undisclosed base	For annealing to the extended cDNA tail added to the 1st DNA strand (above) by SuperScript II Reverse Transcriptase
5' PCR Primer II A	AAGCAGTGGTATCAACGCAGAGT	For targeting the 5' end of SMART IIA oligonucleotide and synthesis of the 2nd (complementary) DNA strand

2.6. Immunohistochemistry staining

Washing cycle = rinse 3 times, wash 5 minutes on shaker, rinse 3 times, wash 5 minutes on shaker and rinse 1 time in PBS-Triton (1X PBS– 0.4% Triton)

Fixed embryos first went through one washing cycle, then blocked with 10% Newborn Calf Serum (NBCS) in PBS-Triton at room temperature for 1 hour. Samples were incubated with primary antibodies (1:1000 if generated in Rabbit, or 1:50 to 1:100 if generated in Mouse) at 4°C overnight. The sample went through one washing cycle, and then incubated with Alexa Fluor secondary antibody (1:300) at room temperature for 2 hours, followed by one washing cycle.

Samples were incubated in 50% glycerol in PBS at room temperature for 15 minutes, and then transferred to 70% glycerol in PBS, stored at 4°C overnight before mounting.

For larval brains, Triton was increased to 1% dissolved in 1x PBS. Samples were incubated with primary antibodies for two nights at 4°C. The rest of the washing and staining steps are the same with that of embryos.

2.7. *in situ* Hybridisation

Preparation of Solutions:

DEPC H_2O
1µL Diethyl Pyrocarbonate in 500ml distilled H_2O
Autoclave

2X Carbonate Buffer (50ml)
120mM Na_2CO_3 (0.636g)
80mM $NaHCO_3$ (0.336g)
Add DEPC H_2O up to 50ml
Adjust pH to 10.2 with NaOH

SSC (20X)
175.3g NaCl
88.2g Sodium Citrate
Add DEPC H_2O up to 1L
Adjust pH to 7.0

3M NaAcetate
12.3g NaAcetate
Add DEPC H_2O up to 50ml
Hybrid Buffer (500ml)
50% Formaldehyde
5X SSC
0.1% Tween-20
Add DEPC H_2O up to 500ml
Adjust pH to 6.5 with HCl

Prehybrid Solution (50ml)
500ul 10mg/ml E.Coli tRNA
50µL 100mg/ml Heparin
Add Hybrid Buffer up to 50ml

TNT Buffer (500ml)
0.1M Tris-Base (6.057g)
0.15M NaCl (4.38g)

0.05% Tween-20 (250µL)
Add DEPC H_2O up to 500ml
Adjust pH to 7.5 with HCl

All solutions were prepared with DEPC H_2O

Probe Preparation:

RNA probes were prepared by mixing the following reagents: 9.5µL of DEPC H_2O, 2µL of Transcription Buffer (Roche), 2µL of 10X DiG Nucleotide Mix (Roche), 4µL of purified PCR product, 2µL of T7 or SP6 Polymerase (Roche), and 0.5µL of RNase inhibitor (Roche). Samples were incubated at 37°C for 2 hours (or at 18°C overnight). 2µL of sample was taken to run on a gel for confirmation (a smear of bands around the appropriate size could be seen). After that, 1µL of DNaseI-RNase Free (NEB) was added and samples were incubated at 37°C for 30 minutes. 31µL of DEPC H_2O and 50µL of 2x Carbonate Buffer were added, and samples were incubated at 60°C for 10 minutes to break down the fragments to 600bp. The reaction was stopped with an addition of 3.5µL of 10% acetic acid and 6.5µL of 3M NaAcetate. 250µL of 100% ethanol was added and samples were incubated at -20°C for at least 1 hour. Samples were centrifuged at maximum speed for 15 minutes and then washed with 70% ethanol. Samples were left to air dry for 1 hour. 20µL of Hybrid Buffer was added to re-suspend the sample. Samples were stored at -20°C for further application. To make the probe, 1µL of sample was diluted in 500µL of Hybrid Buffer.

Day 1

Washing cycle = rinse 3 times, wash 5 minutes on shaker, rinse 3 times, wash 5 minutes on shaker and rinse 1 time in PBS-Tween (1X PBS– 0.4% Tween20)

Fixed embryos first went through one washing cycle, then fixed again in 3.7% formaldehyde for 15 minutes. Next, the sample went through another washing cycle, and then incubated with 0.1% sodium borohydride at room temperature for 10 minutes (the microcentrifuge tube was inverted 3 times during this incubation and the rest of the time the lid was left open). The incubation was stopped with another washing cycle. Samples were then washed in PBS-Tween and Hybrid Buffer mixture (1:1) for 2 minutes, followed by washing in Hybrid buffer for 2 minutes. The supernatant was removed, then 300µL of Prehybrid Solution was added, and samples were incubated at 65°C for 1 hour. The supernatant was removed and 100µL of probe was added, and samples were incubated at 65°C overnight.

Day 2

Samples were washed in Hybrid buffer at 65°C for 2x10 minutes, and then washed in PBS-Tween and Hybrid Buffer mixture (1:1) at 65°C for 2x10 minutes, followed by washing in PBS-Tween at 65°C for 2x10 minutes. After that, samples were washed with PBS-Tween at room temperature for 10 minutes. Samples were blocked in 5% milk powder in PBS-Tween for 20 minutes. The supernatant was removed, and 100µL of 1:100 anti-DIG coupled with HRP was added, and samples were incubated at 4°C overnight.

Day 3

The sample went through one washing cycle. (Optional) PBS-Tween20 was replaced with TNT buffer and the sample went through an additional washing cycle. The supernatant was removed from the sample. 2µL of Fluorescein coupled Tyramide stock solution was dissolved in 100µL of Amplification Diluent (Perkin-Elmer) and added to the sample. Samples were kept in a dark box and incubated at room temperature for 10 minutes. The sample went through one washing cycle. Additional immunohistochemistry staining could be initiated at this stage. Otherwise, samples

were incubated in 50% glycerol in PBS at room temperature for 15 minutes, and then transferred to 70% glycerol in PBS, stored at 4°C overnight before mounting.

2.8. Detection of splicing defects of Cha

Total RNAs were first extracted from either embryos or larval brain of *Elav-Gla4/; ; UAS-BBS/+;*, and control *Elav-Gal4; ; +/+;*, respectively. The RNAs were then reverse transcribed to create cDNA template for PCR. Two pairs of primers were used: Fwd-Cha-Intron 2 and Rev-Cha-Intron 2 to amplify Intron2 and partial sequence of flanking exons; Fwd-Cha-Intron 4-7 and Rev-Cha-Intron 4-7 to amplify Intron 4 to intron 7 and partial sequence of flanking exons; The resulting PCR products were then run on either 1% (Intron 4-7) or 2% (Intron 2) agarose gel. In both cases, the unspliced fragments were gel purified, cloned into PCRII-TOPO vector (Invitrogen), transformed into TOP10 cells (Invitrogen), DNA-purified (Sigma Gen Elute) and sent for sequencing.

2.9. Mapping of *lacW* insertion in *p{lacW}B52^{S2249}*

To map the *lacW* insertion in the *p{lacW}B52^{S2249}* mutant line (Simplified as *p{lacW}B52/TM3*), this fly line was first crossed to *Dr^{Mio}/TM3$^{TwiGAL4;UAS-GFP}$* (simplified as *Dr^{Mio}/TM3$^{Twi-GFP}$*). Progeny with normal eyes and short bristles (*p{lacW}B52/TM3$^{Twi-GFP}$*) were collected and then self-crossed to yield high quantities. Embryos that did not give off green fluorescence under blue light (excitation at 488nm) were selected for genomic DNA extraction. Primers Pry2 and Fwd-B52-genomic (Table 2.2) were used to amplify the corresponding fragment. The PCR product was then gel purified, cloned into PCRII-TOPO vector (Invitrogen), transformed into TOP10 cells (Invitrogen), DNA-purified (Sigma Gen Elute) and sent for sequencing.

2.10. Generation of *B52* null mutant using *Δ2-3, Sb* and *P{lacW}B52/TM3*

To generate mutations in the *B52* gene, we made use of the existing *p{lacW}B52/TM3* mutant line and crossed it to *Δ2-3, Sb/TM6B*^{Ubx}, to yield *p{lacW}B52/Δ2-3, Sb* (phenotypes: speckled eye colour and short bristles). *Δ2-3, Sb* is a construct with a single P element insertion of transposase, which mediates the transposition of all the P elements in the genome of *Drosophila*. In our case, we aimed at removing the P element in *p{lacW}B52*, which was inserted 60bp upstream the start codon of *B52*.

To make sure the genome is not disrupted by genetic recombination, male *p{lacW}B52/Δ2-3, Sb* flies were used to carry out the next cross with female *TM3/TM6B*. After that, male progeny *B52*/TM6B* (phenotypes: white eye colour, normal bristles and humeral) were collected. Confirmation of P element removal was made based on the loss of red eye colour, which was a marker of the previous *p{lacW}* insertion. These flies were referred to as *B52**.

During P-element transposition, endogenous genomic DNA flanking the P-element can also get removed with very low rate, which in our case may cause mutations of the *B52* gene. At this point, each of the male *B52*/TM6B* progeny had the potential of carrying a mutated *B52* gene, and their *B52* gene would be different from one another. The next step was to set up single crosses where each one of the male *B52*/TM6B* flies was allocated in a single vial to mate with three female *TM3/TM6B* flies. Up to 50 individual vials were set up. Both male and female *B52*/TM3* (phenotype: white eye colour and short bristles) progenies were collected from each vial, and they were crossed only to flies of the same genotype collected from the same vial, to yield higher quantities and preserve the genotype. This was followed by a lethality test.

In the next few generations, flies, and therefore the entire line, were trashed if one or more individuals from the same line had got normal bristles, which would indicate that the P element removal was either perfectly accurate and did not cause deletion of *B52* gene, or the inaccurate

removal, if there was any, did not cause a severe functional change of the B52 gene. This is based on previous report that B52 null mutant is homozygous lethal at first- and second-instar larval stages [225].

In the end, only a total of 5 lines passed these phenotypic selections. They were crossed to $Dr^{Mio}/TM3^{Twi\text{-}GFP}$ to yield $B52^{*}/TM3^{Twi\text{-}GFP}$.

2.11. *B52* null mutant – genetic screening

Genomic DNA was extracted from stage 17 embryos collected from the $B52^{*}/TM3^{Twi\text{-}GFP}$ self-cross. The collection was separated into two groups: one with medium level of green fluorescence ($B52^{*}/TM3^{Twi\text{-}GFP}$), and one with no green fluorescence ($B52^{*}/B52^{*}$).

Primers Fwd-B52-genomic and Rev-B52-genomic (Table 2.2) were first used to amplify 2.7kb fragment around original *lacW* insertion site. Then primers -400-B52-start and +400-B52-start (Table 2.2) were used to narrow down the sequence to 800bp. We were able to amplify the corresponding fragments from four of the five $B52^{*}$ mutant lines (L1, L11, L31 and L32). For $B52^{*}$ L24, primers -400-B52-start and Rev-B52-genomic were used to amplify the corresponding fragment, which would give a product of 2.1kb under original circumstance. The resulting PCR fragments were cut out from the gel, cloned into PCRII-TOPO vector (Invitrogen), transformed into TOP10 cells (Invitrogen), and DNA-purified (Sigma Gen Elute). The length of the fragment was checked by EcoRI enzyme restriction.

From the five samples, three of them contained the same length of fragment as that expected from the *p{lacW}B52* genome, indicating in these lines, the removal of P element did not result in major genomic deletions. On the other hand, L24 and L31 each showed different patterns. In L24, 1.5kb was detected instead of the 2.1kb, and in L31, 1.4kb was detected instead of 800bp.

Since deletions are more likely to cause loss of function mutation than duplications or reversions, only L24 was sent for sequencing.

2.12. Microinjection of embryos

Living embryos were dechorionated by hand using double sided tape stuck on a coverslip. Another coverslip was coated with glue (see below) and an area was marked by sticking on a square plastic frame, cut out from transparent self-adhesive book binding foil. Embryos were glued with the ventral side down onto this coverslip. The embryos were desiccated for about 10 minutes (depending on room temperature and humidity). 10 S VOLTALEF oil was applied to cover the embryos one or two minutes after they showed signs of desiccations (a slight wrinkle around the presumptive cephalic furrow). The coverslip was then transferred onto a slide.

For DNA injection, 2hrs old egg lays (25°C) were used. Capillary was inserted into the embryo at a level slightly above the point where the embryo touched the coverslip. For CNTs injection, 1hr or 4hrs egg lay at 25°C were used. For these injection, the capillary was positioned as close as it could be to the coverslip, i.e. at ventral side of the embryo.

The capillary was made with a Micropipette Puller (see below for settings), and then bevelled at an angle of about 20 to 30 degrees. After bevelling, the capillary was washed 3 times in water and 3 times in acetone. During injection, capillary was attached to a 5ml syringe. For loading, 1µL of DNA solution was released onto the 10 S VOLTALEF oil, the capillary tip lowered into the drop and the DNA was sucked into capillary by slowly reversing the syringe piston. Before embryo injection, the pressure inside the syringe and capillary was increased to a level where the solution would just be maintained within the capillary. Upon entry into the embryo, solution diffused freely inside the periplasm without manually applying any pressure to syringe.

<u>Settings of Micropipette Puller (Sutter P-97):</u>

Heat = Ramp – 40

Pull = 40

Velocity = 45

Time = 130

Pressure = 500

Glue Preparation:

Glue was prepared by filling up a 250ml bottle with small fragments of double-sided tape (Scotch) wrapped in a ball shape, together with 125ml of heptane. The bottle was put on a roller overnight at room temperature. The heptane solution which contained the dissolved glue was transferred to a new container.

2.13. Preparation of embryonic fillets in PBS

The glass coverslip containing 4-gut-stage embryos (stage 17, 17hrs to 19hrs old at 25°C) was cut and transferred to a weighing dish, immobilised by applying a small amount of 10 S VOLTALEF oil between it and the dish, and then immersed in PBS-Triton (1x PBS with 0.4% Triton X100). A drawn out pasteur pipette fitted with a rubber bulb was used to rinse off the oil around the embryos. PBS-Triton was first sucked into the pipette, and then released by pointing the tip of the pipette directly to the embryos from above. The pipette was held at an angle of 30 degrees to the surface of the solution in the dish. The tip of the pipette was immersed in the solution at all time to avoid creation of bubbles. While the solution was released by applying pressure to the bulb, the tip of the pipette was moved from the embryo at the bottom to the embryo at the top. This step was repeated several times until most of the Oil 10 S VOLTALEF was removed.

This was followed by three times rinse with PBS (1x). The cut glass coverslip was then transferred to a bigger glass coverslip (22x64mm, wiped with 70% ethanol) surrounded by a silicon ring.The cut coverslip was immobilised by applying a small amount of 10 S VOLTALEF between it and the bigger coverslip, and then immersed in PBS. An injection capillary was used to poke into the dorsal side of the embryo from the posterior all the way to the anterior. The embryo was then lifted up along with the capillary and then gently placed onto the clean, non glue coated glass surface. The van der Waals' force was able to immobilise the ventral nerve cord and the connecting tissue on the glass coverslip. The embryo was cut open from the dorsal side with the capillary and the gut was removed. After gut removal the sides of the embryo were pressed down onto the coverslip. The fixation was done by incubation in 3.7% formaldehyde in PBS for 20 minutes, followed by normal washing and staining steps.

2.14. Transformation

Preparation of Solutions:

Lysis Buffer

10mg/ml lysozyme from chicken egg white in 50% glycerol

STET (50ml)
0.1M NaCL (0.292g)
10mM Tris-HCL (0.06057g)
1mM EDTA (0.01861g)
2.5ml 5% Triton X-100
Add dH_2O up to 50ml
Adjust pH to 8.0

TE Buffer (50ml)
1M Tris (500 µL)
0.5M EDTA (100 µL)
Add dH_2O up to 50ml
Adjust pH to 8.0

LB-Agar medium was prepared as instructed by the manufacturer. For every 500ml of medium, 500µL of 100mg/ml of Carbenicillin was added (final concentration 100ug/ml). 20ul of x-Gal (40mg/ml) was pasted evenly on medium plate and incubated at 37°C for 30 minutes. Invitrogen TOP10 Chemically Competent *E.coli* were taken from -80°C freezer and thawed on ice for 5 minutes. 4µL of DNA sample was mixed gently with 1 µL of Salt Solution (1.2M NaCl, 0.06M $MgCl_2$) and 0.5µL of PCRII-TOPO Vector (Invitrogen TA Cloning Kit). The mixture was left standing at room temperature for 4 minutes, then pipetted into competent cells, gently mixed again and immediately pasted onto the warm LB medium plate. Plates were incubated at 37°C overnight. Single colonies were transferred into 2ml liquid LB medium with Carbenicillin and grown overnight. Cultures were collected with Eppendorf tubes and centrifuged at 6000rpm for 3 minute, supernatant removed. The pellet was resuspended in 350µL STET and 30µL Lysis Buffer, mixed by vortex, and heat shocked at 100 °C for 1 minute. After that, samples were transferred onto ice for cooling for 4 minutes, and then centrifuged at maximum speed for 10 minutes. The pellet was sucked up and discarded by pipetting with a blue tip without disturbing the solution. 1ml isopropanol and 100µL 10M ammonium acetate were added to the solution, vortexed shortly, and stored at -20°C for 20 minutes. Next, samples were centrifuged at maximum speed for 20 minutes at 4°C, supernatant removed. The pellet was washed with 70% ethanol and then left air dry by leaving the tube upside down on a piece of tissue at room temperature for a minimum of one hour. 30µL TE Buffer was added, and samples were stored at -20°C overnight before further application.

Plasmids with an insertion was identified by EcoR1 digest. For sequencing, positive colonies were grown overnight in 100ml LB Medium with Carbenicillin before extraction of the DNA using Sigma GenElute™ Midiprep.

2.15. Sequencing

All sequencing was done by Source BioScience LifeSciences.

2.16. Time lapse recording of larval locomotion

2hrs old embryos were prepared as described in 2.12 but without desiccation. After applying Oil 10 S VOLTALEF, the embryos were kept at 25°C for 10.5hrs until their trachea were filled. HCImage (Hamamatsu) was used for time lapse recording. During recording, embryos were kept in a dark room with temperature set at 20°C. The intensity of light projected to the embryos was set at minimum level which was just enough for the camera to recognise the subject. Time interval between each capture was set at 5 second for a recording period of 2 hours or more.

2.17. Confocal Imaging

Fixed or live samples were recorded using a Zeiss LSM710. For time lapse recording of living embryos, the time interval was set to be 30 seconds and the space interval for Z-stack was 1µm for a total of three Z levels. Scanning was set to bi-directional.

CHAPTER 3: From MP2 Neurons to *B52* Gene – Cell Morphology

3.1. Introduction

In *Drosophila*, a group of four neurons are known as the longitudinal pioneer neurons in each segment, including two descending neurons: dMP2 and MP1, and two ascending neurons: vMP2 and pCC. These pioneer neurons send out their axons simultaneously. The two descending neurons first send out their axons laterally as a bundle to reach the commissure. The axons then separate from each other and project posteriorly. In contrast, the two ascending neurons project axons directly to the anterior. It has been shown that dMP2 also has an anterior axon which is shorter than its posterior axon [226].

MP2 precursors first emerge in stage 8 *Drosophila* embryos and are located as a pair in each segment of the VNC [227]. The MP2 precursors divide asymmetrically once to give rise to vMP2 and dMP2. vMP2 always locate anterior to dMP2 in each segment. In later stages (after embryonic stage 16), the 18 dMP2 neurons located in the anterior sections (LB - A5) of the VNC are eliminated, while the 6 dMP2 neurons in the posterior sections (A6-A8) are maintained throughout larval stages [228]. By stage 13, each of the two daughter MP2 cells display distinct axon trajectories. vMP2 extends its axon anteriorly along with the axon from the pCC cell, whereas dMP2 extends posteriorly and fasciculates with the axon of the MP1 neuron [229]. Initially, both vMP2 and dMP2 neurons were believed to be interneurons since they extend their axons to pioneer the longitudinal tract [230]. However, using membrane reporter *dMP2-Gal4/UAS-myc-EGFP*, the axon of dMP2 was found to exit the VNC and innervate the hindgut in late stage embryos. This is further confirmed by injecting DiI into the hindgut where the dye backfilled to segments A6-8 of stage 17 embryo. Therefore dMP2 is in fact a motor neuron [228]. In contrast to it, the axon of vMP2 (vMP2/pCC) stays in the VNC and making light contact with

the axon of dMP2 (dMP2/MP1) originated from the contiguous segment. Axons of vMP2 and dMP2 remain fasciculated until stage 17, during which they defasciculate from each other and continues to run along the longitudinal axons in a more ventral (vMP2) or dorsal (dMP2) plane [231].

The difference in the projection patterns between vMP2 and dMP2 suggests the two neurons may contribute to different neuronal circuits. The choosing of neuronal circuits involves the selection of several important factors, such as cell morphology, specification of neurotransmitter, and synaptic formation and maintenance.

In order to complete the understanding of the regulatory mechanisms involved in these processes, genes which were differentially expressed between vMP2 and dMP2 were identified. This was achieved by performing single cell transcriptome analysis of vMP2 and dMP2. In three independent experiments, the single cell transcriptome was isolated from each of the two sibling neurons in stage 17 *Drosophila* embryos and compared on three different microarrays (Bossing, Unpublished).

Of 2631 transcripts compared, seven transcripts were up-regulated by two times at least in dMP2. The primary candidate gene chosen was *B52*, whose expression level was over 44 times higher in dMP2. Due to the late embryonic stage selected for transcriptional analysis, *B52* might play a role in the selection of synaptic partners before synaptogenesis takes place and/or maintenance of newly formed synapses. Since synaptic plasticity is subject to change from time to time, the contribution of *B52* might still be needed. From all RNA targets identified for B52, none have been shown to be involved in synaptogenesis or neurotransmission [208, 219, 232-235].

Therefore, the first question addressed was the possible involvement of *B52* in the establishment of cell identity, morphological structure and function (this Chapter). Secondly, we

also examined, whether *B52* contributes to the selection of neurotransmitter (Chapter 5), which ultimately could affect larval behaviour (Chapter 6). All these analyses were carried out using *B52* loss/gain of function and *B52* mutant embryos or larvae (Chapter 4).

3.2. Results

3.2.1. Genes that are differently expressed between vMP2 and dMP2

From microarray analysis of single cell transcriptomes between vMP2 and dMP2, a group of seven genes were found to be differently expressed between the two sibling neurons (Table. 3.2.1). Among these genes, the expression level of *B52* was 44.94 times higher in dMP2 than that in vMP2.

Table 3.1 Genes differently expressed between vMP2 and dMP2

	B52	***CG7433***	***CG31855***	***Fis1***	***wrapper***	***DMAP1***	***trx***
vMP2	1	1	1	1	1	1	1
dMP2	44.94	15.56	19.29	3.14	66.72	0.09	0.14

* "1" represents the standard expression level of that specific gene in vMP2 and is not an indication of quantity.

3.2.2. Expression pattern of B52 and CG7433

In order to get an idea of what roles the candidate genes play in terms of regulating neuronal network formation and function, *in situ* hybridisation was performed with the view to reveal the expression pattern of *B52* and *CG7433*. Our data indicate that *B52* is expressed ubiquitously in the embryo from stage 11 onward, while *CG7433* is expressed along the connectives (Fig. 3.0).

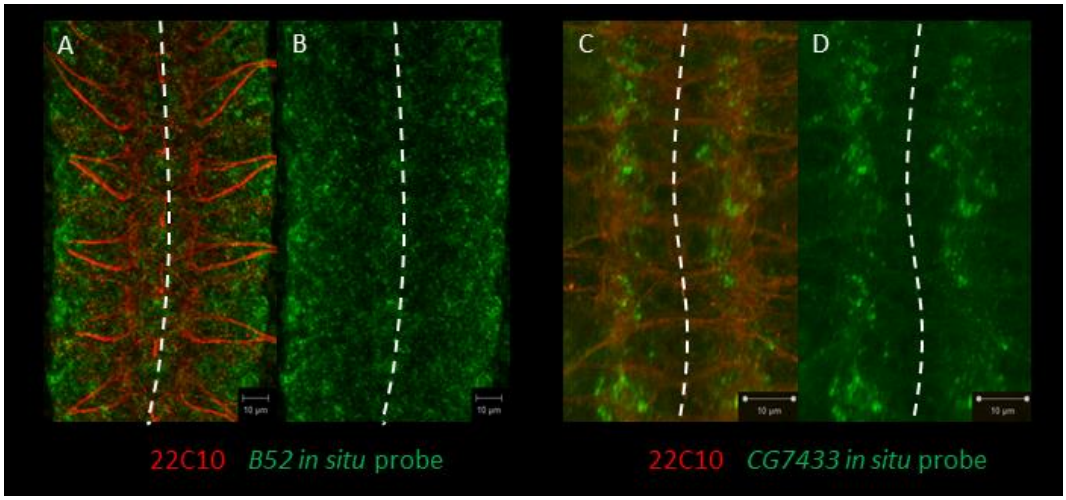

Figure 3.0 in situ hybridisation of B52 and CG7433 in the CNS of stage 17 WT embryos.

CNS of stage 17 WT embryo (n=10), horizontal views, anterior up. Bar = 10µm. Dotted line indicates the location of midline. (A-B) Axons are labelled with 22C10 antibody in red, and *B52 in situ* probe in green. *B52* is expressed ubiquitously, but the expression strength varies from cell to cell. (C-D) Axons are labelled with 22C10 antibody in red, and *CG7433 in situ* probe in green. *CG7433* RNA is localised along the connectives.

3.2.3. Manipulation of B52 activity by introducing B52 Binding Sites through Gal4/UAS system

To study the function of B52, the Gal4/UAS system was used to manipulate the level of B52 in the CNS of *Drosophila* embryos and larvae. The Gal4/UAS system consists of two separate functional units. In one unit the coding sequence of the Gal4 transcription factor was fused downstream of an enhancer which allows for the expression of Gal4 in selected tissues. In the second unit, the sequence of a target gene is expressed from a *UAS* sequence (upstream activation sequence) to which Gal4 binds. Hence, only cells containing both units express the target gene due to its up-regulation by the Gal4 transcription factor [236].

The RNA aptamer B52 Binding Sites (BBS) were introduced to different tissues and developmental stages with the use of different *Gal4* lines. BBS is an artificial construct. A single unit of BBS consists of five high affinity binding sites found among different B52 target RNAs, with each of them forming a hairpin loop structure, and folded in a specific way to have the

formation of a pentameric structure. A fully functional BBS consist of 12 of this pentameric units with head-to-tail connection (Fig. 3.1). It has been shown that the presence of BBS can inhibit the activity of B52 both *in vitro* and *in vivo* due to competition with the endogenous BBS sites [221, 237].

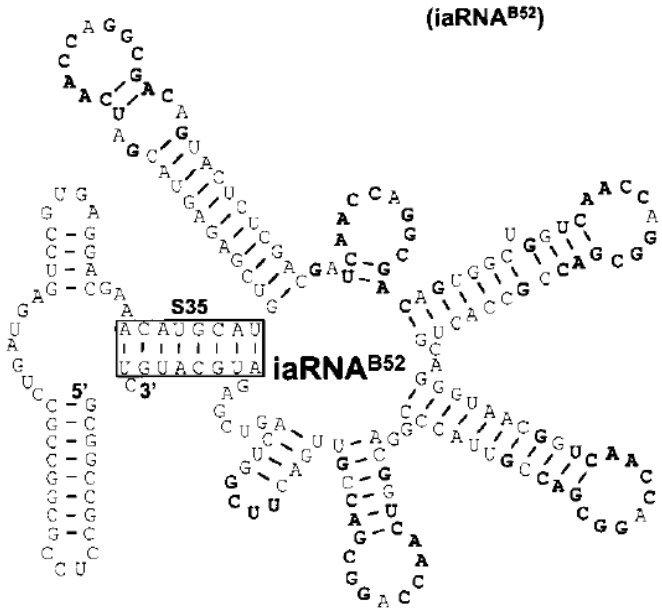

Figure. 3.1 Single unit of B52 Binding Sites

A single unit of BBS consists of five high affinity binding sites found among different B52 target RNAs, with each of them forming a hairpin loop structure, and folded in a specific way to have the formation of a pentameric structure. A fully functional BBS consist of 12 of this pentameric units with head-to-tail connection. Figure taken from Shi et al., 1999.

The choice of Gal4 lines (enhancers) specifies when and where the target gene can be expressed. In *Drosophila*, genetic manipulation is often achieved by bring two different transgenic lines together through fly crossing, and then looking for the phenotypes in the next generation. For example, in one of my experiments, female flies carrying the *elavGal4* line and male flies carrying the *UAS-BBS* line were crossed to each other, and therefore leading to their progenies expressing the Gal4 protein in all differentiated neurons, which is driven by the *elav* enhancer. The Gal4 protein in turn activates the *UAS*, triggering the expression of BBS. The presence of BBS serves as a competitor that saturates the available B52 protein by binding to the RNA recognition

mortif (RRM), and therefore preventing B52 from interacting with its endogenous RNA targets. This is equivalent to inhibiting B52 activity. The results below illustrate the outcomes of introducing BBS to various tissue and at different developmental stages using a selection of *Gal4* lines.

3.2.4. Expression of BBS does not cause defects in axon projection pattern of dMP2 cell

Since axon retraction and alternation of axon trajectory could still occur after the first synaptic contact is made, whether B52 has a role in mediating morphology and possibly synaptic targets of MP2 neurons was examined. *UAS-mCD8-GFP* DNA was injected into *UAS-BBS/+; $Gal4^{Cy27}$/+* embryos to label single dMP2 cells and its axon. The same injection was performed in *$Gal4^{Cy27}$* as control. Anti-Odd staining was performed to identify dMP2 neurons. I compared the projection pattern and length of the dMP2 axon between *$Gal4^{Cy27}$* control and *UAS-BBS/+; $Gal4^{Cy27}$/+* embryos.

In *$Gal4^{Cy27}$*, the axon of dMP2 bifurcates as soon as it extends from the neuron body, projecting both anteriorly and posteriorly. We find no differences in the branching pattern or general axonal course. Yet, we observed a consistent increase in length of the posterior dMP2 branch by an average of 46.41µm in embryos expressing UAS-BBS (n=9, Fig. 3.2).

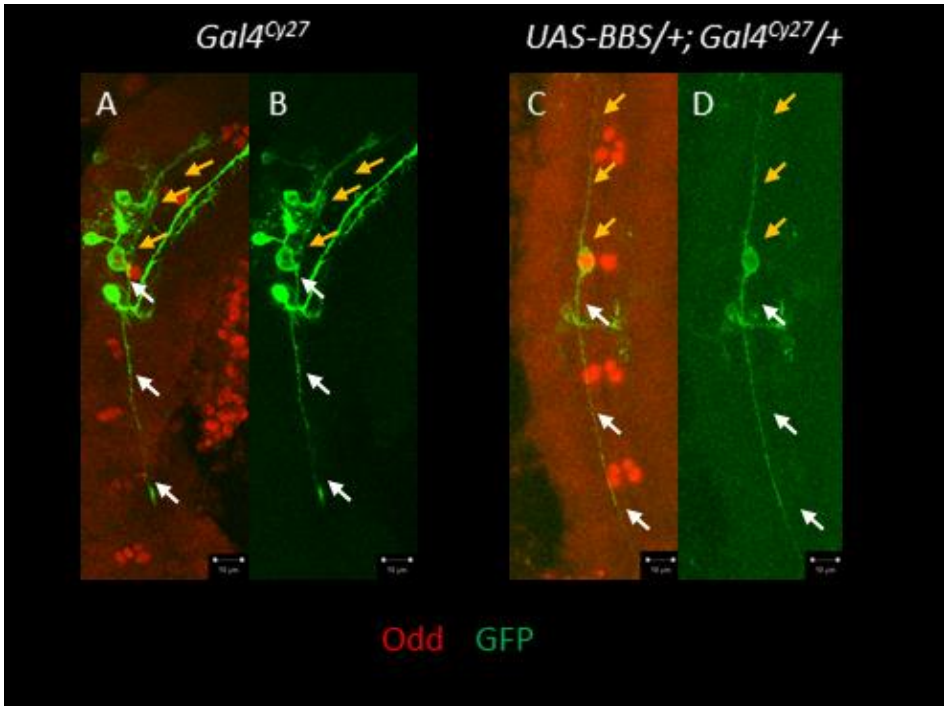

Figure. 3.2a Microinjection of *UAS-mCD8-GFP* DNA reveals the projection of single MP2 neuron in stage 17 embryonic CNS.

The nuclei of dMP2 and MP1 neurons are labelled with Odd antibody in red. Axon and cell body of MP2 neurons are labelled with GFP in green. Horizontal views, anterior up. Bar = 10µm. Yellow arrows indicate anterior axon, white arrows indicate posterior axon. (A-B) *Gal4^{Cy27}* control (n=9) and (C-D) *UAS-BBS/+; Gal4^{Cy27}/+* (n=9). The length of anterior axon is always shorter than posterior axon. The length of posterior axon is longer in *UAS-BBS/+; Gal4^{Cy27}/+* than that in *Gal4^{Cy27}* control.

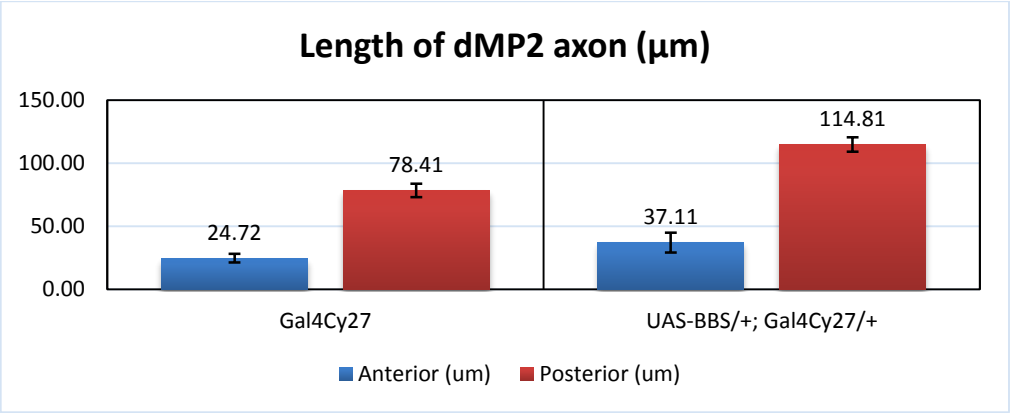

Figure. 3.2b Length of dMP2 axons.

Gal4^{Cy27} on the left and *UAS-BBS/+; Gal4^{Cy27}/+* on the right. Anterior axon is represented by blue and posterior axon by red. The difference in the length of anterior axon between *Gal4^{Cy27}* and *UAS-BBS/+; Gal4^{Cy27}/+* is not significant. In *UAS-BBS/+; Gal4^{Cy27}/+*, the posterior axon is much longer than that in *Gal4^{Cy27}* control.

3.2.5. Expression of BBS in eagle-Gal4 (eagleGal4) does not induce morphological change

The possible role of B52 in regulating cell morphology was further examined in a subset of neurons derived from NB2-4, NB3-3, NB6-4 and NB7-3 [214]. *BBS* was introduced by generating *UAS-BBS/ +; egGal4, UAS-mCD8-GFP/ +*, and *egGal4, UAS-mCD8-GFP* was used as control.

In stage 17 embryo, there was no obvious changes in cell morphology, number of neurons and projection patterns of axons between *egGal4, UAS-mCD8-GFP* control and *UAS-BBS/ +; egGal4, UAS-mCD8-GFP/ +* (Fig. 3.3).

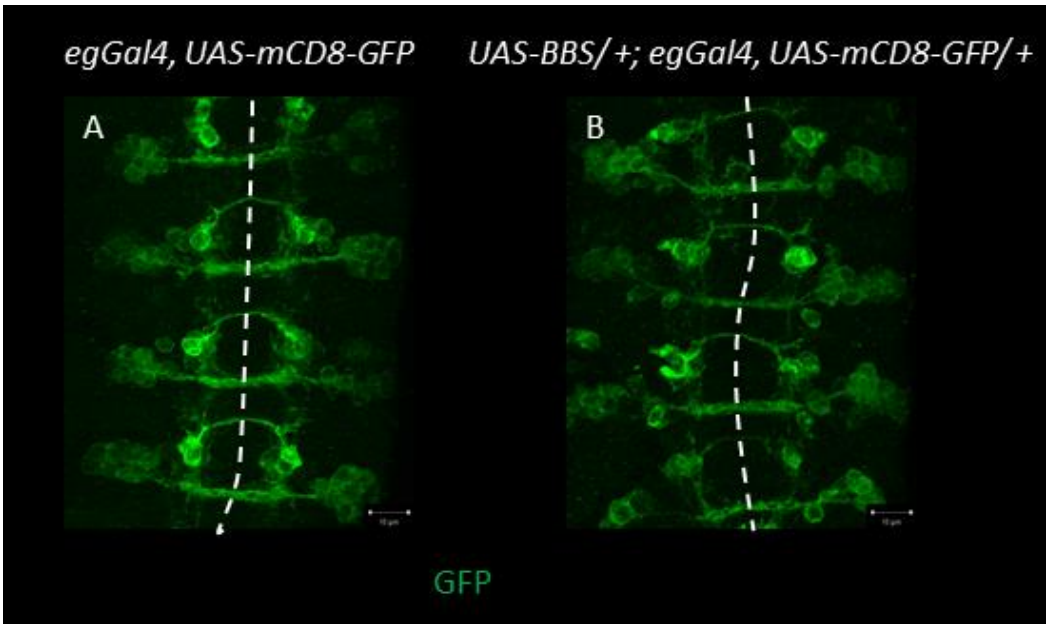

Figure. 3.3 GFP staining in neuronal subsets in stage 17 embryonic CNS.

GFP in green. Horizontal views, anterior to the left. Bar = 10µm. Dotted line indicates the location of midline. (A) *egGal4, UAS-mCD8-GFP* control (n=23) and (B) *UAS-BBS/ +; egGal4, UAS-mCD8-GFP/ +* (n=18). Locations and projection patterns of neurons are not different between *egGal4, UAS-mCD8-GFP* control and *UAS-BBS/ +; egGal4, UAS-mCD8-GFP/ +*.

3.2.6. Morphology and projection pattern of dMP2 dendrites do not show obvious defects when BBS is over-expressed

In addition to axons, dendrites also play an important part in mediating the communication process between pre- and post-synaptic sites during synaptic formation. To find out if B52 is involved in the regulation of dendritic development and guidance in dMP2 neurons, comparison was made between *Gal4^{Cy27}, UAS-Denmark/+; UAS-BBS/+* and the control *Gal4^{Cy27}, UAS-Denmark*. In these lines, dendrites of dMP2 cells were labelled with RFP, which allow us to see if the presence of *BBS* causes any defects in the dendritic network of dMP2 cells in stage 17 embryo.

I observed some weakening in the expression of UAS-Denmark along the dendrites of *Gal4^{Cy27}, UAS-Denmark/+; UAS-BBS/+*. This weakening in red fluorescence is likely to be caused by the use of one *Gal4* driver to activate two *UAS* constructs, which may lead to reduced *UAS* expression. The general weakness in expression is most likely not due to dendritic defects. Despite that, dendrites in *Gal4^{Cy27}, UAS-Denmark/+; UAS-BBS/+* were restricted to their supposed locations as those in *Gal4^{Cy27}, UAS-Denmark* control. No misarborisation was observed (Fig. 3.4).

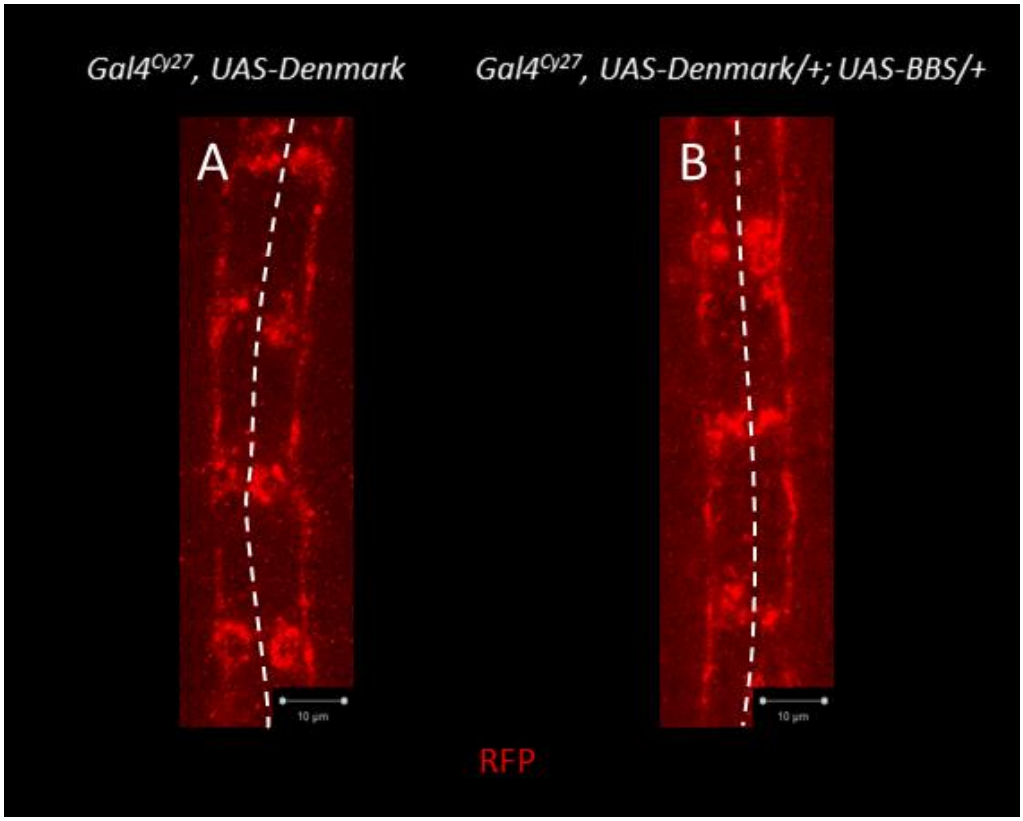

Figure 3.4 Dendrites of dMP2 cells in stage 17 embryonic CNS.

Dendrites and cell body of dMP2 neurons are labelled with RFP in red. Horizontal views, anterior up. 1 Bar = 10µm. Dotted line indicates the location of midline. (A) *Gal4^{Cy27}, UAS-Denmark* control (n=6) and (B) *Gal4^{Cy27}, UAS-Denmark/+; UAS-BBS/+* (n=15). There are obvious gaps along the dendritic path of *Gal4^{Cy27}, UAS-Denmark/+; UAS-BBS/+* and also *Gal4^{Cy27}, UAS-Denmark/+*. Most of the staining is not limited to dendrites but is along the axons. The dendrites of dMP2 axons are not separate from the axon (see spines along axon in Fig. 3.2A).

3.2.7. Morphology and projection patterns of 19H09Gal4 (subsets of type II neuroblasts and progenies) dendrites are not affected by the presence of BBS or overexpression of B52

To find out if B52 is involved in regulation of dendritic development and guidance in larval stage, comparison was made among *19H09Gal4, UAS-myrm::RFP/UAS-BBS*, *19H09Gal4, UAS-myrm::RFP/UAS-GFP-B52* and the *19H09Gal4, UAS-myrm::RFP* control, to see if the presence of *BBS* or excessive *B52* can cause any defects in the dendritic network of single motorneuron in the abdominal segment 4-8, labelled by the *19H09Gal4* line, 84hrs larval brain.

There were no significant changes in the morphology of *19H09Gal4* neurons or defects in the projection patterns of dendrites in either *19H09Gal4, UAS-myrm::RFP/UAS-BBS* or *19H09Gal4, UAS-myrm::RFP/UAS-GFP-B52*, when compared with *19H09Gal4, UAS-myrm::RFP* control (Fig. 3.5).

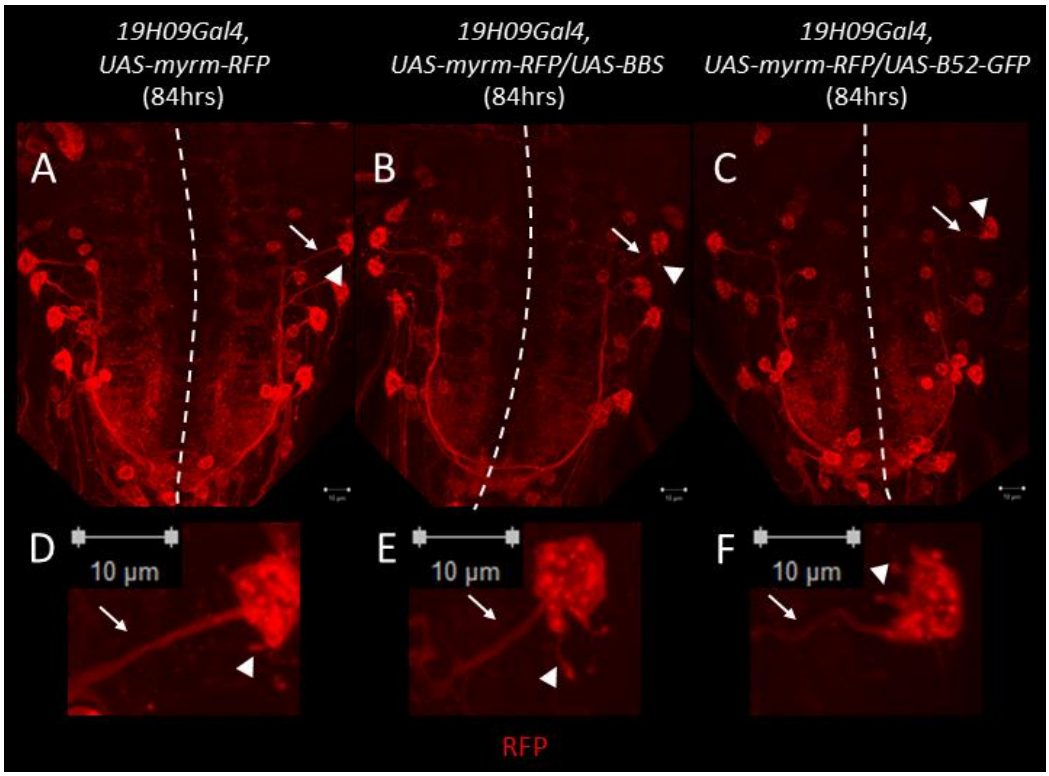

Figure 3.5 Dendrites of 19H09Gal4 neurons in 72hrs larval brains.

RFP in red. Horizontal views, anterior up. Bar = 10µm. Dotted line indicates the location of midline. Arrowheads label dendrites and arrows label axon. (A) *19H09Gal4, UAS-myrm::RFP* Control (n=8), (B) *19H09Gal4, UAS-myrm::RFP/UAS-BBS* (n=8) and (C) *19H09Gal4, UAS-myrm::RFP/UAS-GFP-B52* (n=6). Close-up of single motor neuron of (D) *19H09Gal4, UAS-myrm::RFP* Control, (E) *19H09Gal4, UAS-myrm::RFP/UAS-BBS*, and (F) *19H09Gal4, UAS-myrm::RFP/UAS-GFP-B52*. *19H09Gal4* labels motor neurons located near the lateral sides of the abdominal segment of larval brain. There are no significant differences in dendritic morphology or projection patterns among the three lines.

3.2.8. Reducing B52 function by expression of BBS in all neurons does not affect axon fasciculation, glial cell localisation or muscle innervation

Since glial cells have been shown to play a role in both guidance of axons and synapse formation [126, 130-134], distribution of these cells in the CNS and muscle field was examined by performing anti-repo staining in stage 17 embryo of *elavGal4* control and *UAS-BBS/+; elavGal4/+*. It has been shown that in addition to neurons, Elav protein is expressed in the glial lineage of the longitudinal glioblast (LGB), in *Drosophila* embryos. LGB is functionally similar to a neuroblast, but gives rise to glial cells only. Therefore the *elavGal4* line not only serves to drive expression of target genes in postmitotic neurons, but also in neural progenitor cells and nearly all embryonic glial cells [238]. However, the expression of *Elav* is rather transient in the LGB. Also, DiI labelling, which is the injection of membrane diffusible fluorescent lipophilic cationic indocarbocyanine dye to label target cell, shows each LGB gives rise to 7 to 10 progenies [239] out of 23 glial cells per segment [240] by the end of embryogenesis, which is less than a half of all glia. It is therefore very unlikely that the short and weak expression of *BBS* in these glia will have any phenotypes at all.

Fasciculation is a key feature contributing to the guidance of longitudinal axons. This process provides the framework for the subsequent pathfinding of newly emerging axons via cell adhesion mediated by FasII [241]. Fasciculation of axons originating from multiple neurons is critical in axon guidance towards their target. To test if fasiciculation is affected by the presence of *BBS*, anti-FasII staining was also performed.

There was no obvious mislocalisation or morphological changes of these glial cells between *elavGal4* control and *UAS-BBS/+; elavGal4/+*. The glial cells were found in their normal positions around the axons. This is expected because the expression of BBS in glia cells is too short plus only a sub population of glia cells are affected by the *elavGal4* line to cause serious phenotypic changes in this case. Also, compared to the *elavGal4* control, there was no obvious

misfasciculation or thinning of axon bundles observed in the CNS or any abnormal muscle innervation in *UAS-BBS/+; elavGal4/+* (Fig. 3.6).

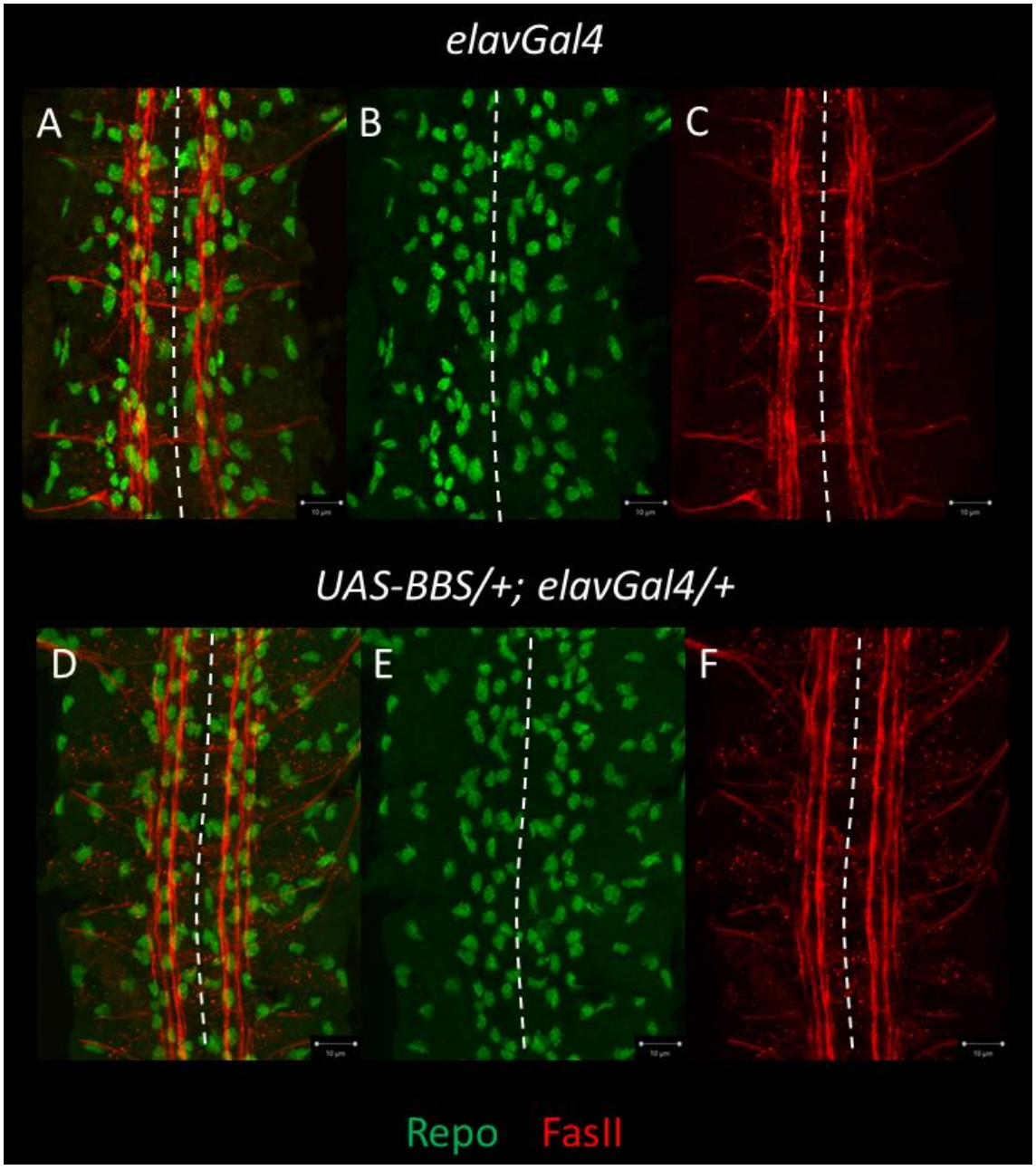

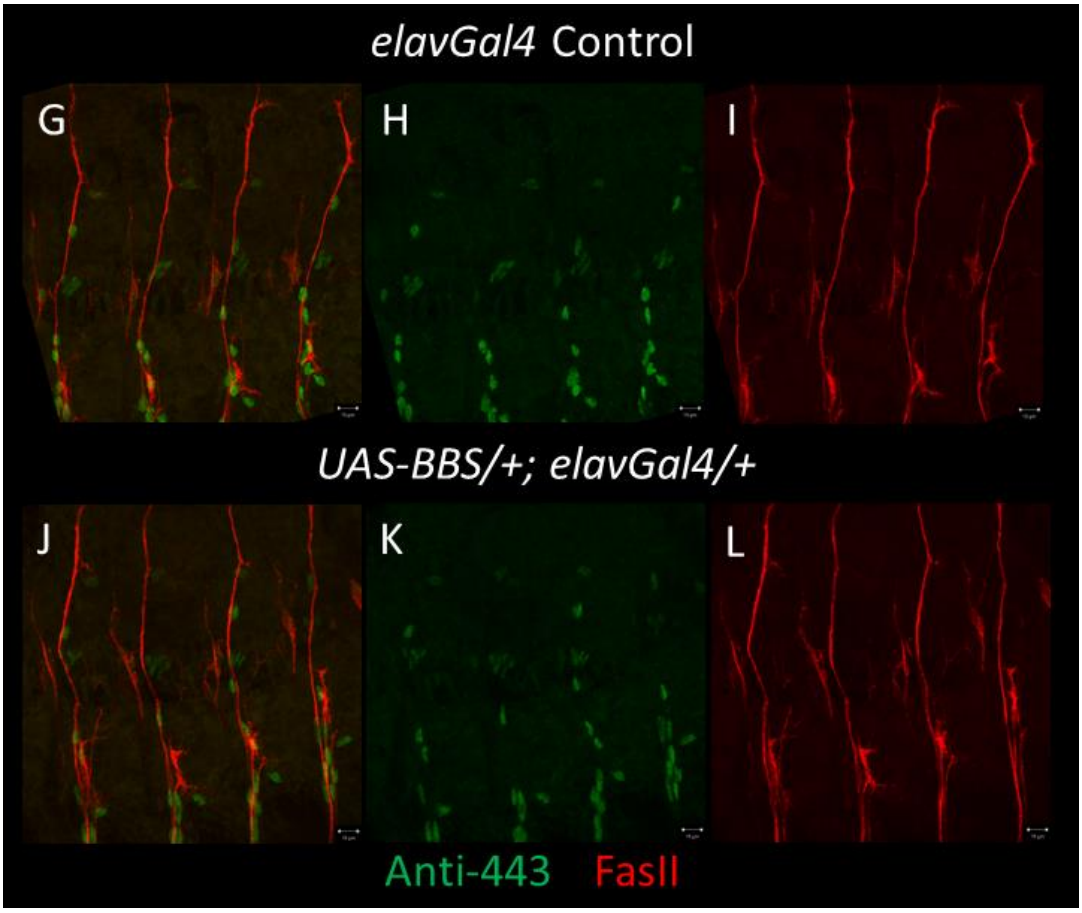

Figure. 3.6 Repo and FasII staining of stage 17 embryonic CNS and peripheral motor neuron axons. FasII in red and Repo in green. Horizontal views, anterior to the left. Bar = 10µm. Dotted line indicates the location of midline. (A-C) CNS of *elavGal4* control (n=10) and (D-F) *UAS-BBS/+; elavGal4/+* (n=7). (G-I) Muscle innervation of *elavGal4* control (n=20) and (J-L) *UAS-BBS/+; elavGal4/+* (n=20). There are no obvious differences in the distribution of glial cells between *elavGal4* and *UAS-BBS/+; elavGal4/+*. Patterns of innervations and branching of motorneurons also appear to be normal in *UAS-BBS/+; elavGal4/+*.

3.2.9. No defects in fasciculation in 48hrs larval brain of p{lacW}B52 homozygous mutants

Because *B52* is expressed throughout the whole life cycle of *Drosophila*, fasciculation was examined also in 48hrs larval brain of *p{lacW}B52* homozygous mutant. Heterozygous mutant *p{lacW}B52/TM3*$^{Twi\text{-}GFP}$ was used as control. The *p{lacW}B52* line was first created by Ring and Lis (1994). It contains a P-element transposase-*lacZ* fusion inserted in the open reading frame of

B52 gene. According to the authors, *B52* RNA was not detected in the total RNA extraction of 2nd instar homozygous *p{lacW}*B52, and anti-B52 staining showed B52 protein was completely gone in the nuclei of 2nd instar larvae homozygous *p{lacW}*B52 [209]. However, I did not re-confirm the RNA or protein level of B52 before doing the assays below. Because more than two decades have passed since the line was first created, the mutated *B52* gene may have already been selected out. Therefore, the expression level of B52 in the *p{lacW}B52* line may not be different from that of the wild type.

Compared to the heterozygous control, there is no obvious defect in *p{lacW}B52* homozygous mutant in terms of the distribution of fasciclin2. However, the intensity of FasII staining is stronger in *p{lacW}B52* homozygous mutant (Fig. 3.7).

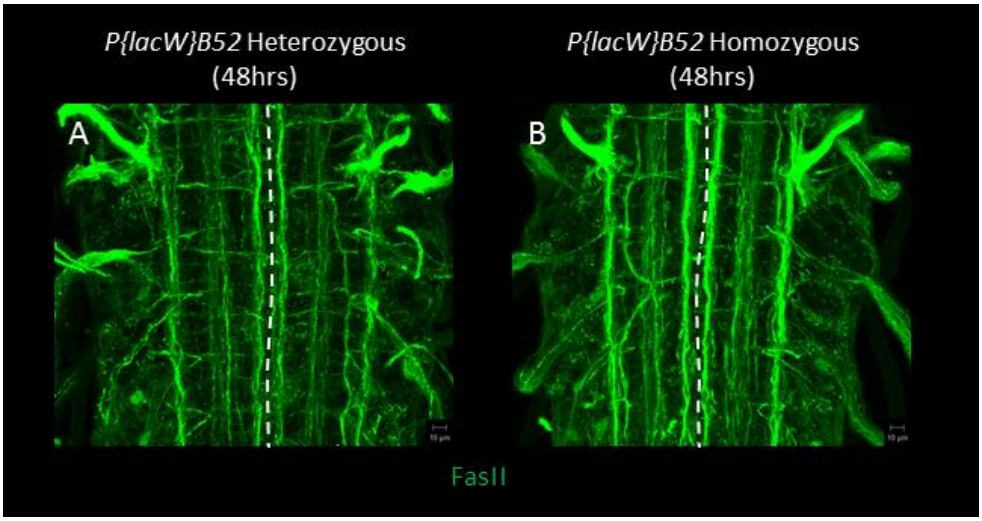

Figure. 3.7 FasII staining of 48hrs larval brains.

FasII in green. Horizontal views, anterior up. Bar = 10µm. Dotted line indicates the location of midline. (A) *p{lacW}B52/TM3*$^{Twi\text{-}GFP}$ control (n=9) and (B) *p{lacW}B52* homozygous mutant (n=10). Apart from a slight elevation of FasII signal in *p{lacW}B52* homozygous mutant, there is no significant difference in fasciculation of axons between *p{lacW}B52/TM3*$^{Twi\text{-}GFP}$ control and *p{lacW}B52* homozygous mutant.

3.2.10. No defects in fasciculation in 72hrs larval brain where B52 is overexpressed maternally

Fasciculation was further examined in 72hrs larval brain of *Gal4^{V2h}/+; ; UAS-GFP-B52/+*, where expression of *B52* was elevated until embryonic stage 14 [216]. *Gal4^{V2h}* was used as control. This is to test whether over-expression of *B52* would cause any problem with embryos hatching and developing into mature larvae.

Compared to *Gal4^{V2h}* control, distribution and quantity of fasciculation in *Gal4^{V2h}/+; ; UAS-GFP-B52/+* are normal (Fig. 3.8).

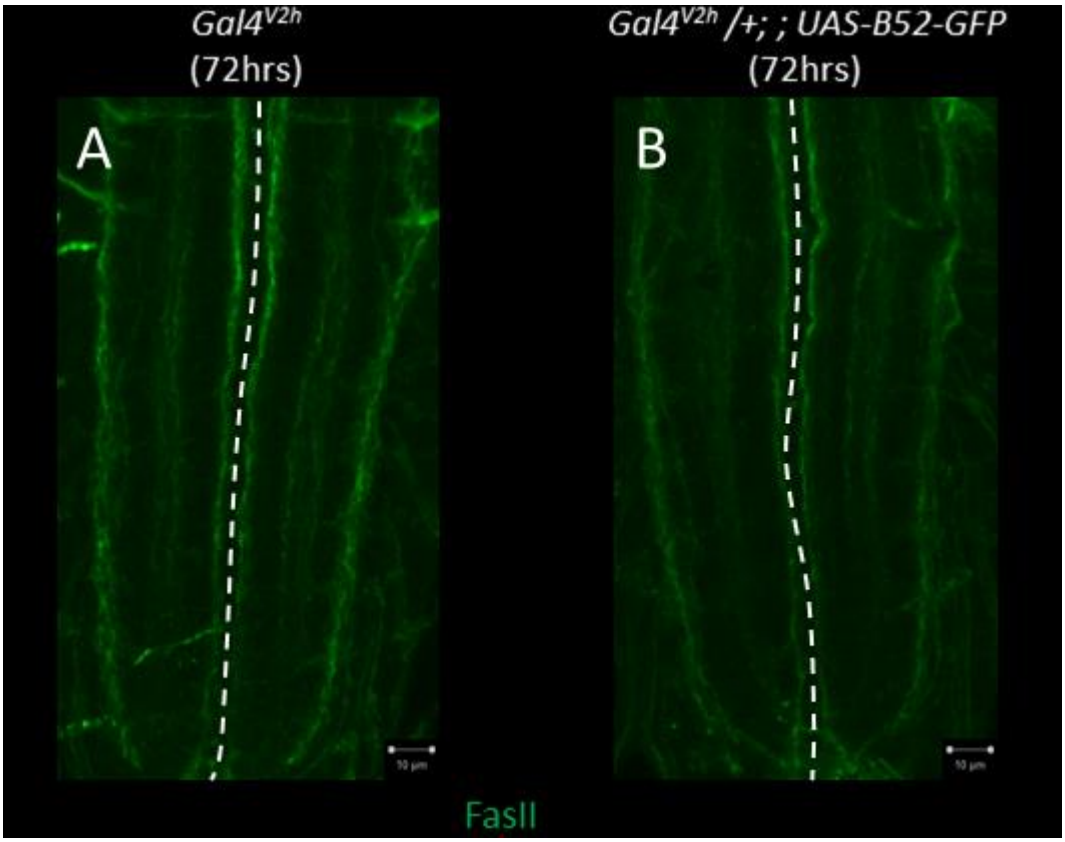

Figure. 3.8 FasII staining of 72hrs larval brains.

FasII in green and FasII in red. Horizontal views, anterior to the left. Bar = 10µm. Dotted line indicates the location of midline. (A) *Gal4^{V2h}* control (n=3) and (B) *Gal4^{V2h} /+; ; UAS-GFP-B52* (n=3). There is no obvious defect in fasciculation of axons between *Gal4^{V2h} /+; ; UAS-GFP-B52* and *Gal4^{V2h}* control.

3.2.11. No defects in fasciculation in 72hrs larval brain where B52-RNAi is induced maternally

Fasciculation was examined in 72hrs larval brain of *Gal4^{V2h}/+; ; UAS-B52-TRiP-RNAi/+*. *Gal4^{V2h}* was used as control.

Compared to *Gal4^{V2h}* control, fasciculation in *Gal4^{V2h}/+; ; UAS-B52-TRiP-RNAi/+* is normal (Fig. 3.9).

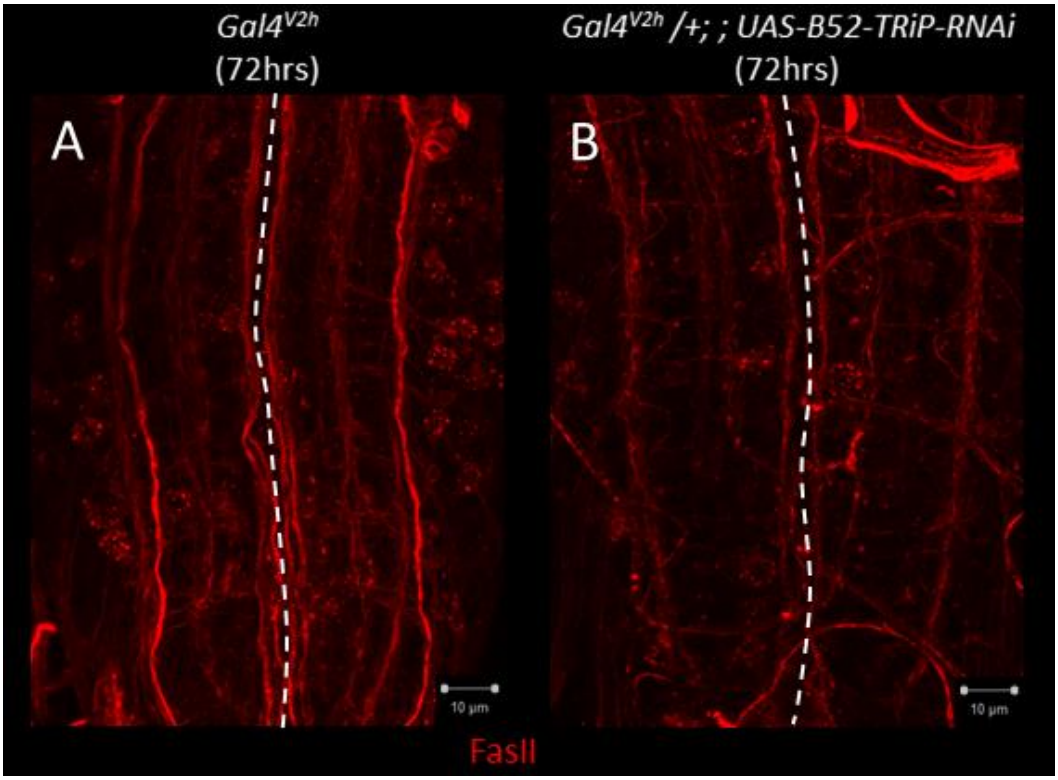

Figure. 3.9 FasII staining of 72hrs larval brains.

FasII in red. Horizontal views, anterior to the left. Bar = 10µm. Dotted line indicates the location of midline. (A) *Gal4^{V2h}* control (n=3) and (B) *Gal4^{V2h}/+; ; UAS-B52-TRiP-RNAi/+* (n=3). There is no obvious fasciculation defect in *Gal4^{V2h} /+; ; UAS-B52-TRiP-RNAi* compared to *Gal4^{V2h}* control.

3.2.12. No defects in fasciculation in 24hrs larval brain of B52*L24 homozygous mutant embryos

Fasciculation was examined in 24hrs larval brain of *B52*L24* homozygous mutant. *B52*L24* heterozygous mutant was used as control.

Compared to *B52*L24* heterozygous controls, there is no obvious defect in fasciculation of *B52*L24* homozygous mutants (Fig. 3.10).

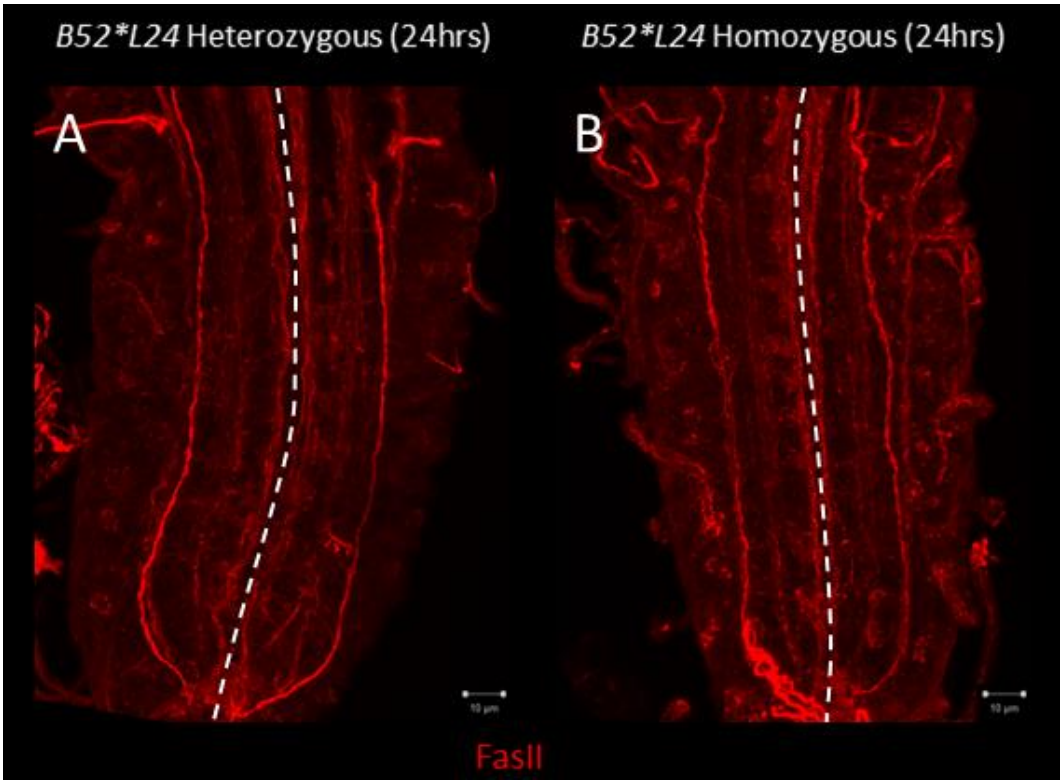

Figure. 3.10 FasII staining of 24hrs larval brains.

FasII in red. Horizontal views, anterior up. Bar = 10µm. Dotted line indicates the location of midline. (A) *B52*L24* heterozygous control (n=3) and (B) *B52*L24* homozygous mutants (n=3). Compared to *B52*L24* heterozygous control, there is no obvious defect in fasciculation in *B52*L24* homozygous mutants.

3.3. Discussion

3.3.1. B52 has no effect on cell determination

It has previously been shown that Odd-skipped (Odd) is expressed in dMP2 and MP1 from stage 11 in the embryo [242]. Therefore, anti-Odd was used to detect the distribution and level of the corresponding cell marker protein in *UAS-BBS/+; Gal4^{Cy27}/+*. Antagonising B52 activity in the dMP2 cell did not trigger any change of Odd expression. All dMP2 and MP1 neurons in *UAS-BBS/+; Gal4^{Cy27}/+* reside in exactly the same locations as their control counterparts. Also, single cell labelling showed that the projection trajectories of both anterior and posterior axons of dMP2 were not affected in *UAS-BBS/+; Gal4^{Cy27}/+*.

3.3.2. Overshooting axon of dMP2 neuron in UAS-BBS/+; Gal4^{Cy27}/+

In the single cell labelling experiment, overshooting of the posterior axon of dMP2 was observed in *UAS-BBS/+; Gal4^{Cy27}/+*, indicating down-regulation of B52 activity in dMP2 neurons leads to defects in axon extension.

B52 has been shown, by both microarray analysis and genomic SELEX, to target *lola*, a transcription factor gene [219, 234]. Seeger et al. (1993) first observed stalled longitudinal axons that failed to make connection with the segmental ganglia in *lola* mutants. This pathfinding defect in *lola* mutants is reminiscent of that seen in *Delta* and *Notch* mutants [243]. *lola* can give rise to 19 different isoforms (predicted 20) through RNA splicing. All of these isoforms share a common BTB/POZ dimerisation domain, whereas 17 of these isoforms also have unique zinc finger DNA-binding domains [244]. These 19 *lola* splice variants display various expression patterns, ranging from whole embryo to specific subsets of cells such as gonad, imaginal discs, or dorsal cell layer of the CNS [244]. Several unique features of *lola* isoforms have been revealed. Expression of Lola is needed in both the motorneurons of spinal nucleus of the bulbocavernosus (SNB) and their innervating targets, the ventral muscles in stage 17 *Drosophila* embryo, to

complete the targeting process [245]. Loss of Lola causes wiring defects in both axons and dendrites of all lineages of projection neurons in adult fly brain [246].

Expression microarray analysis of *lola* mutant embryos (10-12 hours after egg lay), identified a key regulator in axon growth, which was named Spire [247]. Spire is known for its roles in regulating oocyte cytoskeleton and cytoplasmic streaming through actin nucleation and also crosslinking of microtubule and microfilament [248, 249]. Apart from these, several other downstream targets of Lola have also been identified such as DSCAM and Frazzled (axon patterning) and katanin80 and stathmin (microtubule and motor development) [247].

In addition to *lola*, B52 has been shown to bind to the RNA transcripts of Syndecan (Sdc) and RhoGAP16F [234]. In Sdc mutant, there is a higher rate of dorsal branches of the tracheal system which fails to establish anastomosis in third instar larvae [250]. This phenotype resembles that seen in the mutant of *Slit* or *Robo* [251]. Loss of Slit or Robo function restores the dorsal branch phenotype in Sdc mutant, whereas overexpression of Robo causes enhanced dorsal branch fusion defects [250]. This indicates Sdc acts as a suppressor for the Slit/Robo signalling. In a different study, Sdc has been shown to regulate cell migration and axon guidance in *C.elegans*, and this too involves the Slit/Robo pathway [252].

RhoGAP16F belongs to the RhoGAP family protein. Both RhoGAP (Rho GTPase activating protein) and RhoGEF (Rho guanine nucleotide exchange factor) are responsible for regulating the activation state of GTPase. The function of RhoGAP16F has only been examined in the leg of *Drosophila* so far, and loss of RhoGAP16F function by inducing RNAi causes bent tibia and femur, as well as tendon necrosis [253]. However, study of other members of this RhoGAP family has shown strong connection between them and axon pathfinding. RNAi inactivation of mammalian *RhoGAPp190* in *Drosophila* mushroom body (OK107Gal4) leads to axon retraction. RNAi targeting *RacGAP50C* (*tum* in flybase) and *RhoGAP71E* in mushroom body leads to various cell

morphological defects such as cell number reduction, enlarged cells, axon overextension and axon misguidance [254].

Axon overshooting is a common defect caused by misregulated signalling. For example, overexpression of the previously mentioned *RhoGAPp190* leads to overextension of dorsal axon branch in mushroom body [254]. In a study of Jun N-terminal kinase (JNK) in the mushroom body of *Drosophila*, partial loss of *bsk* function caused by RNAi leads to overextension of mushroom body axons [255]. This time, instead of translational regulation, direct protein-protein interaction between peptides of B52 and Bsk has been reported by examining the protein complex using LC-MS [256].

In summary, overshooting of posterior axon of dMP2 in *UAS-BBS/+; Gal4^{Cy27}/+* is likely to be caused by the misregulation of B52 splicing targets, including the above mentioned *lola*, *Sdc* and *RhoGAP16F*, which in turn act upon key axon singling cues Lola and Notch.

3.3.3. Fasciculation of axons is not affected by B52 activity

Fasciculation of longitudinal axons appear to be normal in all of the mutant lines tested, including *UAS-BBS/+; Gal4^{Cy27}/+*, *UAS-BBS/ +; egGal4, UAS-mCD8-GFP/ +, UAS-BBS/+; elavGal4/+* and *B52*L24* mutant, ranging from stage 17 embryos to 3rd instar larvae. This indicates expression of the cell adhesion molecule Fasciclin II (FasII) is not affected by B52 activity.

However, in *lola* mutants, anti-FasII staining in stage 17 embryos revealed the midline axons were severely disrupted in stage 17 embryos [257]. Even though B52*L24 homozygous mutants die at 36hrs post hatching, there is no collapse of these longitudinal connectives highlighted by anti-FasII up to 12hrs before the death of larvae. One possible explanation is that the presence of other splicing factors, which share common targets as B52, helps to complement defects in Lola splicing caused by the loss of B52 function. Or, maternally supplied B52 is sufficient to

ensure Lola splicing and FasII expression during embryogenesis, and once fasciculation is established, Lola is no longer required.

3.3.4. Loss of B52 activity in all differentiated neurons does not induce changes in the morphology or distribution of glia

In *Drosophila*, midline cells consists of both neurons and glia. They form an integral part and persist throughout development and function as the directing centre for axon guidance.

For example, expression of *Notch* in glia is essential for the correct guidance of longitudinal pioneer axons. In $Notch^{ts}$ mutants, axons of dMP2 and vMP2 cease to grow and fail to make contact with their targets in late stage 13 embryos [243, 258]. It has been shown that there is a gap between the advancing longitudinal growth cones and the interface glia, and this gap is filled by a thin meshwork of neuronal tissue which shows positive to neuronal membrane markers anti-HRP, BP102, and anti-Frazzled [259]. In $Notch^{ts}$ mutants, the continuity of this neuronal meshwork is largely disrupted and in some cases the meshwork is absent between the interface glia and the stalled axons [259]. Also, reduction of Notch signal by inducing RNAi in glia dramatically enhances the axon growing defects [259]. These growing defects are largely rescued by expressing *Notch* in all glia (*repoGal4*), interface glia (*htlGal4*), or just dMP2 and vMP2 (*15J2Gal4*), suggesting Notch mediates growth of pioneer longitudinal axon both autonomously in vMP2 and dMP2, and also non-autonomously in the surrounding glia [259]. Ablation of longitudinal glia causes longitudinal axons to stall or make an early turn away from the connectives. Similar effects were seen in ablation of midline glia, which led to longitudinal axons crossing the midline [251].

Previous study has also shown that pioneer axons follow their longitudinal path by tracking Frazzled and Netrin [260]. Disturbance of Frazzled and Netrin patterns have been observed in $Notch^{ts}$ mutant [259]. In $Notch^{ts}$ mutant, the position and morphology of glia appear to be

normal [259]. This is reminiscent of the situation seen in *UAS-BBS/+; elavGal4/+* with anti-repo staining in this study. Our *in situ* staining shows that *B52* is nearly absent along the connectives and hence B52 is either not or very weakly expressed in longitudinal glial cells (Fig. 3.1). Yet, for a definite clarification of the role of B52 in glial cells requires the expression of *UAS-BBS* and *UAS-GFP-B52* with drivers with a prolonged and strong glial expression such as *repoGal4*. In addition, there are no obvious defects in longitudinal axon patterning in any of the mutant line mentioned above, as revealed by anti-FasII staining, suggesting the distribution of Netrin is not affected by B52 activity.

3.3.5. Down-regulation of B52 activity does not induce obvious defects in dendrite formation

Dendritic pattern is an important aspect of synapse formation, especially during axon-dendritic interaction. The dendritic condition was first examined in stage 17 embryos, where B52 activity in dMP2 was down-regulated in the line *Gal4^{Cy27}, UAS-Denmark/+; UAS-BBS/+*. In another assay, B52 activity was down-regulated in subsets of abdominal motorneurons in the line *19H09Gal4, UAS-myrm::RFP/UAS-BBS*. In both essays, the dendritic morphology is not affected by a reduction in B52 activity.

3.4. Summary

The above results indicate it is possible that B52 regulates axon extension through its splicing targets which include *lola*, *Sdc* and *RhoGap16F*, and therefore is able to affect the projection of posterior axon of dMP2. In the single cell labelling assay, antagonising of B52 activity is achieved by inducing *BBS* at stage well before the time single cell transcriptomes of vMP2 and dMP2 are obtained. Therefore, expression level of B52 are also important at early embryonic stages but only for axon extension and not for cell determination, axonal pathfinding or dendrite formation.

Chapter 4 B52 – Generation of B52 Mutants

4.1. Introduction

Recent studies have identified several RNAs targeted by B52 during splicing, including those involved in cell cycle control [233], and eye development [219, 232]. In loss of B52 mutants, splicing of *de2f1* is impeded, correlating with a reduction in dE2F2, a cell proliferation regulator [233]. Overexpression of B52 in the eye (*GMR-Gal4* and *ey-Gal4*) leads to severe defects of eye development. The phenotype is typically stronger in *ey-Gal4* where the shape of the eye is completely distorted in adult flies, same as those experiencing reduced level of *eyeless* expression [232]. Later it has been shown that B52 regulates the RNA splicing of *eyeless*, and the previous eye phenotype is caused by splicing out of exon 2 in *eyeless,* which plays an essential role in eye development. The longer isoform of *eyeless* is involved in limiting the size of the eye, while the shorter isoform is responsible for regulating both size and shape of the eye, and B52 regulates the availability of these two isoforms through RNA splicing [232]. In a different publication, *GMR*-driven expression of B52 results in disorganisation of R and cone cells in eye imaginal discs in the third-instar larvae [219]. These authors have also identified several B52-interacting mRNAs by performing co-immunoprecipitation of B52 proteins, using dASF overexpression as a control. RNAs bound to both proteins were reverse transcribed, amplified and analysed on microarrays [219]. Some of these targets are in agreement with the result of genomic SELEX (Systematic Evolution of Ligands with EXponential enrichment) where full length Baculovirus-expressed B52, is used as a bait to attract potential RNA targets that have high affinity for B52 [234]. In addition to its mRNA-splicing function, B52 is also involved in direct protein-protein interactions, such as the recruitment of Topoisomerase I to the transcription site [208]. Potential targets of B52 have been screened by genomic SELEX and microarrays [219, 234]. Some of them are listed in table 4.1.

Table 4.1 Potential targets of B52 mRNA splicing factor

Genomic SELEX [219, 234])	**Microarray** [219, 234]
Ecdysone Receptor	White
Ladybird late (EcR)	Longitudinals lacking
Frizzled (fz)	DDB1
Furin 1 (Fur1)	Polychaetoid
Longitudinals lacking (lola)	Flotillin
Rx	Tropomyosin 1
Skiff (skf)	Fau
Mlx interactor (Mio)	Minibrain
RhoGAP16F	Beta-tubulin at 56D
Syndecan (Sdc)	Imaginal disc growth factor 3
Faint sausage (fas)	C-terminal binding protein

Several loss/gain of function lines have been used for this study, including *UAS-BBS* (an RNA aptamer that resembles B52 targets sequence and serves as a competitor for the available B52 proteins) [261], *UAS-GFP-B52* (B52 overexpression tagged with GFP) [219], *p{lacW}B52*^{S2249} (insertion of *lacW* sequence into *B52* gene) [225].

To further study the impact of B52 on neuronal circuit formation, a B52 mutant line *B52*L24* was created for this study, which is detailed below. The process for generating this mutant has been described in Section 2.10. Basically, the mutant was generated by re-editing an existing B52 mutant line *p{lacW}B52*^{S2249}, which basically was the removal of the inserted *p{lacW}* sequence, along with its flanking regions. As mentioned in previous chapters, *p{lacW}B52*^{S2249} carries a P element insertion in the *B52* gene and the coding product of *Δ2-3* is a transposase which excises P elements. Hence expression of the transposase will remove the P element inserted after 3R:13,659,314 locus in the genome (S2249 is a line ID, and it does not represent

the insertion site or have any meaning associated with the *B52* mutation). Because of this there is a very low chance that the excision of the P element triggers imprecise removal of fragments flanking the original P element site. This can disrupt the endogenous *B52* gene in the genome thereby creating a fly line devoid of the B52 protein. *p{lacW}* consists of a P element and the gene sequence encoding *lacW*, a modified version of beta-galactosidase.

4.2. Results

4.2.1. Mapping of lacW insertion in p{lacW}B52^{S2249}

Mapping of the *p{lacW}* insertion in the line *p{lacW}B52S^{2249}* was performed to confirm that *p{lacW}* was inserted after the first 3bp of *B52* gene (*B52* start codon ATG is at the 64th to 66th base pair of the gene).

One pair of primers, Fwd-B52-genomic and Pry2, was used to amplify a fragment of 1001bp in length from *p{lacW}B52S^{2249}* genomic DNA as described in section 2.4 and 2.9. This fragment consists of the last 187bp of *Hrb87F*, 780bp of *B52* 5' untranslated region (5'-UTR), plus the first 3bp of *B52* gene, and 30bp of the 3' end of *p{lacW}*. Fwd-B52-genomic overlaps with the sequence in the end of *Hrb87F*, which is 779bp upstream of *B52* in the *Drosophila* genome. Pry2 overlaps with the sequence in the 3' end of *p{lacW}*. The locations of both primers relative to the genome of *p{lacW}B52^{2249}* are illustrated in Fig. 4.1.

The PCR product was cloned into PCRII-TOPO vector (Invitrogen), transformed, DNA-purified and sent for sequencing as described in section 2.14 and 2.15. For plasmid map of the vector, see *https://tools.lifetechnologies.com/content/sfs/vectors/pcriitopo_map.pdf*. PCRII-TOPO vector is 4.0kb long and consists of M13 Forward Primer (M13F) site and M13 Reverse Primer (M13R) site inside the fragment encoding lacZ (for blue-white screen), plus two origins of replication and

sequences encoding products that provide resistance to ampicillin and kanamycin. M13F and M13R sites are the places where polymerisation initiates. Up to 1.6kb fragment downstream/upstream of M13F/M13R can be synthesised with a single primer for sequencing. The location where the PCR product is inserted is about 100bp away from both M13 sites. There are two EcoRI sites flanking the location where the PCR product is inserted (about 9bp away from either end). This allows the isolation of PCR product by EcoRI digestion. Fig. 4.2 illustrates the EcoRI digested product after transformation. There are two distinct bands, one at 4.0kb (PCRII-TOPO vector) and one at 1.0kb (PCR product insertion).

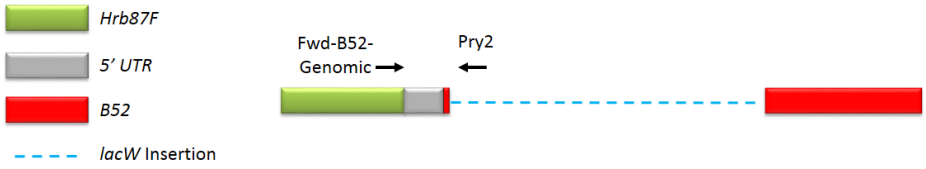

Figure 4.1 Schematic view of *B52* gene and *lacW* insertion in *p{lacW}B52.*

p{lacW} is inserted 3bp after the start of *B52* gene. Fwd-B52-genomic covers from the last 187bp of *Hrb87F* gene, which locates 780bp upstream of *B52* gene, to the right. Pry2 covers from the first 30bp fragment of *p{lacW}*3' end (as indicated by the sequencing result presented below), which is followed by the first 3bp of *B52* gene in $p\{lacW\}B52S^{2249}$ to the left. The PCR product is therefore 1.0kb.

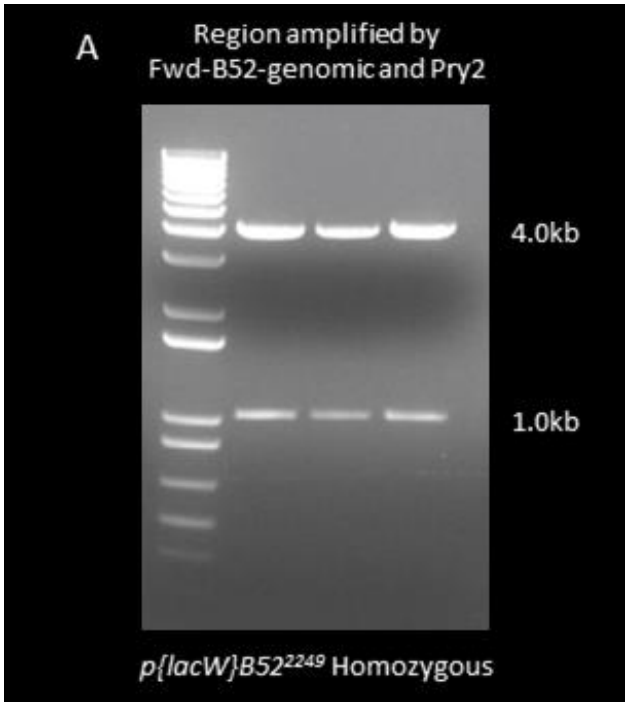

Figure 4.2 PCR of Fwd-B52-genomic and Pry2 from embryonic DNA. 1kb DNA ladder.

(A) The bands near the 1.0kb marker represent the fragment amplified by Fwd-B52-genominc and Pry2, using genomic DNA of *p{lacW}B52*^{2249} embryos as template.

The transformation product was sent for sequencing after DNA-purification. Alignment of the sequence with the corresponding gene region in wild type *Drosophila* indicates the insertion is at the right location, i.e. 3bp after the start of *B52* gene. However, the mapping result shows that *p{lacW}* is inserted in the reverse direction (Fig. 4.1), which has already been justified by the use of Pry2 primer, instead of Plac1 for the 5' end of *p{lacW}* (sequence not shown).

Figure 4.3A Sequences amplified by Fwd-B52-Genomic and Pry2 from DNA extract of *p{lacW}^{S2249}* homozygous mutants

Input of sequence amplified by Fwd-B52-genomic and Pry2 for alignment

--- *B52* start codon ATG is in bold and underlined

Primers = **XXXX** Overlapping regions between B52{lacW}^{S2249} and WT B52 gene = XXXX

>lacW_M13F_RC (sequence downstream of M13F in the transformation product – reverse complement)

NTNANNNNNNNNNNNANNNNANNNNNNNNNNCNNNNNCNTNCCNNNNNNNNNNNTNNTANGCAGNTGNNNNN
NNNNNNNCGNNNGAAAGNNNNNNNNNAGNGNNNNNNNNANNNGAGTAGNNNNNTCNTAGNNNCCCAGNTTNNNN
CTTNATGNNNGNTCGNNNNTNNGNGGANTNTGAGCGGANANATTTCACNCNGNANCAGCTATGNCCATNNTACNCCAA
GCTATTTNGNGACNCTATAGAATACTCAAGCTATGCATCAAGCTTGGTACCGAGCTCGGANCCACTAGTAACGGCCGCCAG
TGTGCTGGAATTCGCCCTT**TTCACCATCGTCGTAGTTTCC**GTTGGAATCGTTTTGTTCCGCCATTCTCTCCTTGGTTGTTCAAG
AAGCTGGAAAGTTTAAACACCGAACGCAGGAAATATTTTTTTTGTTTTTGTTCTTTTTTGACGGCAGACTGGCAATAAATGAA
ATGTACAGCACGCACAATGAGAATGGAGTGAGCAGTATGACCAGGTGTCGAGAACGGGGGTAAAGTCGGAAAATCGGACGC
CACGTGGAATCGGAACGATTGTTTCGGTGCGTTAGGGGTGTTCCTCGACAATTAAGCTGATGCCACACTTGATTTTATATATC
TTCATATAAATTTGTATTCGTCTAGTAAGGGCTTAAAAATATTAGACAAGTTTATTGTATATATTTCTGAACAAACGGATTTGA
ATGTATTATCTTTATAAATGGATTATGATAATTACTACCACGATAACCCAAGAAACATTTAATATGTTTAACTTTTTAGCTAAA
TATGTATTATTATTAATACCGCTTACATAACTCTTTCTGCGAGCATTCGCTTTAGCTGGGGCGATGGTAGGCTTCACTTTAAGA
GATAACTTGTAAATTATTTTGTATTGAATTGTATATTTGTAAGTAGCCAGCTAAGGGTCAATCAATATTACAATTACGGGATC
TATGAGGCATTTGGGAATAAAAAAAGACATCGTGCGAAATAAATTAATAAATCCAGAAACATTTTATGTATATCATCAAATC
AGAAACGTTAAAAAATGCTAATGAGTGCTTGCTAGCAGATATCAAAATAAAAAGGTTGTTAACAGTATATTCAAATGCTACT
ACTAAGTATATTTAATGTTTATTCTTTTCATAGCGGAACACGAACAGCAACTGGAATACCCTTAACGCAGCGAAACGCATTGC
CCGCCCAAAATATCGATAGGCGAAAAAGTATCGTTCCATTCCGCCTTTGGAATGACTGTCAAACATCGCTTTCGTCTGTCACA
TGATGAA**ATAACATAAGGTGGTCCCGTCGGCAAG**AAGGGCGAATTCTGCAGATATCCATCACACTGGCGGCCGCTCGAGC
ATGCATCTAGAGGGCCCAATCGCCCNNNNNNNNNN

>lacW_M13R (sequence upstream of M13R in the transformation product)

NNNNTNNNNGTGNNCTATAGNNTACTCAAGCTATGCATCAAGCTTGGTACCGAGCTCGGATCCACTAGTAACGGCCGCCA
GTGTGCTGGAATTCGCCCTT**TTCACCATCGTCGTAGTTTCC**GTTGGAATCGTTTTGTTCCGCCATTCTCTCCTTGGTTGTTCAA
GAAGCTGGAAAGTTTAAACACCGAACGCAGGAAATATTTTTTTTGTTTTTGTTCTTTTTTGACGGCAGACTGGCAATAAATGA
AATGTACAGCACGCACAATGAGAATGGAGTGAGCAGTATGACCAGGTGTCGAGAACGGGGGTAAAGTCGGAAAATCGGAC
GCCACGTGGAATCGGAACGATTGTTTCGGTGCGTTAGGGGTGTTCCTCGACAATTAAGCTGATGCCACACTTGATTTTATAT
ATCTTCATATAAATTTGTATTCGTCTAGTAAGGGCTTAAAAATATTAGACAAGTTTATTGTATATATTTCTGAACAAACGGATT
TGAATGTATTATCTTTATAAATGGATTATGATAATTACTACCACGATAACCCAAGAAACATTTAATATGTTTAACTTTTTAGCT
AAATATGTATTATTATTAATACCGCTTACATAACTCTTTCTGCGAGCATTCGCTTTAGCTGGGGCGATGGTAGGCTTCACTTTA
AGAGATAACTTGTAAATTATTTTGTATTGAATTGTATATTTGTAAGTAGCCAGCTAAGGGTCAATCAATATTACAATTACGGG
ATCTATGAGGCATTTGGGAATAAAAAAAGACATCGTGCGAAATAAATTAATAAATCCAGAAACATTTTATGTATATCATCAA
ATCAGAAACGTTAAAAAATGCTAATGAGTGCTTGCTAGCAGATATCAAAATAAAAAGGTTGTTAACAGTATATTCAAATGCT

ACTACTAAGTATATTTAATGTTTATTCTTTTCATAGCGGAACACGAACAGCAACTGGAATACCCTTAACGCAGCGAAACGCAT
TGCCCGCCCAAAATATCGATAGGCGAAAAAGTATCGTTCCATTCCGCCTTTGGAATGACTGTCAAACATCGCTTTCGTCTGTC
ACATGATGAA**ATAACATANNTGNNCCGTCGGCAAG**AAGGGCGAATTCTGCAGANNTCCATCACACTGGCGNCCGCTCGN
GCATGCATCTAGAGGGNCCAATTCGCCNATAGTGAGTCGTANTANNATTCACTNNNGTCNTTTTACANNTCNNGACTGGG
NAANCCNNNNTNCCCANTNNNGCNNNAGCNCNATCCCCTTTCNCNNCTNNCGTANNNNCNAANNNNNNCNCNNATCNC
NNNNNNNCNNNNNNNNNNNNNNNNANGGNNNCNNCCNGNNNNGNNCNTANCNNNNNNNNNNNNNNNCNNNNN
NNNNCNNNANNNNNNNANNNCCNNNNNNNN

>WT_B52_extended_gene_region (starts with overlapping sequence of Fwd-B52-genomic)

TTCACCATCGTCGTAGTTTCCGTTGGAATCGTTTTGTTCCGCCATTCTCTCCTTGGTTGTTCAAGAAGATGGAAAGTTTAAACA
CCGAACGCAGGAAATATTTTTTTTGTTTTTGTTCTTTTTTGACGGCAGACTGGCAATAAATGAAATGTACAGCACGCACAATG
AGAATGGAGTGAGCAGTATGACCAGGTGTCGAGAACGGGGTAAAGTCGGAAAATCGGACGCCACGTGGAATCGGAACGA
TTGTTTCGGTGCGTTAGGGGTGTTCCTCGACAATTAAGCTGATGCCACACTTGATTTTATATATCTTCATATAAATTTGTATTC
GTCTAGTAAGGGCTTAAAAATATTAGACAAGTTTATTGTATATATTTCTGAACAAACGGATTTGAATGTATTATCTTTATAAAT
GGATTATGATAATTACTACCACGATAACCCAAGAAACATTTAATATGTTTAACTTTTTAGCTAAATATGTATTATTATTAATAC
CGCTTACATAACTCTTTCTGCGAGCATTCGCTTTAGCTGGGGCGATGGAAGGCTTCACTTTAAGAGATAACTTGTAAATTATT
TTGTATTGAATTGTATATTTGTAAGTAGCCAGCTAAGGGTCAATCAATATTACAATTACGGGATCTATGAGGCATTTGGGAAT
AAAAAAAGACATCGTGCGAAATAAATTAATAAATCCAGAAACATTTTATGTATATCATCAAATCAGAAACGTTAAAAAATGC
TAATGAGTGCTTGCTAGCAGATATCAAAATAAAAAGGTTGTTAACAGTATATTCAAATGCTACTACTAAGTATATTTAATGTT
TATTCTTTTCATA`GCGGAACACGAACAGCAACTGGAATACCCTTAACGCAGCGAAACGCATTGCCCGCCCAAAATATCGATA
GGCGAAAAAGTATCGTTCCATTCCGCCTTTGGAATGACTGTCAAACATCGCTTTCGTCTGTCACTTTCACTTCCGTTTGTGTCG
AGTCGCTTGCGTTTTTTCGTGTGGGAAAGCCTGAAAAAGAGAGAGTACGGCAGCGACTTAATTGTAAATTTGCCACAAATAT
CCTTCACTGAACGCACCTGCTCCAGATACGTAAGGAACCGTTATC**ATG**GTGGGATCTCGAGTGT

>Fwd-B52-genomic

TTCACCATCGTCGTAGTTTCC

>Pry2_RC (revers complement of Pry2 primer)

ATAACATAAGGTGGTCCCGTCGGCAAG

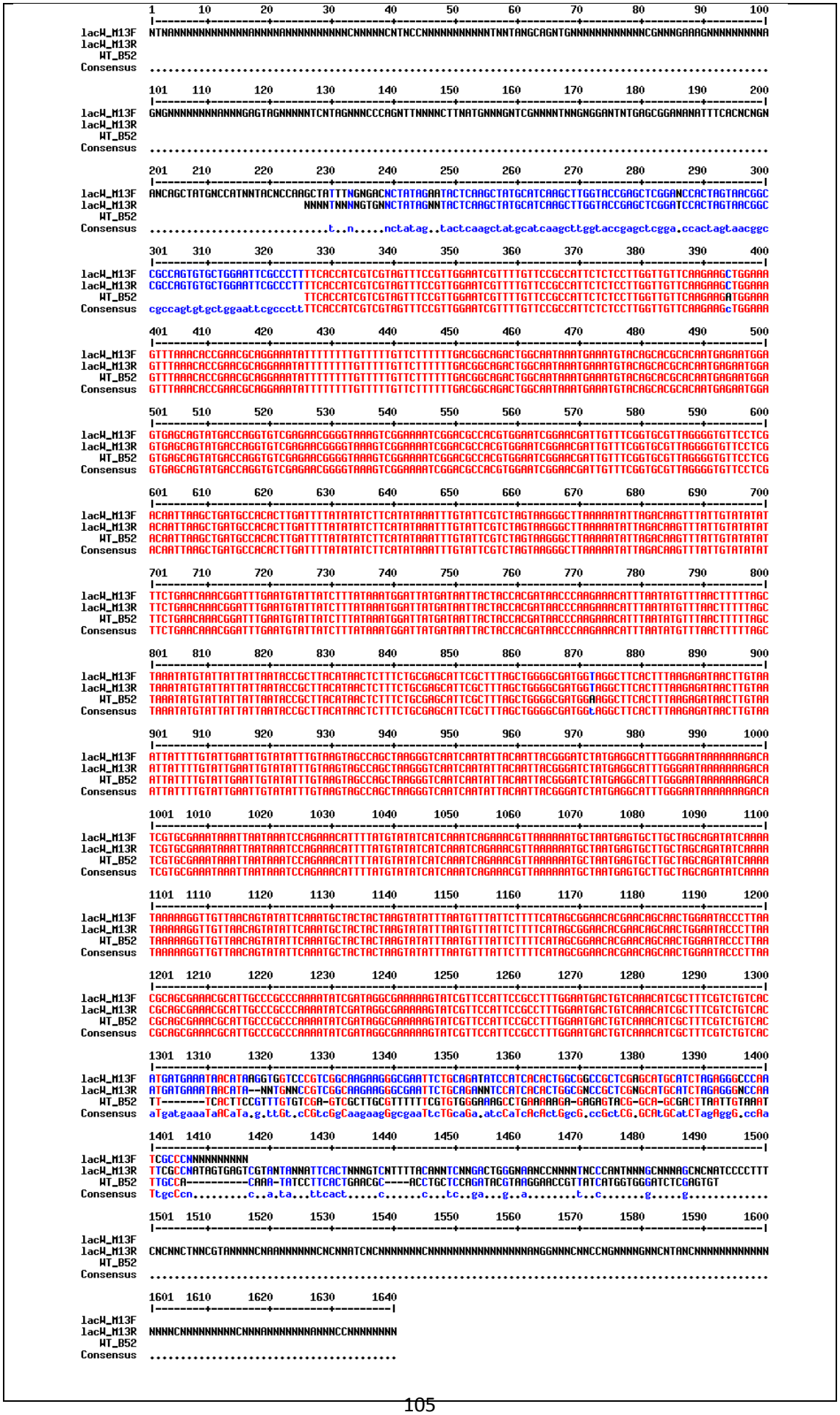
lacW_M13F
lacW_M13R
WT_B52
Consensus

Figure 4.3B Sequences amplified by Fwd-B52-Genomic and Pry2 from DNA extract of *p{lacW}^{S2249}* homozygous mutants

lacW_M13F_RC and **lacW_M13R** are sequences amplified by primers Fwd-B52-Genomic and Pry2 from DNA extract of *p{lacW}^{S2249}* homozygous mutants. They represent the same gene region, but are synthesised from different ends of the M13 plasmid for sequencing purpose. The sequence was compared with the corresponding region in wild type *Drosophila*, which is named **WT_B52_extended_gene_region**. As highlighted with yellow background, the corresponding DNA sequence of *p{lacW}^{S2249}* is identical to that in wild type, indicating the insertion is at the right place in the B52 gene. Sequences of the primers are in bold and underlined. Note the reverse primer Pry2 only overlaps with **lacW_M13F_RC** and **lacW_M13R**. This is because the sequence is from the *lacW* insertion, and is not present in the *B52* gene in wild type.

4.2.2. Generation of a B52 null mutant

After confirming that *p{lacW}* was indeed inserted close to the open reading frame (ORF) of *B52*, the *p{lacW}B52S^{2249}* line was used to create a *B52* null mutant as described in section 2.10 and 2.11. Two separate pairs of primers were used to amply specific regions of the *B52* gene in the mutants. The first pair: U400-B52-start and Rev-B52-genomic (from 400bp upstream the start of *B52* gene to 1667bp downstream the start of *B52* gene in wild type *Drosophila*) for *B52*L24* (Fig. 4.4). The second pair: U400-B52-start and D400-B52-start (from 400bp upstream the start of *B52* gene to 400bp downstream the start of *B52* gene in wild type *Drosophila*) for *B52*L31* (primer location not shown in Fig 4.3 because the resulting line is not a null mutant and therefore not sequenced, see Fig 4.4 agarose gel). The resulting PCR products were cloned into PCRII-TOPO vector (Invitrogen), transformed, and DNA-purified as described in section 2.14.

Fig. 4.5 illustrates the EcoRI digested products after transformation of both lines. Note different primers covering fragments of different length in wild type were used (as mentioned above). In both cases there are bands at 4.0kb, which represent the PCRII-TOPO vector. For *B52*L31*, the PCR insertion is digested by EcoRI, and results in two separate bands at approximately 0.9kb and 0.6kb, respectively (Fig. 4.5A). Since the length of the corresponding fragment in wild type is 0.8kb, this indicates there is an insertion mutation of *B52* gene in *B52*L31*. Because this type of mutation is unlikely to cause loss of gene function, *B52*L31* line was not sent for sequencing. In

contrast to it, *B52*L24* has a deletion of approximately 0.7kb fragment from the *B52* gene (Fig. 4.5B), since the corresponding fragment is reduced from 2.1kb (in wild type) to 1.4kb. Therefore, *B52*L24* was sent for sequencing.

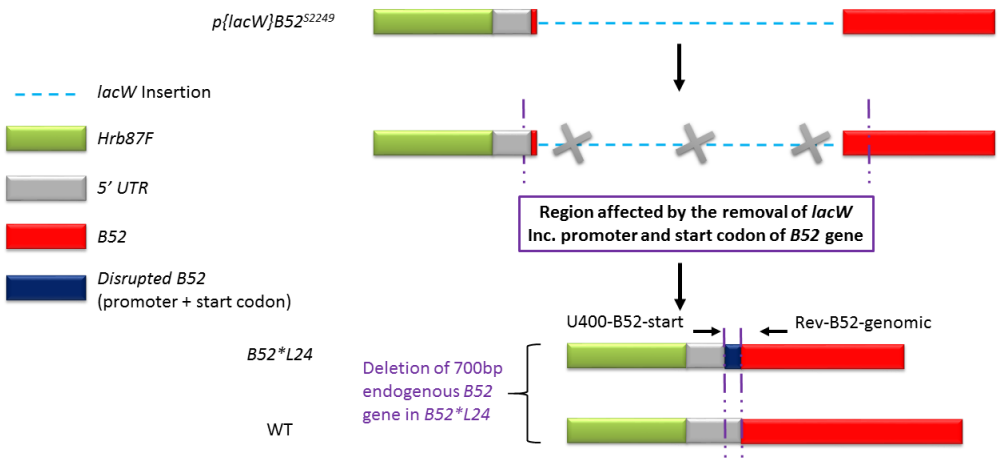

Figure 4.4 Schematic view of sequences flanking the *B52* start codon in *B52*L24.*

U400-B52-start covers from 400bp upstream the start of the *B52* gene to the right. Rev-B52-genomic covers from 1667bp downstream the start of *B52* gene to the left. The removal of *lacW* triggers non-homologous recombination DNA repair mechanism, and thus inducing deletion of nucleotides in *B52* endogenous gene, causing mismatches and missing of nucleotides in the promoter and start codon of *B52* gene in *B52*L24*, and therefore disruption of *B52* open reading frame compared to the wild type.

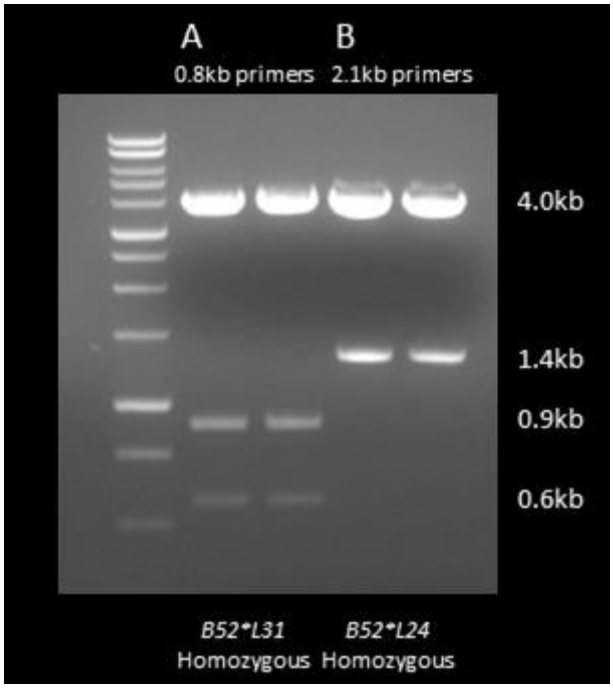

Figure 4.5 PCR of 0.8kb primer pair and 2.1kb primer pair from embryonic DNA

1kb DNA ladder. 0.8kb primers = U400-B52-start and D400-B52-start, and 2.1kb primers = U400-B52-start and Rev-B52-genomic. In both cases, there are 4.0kb bands on top of the gel which represent the PCRII-TOPO vector. (A) There are two bands present in the *B52*L31* homozygous mutant. This is caused by digestion of EcoRI which cuts the 1.5kb PCR product amplified by primers U400-B52-start and D400-B52-start. Since the primers cover a region of 800bp in wild type, this result indicates there is an increase of 700bp fragment, possibly caused by duplication, in the *B52*L31* homozygous mutant. (B) The 1.4kb bands represent the PCR product amplified by U400-B52-start and Rev-B52-genomic. In wild type, the primers cover a fragment of 2.1kb in length. This indicates there is a deletion of 700bp in the *B52* gene in the *B52*L24* homozygous mutant, as compared to wild type.

The sequencing result of the fragment amplified by primers U400-B52-start and Rev-B52-genomic from *B52*L24* genomic DNA is illustrated below. Alignment of this sequence with the corresponding *B52* sequence from wild type (including the 200bp sequence flanking the *B52* start codon) indicates there are nucleotides mismatched and missing in the *B52* gene of *B52*L24*. Note right after the first nucleotide "A" of the *B52* start codon ATG, there are 7bp (including the "TG"), missing in the sequencing results (around 830bp marked in the alignment result). This, plus the mismatches and missing nucleotides up/downstream the supposed ATG site, indicates the promoter and start codon of *B52* gene is completely disrupted in *B52*L24*. At the same time,

the gene sequence of *Hrb87F* is assumed to be intact, since most of the sequence upstream of *B52* start codon is identical with that of wide type, despite very few mismatches which might be caused by sequencing errors. The outcome of the deletion is illustrated in Fig. 4.4.

Figure 4.6A Sequences amplified by U400-B52-start and Rev-B52-Genomic from DNA extract of B52*L24 homozygous mutants

Input of sequence amplified by U400-B52-start and Rev-B52-genomic for alignment

--- *B52* start codon ATG is in bold and underlined

Primers = **XXXX** Overlapping regions between B52{lacW}^{S2249} and WT B52 gene = XXXX

*** = the location of B52 start codon ATG in reference to WT (missing in B52^L24 homozygous mutants)

>*B52*L24*_M13F (sequence downstream of M13F in the transformation product)

AATCAATAGGGCGATTGGCCCTCTAGATGCATGCTCGAGCGGCCCCAGTGTGATGGATATCTGCAGAATTCGCCCTTGGTCA
ATCAATATTACAATTACGGGATCTATGAGGCATTTGGGAATAAAAAAAGACATCGTGCGAAATAAATTAATAAATCCAGAAA
CATTTTATGTATATCATCAAATCAGAAACGTTAAAAAATGCTAATG***AGTGCTTGCTAGCAGATATCAAAATAAAAAGGTT
GTTAACAGTATATTCAAATGCTACTACTAAGTATATTTAATGTTTATTCTTTTCATAGCGGAACACGAACAGCAACTGGAATA
CCCTTAACGCAGCGAAACGCATTGCCCGCCCAAAATATCGGTATCGATGAAAAAAATCGGTTAAAAAATCGATTTGAAGACA
TTTCTGCATTTCTCTGTTTGTCTATAGGTTTCCTAACATTTCAAGCCGACCCTTGAATACTTTTTTTTTCTTTTTGAACCTATATTT
GTTCCATCATTTGTCTGTCAAATACAGTGACGCTTAAAAACTGTTCTTAAATTCACCCAGCGTATTTCCATAAGAGTATGCACA
GGCAGGGTAGCTTCAATACTAATTCCATAATCAATACTAATCACTAATTGAATTTTCAGGAATTCGAAGACTATCGTGATGCC
GACGATGCCGTCTATGAACTGAATGGCAAAGAGCTGCTTGGCGAACGGTGAGTTGTTAGATATAAGCCAAAGTACGAAATG
ACTCACGATTGTATGTTCTATATTTTTGCAGTGTGGTTGTTGAACCCGCCAGGGTACCGCTCGTGGCAGCAACCGCGACCGCT
ACGACGATCGATATGGTGGTCGGCGGGGCGGCGGCGGCGGTCGTTACAACGAAAAGTAAGTAGTACTGCCAGCGGACCTT
AAAACCGGACCAAAGTAGCGACGATATCGTCCTCCAACTTTGTTTGCGTTGAAGTTTGCCCTAGAATTAGCACTGCCAATTTG
TTTCGTTTGATATCTCCATACACACAGATGCAACCAGCTTAGATCGTGCAAAATCTATATACCTATAATATTAGCTACTTGCGA
TATATATAAAAAACATCAGTTTATTATATATTGACTTCTATAATTTTATACACTTTTGGTAGTGCAATCGTATAAGCTGATTTCT
TCTGCGTGGAAGGGAACCAAAAGACACTGACTTGCTGTTAATATTATCATTTCCAAGACGCTCCGTTTTCCTATGCATACTAT
TGTTGCTTTTATTTGCACGTTCCACCCATCCGCAAAGTATGTAAAATGTTTGATTTGTTGCGCATAACCCAAATGTAAATATGC
ATATCCTGGAATATATTCACCATTAGCGTTAATTTTTTGTGATGGAGCATCAGGGAGCAGCAGGCAGTTGTCAATACCTAATT
AGCGAATCCCTTTCAATTATTTCCCCAGAAACAAAAATTCCAGAATCATCCTCTTCGTTATGGCCCACCCGTTGCGCACTTGAG
AACCGACTTGATTTGGGGAAATTTGTCTAACCCGAAGCCGAAATTTCAAGGCCACTTGGCGGGCCGTTACATAGTGGGTCCC
GAGCTCGGAACCAAGCTTTGATGCATAAGCTTGGAGTATCCTAAAGGTGCCCCCTAAAAAGACTTGGGGAAAACAAGGGGC
AAAAGCGGT

>*B52*L24*_M13R_RC (sequence upstream of M13R in the transformation product – reverse complement)

CGGCGTGTGTAAACCGCCGGCCAGGGAAATGTAATCCCGCCCCACCTATGGGCGAAATTGGGCCCCTCTAGATGCATGCTC
GACGGCCGCCCAATGTGAATGGAATCCTGCAAGAATTCGCCCTTGGGCAATCCAATTTTCCAATTCCGGGATCTTTGAGGCA
TTTGGGAATAAAAAAAGGCATTGTGCGAAATAAATTAATAAATCCAGAAACATTTTTATGTATTTCATCAAATCAGAAACGTT
AAAAAATGCTAATG***AGTGCTTGCTAGCAGATTTCAAAATAAAAAGGTTGTTAACAGTATATTCAAATGCTCCTACTAAGT
ATATTTAATGTTTATTCTTTTCATAGCGGAACACGAACAGCAACTGGAATACCCTTAACGCAGCGAAACGCATTGCCCGCCCA
AAATATCGGTATCGATGAAAAAAATCGGTTAAAAAATCGATTTGAAGACATTTCTGCATTTCTCTGTTTGTCTATAGGTTTCCT
AACATTTCAAGCCGACCCTTGAATACTTTTTTTTTCTTTTTGAACCTATATTTGTTCCATCATTTGTCTGTCAAATACAGTGACG

CTTAAAAACTGTTCTTAAATTCACCCAGCGTATTTCCATAAGAGTATGCACAGGCAGGGTAGCTTCAATACTAATTCCATAAT
CAATACTAATCACTAATTGAATTTTCAGGAATTCGAAGACTATCGTGATGCCGACGATGCCGTCTATGAACTGAATGGCAAA
GAGCTGCTTGGCGAACGGTGAGTTGTTAGATATAAGCCAAAGTACGAAATGACTCACGATTGTATGTTCTATATTTTTGCAG
TGTGGTTGTTGAACCCGCCAGGGGTACCGCTCGTGGCAGCAACCGCGACCGCTACGACGATCGATATGGTGGTCGGCGGG
GCGGCGGCGGCGGTCGTTACAACGAAAAGTAAGTAGTACTGCCAGCGGACCTTAAAACCGGACCAAAGTAGCGACGATAT
CGTCCTCCAACTTTGTTTGCGTTGAAGTTTGCCCTAGAATTAGCACTGCCAATTTGTTTCGTTTGATATCTCCATACACACAGA
TGCAACCAGCTTAGATCGTGCAAAATCTATATACCTATAATATTAGCTACTTGCGATATATATAAAAAACATCAGTTTATTATA
TATTGACTTCTATAATTTTATACACTTTTGGTAGTGCAATCGTATAAGCTGATTTCTTCTGCGTGGAAGGGAACCAAAAGACA
CTGACTTGCTGTTAATATTATCATTTCCAAGACGCTCCGTTTTCCTATGCATACTATTGTTGCTTTTATTTGCACGTTCCACCCA
TCCGCAAAGTATGTAAAATGTTTGATTTGTTGCGCATAACCCAAATGTAAATATGCATATGCTGGAATATATTCACCATTAGC
GTTAATTTTTGTGATGGAGCATCAGGAGCAGCAGCGCAGTGTCAATACTAATTAGCGAATCCATTCAATTATTCACCAGAAA
CAAAAATTCCAGATCATCCTCTCGTTATGGCCCACCGTTGCGCACTGAGTACCGACTGATTGTGGAGAATTTGTCTAGCGAA
GGGCGAATTCCAGCACACTGGCGGCCGTTACTAGTGGATCCGAGCTCGGTACCAAGCTTGATCATAGCTTGAGTATTCTATA
GTTCCCCTAAATTT

>2.1kb_WT (2.1kb sequence covered by primers U400-B52-start and Fwd-B52-genomic)

CTTGTAAATTATTTTGTATTGAATTGTATATTTGTAAGTAGCCAGCTAAGGGTCAATCAATATTACAATTACGGGATCTATGA
GGCATTTGGGAATAAAAAAAGACATCGTGCGAAATAAATTAATAAATCCAGAAACATTTTATGTATATCATCAAATCAGAAA
CGTTAAAAAATGCTAATGAGTGCTTGCTAGCAGATATCAAAATAAAAAGGTTGTTAACAGTATATTCAAATGCTACTACTAA
GTATATTTAATGTTTATTCTTTTCATAGCGGAACACGAACAGCAACTGGAATACCCTTAACGCAGCGAAACGCATTGCCCGCC
CAAAATATCGATAGGCGAAAAAGTATCGTTCCATTCCGCCTTTGGAATGACTGTCAAACATCGCTTTCGTCTGTCACTTTCAC
TTCCGTTTGTGTCGAGTCGCTTGCGTTTTTTCGTGTGGGAAAGCCTGAAAAAGAGAGAGTACGGCAGCGACTTAATTGTAAA
TTTGCCACAAATATCCTTCACTGAACGGTACGTGCTAGTGAGTACGCTTAAGTGAAGAACAGCGCGTATTTCGCGTTGTTAA
ATTAACTCGTTTTTGCAGCGGTTCTGTACACCCGGTACATTGCGAGCGTGTGTGTGTGTATGTGGTGGCCGCCATCTTGGCG
AAACATACACGGCGCGTACATATGTGCGTTTTTTTTTTCTTCCATTCCTAAAGGACAGTCGAGCAAAATAGAAGCTGCAAACT
GCAACGGTTCCCTTGCTGATATATATATATATACTTCACTATTTTATAGCACCTGCTCCAGATACGTAAGGAACCGTTATC**ATG**
GTGGGATCTCGAGTGTATGTGGGCGGTCTGCCCTACGGAGTGCGCGAGCGCGATTTGGAGCGCTTTTTCAAAGGCTACGGC
CGCACACGCGACATCCTCATCAAAAATGGCTACGGCTTTGTGGTGAGTACAAAATATCATATTTAACTGGAATATGTAAAAA
AAAAAAATCGGTTAAATTTGATTTGAAGACATTTCTGCATTTCTCTGTTTGTCTATAGGTTTCCTAACATTTCAAGCCGACCCT
TGAATACTTTTTTTTTCTTTTTGAACCTATATTTGTTCCATCATTTGTCTGTCAAATACAGTGACGCTTAAAAACTGTTCTTAAAT
TCACCCAGCGTATTTCCATAAGAGTATGCACAGGCAGGGTAGCTTCAATACTAATTCCATAATCAATACTAATCACTAATTGA
ATTTTCAGGAATTCGAAGACTATCGTGATGCCGACGATGCCGTCTATGAACTGAATGGCAAAGAGCTGCTTGGCGAACGGT
GAGTTGTTAGATATAAGCCAAAGTACGAAATGACTCACGATTGTATGTTCTATATTTTTGCAGTGTGGTTGTTGAACCCGCCA
GGGGTACCGCTCGTGGCAGCAACCGCGACCGCTACGACGATCGATATGGTGGTCGGCGGGGGGGCGGGGGCGGTCGTTA
CAACGAAAAGTAAGTAGTACTGCCAGCGGACCTTAAAACCGGACCAAAGTAGCGACGATATCGTCCTCCAACTTTGTTTGCG
TTGAAGTTTGCCCTAGAATTAGCACTGCCAATTTGTTTCGTTTGATATCTCCATCCACACAGATGCAACCAGCTTAGATCGTGC
AAAATCTATATACCTATAATATTAGCTACTTGCGATATATATAAAAAACATCAGTTTATTATATATTGACTTCTATAGTTTTATA
CACTTTTGGTAGTGCAATCGTATAAGCTGATTTCTTCTGCGTGGAAGGGAACCAAAAGACACTGACTTGCTGTTAATATTATC
ATTTCCAAGACGCTCCGTTTTCCTATGCATACTATTGTTGCTTTTATTTGCACGTTCCACCCATCCGCATAGTATGTAAAATGTT
TGATTTGTTGCGCATAACCCAAATGTAAATATGCATATGCTGGAATATATTCACCATTACCGTTAATTTTTGTGATGGAGCAT
CAGGAGCAGCAGCGCAGTGTCAATACTAATTAGCGAATCCATTCAATTATTCACCAGAAACAAAAATTCCAGATCATCCTCTC
GTTATGGCCCACCGTTGCGCACTGAGTACCGACTGAT**TGTGGAGAATTTGTCTAGCCG**

>200bp_sequence_flanking_B52_start_codon

TCCCTTGCTGATATATATATATATACTTCACTATTTTATAGCACCTGCTCCAGATACGTAAGGAACCGTTATC**ATG**GTGGGATC
TCGAGTGTATGTGGGCGGTCTGCCCTACGGAGTGCGCGAGCGCGATTTGGAGCGCTTTTTCAAAGGCTACGGCCGCACACG
CGACATCCTCATCAAAAATGGCTACGGCTTTGTGG

>U400-B52-start

CTTGTAAATTATTTTGTATTGAATTGTATATTTGTAA

>Rev-B52-genomic_RC

TGTGGAGAATTTGTCTAGCCG

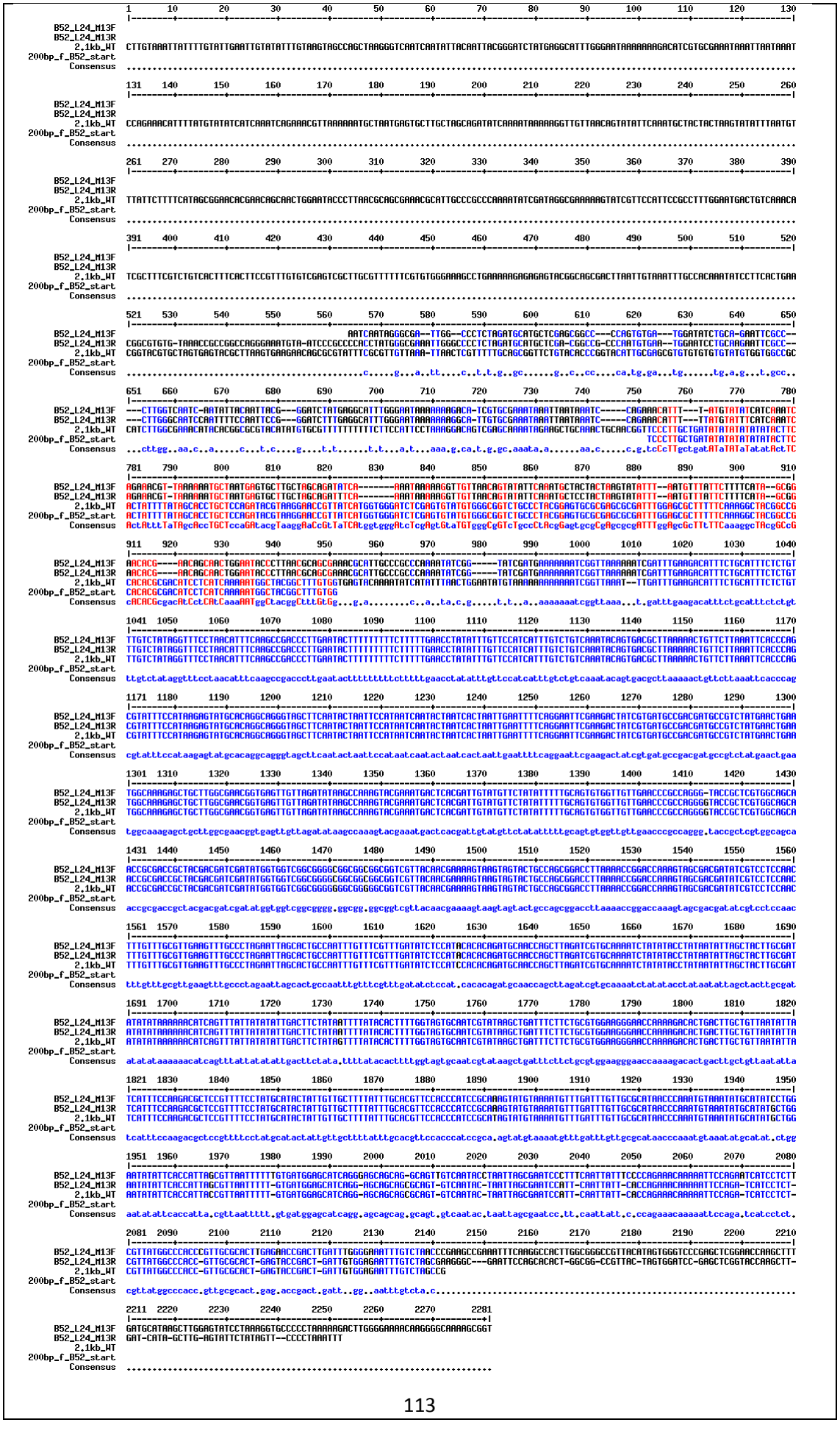
B52_L24_M13F
B52_L24_M13R
2.1kb_WT
200bp_f_B52_start
Consensus

Figure 4.6B Sequences amplified by U400-B52-start and Rev-B52-Genomic from DNA extract of B52*L24 homozygous mutants

B52*L24_M13F and **B52*L24_M13**R_RC are sequences amplified by primers U400-B52-start and Rev-B52-Genomic from DNA extract of B52*L24 homozygous mutants. They represent the same gene region, but are synthesised from different ends of the M13 plasmid for sequencing purpose. The sequence was compared with the corresponding region in wild type *Drosophila*, which is named **2.1kb_WT**. As highlighted with yellow background, the corresponding DNA sequence of B52 in B52*L24 still share similarity with that in the wild type. However, when compared the sequence with the 200bp region around B52 start codon (166bp upstream of the sequence marked with yellow background), as indicated by **200bp_sequence_flanking_B52_start_codon**, there is no overlapping between the two. This indicates the reading frame of B52 gene has been disrupted in B52*L24 homozygous mutants. Note the start codon ATG of B52 cannot be found in the corresponding regions from the M13 sequencing results. Sequences of the primers are in bold and underlined.

4.2.3. Detection of B52 RNA in the larval brain of B52*L24 homozygous mutant animals

The RNA level of *B52* was examined in *B52*L24* homozygous mutants. Since the accumulated maternal RNA might still present in late stage embryos, the level of *B52* RNA was only examined in the brains of 36hrs post-hatching larvae of *B52*L24* homozygous mutant, which is around the time they die (see Chapter 6, only living larvae were used for RNA extraction), where *B52*L24* heterozygotes were used as control. Primers B52-SP6 and B52-T7 were used to amplify all transcripts of *B52*. This pair of primer covers around 1.0kb sequence of *B52* transcript in wild type *Drosophila*. As shown in Fig. 4.7, *B52* RNA is only detected in *B52*L24* heterozygous animals, indicating *B52*L24* homozygotes are null mutants for B52.

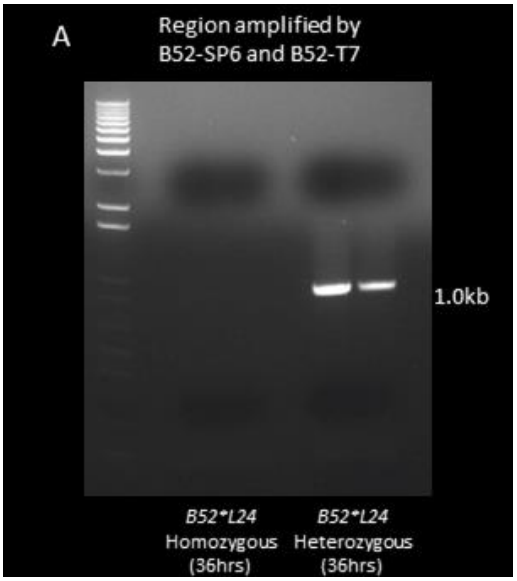

Figure 4.7 PCR of B52-SP6 and B52-T7 from larval RNA.

1kb plus DNA ladder. (A) The 1.0kb band which represents *B52* RNA is only detected in *B52**L24 heterozygous mutant.

4.3. Discussion

The generation of this *B52^L24* mutant further facilitates the study of B52 function, since this is the only mutant line, in this study, that has been confirmed by DNA sequencing to be devoid of the *B52* gene (as indicated by the complete disruption of *B52* reading frame, along with the missing of *B52* start codon). Compared to other lines such as *UAS-BBS* or *UAS-B52-RNAi*, which only lower the activity levels of B52 without completely removing *B52* (plus there is no direct evidence indicating that the B52 RNA or protein is actually absent as a result of BBS or B52-RNAi), the *B52^L24* homozygous mutant is deficienct in the B52 RNA in the brain of 36hrs post hatching larvae. In addition, their death after the 1st instar and their much smaller body size compared to the control are clear phenotypes of the *B52^L24* homozygous mutant. These phenotypes are absent from *UAS-BBS* or *UAS-B52-RNAi* flies.

This *B52^L24* mutant is in fact generated in a similar way to that of *B52*^{28} strain in which the authors induced the removal of the randomly inserted *p{lacW}* sequence from the previously mentioned *p{lacW}B52S*^{2249} line to create a partial deletion mutant [208]. This *B52*^{28} mutant line does not survive after the 2nd instar larval stage. This phenotype is not connected to changes on the splicing patterns of several B52 targets such as a gene named *ftz* [235].

This *B52^L24* mutant line ultimately serves as a touchstone to backup or oppose the results of all analyses done regarding to B52.

Chapter 5 From B52 to neurotransmitter

5.1. Introduction

Neuronal network formation is a developmental process controlled by many factors, including genetically regulated and activity dependent mechanisms. A simple functional neuronal circuit controlling locomotion consists of three subsections: sensory neuron, interneuron and motor neuron. Each of the three different types of neurons can have different roles which are determined by its location, axon projection pattern, synaptic connection, neurotransmitter expression and electrophysiological properties.

As an essential part contributing towards neuronal circuit function, the neurotransmitter plays a primary role in determining specific features of neurons. It is known that most neuron types express exclusively one particular neurotransmitter, and expression of the neurotransmitter phenotype is specified genetically during development [262]. This process requires the transcription of several kinds of proteins, including enzymes involved in the synthesis of neurotransmitters, vesicular transporters and receptors found on the neuronal cell body. A series of events controlling the expression of corresponding units for a single neurotransmitter can be regulated by either a single transcriptional unit [263, 264] or several throughout the genome [265].

Neurotransmitter selection has been extensively studied at neuromuscular junctions in *Drosophila* [266]. Studies of *Drosophila* motor neurons have identified several transcription factors, including Even-skipped, Islet, Lim3 and Hb9 [267-270]. These factors are expressed at different levels between motor neurons and subsets of interneurons [267, 269, 271]. Islet is required by both serotonergic and dopaminergic neurons, and ectopic expression of Islet induces the synthesis of tyrosine hydroxylase in certain neurons [271].

In vertebrates, most of the mature neuromuscular junctions are cholinergic, and motor neurons express Islet, MNR2 and Lhx3. Ectopic expression of MNR2 in interneurons leads to development of motor-neuron like features such as the expression of choline acetyltransferase (ChAT), which is which is characteristic but not exclusive of motor neurons [272].

The majority of interneurons are either inhibitory (expressing GABA or glycine), or excitatory (expressing glutamate). Studies of mouse dorsal horn neurons have revealed that specification of neurotransmitter is regulated by two transcription factors, TLX3 and LBX1. TLX3 favours the up-regulation of glutamate while inhibiting the expression of GABA [273], whereas LBX1 promotes the GABAergic phenotype while supressing the glutamatergic phenotype [274]. In this case, transcriptional regulation of neurotransmitter selection is controlled by only two factors. In most other situations, more than two transcription factors are combined together to specify the neurotransmitter [275].

Recent studies of *Xenopus* embryos have demonstrated that re-specification of neurotransmitters can be triggered by regulation of Ca^{2+} levels in both central interneurons and motor neurons [276, 277]. Reduction of Ca^{2+} level by expressing the $Kir_{2.1}$ K+ channel results in up-regulation of excitatory neurotransmitters, glutamate and acetylcholine (ACh). In contrast, increasing of Ca^{2+} level by overexpressing voltage-gated Na^{+} channel leads to increase of inhibitory neurotransmitters, GABA and glycine [276]. Activity-dependent regulation targets transcription factors Tlx3 and Lmx1b in chick and mouse spinal cord [277, 278].

The re-specification of neurotransmitter is thought as a way to balance the input of excitatory and inhibitory signals, thus maintaining a stable environment for neuronal development. Disturbance in this excitatory and inhibitory balance is thought to results in neurological disorders, such as seizure, autism and schizophrenia [279].

It is known that the splicing of the mRNA of a particular gene can lead to generation of sequences that later translate into proteins of different functions. Taking ChAT as an example, the splicing of the *ChAT* RNA not only produces different isoforms of *ChAT* transcripts, but also for vesicle acetylcholine transferase (VAChT), which is involved in acetylcholine transport into synaptic vesicles. Therefore, like with most genes, RNA splicing is a necessary step to go through before DNA can be correctly decoded into functional proteins. For example, there are two different splice variants of *ChAT* (flybase.org). One of them is the soluble form and another one is non-ionically membrane-bound form [280]. The soluble form contributes to 80-90% of the total enzyme activity [281]. Alignment result of the *Drosophila* ChAT protein isoforms is shown in Fig. 5.0. They differ only by an extra 7 amino acid which is present exclusively in the ChAT_PA isoform. In rats, the membrane-bound form, which is the longer ChAT_PA, is referered to as common type ChAT because it presents in both the central nervous system (CNS) and peripheral nervous system (PNS), whereas ChAT_PB, the shorter form is referred to as peripheral type ChAT due its exclusive expression in the PNS [282].

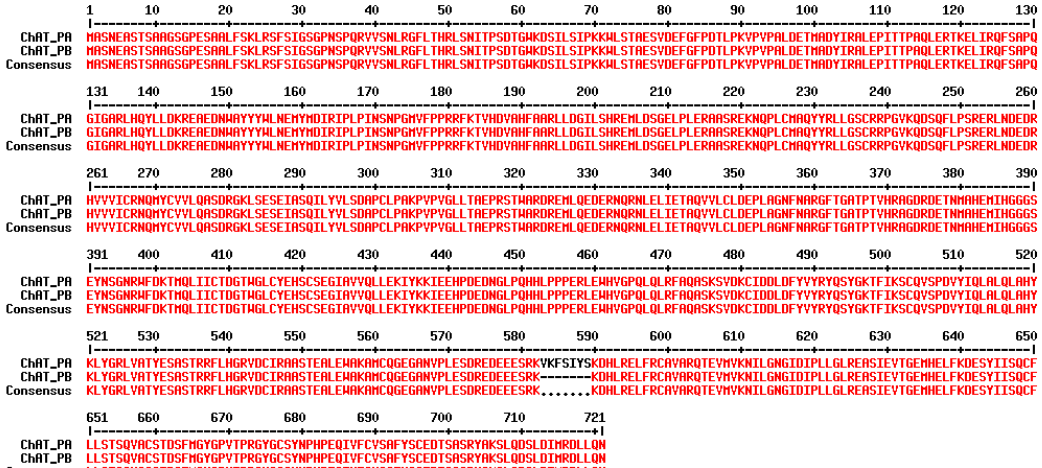

Figure. 5.0 Aliment of ChAT protein isoforms

ChAT_PA, the common type ChAT, has an extra 7 amino acid near the end, compared to ChAT-PB, the peripheral type ChAT.

In my study, the genetic components governing the expression of neurotransmitter has been examined. The first target neurotransmitters analysed were acetylcholine and glutamate, since these neurotransmitters were expressed by vMP2 interneuron and dMP2 motor neuron, respectively. Apart from that, the expression level of GABA, 5-hydroxytraptamine (5-HT, also known as serotonin) and tyrosine hydroxylase (TH, an enzyme responsible for the biosynthesis of L-3, 4-dihydroxyphenylalanine, the precursor of dopamine) relative to the activity of B52 were also examined.

5.2. Results

5.2.1. Reduction in 5-HT, but no difference in levels of ChAT, v-Glut or GABA when B52 activity is antagonised in *elavGal4* neurons in the ventral nerve cord (VNC) of 24hrs larval brains

The level of ChAT, v-Glut, GABA and 5-HT were examined by immunohistochemistry staining with corresponding antibodies in 24hrs larval brain where *BBS* was expressed with *elavGal4* in neurons (*UAS-BBS/+; elavGal4/+*). In most cases, two of the above mentioned primary antibodies were used together (different species), for the same group of larval brains, followed by stained with corresponding secondary antibodies. Larval brains of different genotypes were separated into two glass wells. The antibody solution was evenly separated (volume and concentration) into two from the same master mix. These brains were mounted in different areas on the same slide marked by ring-shaped tape based on genotypes. This methodology also applied to the other antibody stainings described subsequently.

To confirm the result, the staining was often repeated once or twice more using new samples, especially in cases where there was a difference in the phenotype. The number of samples (n=)

mentioned in the legend section of figures in this Chapter only corresponds to the number of samples prepared and stained at the same time relative to its counterpart(s), where results also show consistency with either the previous staining or one of the two previous stainings, i.e. the total number of samples stained with a specific antibody for one genotype is around twice more than that number if pilot staining (including stainings performed at different days between two or among three different genotypes) is also included. However, those samples were not included in "n=" for analysis, because the difference in preparation conditions may induce more variable factors. This applies to all antibody stainings.

The fluorescence intensity (FI) was measured with the ZEN software. The control and mutant line, for example *elavGal4* (III) control and *UAS-BBS/+; elavGal4/+*, were brought to the same Z level where a clear midline gap can be seen. Two circles of 100um^2 each were then drawn at the most posterior end (one on the left and one on the right side as separated by the midline) of the larval brain for intensity measurement. The average intensity value of the two areas was calculated and then used for t-test (assuming equal variance) between control and the mutant line. All the images shown below are superimposed images (or maximum z-stack projection).

Compared to *elavGal4* (III) control, the level of 5-HT (Fig. 5.4) is significantly lower in *UAS-BBS/+; elavGal4/+*. Levels of v-Glut (Fig. 5.2) appear to be the same between the two genotypes. More samples are needed to confirm the expression levels of ChAT (Fig. 5.1) and GABA (Fig5.3), where the sample population gives a biased result due to relatively large difference between mean and median values for the intensity of corresponding antibodies.

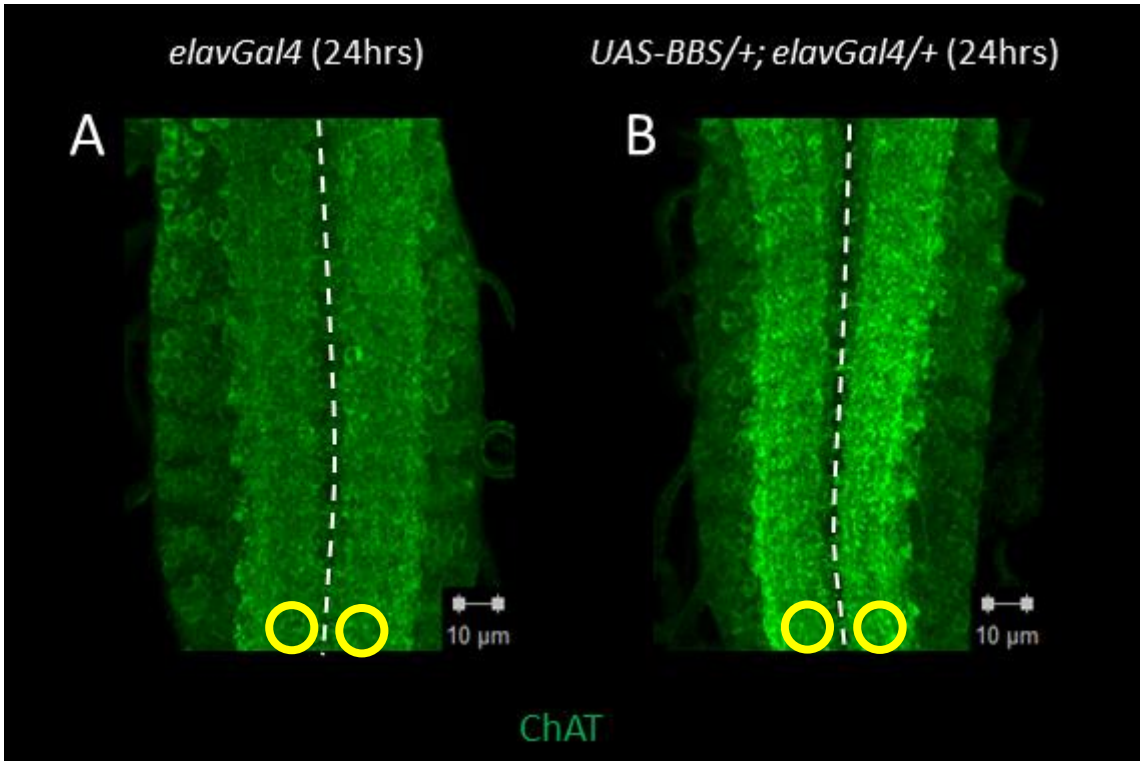

Figure. 5.1a ChAT staining of 24hrs larval brains

ChAT in green. Horizontal views, anterior up. Bar = 10um. Dotted line indicates the location of the ventral midline. Yellow circles indicate the areas taken for intensity measurement. (A) *elavGal4* (III) control (n=5) and (B) *UAS-BBS/+; elavGal4/+* (n=7).

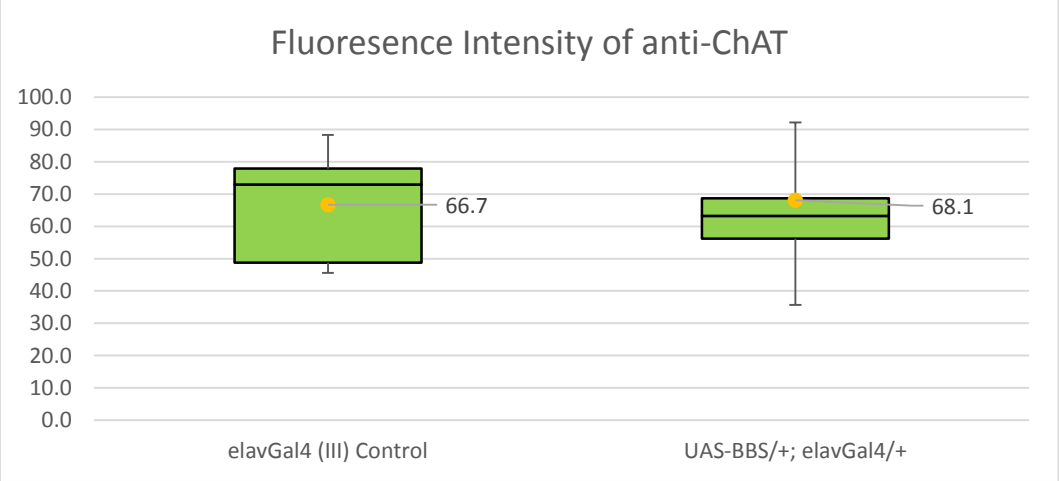

Figure. 5.1b Fluorescence intensity of anti-ChAT

Yellow dots represent mean value of intensity, and the middle line in the green box represents the median value which separates the populations in half. The level of ChAT on average appear to be higher in *UAS-BBS/+; elavGal4/+*, as indicated by the mean value represented by the yellow dots. However, the difference in intensity between *elavGal4* (III) control and *UAS-BBS/+; elavGal4/+* is not statistically significant (p=0.9065). In fact, more than 75% of samples from *UAS-BBS/+; elavGal4/+* do not reach the

average ChAT intensity (value of quartile 3, the top line of the box, is slightly higher than the yellow dot), and the high average intensity value is caused only by a small population (in this case 1 quarter of the total), as indicated by the top whisker (error bar). On the other hand, the mean and median values of ChAT intensity are rather close to each other for *elavGal4* (III) control samples, indicating the mean intensity indeed reflects the true value of the *elavGal4* (III) control. This somehow suggests the level of ChAT is lower in *UAS-BBS/+; elavGal4/+* compared to *elavGal4* (III) control. However, since there is a clear sign of bias from *UAS-BBS/+; elavGal4/+* (75% of population falls below mean value), more samples should be collected to confirm the phenotypes.

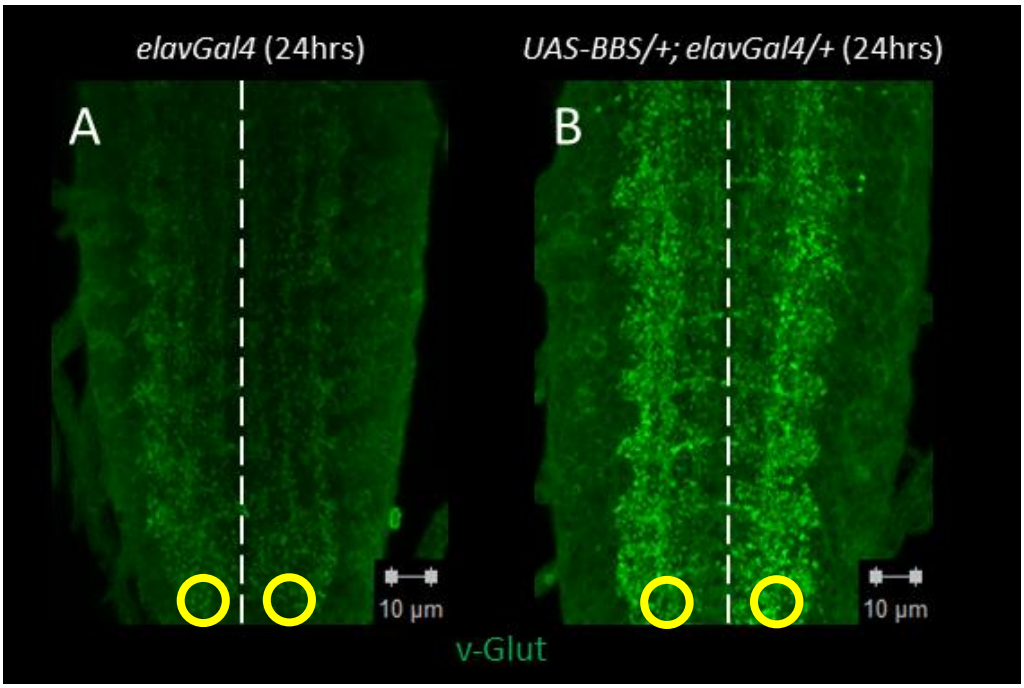

Figure. 5.2a v-Glut staining in 24hrs larval brains

v-Glut in green. Horizontal views, anterior up. Bar = 10um. Dotted line indicates the location of the ventral midline. (A-C) *elavGal4* control (n=6) and (D-F) *BBS/+; elavGal4/+* (n=7).

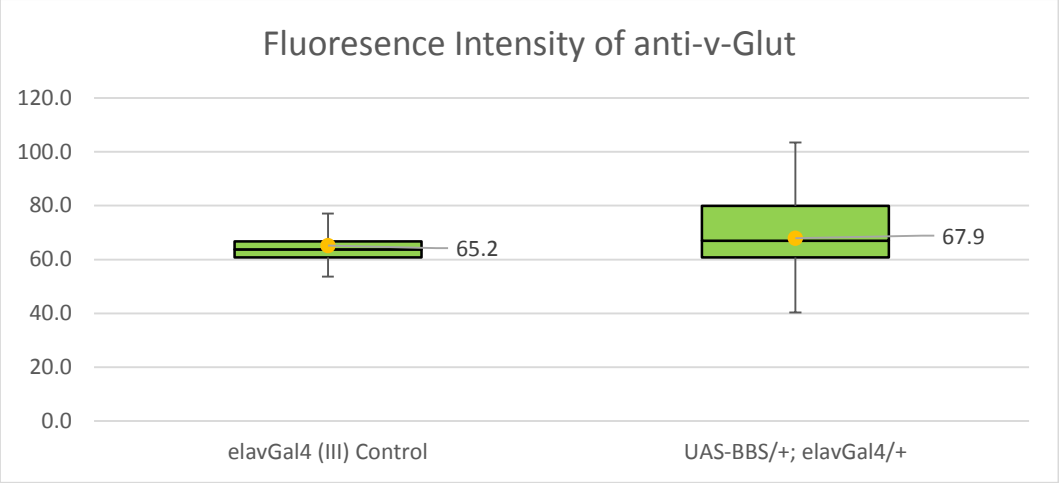

Figure. 5.2b Fluorescence intensity of anti-v-Glut

Yellow dots represent mean value of intensity, and the middle line in the green box represents the median value which separates the populations in half. The level of v-Glut is slightly higher in *UAS-BBS/+; elavGal4/+*. However, the difference in intensity between *elavGal4* (III) control and *UAS-BBS/+; elavGal4/+* is not statistically significant (p= 0.7221). This time the two mean values and median values of v-Glut intensity between the two different genotypes are more or less the same, respectively, indicating an even distribution, and an accurate reflection of v-Glut levels between the two genotypes.

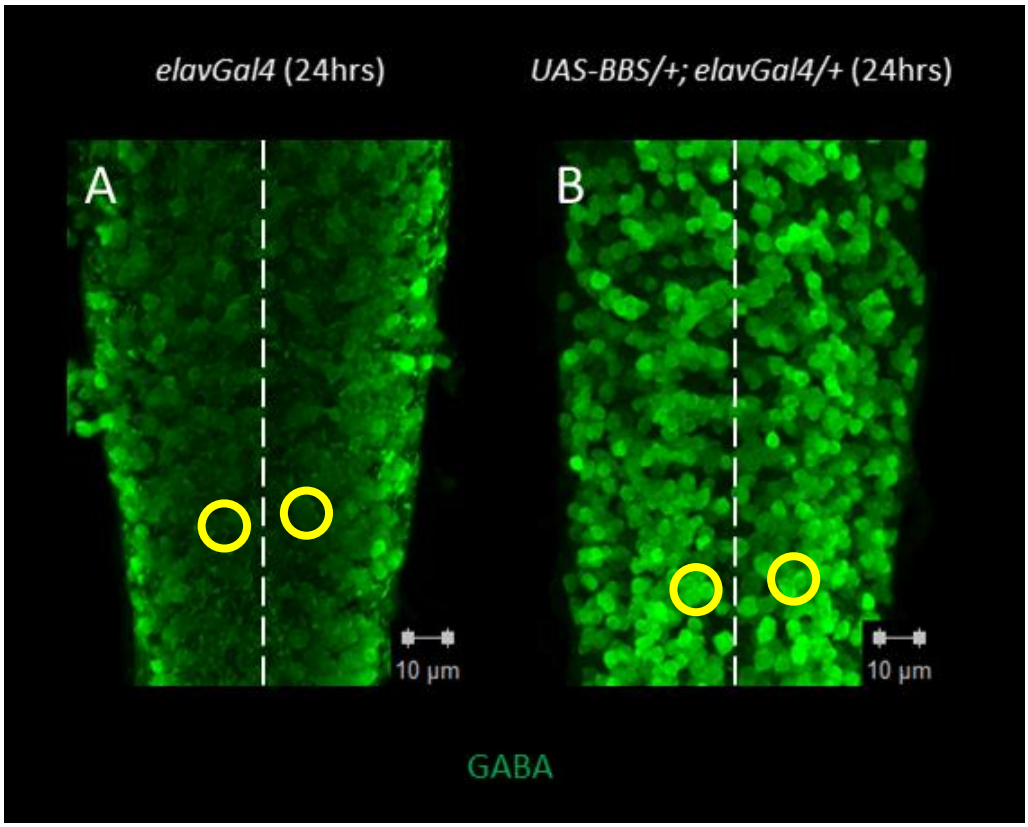

Figure. 5.3a GABA staining of 24hrs larval brains

GABA in green. Horizontal views, anterior up. Bar = 10um. Yellow circles indicate the areas taken for intensity measurement. (A) *elavGal4* control (n=4) and (B) *UAS-BBS/+; elavGal4/+* (n=4).

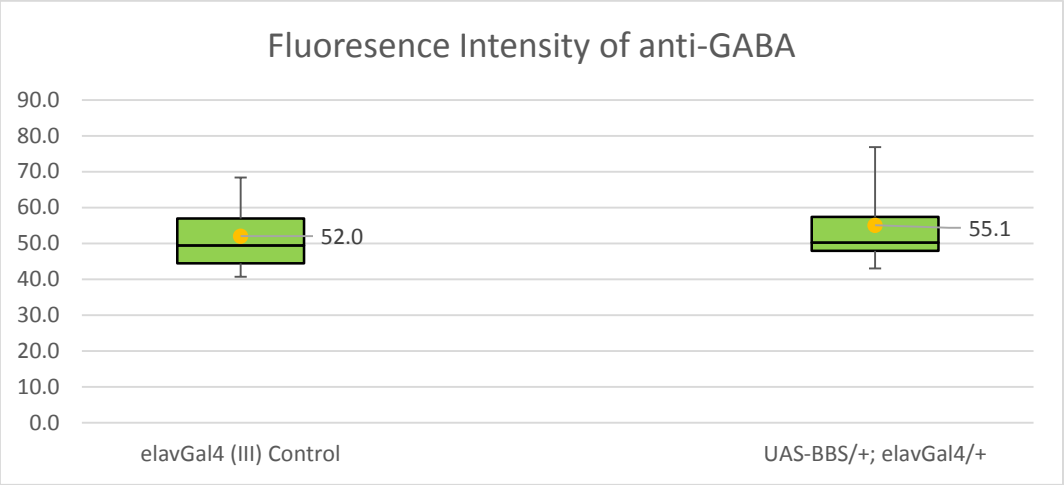

Figure. 5.3b Fluorescence intensity of anti-GABA

Yellow dots represent mean value of intensity, and the middle line in the green box represents the median value which separates the populations in half. The level of GABA is slightly higher in *UAS-BBS/+; elavGal4/+*. However, the difference in intensity between *elavGal4* (III) control and *UAS-BBS/+; elavGal4/+* is not statistically significant (p= 0.6880). Around 70% of samples from *UAS-BBS/+; elavGal4/+* falls below average ChAT level, indicating more samples should be collected to confirm the phenotypes.

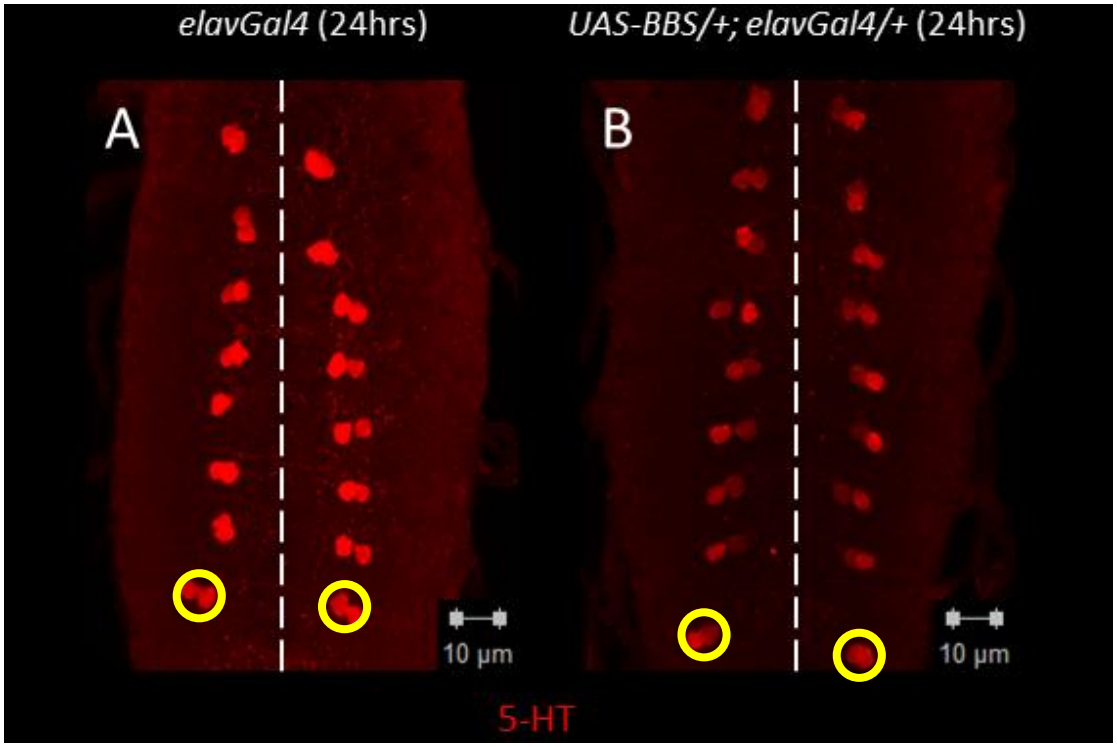

Figure. 5.4a 5-HT staining of 24hrs larval brains

5-HT in red. Horizontal views, anterior up. 1 unit scale bar = 10um. Dotted line indicates the location of midline. Yellow circles indicate the areas taken for intensity measurement. (A) *elavGal4* control (n=5) and (B) *UAS-BBS/+; elavGal4/+* (n=7).

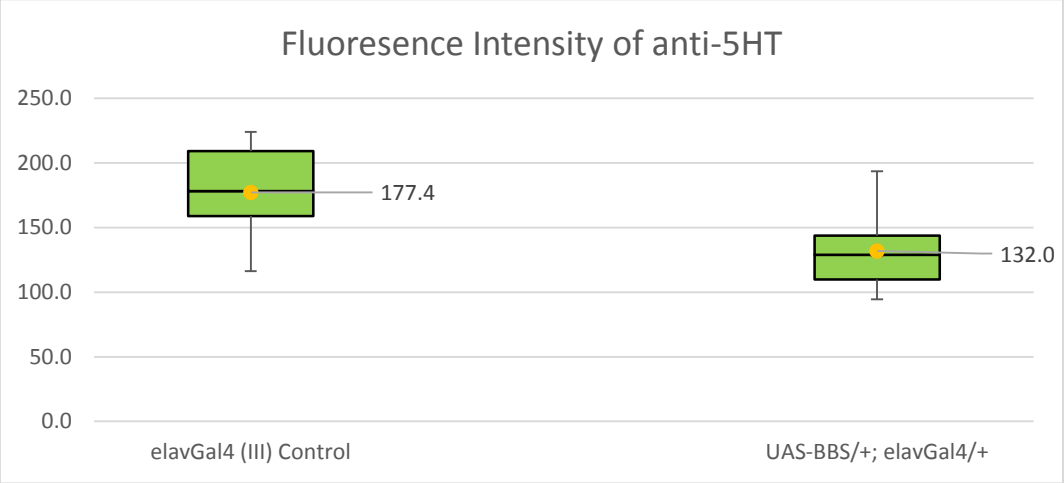

Figure. 5.4b Fluorescence intensity of anti-5-HT

Yellow dots represent mean value of intensity, and the middle line in the green box represents the median value which separates the populations in half. Compared to *elavGal4* (III) control, the level of 5-HT is significantly reduced in *UAS-BBS/+; elavGal4/+* (p=0.0319). The mean and median values are close to each other within both genotypes, indicating an unbiased sample collection. Therefore, the result accurately reflects levels of 5-HT between the two phenotypes.

5.2.2. No significant difference in levels of ChAT or 5-HT in 24hrs larval brains between p{lacW}B52 homozygous and heterozygous mutants

The level of ChAT and 5-HT were examined in 24hrs larval brains of *p{lacW}B52* homozygous mutant. Heterozygous mutant *p{lacW}B52/TM3*$^{Twi\text{-}GFP}$ was used as control.

There is no significant difference in levels of 5-HT (Fig. 5.6) between the two genotypes. More samples are needed to confirm the ChAT phenotype (Fig. 5.5) of *p{lacW}B52* homozygous control.

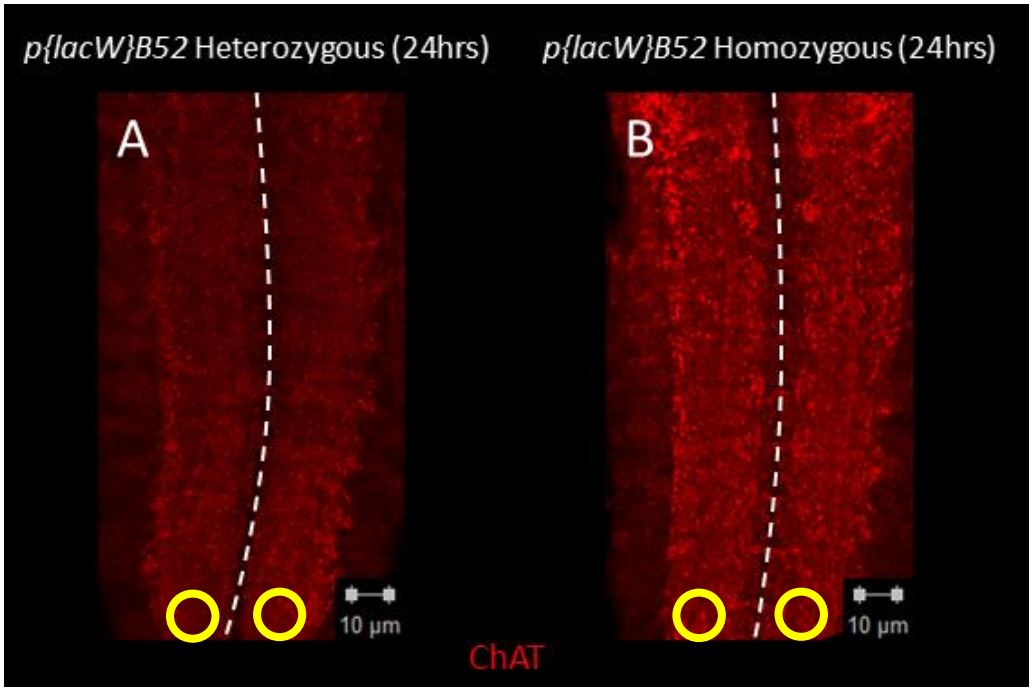

Figure. 5.5a ChAT staining of 24hrs larval brains

ChAT in red. Horizontal views, anterior up. Bar = 10um. Yellow circles indicate the areas taken for intensity measurement. (A) *p{lacW}B52/TM3*$^{Twi\text{-}GFP}$ control (n=8) and (DB) *p{lacW}B52* homozygous mutant (n=10).

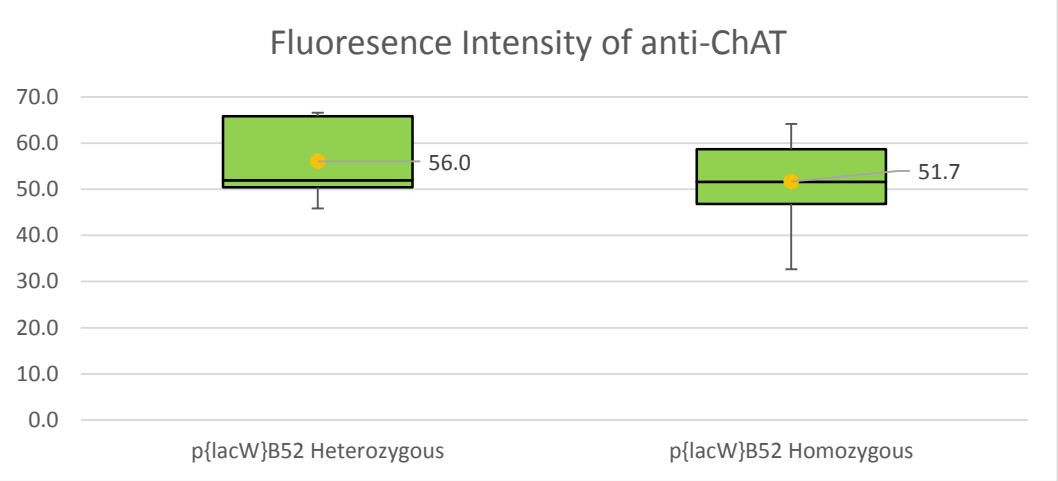

Figure. 5.5b Fluorescence intensity of anti-ChAT

Yellow dots represent mean value of intensity, and the middle line in the green box represents the median value which separates the populations in half. Compared to *p{lacW}B52* heterozygous control, the level of ChAT is reduced in *p{lacW}B52* homozygous mutants. However, the difference in intensity between *p{lacW}B52* heterozygous control and *p{lacW}B52* homozygous is not statistically significant (p= 0.3178). As indicated by the median and mean value of anti-ChAT intensity, more than half of the samples of *p{lacW}B52* heterozygous do not reach mean intensity value. This is similar to the previous

case with *elvaGla4* (III) control and *UAS-BBS/+; elavGal4/+*. Therefore more samples are needed to confirm the phenotype.

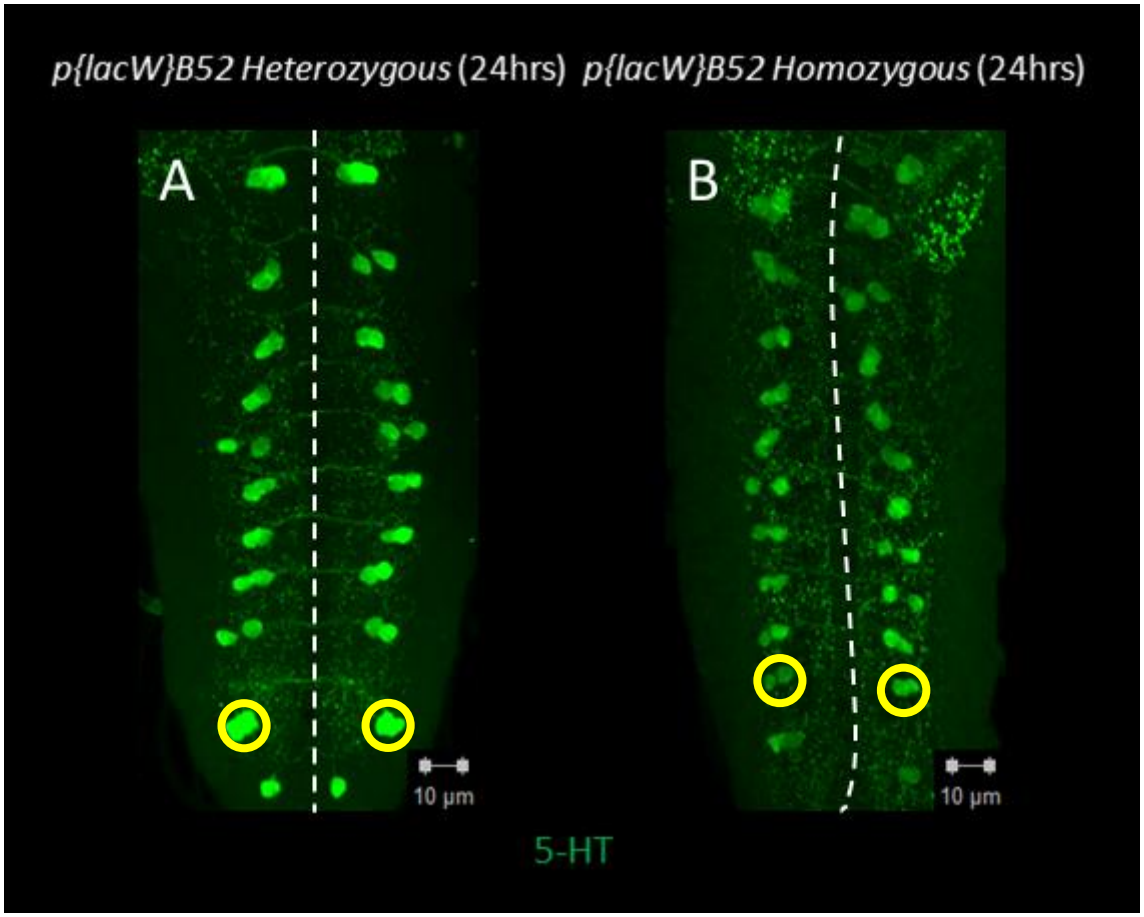

Figure. 5.6a 5-HT staining of 24hrs larval brains

5-HT in green. Horizontal views, anterior up. Bar = 10um. Dotted line indicates the location of midline. Yellow circles indicate the areas taken for intensity measurement. (A) *p{lacW}B52/TM3*$^{Twi\text{-}GFP}$ control (n=9) and (B) *p{lacW}B52* homozygous mutant (n=10).

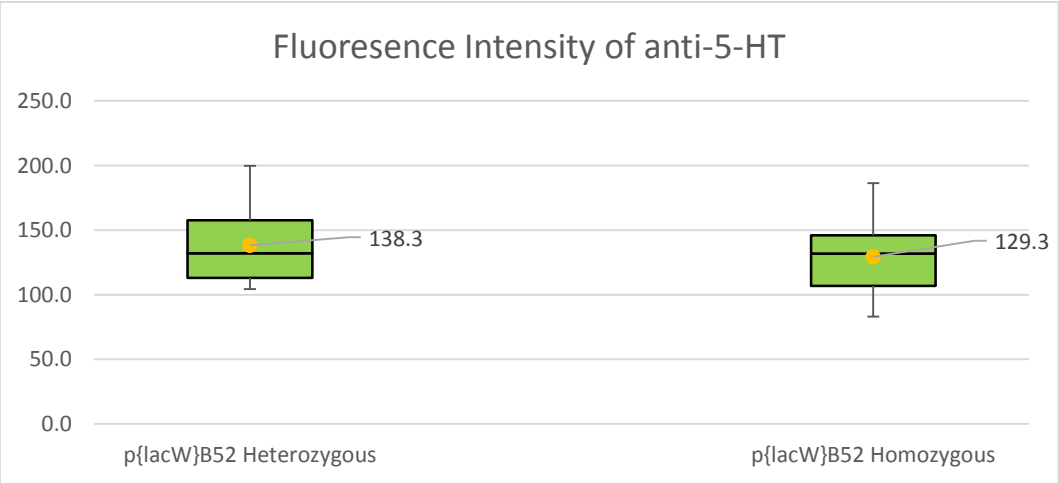

Figure. 5.6b Fluorescence intensity of anti-5-HT

Yellow dots represent mean value of intensity, and the middle line in the green box represents the median value which separates the populations in half. Despite a slightly higher mean intensity value of anti-5-HT for *p{lacW}B52* heterozygous, the median value is in fact below that of *p{lacW}B52* homozygous mutants. This suggests the level of 5-HT is likely to be the same between the two genotypes (p= 0.6021).

5.2.3. No significant difference in ChAT or v-Glut level in 48hrs larval brain when *B52* is overexpressed in *elavGal4* neurons

The levels of ChAT and v-Glut were examined in 48hrs larval brains where *B52* was overexpressed with *elavGal4* in neurons (*elavGal4/+; ; UAS-GFP-B52/+*).

Levels of both ChAT (Fig. 5.7) and v-Glut (Fig. 5.8) are the same, respectively, between *elavGal4/+; ; UAS-GFP-B52/+* and *elavGal4* (X) control.

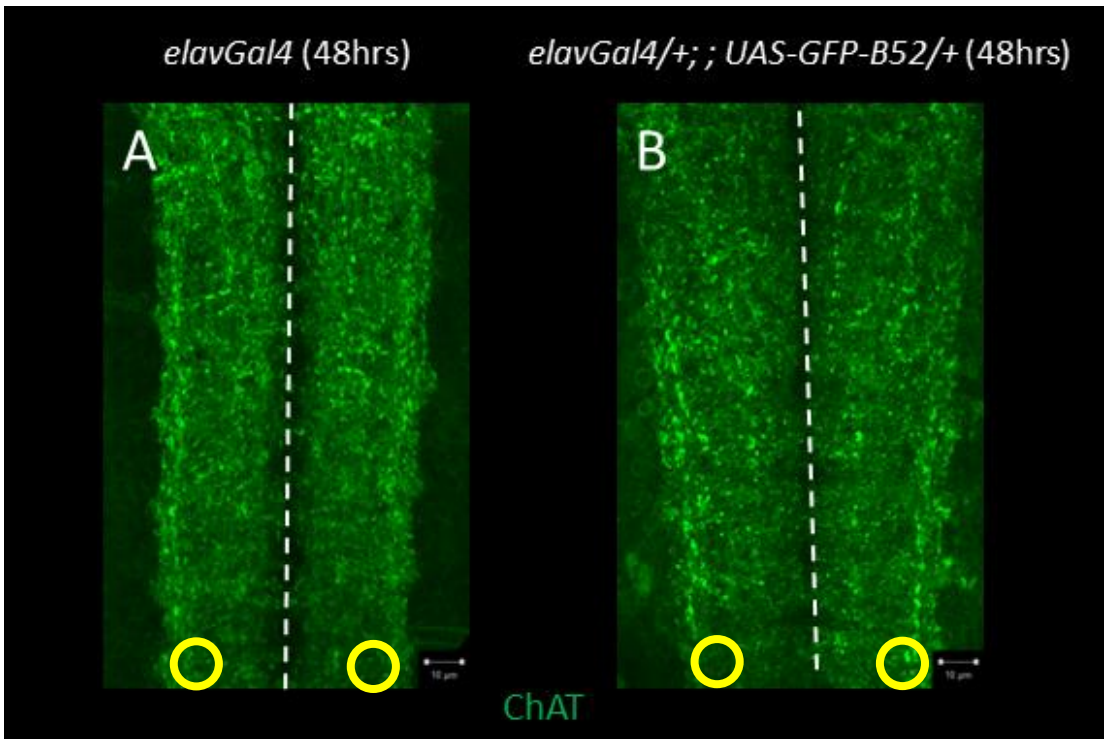

Figure. 5.7a ChAT staining of 48hrs larval brains

ChAT in green. Horizontal views, anterior up. Bar = 10um. Dotted line indicates the location of midline. Yellow circles indicate the areas taken for intensity measurement. (A) *elavGal4* control (n=3) and (B) *elavGal4/+; ; UAS-GFP-B52/+* (n=3).

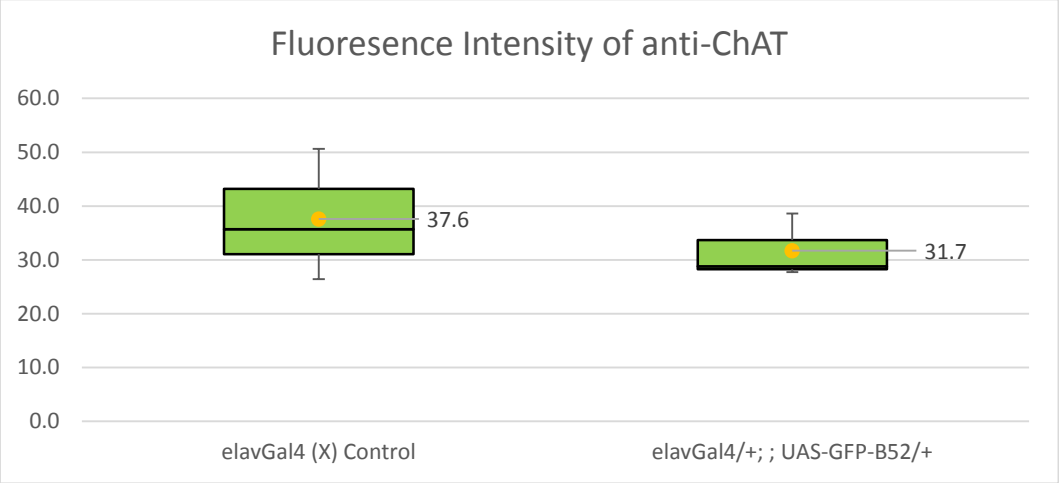

Figure. 5.7b Fluorescence intensity of anti-ChAT

Yellow dots represent mean value of intensity, and the middle line in the green box represents the median value which separates the populations in half (median value overlaps with Q1 in this case). Regardless of a relatively biased sample population for *elavGal4/+; ; UAS-GFP-B52/+*, since both the mean and median values for anti-ChAT intensity are lower in *elavGal4/+; ; UAS-GFP-B52/+* than those in *elavGal4* (X) control, the level of ChAT is indeed lower in *elavGal4/+; ; UAS-GFP-B52/+*. However, the difference in intensity between *elavGal4* (X) control and *elavGal4/+; ; UAS-GFP-B52/+* is not statistically significant (p= 0.4962).

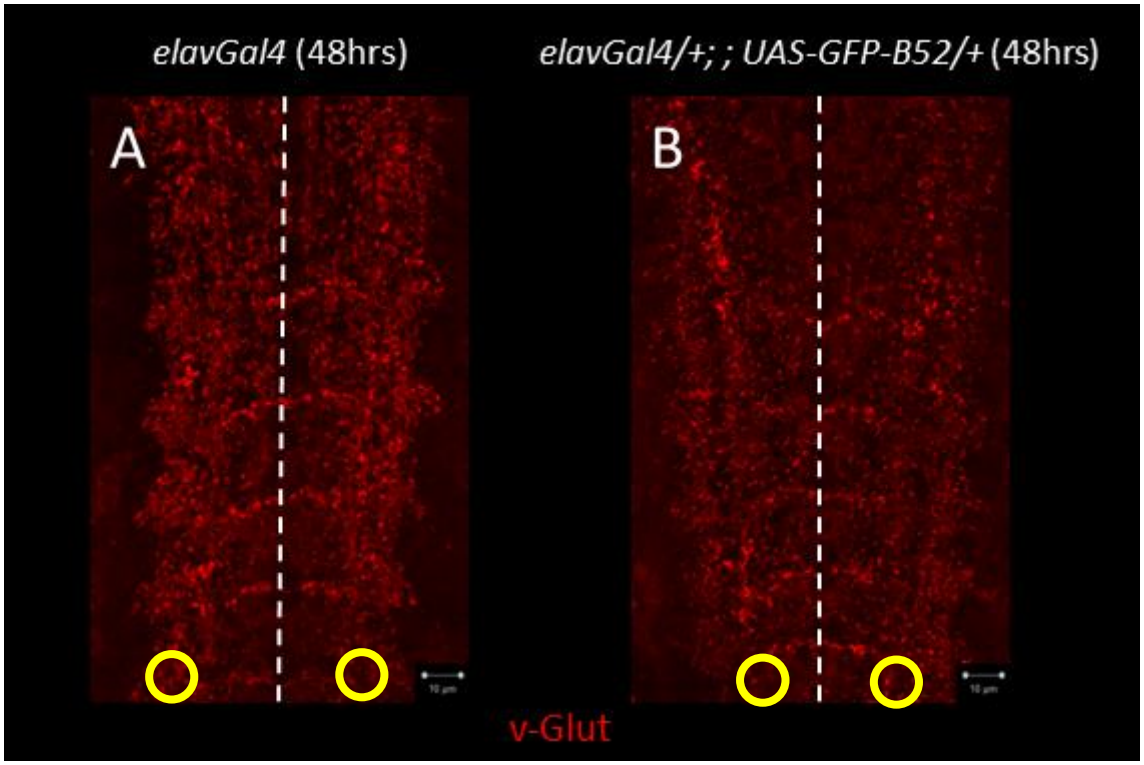

Figure. 5.8a v-Glut staining of 48hrs larval brains

v-Glut in red. Horizontal views, anterior up. Bar = 10um. Dotted line indicates the location of midline. Yellow circles indicate the areas taken for intensity measurement. (A) *elavGal4* control (n=3) and (B) *elavGal4/+; ; UAS-GFP-B52/+* (n=3).

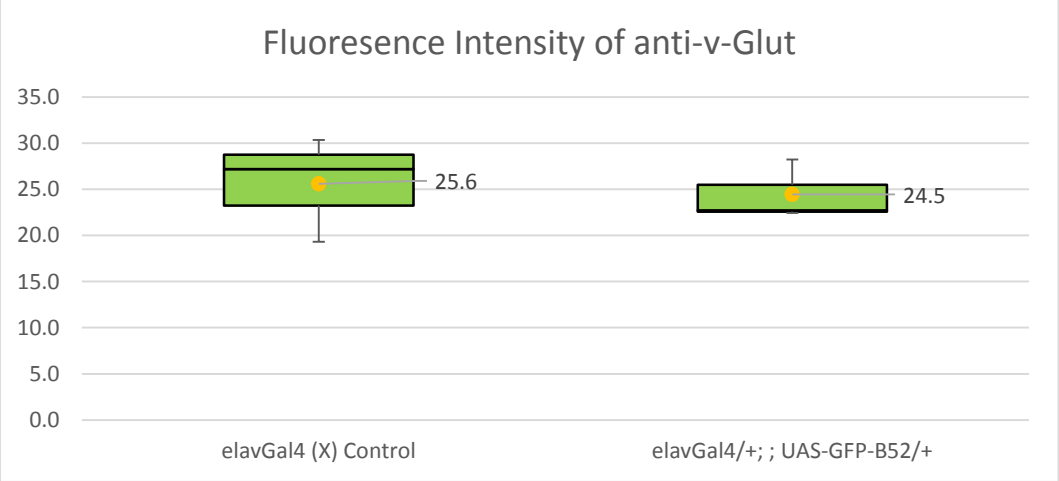

Figure. 5.8b Fluorescence intensity of anti-v-Glut

Yellow dots represent mean value of intensity, and the middle line in the green box represents the median value which separates the populations in half (median value overlaps with Q1 in this case). Regardless of a relatively biased sample population for *elavGal4/+; ; UAS-GFP-B52/+*, since the median value for anti-v-Glut intensity is lower in *elavGal4/+; ; UAS-GFP-B52/+* than those in *elavGal4* (X) control, plus the mean values of intensity are more or less the same between the two genotypes, this suggests

the level of v-Glut is slightly lower in *elavGal4/+; ; UAS-GFP-B52/+*. However, as indicated by T-test, levels of v-Glut are in fact the same between *elavGal4/+; ; UAS-GFP-B52/+*. and *elavGal4* (X) control (p= 0.7762).

5.2.4. No significant differences in levels of ChAT, v-Glut, GABA, 5-HT and TH are observed in 72hrs larval brains when *B52* is overexpressed maternally

Levels of ChAT, v-Glut, GABA, 5-HT and TH were examined in 72hrs larval brains where *B52* was overexpressed from maternal stages onwards (*$Gal4^{V2h}$/+; ; UAS-GFP-B52/+*). *$Gal4^{V2h}$* was used as control.

Compared to the *$Gal4^{V2h}$* control, levels of ChAT, v-Glut, 5-HT and TH are slightly reduced in *$Gal4^{V2h}$ /+; ; UAS-GFP-B52/+*, although none of the differences are statistically significant. Levels of GABA were more or less the same between the two. levels of GABA are more or less the same between the two genotypes. (Fig. 5.9 to Fig. 5.13)

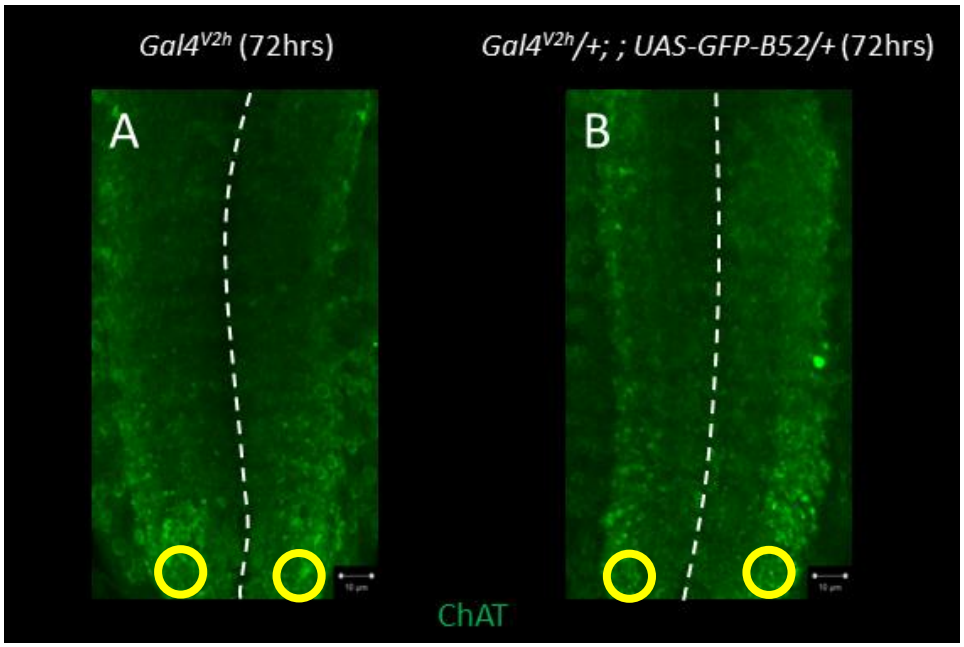

Figure. 5.9a ChAT staining of 72hrs larval brains

ChAT in green. Horizontal views, anterior up. Bar = 10um. Dotted line indicates the location of midline. Yellow circles indicate the areas taken for intensity measurement. (A) *Gal4^{V2h}* control (n=3) and (B) *Gal4^{V2h} /+; ; UAS-GFP-B52* (n=3).

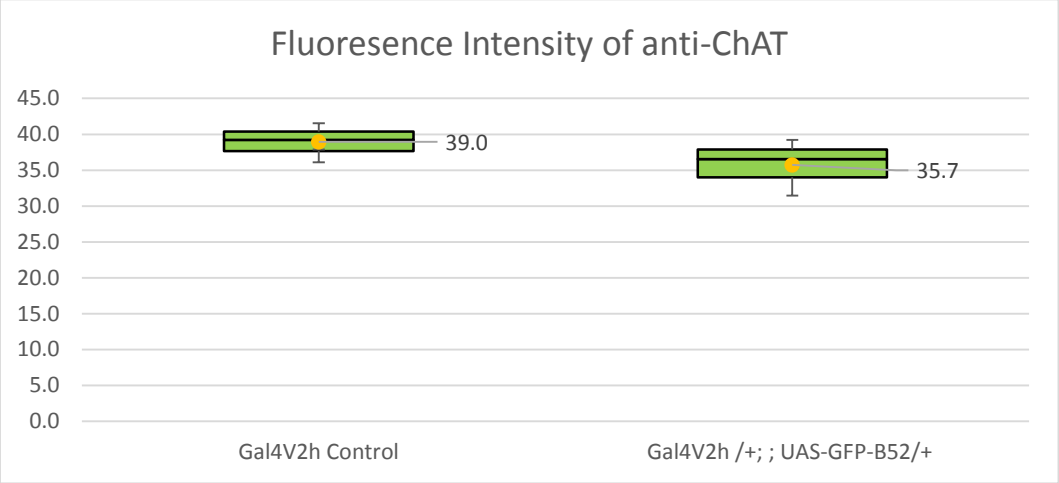

Figure. 5.9b Fluorescence intensity of anti-ChAT

Yellow dots represent mean value of intensity, and the middle line in the green box represents the median value which separates the populations in half. The level of ChAT is slightly lower in *Gal4^{V2h} /+; ; UAS-GFP-B52*. However, the difference in intensity between *Gal4^{V2h}* control and *Gal4^{V2h} /+; ; UAS-GFP-B52* is not statistically significant (p= 0.3087).

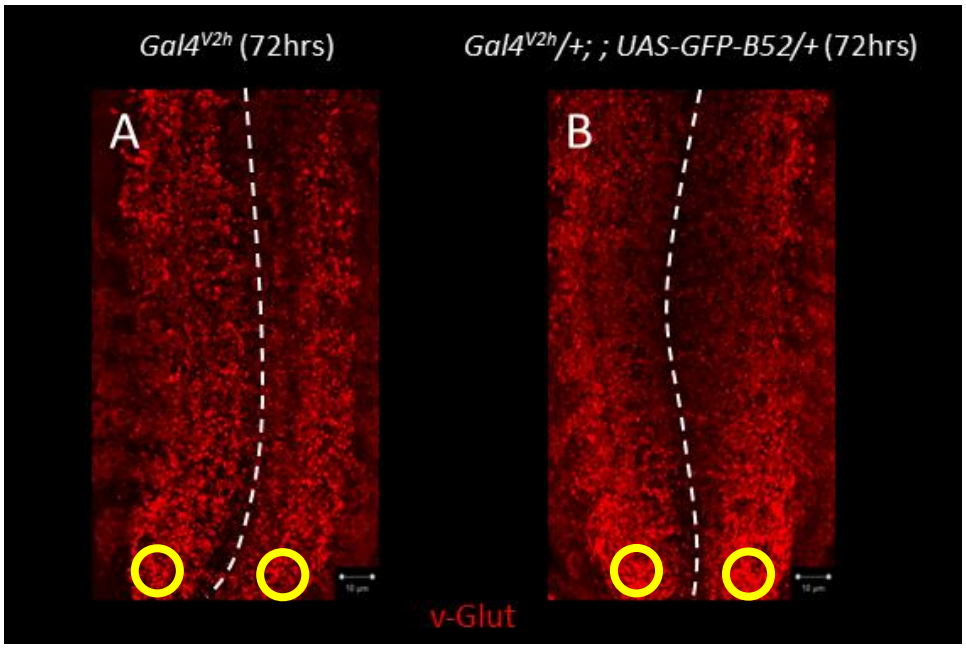

Figure. 5.10a Anti-v-Glut staining of 72hrs larval brains

v-Glut in red. Horizontal views, anterior up. Bar = 10um. Dotted line indicates the location of midline. Yellow circles indicate the areas taken for intensity measurement. (A) *Gal4^{V2h}* control (n=3) and (B) *Gal4^{V2h} /+; ; UAS-GFP-B52* (n=3).

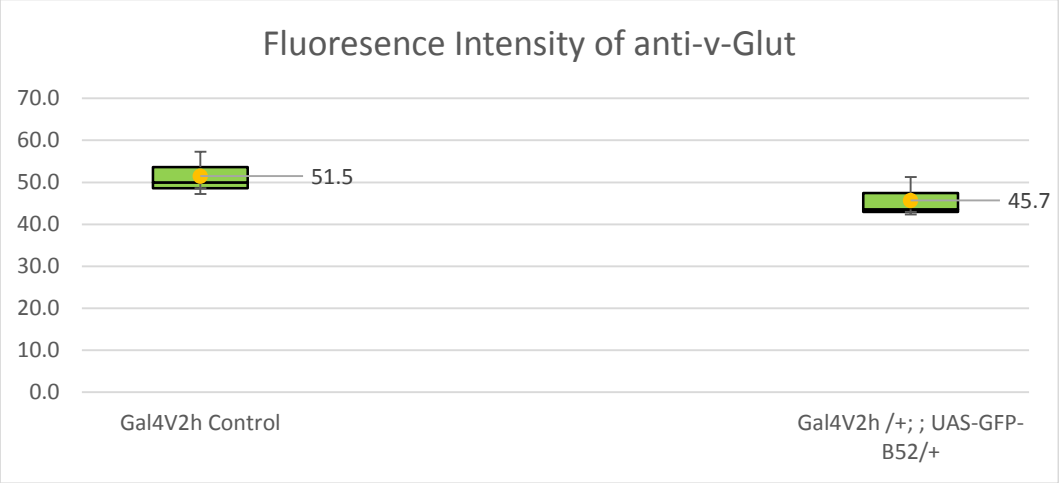

Figure. 5.10b Fluorescence intensity of anti-v-Glut

Yellow dots represent mean value of intensity, and the middle line in the green box represents the median value which separates the populations in half (median value overlaps with Q1 in this case). The level of v-Glut is slightly lower in *Gal4^{V2h} /+; ; UAS-GFP-B52*. However, the difference in intensity between *Gal4^{V2h}* control and *Gal4^{V2h} /+; ; UAS-GFP-B52* is not statistically significant (p= 0.2333).

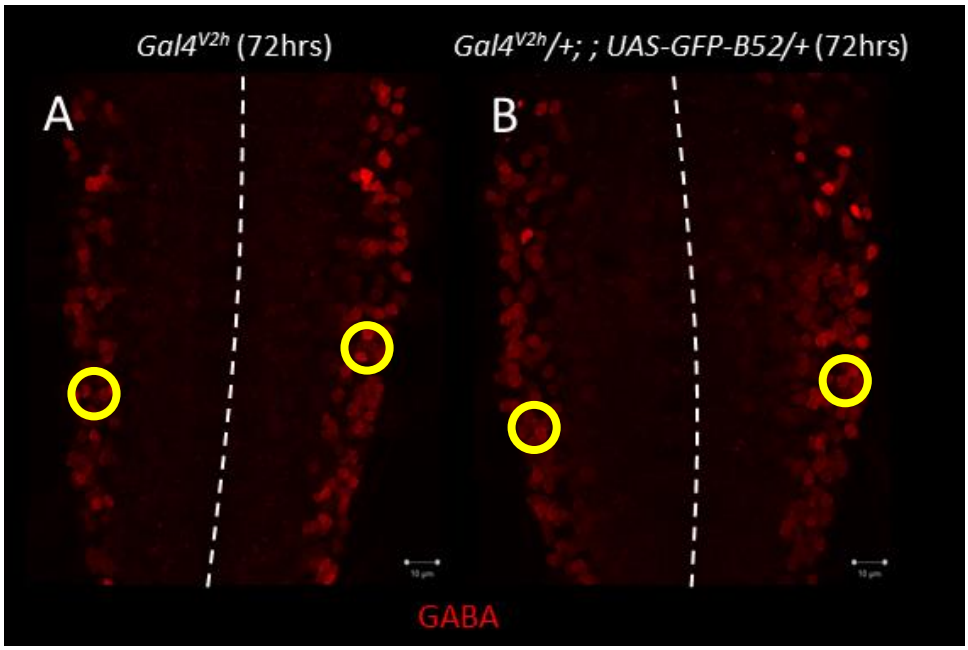

Figure. 5.11a GABA staining of 72hrs larval brains

GABA in red. Horizontal views, anterior up. Bar = 10um. Dotted line indicates the location of midline. (A-C) *Gal4^{V2h}* control (n=3) and (D-F) *Gal4^{V2h} /+; ; UAS-GFP-B52* (n=3).

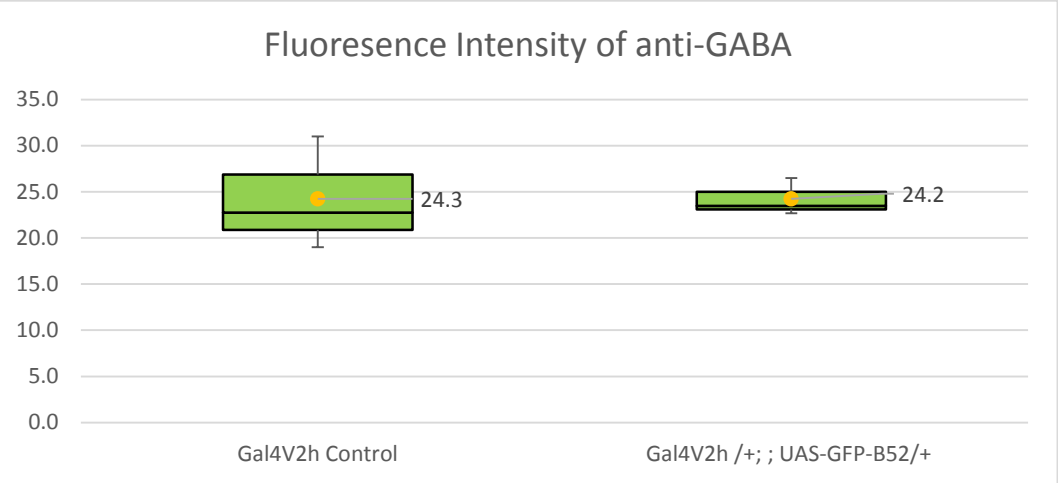

Figure. 5.11b Fluorescence intensity of anti-GABA

Yellow dots represent mean value of intensity, and the middle line in the green box represents the median value which separates the populations in half (median value overlaps with Q1 in this case). Levels of GABA are more or less the same between *Gal4^{V2h} /+; ; UAS-GFP-B52* and *Gal4^{V2h}* control (p=0.9946).

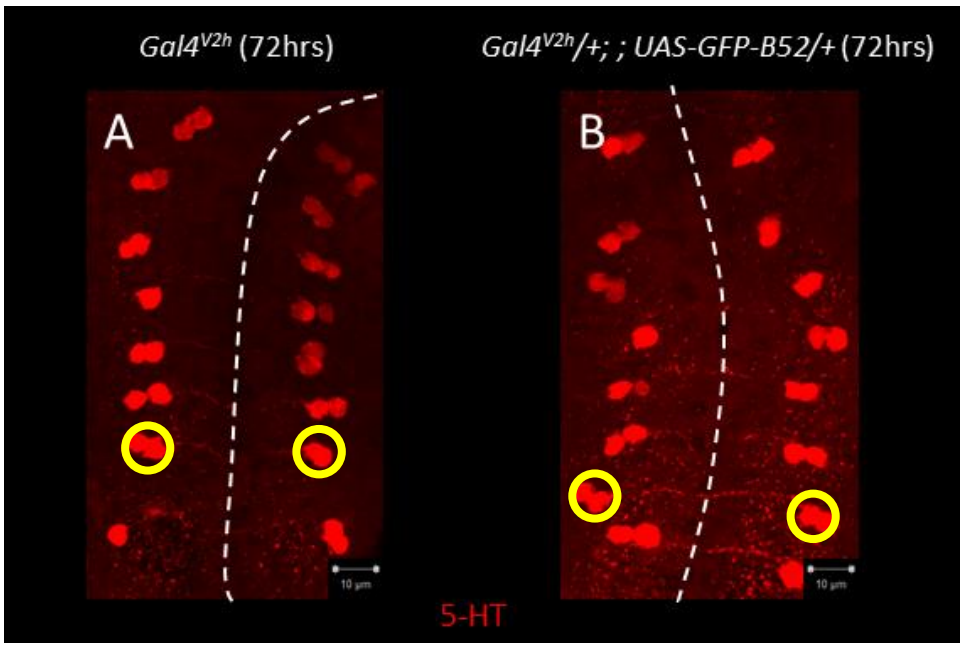

Figure. 5.12a 5-HT staining of 72hrs larval brains

5-HT in red. Horizontal views, anterior up. Bar = 10um. Dotted line indicates the location of midline. (A-C) *Gal4^{V2h}* control (n=3) and (D-F) *Gal4^{V2h} /+; ; UAS-GFP-B52* (n=3).

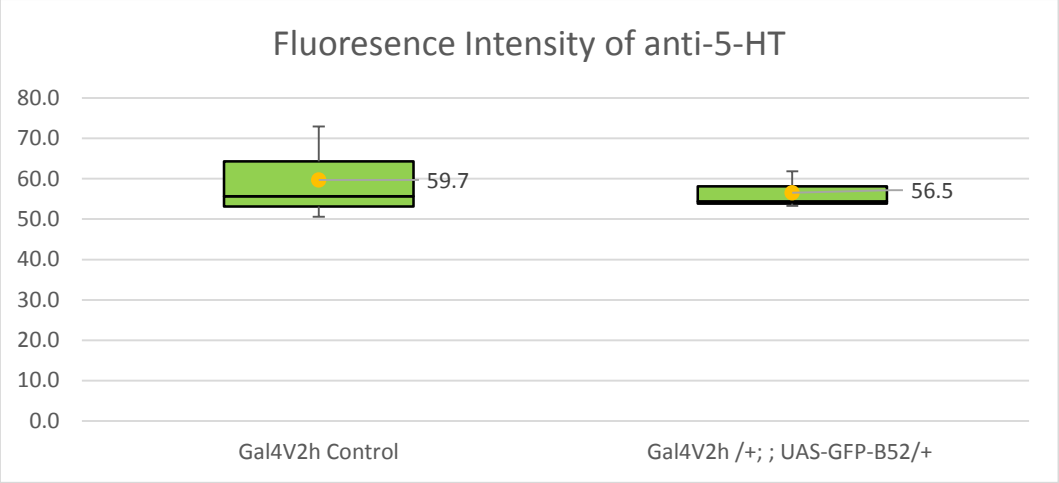

Figure. 5.12b Fluorescence intensity of anti-5-HT

Yellow dots represent mean value of intensity, and the middle line in the green box represents the median value which separates the populations in half (median value overlaps with Q1 in this case). The level of 5-HT is slightly lower in *Gal4^{V2h} /+; ; UAS-GFP-B52*. However, the difference in intensity between *Gal4^{V2h}* control and *Gal4^{V2h} /+; ; UAS-GFP-B52* is not statistically significant (p= 0.6794).

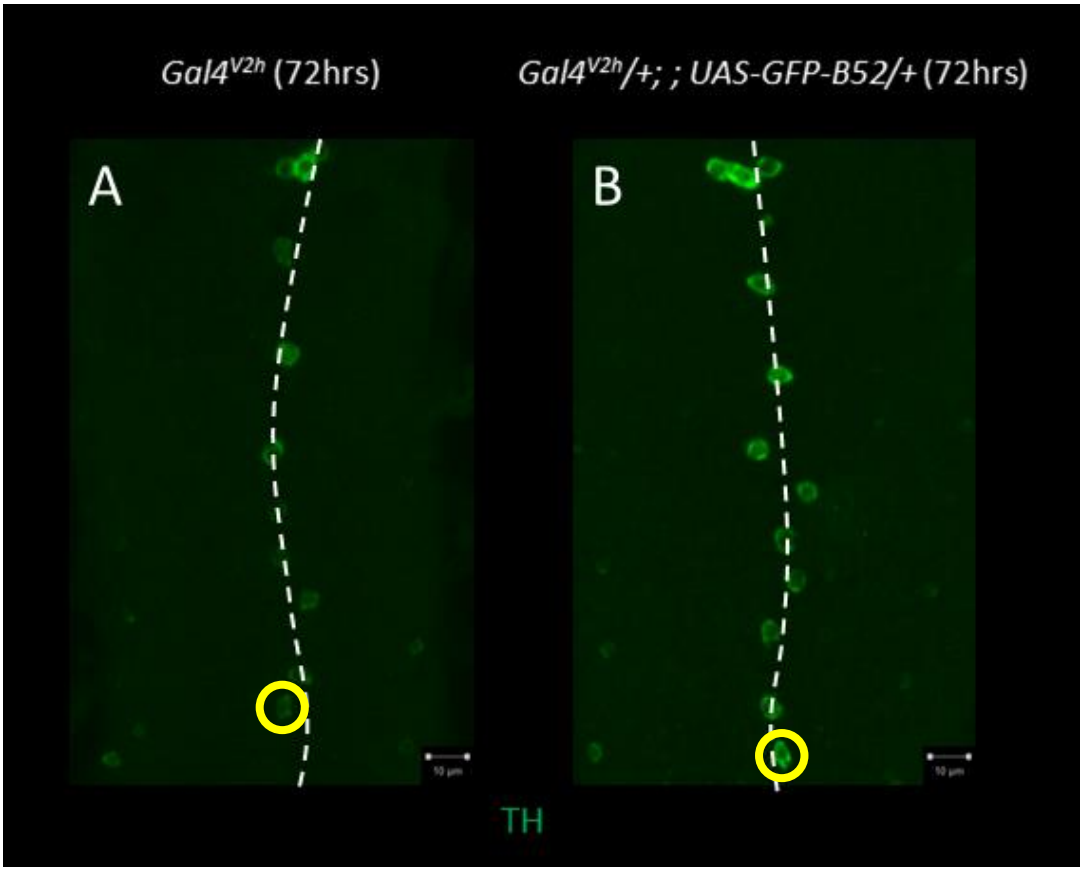

Figure. 5.13a TH staining of 72hrs larval brains

TH in green. Horizontal views, anterior up. Bar = 10um. Dotted line indicates the location of midline. (A-C) *Gal4^{V2h}* control (n=3) and (D-F) *Gal4^{V2h} /+; ; UAS-GFP-B52* (n=3).

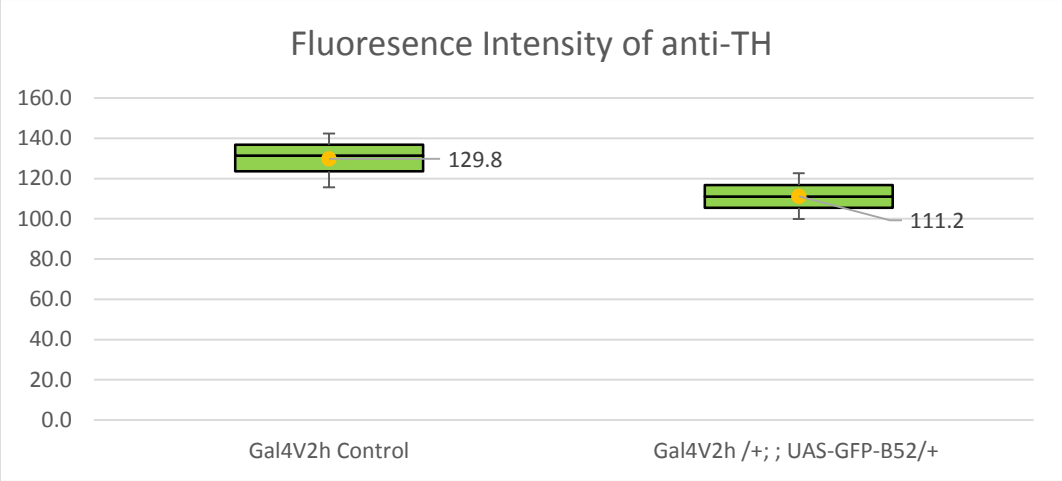

Figure. 5.13b Fluorescence intensity of anti-TH

Yellow dots represent mean value of intensity, and the middle line in the green box represents the median value which separates the populations in half. The level of TH is lower in *Gal4^{V2h} /+; ; UAS-GFP-B52*. However, the difference in intensity between *Gal4^{V2h}* control and *Gal4^{V2h} /+; ; UAS-GFP-B52* is not statistically significant (p= 0.1404).

5.2.5. No significant differences in levels of ChAT, v-Glut, GABA, 5-HT and TH are observed in 72hrs larval brains when *B52-RNAi* was induced maternally

Levels of ChAT, v-Glut, GABA, 5-HT and TH were examined in 72hrs larval brain of *Gal4^{V2h}/+; ; UAS-B52-TRiP-RNAi/+*. *Gal4^{V2h}* was used as control.

Compared to *Gal4^{V2h}* control, levels of ChAT (Fig. 5.14) and v-Glut (Fig. 5.15) are slightly higher in *Gal4^{V2h} /+; ; UAS-GFP-B52/+*, although none of the differences is statistically significant. More samples are needed to confirm the phenotypes for GABA, 5-HT and TH (Fig. 5.16 to Fig. 5.18).

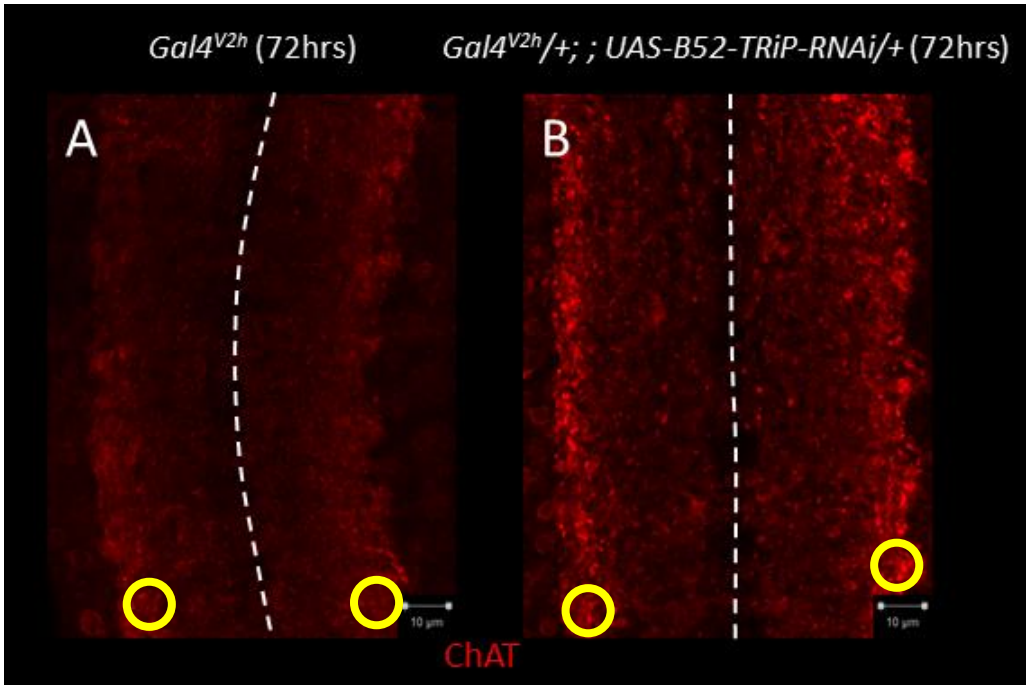

Figure. 5.14a ChAT staining of 72hrs larval brains

ChAT in red. Horizontal views, anterior to the left. Bar = 10um. Dotted line indicates the location of midline. Yellow circles indicate the areas taken for intensity measurement. (A) *Gal4^{V2h}* control (n=3) and (B) *Gal4^{V2h}/+; ; UAS-B52-TRiP-RNAi/+* (n=3).

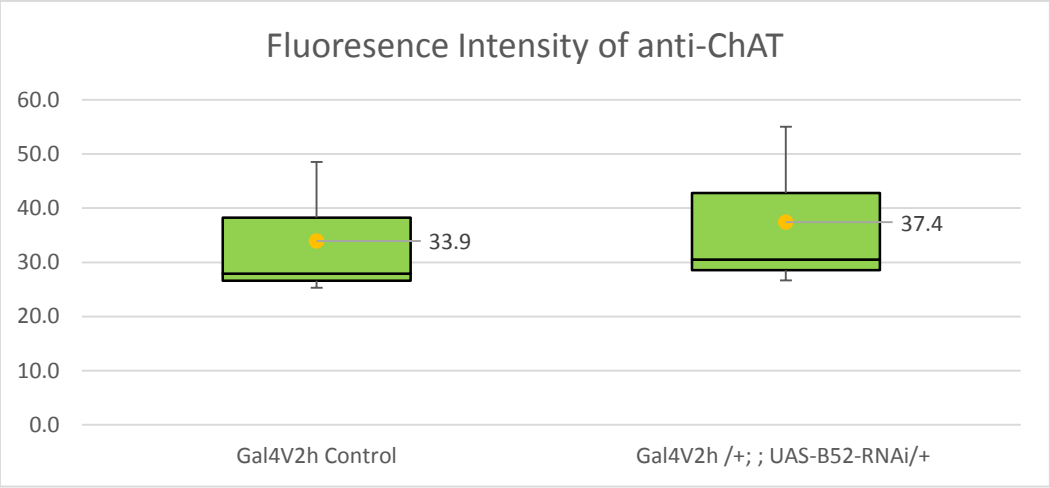

Figure. 5.14b Fluorescence intensity of anti-ChAT

Yellow dots represent mean value of intensity, and the middle line in the green box represents the median value which separates the populations in half. The level of ChAT is slightly higher in *Gal4^{V2h}/+; ; UAS-GFP-B52*. However, the difference in intensity between *Gal4^{V2h}* control and *Gal4^{V2h}/+; ; UAS-B52-RNAi* is not statistically significant (p= 0.7778). Although both sample population show biased distribution, the overall patterns are similar between them, i.e. towards higher intensity. Therefore, the result is relatively accurate.

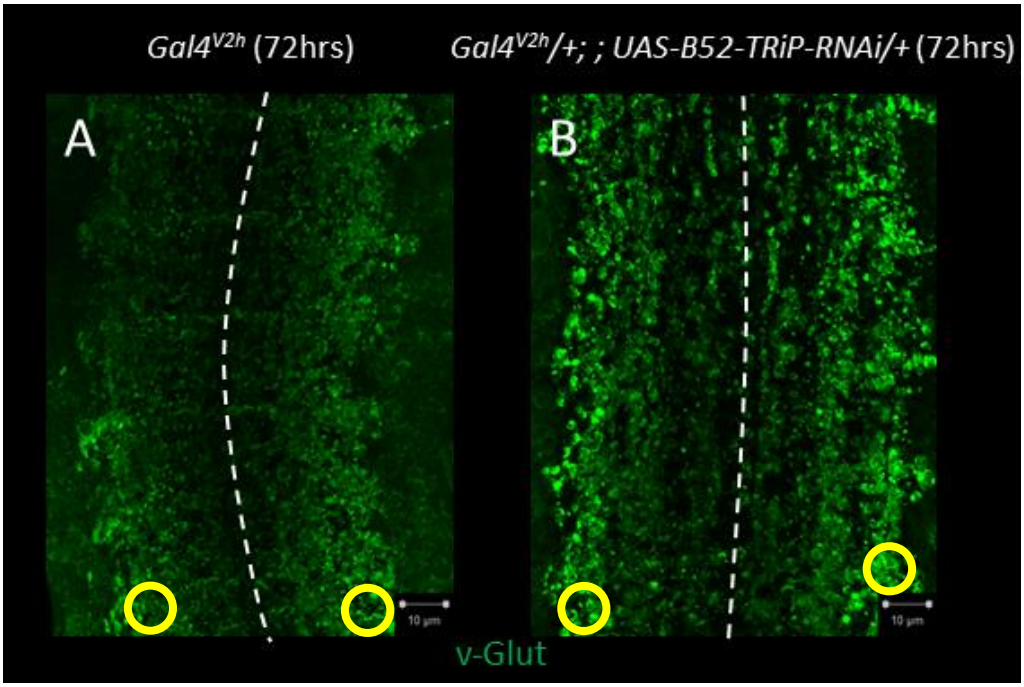

Figure. 5.15a v-Glut staining of 72hrs larval brains

v-Glut in green. Horizontal views, anterior to the left. Bar = 10um. Dotted line indicates the location of midline. Yellow circles indicate the areas taken for intensity measurement. (A) *Gal4^{V2h}* control (n=3) and (B) *Gal4^{V2h}/+; ; UAS-B52-TRiP-RNAi/+* (n=3).

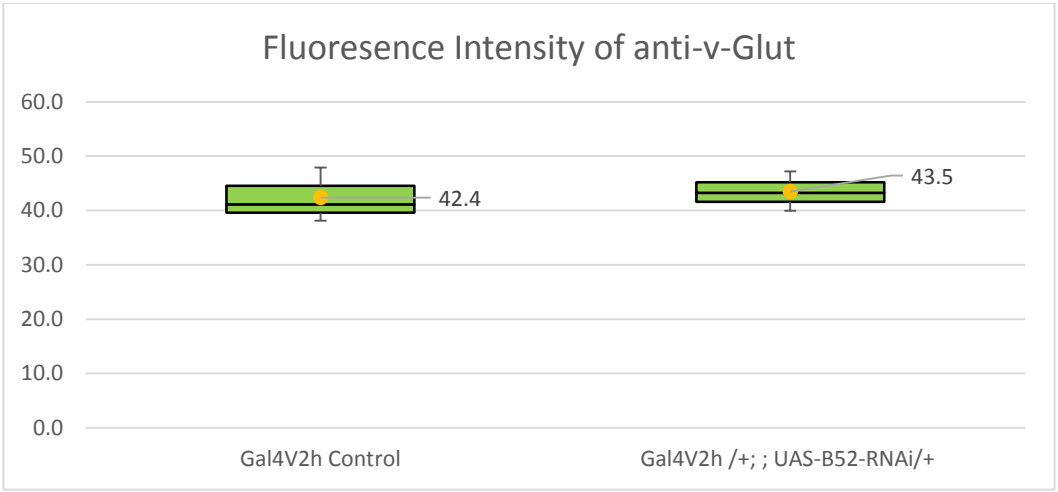

Figure. 5.15b Fluorescence intensity of anti-v-Glut

Yellow dots represent mean value of intensity, and the middle line in the green box represents the median value which separates the populations in half. The level of v-Glut is more or less the same between *Gal4^{V2h}/+; ; UAS-B52-RNAi* and *Gal4^{V2h}* control (p= 0.7769).

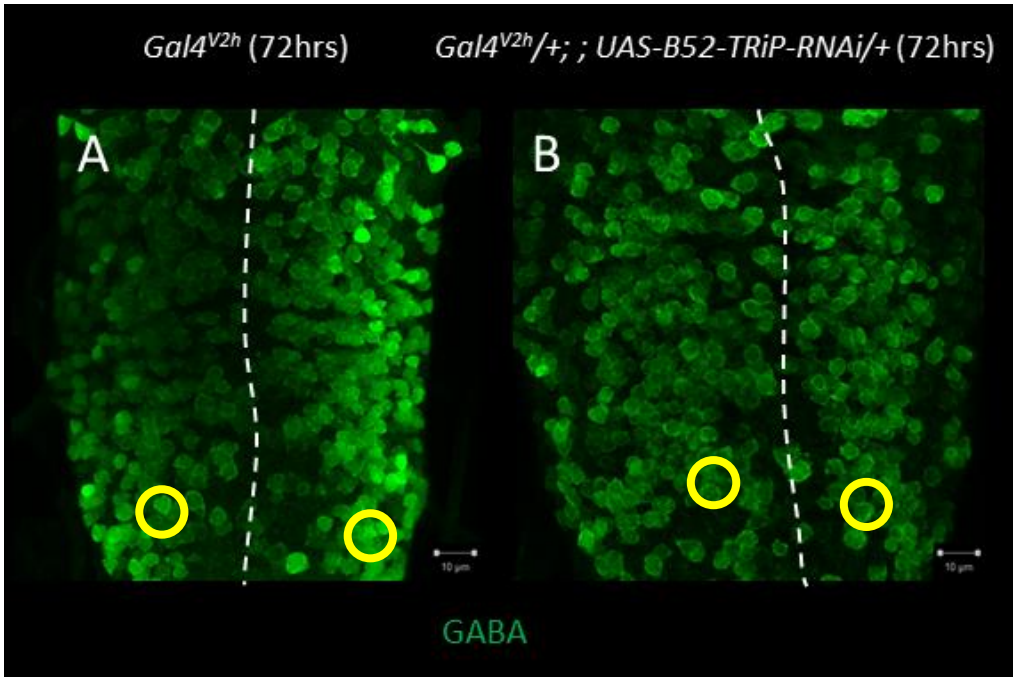

Figure. 5.16a GABA staining of 72hrs larval brains

GABA in green. Horizontal views, anterior to the left. Bar = 10um. Dotted line indicates the location of midline. Yellow circles indicate the areas taken for intensity measurement. (A) *Gal4^{V2h}* control (n=3) and (B) *Gal4^{V2h}/+; ; UAS-B52-TRiP-RNAi/+* (n=3).

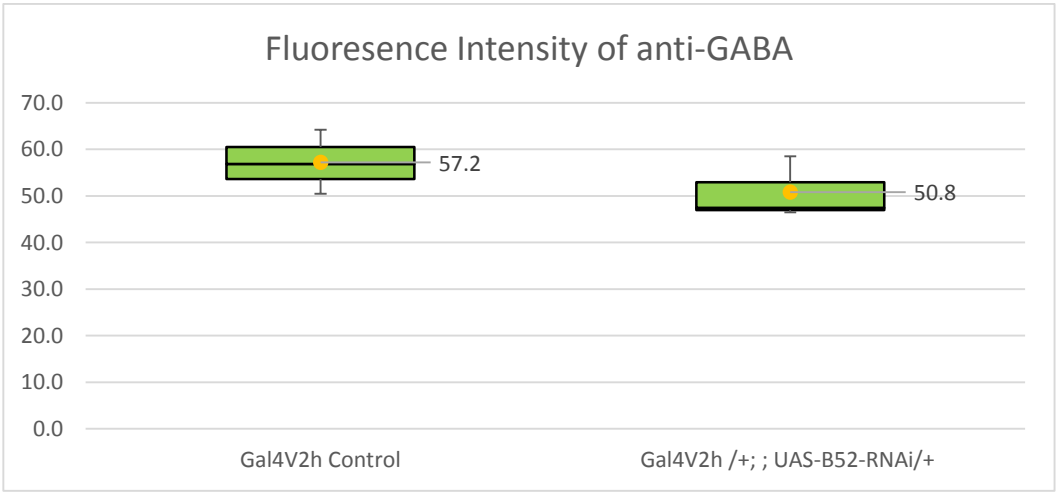

Figure. 5.16b Fluorescence intensity of anti-GABA

Yellow dots represent mean value of intensity, and the middle line in the green box represents the median value which separates the populations in half (median value overlaps with Q1 in this case). The level of GABA is slightly reduced in *Gal4^{V2h}/+; ; UAS-B52-RNAi*. However, the difference in intensity between *Gal4^{V2h}* control and *Gal4^{V2h}/+; ; UAS- B52-RNAi* is not statistically significant (p= 0.3141). Because the distribution for *Gal4^{V2h}/+; ; UAS-B52-RNAi* is biased due to difference in mean and median

value and also overlapping of Q1 and median value, more samples for *Gal4^{V2h}/+; ; UAS-B52-RNAi* may be needed to confirm the phenotype.

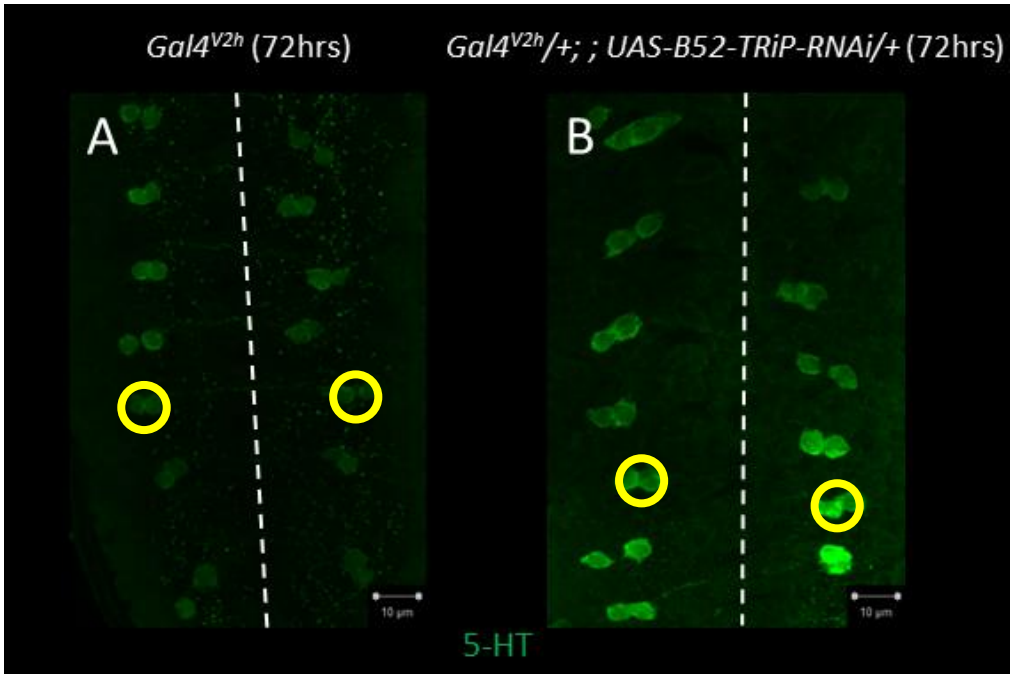

Figure. 5.17a 5-HT staining of 72hrs larval brains

5-HT in green. Horizontal views, anterior to the left. Bar = 10um. Dotted line indicates the location of midline. Yellow circles indicate the areas taken for intensity measurement. (A) *Gal4^{V2h}* control (n=3) and (B) *Gal4^{V2h}/+; ; UAS-B52-TRiP-RNAi/+* (n=3).

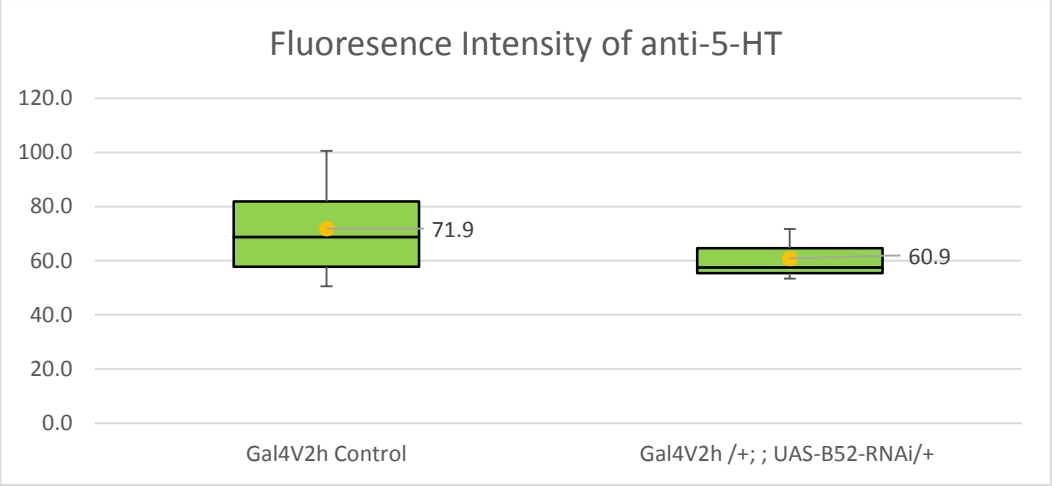

Figure. 5.17b Fluorescence intensity of anti-5-HT

Yellow dots represent mean value of intensity, and the middle line in the green box represents the median value which separates the populations in half (median value overlaps with Q1 in this case). The level of 5-HT is elevated in *Gal4^{V2h}/+; ; UAS-B52-RNAi*. However, the difference in intensity between *Gal4^{V2h}* control and *Gal4^{V2h}/+; ; UAS-B52-RNAi* is not statistically significant (p= 0.4131). Because the

distribution for *Gal4^{V2h}/+; ; UAS-B52-RNAi* is biased due to difference in mean and median value and also overlapping of Q1 and median value, more samples for *Gal4^{V2h}/+; ; UAS-B52-RNAi* may be needed to confirm the phenotype.

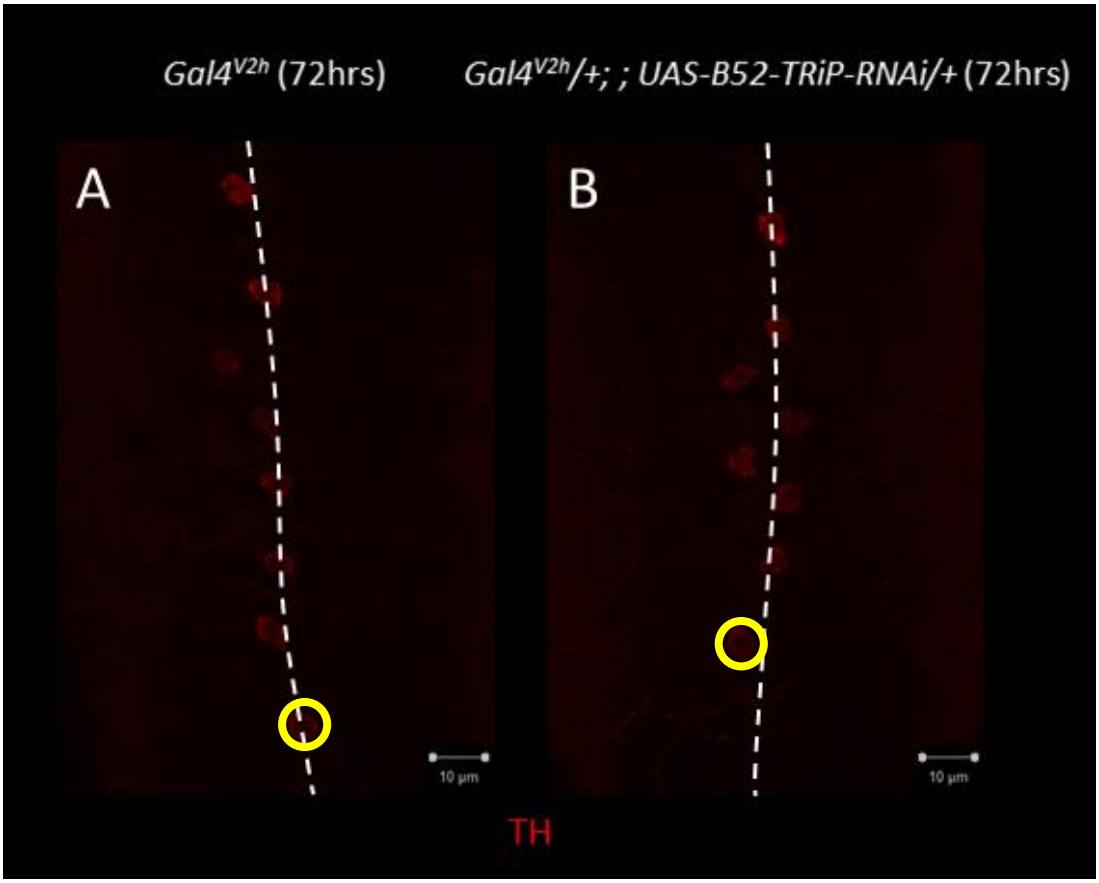

Figure. 5.18a TH staining of 72hrs larval brains

TH in green. Horizontal views, anterior to the left. Bar = 10um. Dotted line indicates the location of midline. Yellow circles indicate the areas taken for intensity measurement. (A) *Gal4^{V2h}* control (n=3) and (B) *Gal4^{V2h}/+; ; UAS-B52-TRiP-RNAi/+* (n=3).

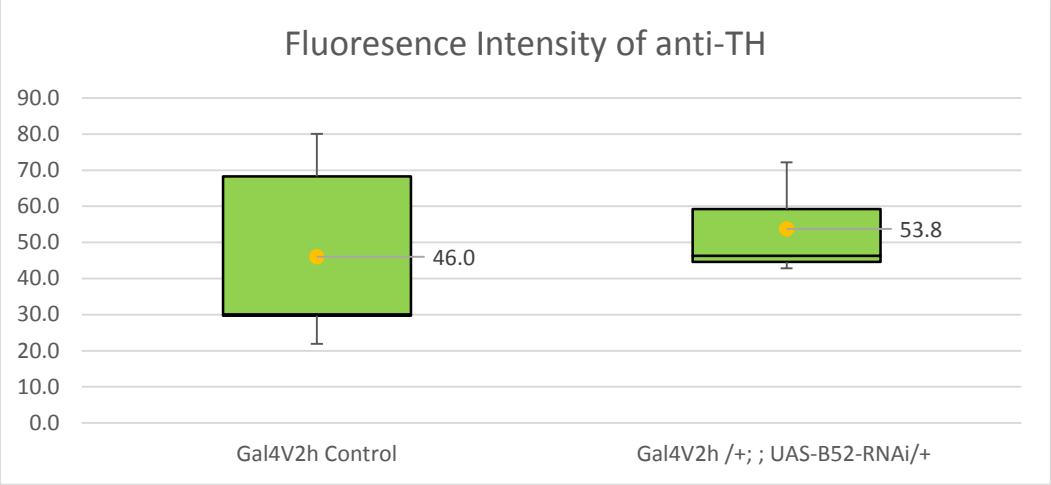

Figure. 5.18b Fluorescence intensity of anti-TH

Yellow dots represent mean value of intensity, and the middle line in the green box represents the median value which separates the populations in half (median value overlaps with Q1 in this case). The level of TH is elevated in *Gal4^{V2h}/+; ; UAS-GFP-B52*. However, the difference in intensity between *Gal4^{V2h}* control and *Gal4^{V2h}/+; ; UAS-GFP-B52* is not statistically significant (p= 0.6640). Also, the population distribution are strongly biased for both groups. Therefore, more samples are needed to confirm the phenotypes.

5.2.6. Antagonising B52 activity with *BBS* in *19H09Gal4* neurons does not induce significant changes in ChAT or v-Glut levels in 84hrs old larval brains

To test if B52 is involved in specifying identities and functions of individual neuronal cells, *BBS* was introduced to a subset of type II NBs and their progenies by constructing the *19H09Gal4, UAS-myrm::RFP/UAS-BBS* line.

Levels of both ChAT (Fig. 5.19) and v-Glut (Fig. 5.20) were elevated in the VNC of 84hrs larval brains of *19H09Gal4, UAS-myrm::RFP/UAS-BBS* when compared to *19H09Gal4, UAS-myrm::RFP* control. However, none of the differences is statistically significant.

5.2.7. Overexpression of *B52* in *19H09Gal4* neurons does not induce significant changes in ChAT or v-Glut levels in 84hrs old larval brains

In parallel to the down-regulation of B52 activity, overexpression of *B52* was also performed by constructing the *19H09Gal4, UAS-myrm::RFP/UAS-GFP-B52* line.

Levels of both ChAT (Fig. 5.19) and v-Glut (Fig. 5.20) in the VNC of 84hrs larvae were slightly lower in *19H09Gal4, UAS-myrm::RFP/UAS-GFP-B52* than those in *19H09Gal4, UAS-myrm::RFP* control (Fig. 5.15). However, none of the differences is statistically significant.

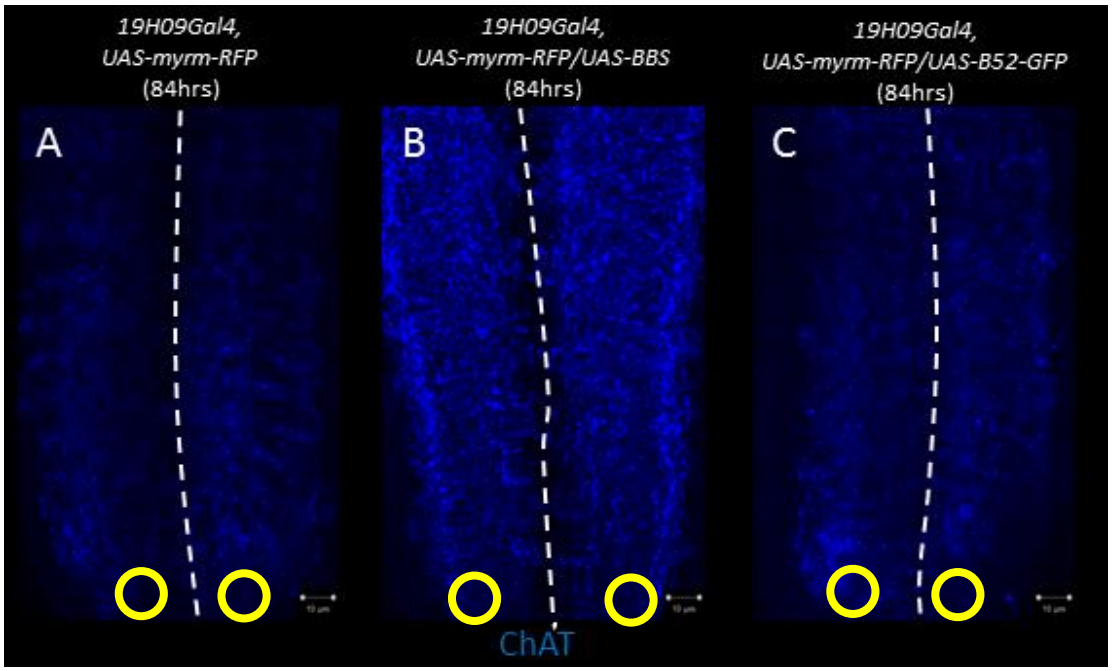

Figure. 5.19a ChAT of 84hrs larval brains

ChAT in blue. Horizontal views, anterior up. Bar = 10um. Dotted line indicates the location of midline. Yellow circles indicate the areas taken for intensity measurement. (A) *19H09Gal4, UAS-myrm::RFP* Control (n=3), (B) *19H09Gal4, UAS-myrm::RFP/UAS-BBS* (n=8) and (C) *19H09Gal4, UAS-myrm::RFP/UAS-GFP-B52* (n=3).

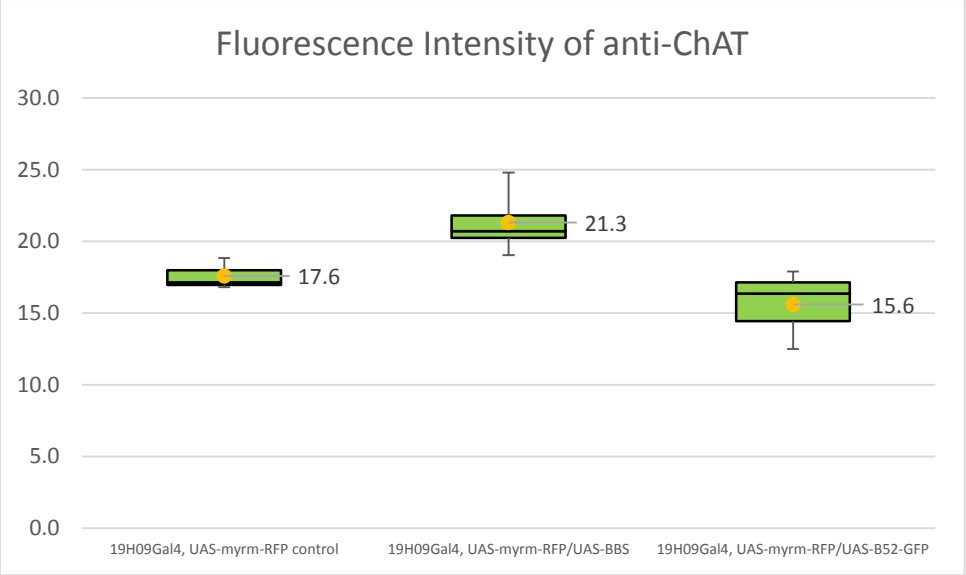

Figure. 5.19b Fluorescence intensity of anti-ChAT

Yellow dots represent mean value of intensity, and the middle line in the green box represents the median value which separates the populations in half (median value overlaps with Q1 in this case). Compared to *19H09Gal4, UAS-myrm::RFP control*, the level of ChAT is elevated in *19H09Gal4, UAS-myr∴mRFP/UAS-BBS*, and slightly reduced in *19H09Gal4, UAS-myr∴mRFP/UAS-GFP-B52.* However, the difference in intensity between *19H09Gal4, UAS-myr::mRFP/UAS-BBS* and *19H09Gal4, UAS-myr∴mRFP* (p= 0.0930), and between *19H09Gal4, UAS-myr∴mRFP/UAS-GFP-B52* and *19H09Gal4, UAS-myr∴mRFP* control (p= 0.6518) are not statistically significant. The difference between mean and median values are relatively small within different genotypes, and thus indicating the samples collected represent the normal situations.

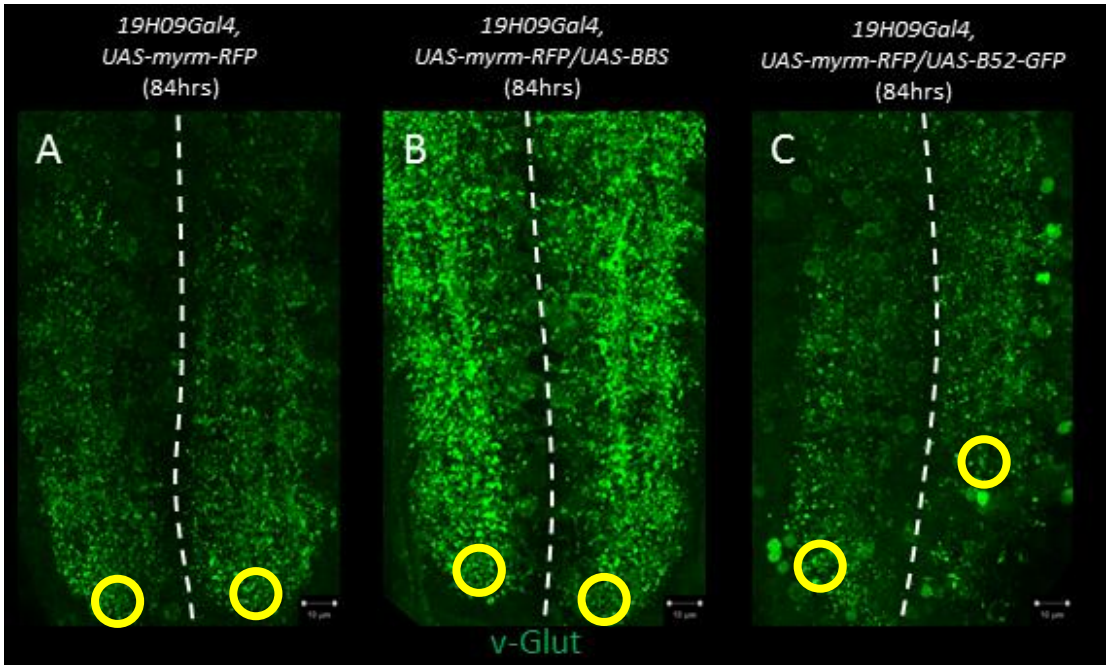

Figure. 5.20a v-Glut of 84hrs larval brains

v-Glut in green. Horizontal views, anterior up. Bar = 10um. Dotted line indicates the location of midline. Yellow circles indicate the areas taken for intensity measurement. (A) *19H09Gal4, UAS-myr∴mRFP* Control (n=3), (B) *19H09Gal4, UAS-myr∴mRFP/UAS-BBS* (n=8) and (C) *19H09Gal4, UAS-myr:mRFP/UAS-GFP-B52* (n=3). *19H09Gal4* neurons show up in (C) *19H09Gal4, UAS-myr∴mRFP/UAS-GFP-B52* and due to expression of GFP.

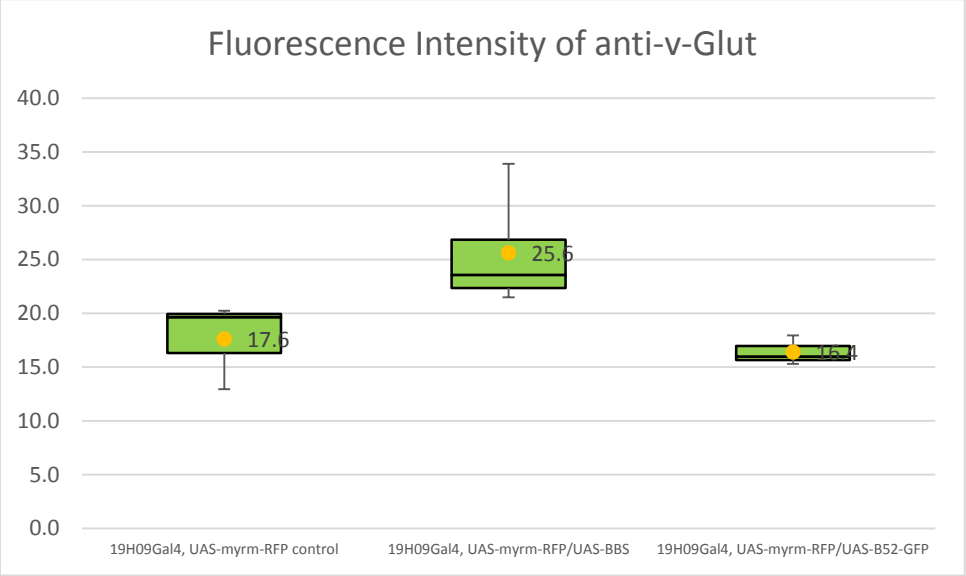

Figure. 5.20b Fluorescence intensity of anti-v-Glut

Yellow dots represent mean value of intensity, and the middle line in the green box represents the median value which separates the populations in half (median value overlaps with Q1 in this case). Compared to *19H09Gal4, UAS-myrm::RFP control*, the level of v-Glut is elevated in *19H09Gal4, UAS-myrm::RFP/UAS-BBS*, and slightly reduced in *19H09Gal4, UAS-myrm::RFP/UAS-GFP-B52*. However, the difference in intensity between *19H09Gal4, UAS-myrm::RFP/UAS-BBS* and *19H09Gal4, UAS-myrm::RFP* (p= 0.0605), and between *19H09Gal4, UAS-myrm::RFP/UAS-GFP-B52* and *19H09Gal4, UAS-myrm::RFP* control (p= 0.3104) are not statistically significant. There are large differences in mean and median values within the same group of samples, suggesting more samples are needed to confirm the phenotypes.

5.2.8. Elevation of ChAT and v-Glut, but no significant difference in GABA, 5-HT or TH in 24hrs larval brain of *B52*L24* mutants

Levels of ChAT, v-Glut, GABA, 5-HT and TH were examined in 24hrs larval brain of *B52*L24* homozygous mutant. *B52*L24* heterozygous mutant was used as control.

Compared to control *B52*L24* heterozygous mutants, there were significant increases in levels of both ChAT ($p<0.05$, Fig. 5.21) and v-Glut ($p<0.05$, Fig. 5.22) in the VNC of *B52*L24* homozygous mutant. Levels of GABA (Fig. 5.23) stayed the same between the two genotypes. More samples are needed to confirm the phenotypes of 5-HT (Fig. 5.24) and TH (Fig. 5.25.

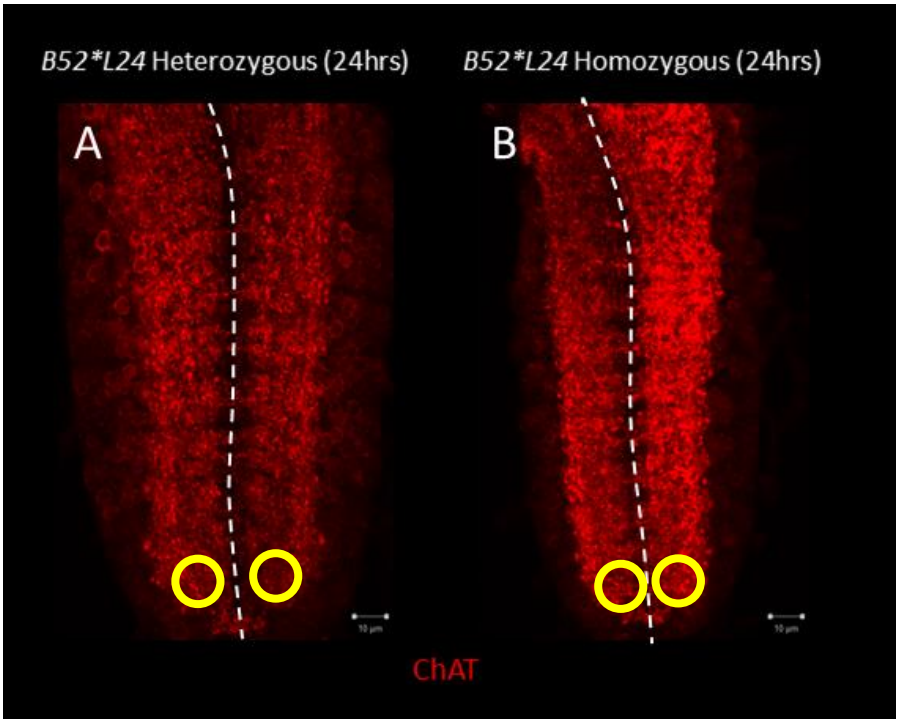

Figure. 5.21a ChAT staining of 24hrs larval brains

ChAT in red. Horizontal views, anterior up. Bar = 10um. Dotted line indicates the location of midline. Yellow circles indicate the areas taken for intensity measurement. (A) *B52*L24* heterozygous control (n=3) and (B) *B52*L24* homozygous mutant (n=3).

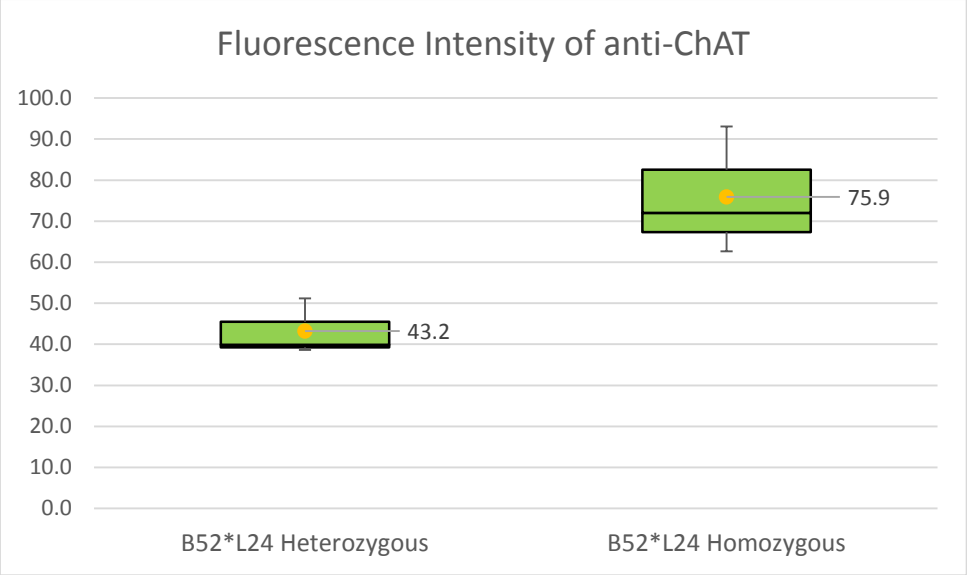

Figure. 5.21b Fluorescence intensity of anti-ChAT

Yellow dots represent mean value of intensity, and the middle line in the green box represents the median value which separates the populations in half (median value overlaps with Q1 in this case). The level of ChAT is significantly higher in *B52*L24* homozygous mutants when compared to *B52*L24* heterozygous mutants (p= 0.0294).

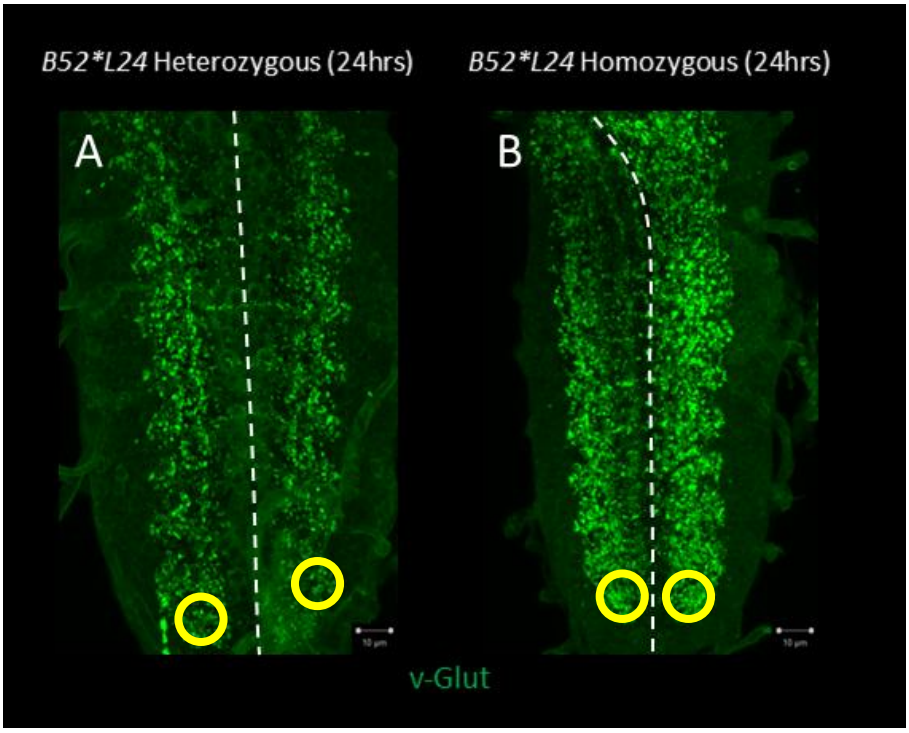

Figure. 5.22a v-Glut staining of 24hrs larval brains

v-Glut in green. Horizontal views, anterior up. Bar = 10um. Dotted line indicates the location of midline. Yellow circles indicate the areas taken for intensity measurement. (A) *B52*L24* heterozygous control (n=3) and (B) *B52*L24* homozygous mutant (n=3).

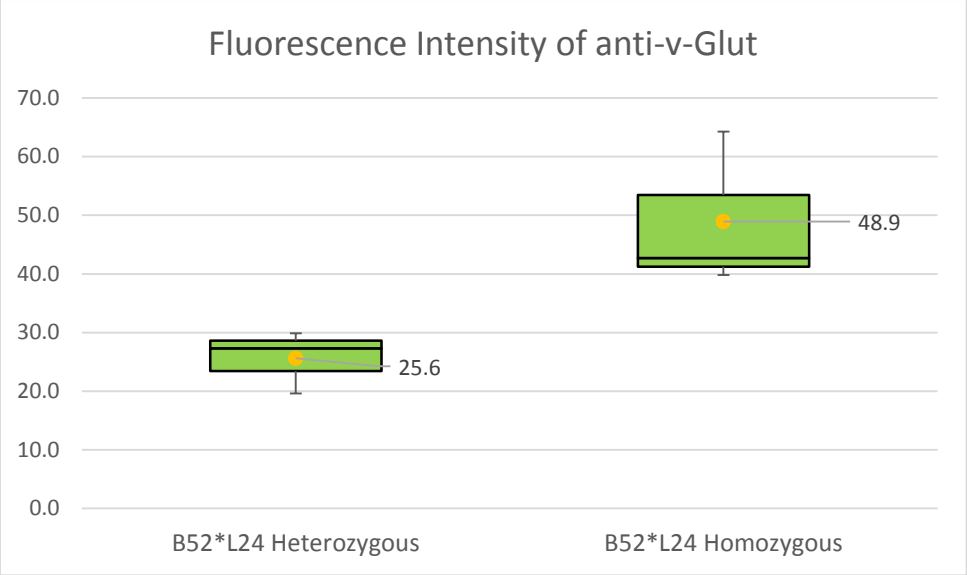

Figure. 5.22b Fluorescence intensity of anti-v-Glut

Yellow dots represent mean value of intensity, and the middle line in the green box represents the median value which separates the populations in half. The level of v-Glut is significantly elevated in *B52*L24* homozygous mutants when compared to *B52*L24* heterozygous mutants (p= 0.0485).

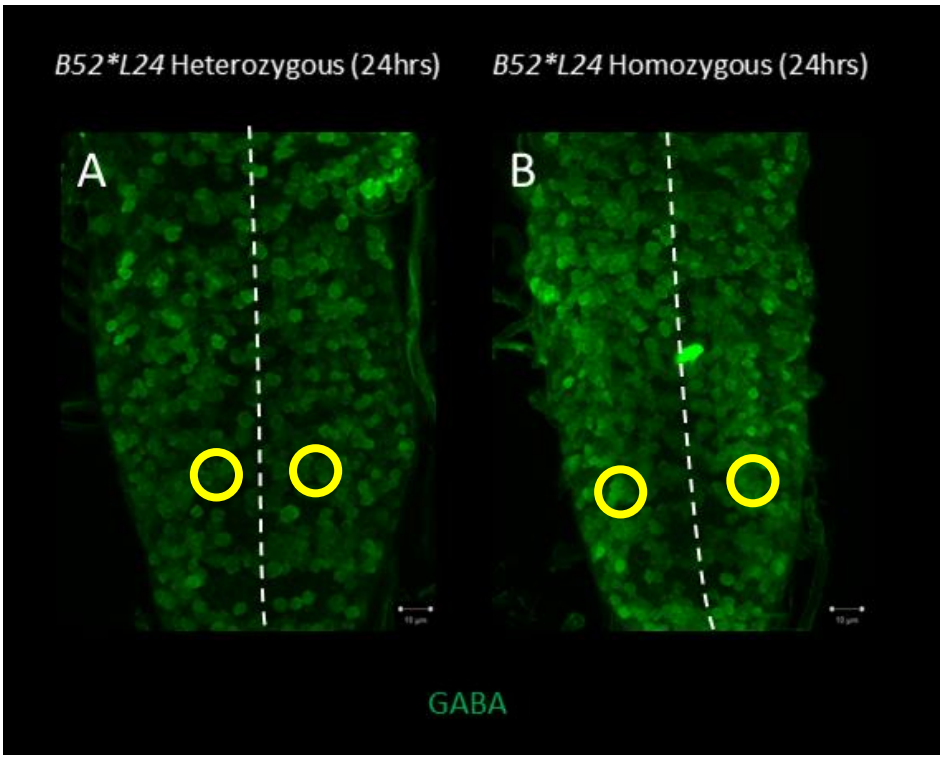

Figure. 5.23a GABA staining of 24hrs larval brains

GABA in green. Horizontal views, anterior up. Bar = 10um. Dotted line indicates the location of midline. Yellow circles indicate the areas taken for intensity measurement. (A) *B52*L24* heterozygous control (n=3) and (B) *B52*L24* homozygous mutant (n=3).

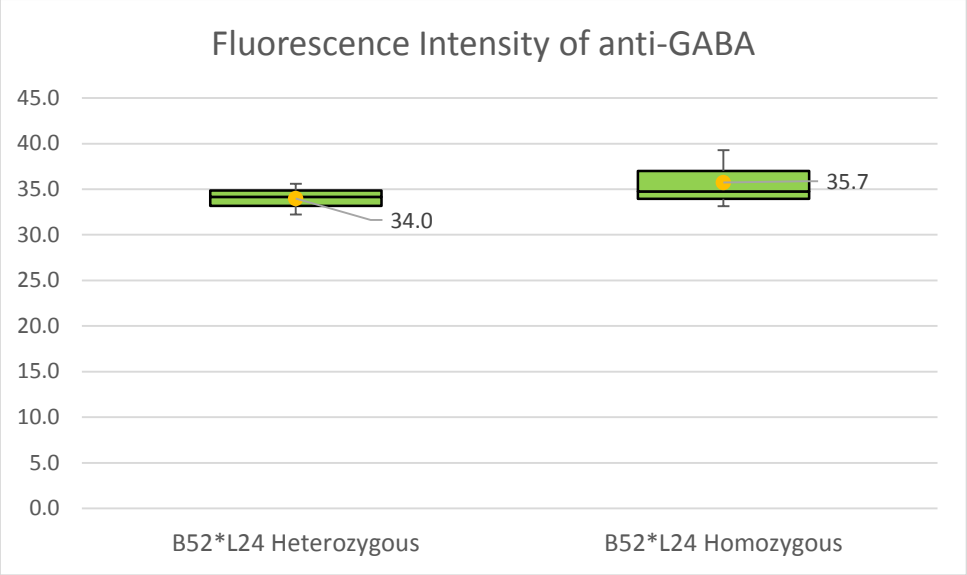

Figure. 5.23b Fluorescence intensity of anti-GABA

Yellow dots represent mean value of intensity, and the middle line in the green box represents the median value which separates the populations in half. The levels of are more or less the same between *B52*L24* homozygous mutants and heterozygous mutants (p= 0.4492).

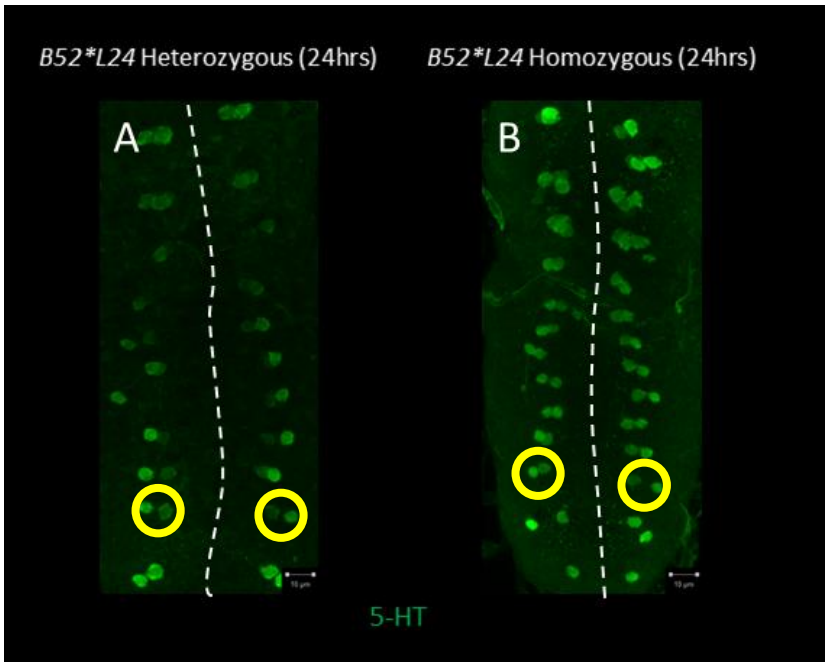

Figure. 5.24a 5-HT staining of 24hrs larval brains

5-HT in green. Horizontal views, anterior up. Bar = 10um. Dotted line indicates the location of midline. Yellow circles indicate the areas taken for intensity measurement. (A) *B52*L24* heterozygous control (n=3) and (B) *B52*L24* homozygous mutant (n=3).

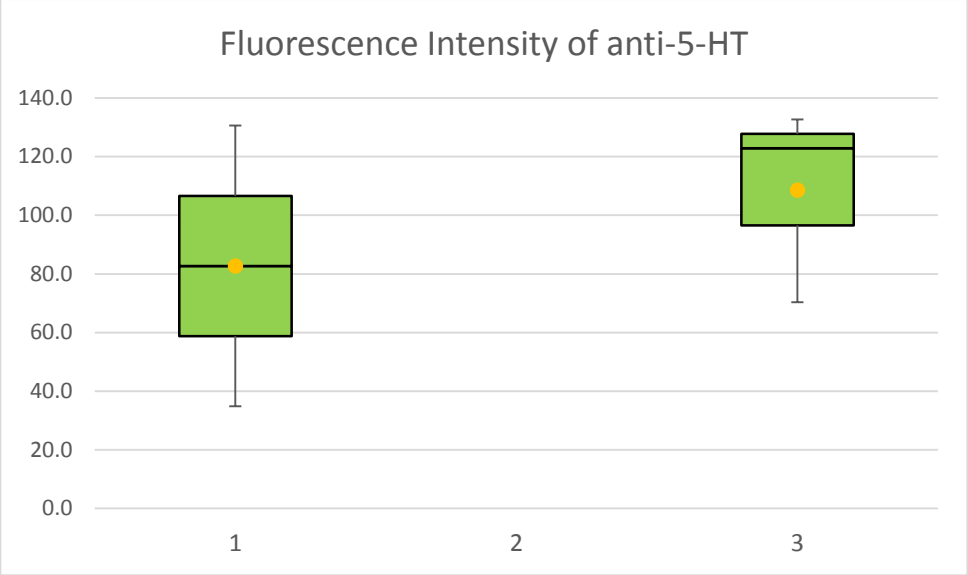

Figure. 5.24b Fluorescence intensity of 5-HT

Yellow dots represent mean value of intensity, and the middle line in the green box represents the median value which separates the populations in half. The level of 5-HT is elevated in *B52*L24* homozygous mutants when compared to *B52*L24* heterozygous mutants. However, the difference is not statistically significant (p= 0.4855). More samples could be collected for *B52*L24* homozygous mutants to confirm the phenotype.

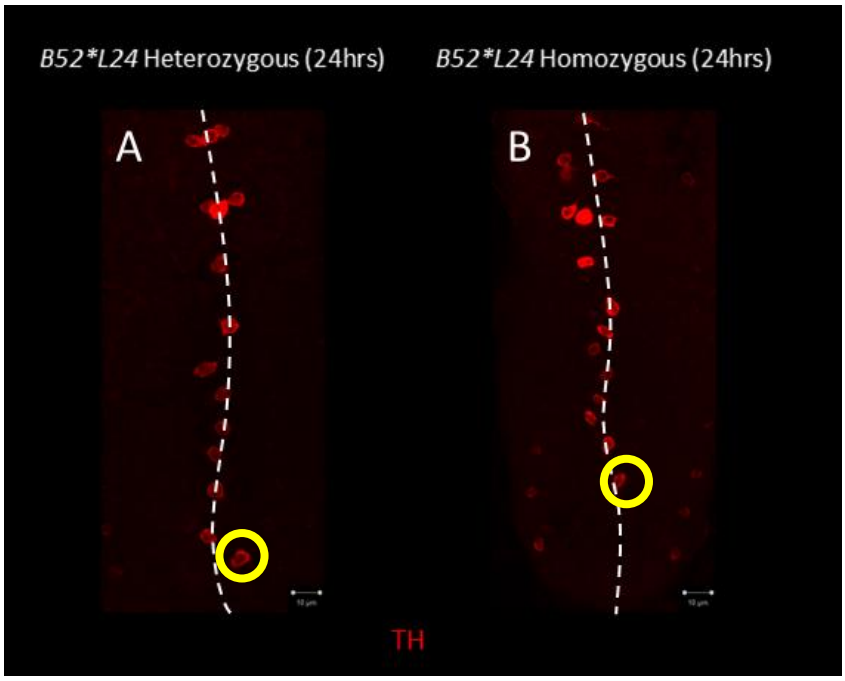

Figure. 5.25a TH staining of 24hrs larval brains

TH in red. Horizontal views, anterior up. Bar = 10um. Dotted line indicates the location of midline. Yellow circles indicate the areas taken for intensity measurement. (A) *B52*L24* heterozygous control (n=3) and (B) *B52*L24* homozygous mutant (n=3).

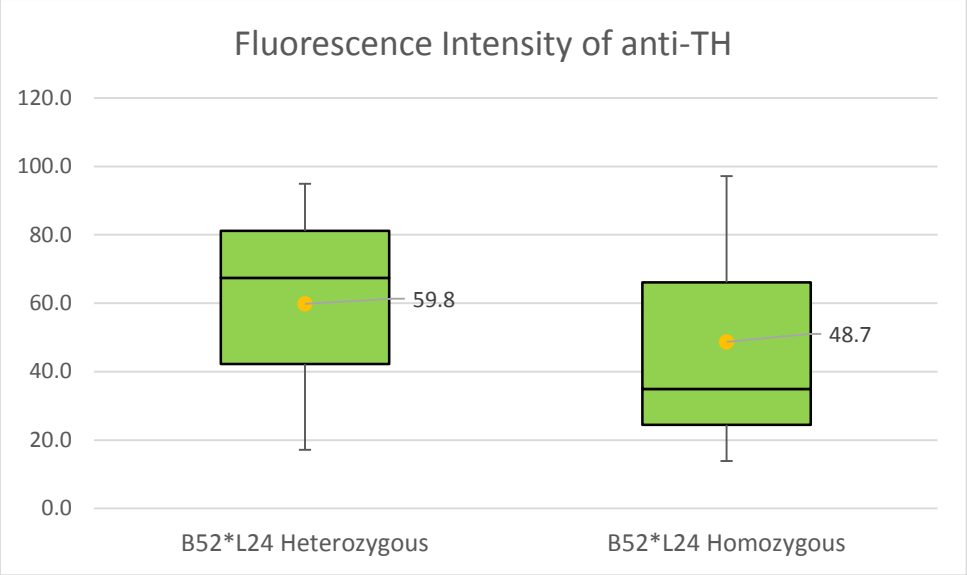

Figure. 5.25b Fluorescence intensity of TH

Yellow dots represent mean value of intensity, and the middle line in the green box represents the median value which separates the populations in half. The level of TH is reduced in *B52*L24* homozygous mutants when compared to *B52*L24* heterozygous mutants. However, the difference is not statistically significant (p= 0.7587). More samples could be collected for *B52*L24* homozygous mutants to confirm the phenotype.

5.2.9. Elevation of ChAT and v-Glut level in 36hrs old larval brains of *B52*L24* mutants

Due to previous results, only expression levels of ChAT and v-Glut were examined further in 36hrs larval brain of *B52*L24* mutants. Once again, the target mutant was *B52*L24* homozygous line. *B52*L24* heterozygotes were used as control and WT was also included for reference.

Compared to both WT and *B52*L24* heterozygous mutants, the level of ChAT ($p<0.001$ in both comparisons, Fig. 5.26) was higher in B52*L24 homozygous mutants, whereas levels of ChAT (Fig. 5.26) between *B52*L24* heterozygous mutants and WT were similar. The level of v-Glut was significantly higher in *B52*L24* homozygous homozygous mutants when compared to WT, but not when compared to *B52*L24* heterozygous mutants. In addition to the molecular phenotypes, the size of VNCs of *B52*L24* homozygous mutants was much smaller than that of both *B52*L24*

heterozygous mutant and WT. This result is consistent with the difference in larval body size between the *B52*L24* homozygous mutant and *B52*L24* heterozygous control. These results will be presented in Chapter 6.

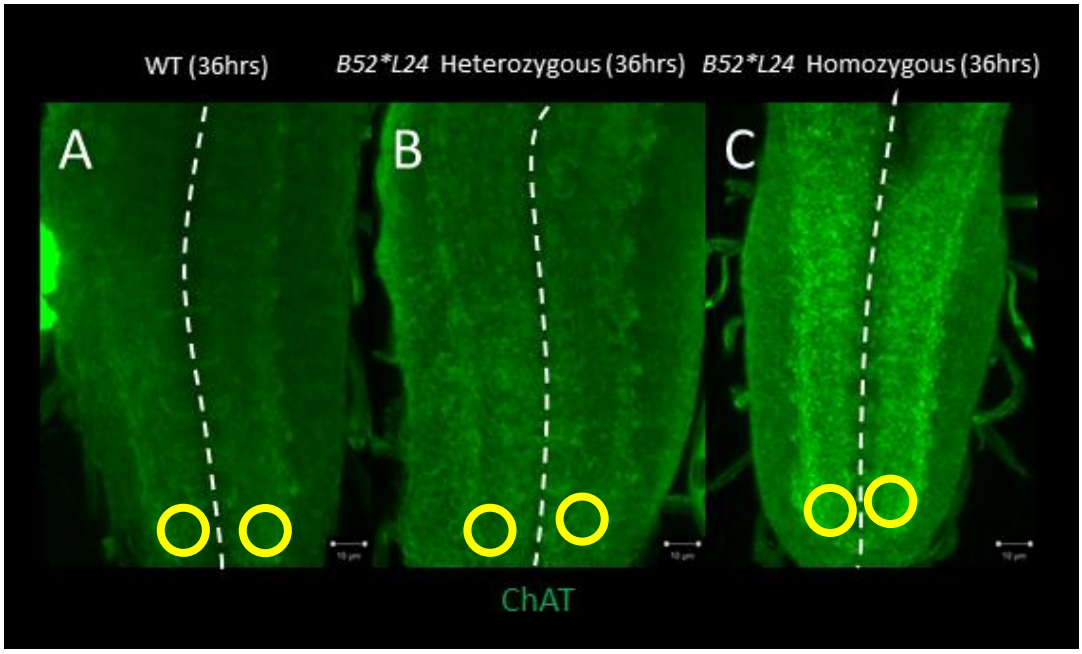

Figure. 5.26a ChAT staining of 36hrs larval brains

ChAT in green. Horizontal views, anterior up. Bar = 10um. Dotted line indicates the location of midline. Yellow circles indicate the areas taken for intensity measurement. (A) WT (n=5), (B) *B52*L24* heterozygotes (n=5) and (C) *B52*L24* homozygous mutant (n=5). Compared to both WT and *B52*L24* homozygous mutants, level of ChAT is significantly elevated in the *B52*L24* homozygous mutant.

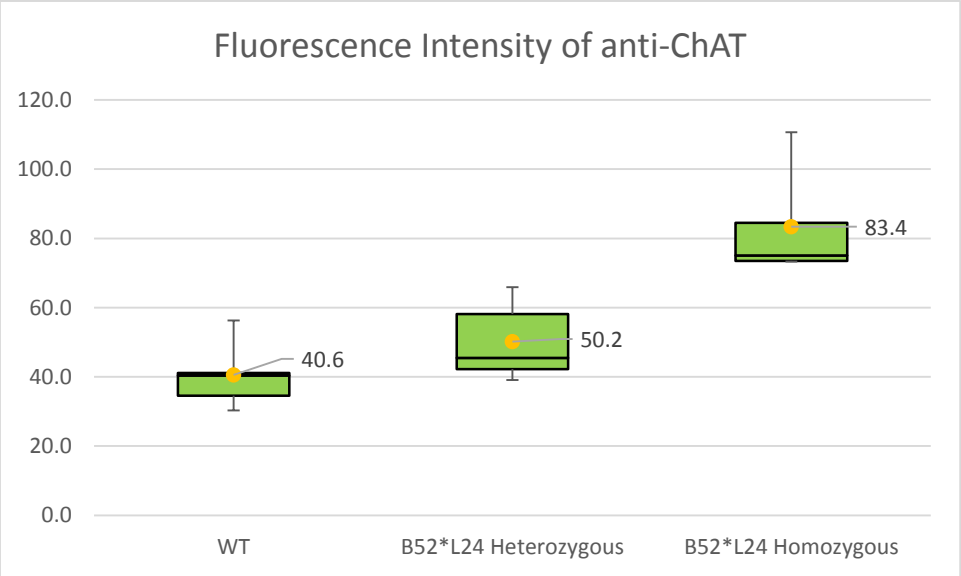

Figure. 5.26b Fluorescence intensity of anti-ChAT

Yellow dots represent mean value of intensity, and the middle line in the green box represents the median value which separates the populations in half (median value overlaps with Q1 in this case). Compared to both WT (p= 0.0009) and *B52*L24* heterozygous mutants (p= 0.0053), the level of ChAT is significantly elevated in B52*L24 homozygous mutants. More samples could be collectd to further confirm the phenotype distrubution for *B52*L24* homozygous mutants.

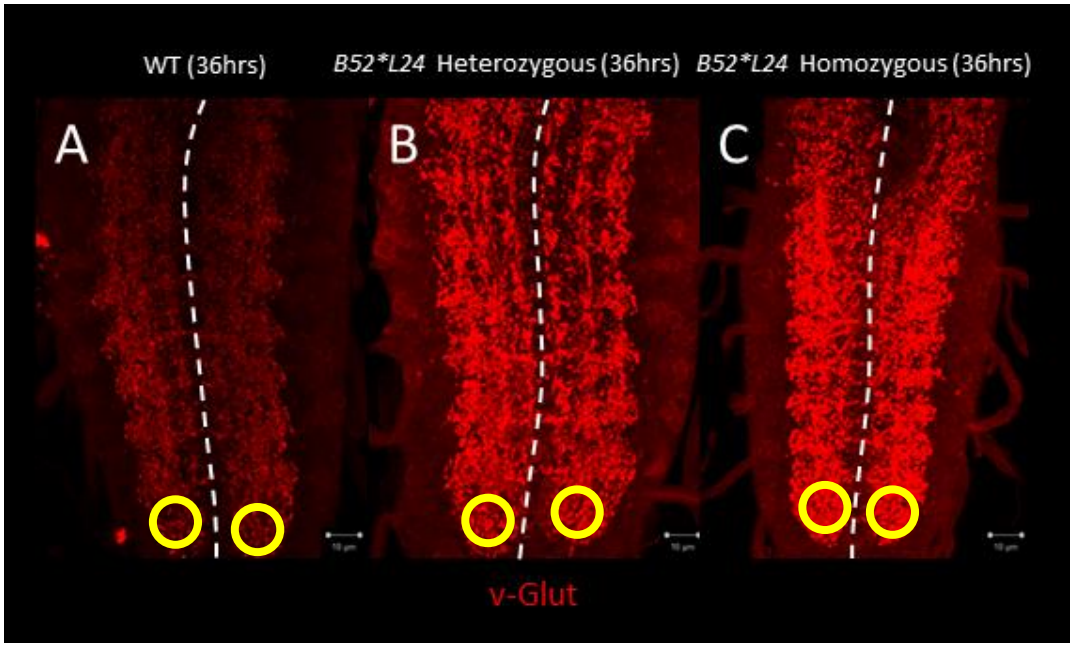

Figure. 5.27a v-Glut staining of 36hrs larval brains

v-Glut in red. Horizontal views, anterior up. Bar = 10um. Dotted line indicates the location of midline. Yellow circles indicate the areas taken for intensity measurement. (A) WT (n=5), (B) *B52*L24* heterozygotes (n=5) and (C) *B52*L24* homozygous mutant (n=5). Compared to WT, level of v-Glut is significantly elevated in both *B52*L24 B52*L24* heterozygous and homozygous mutants.

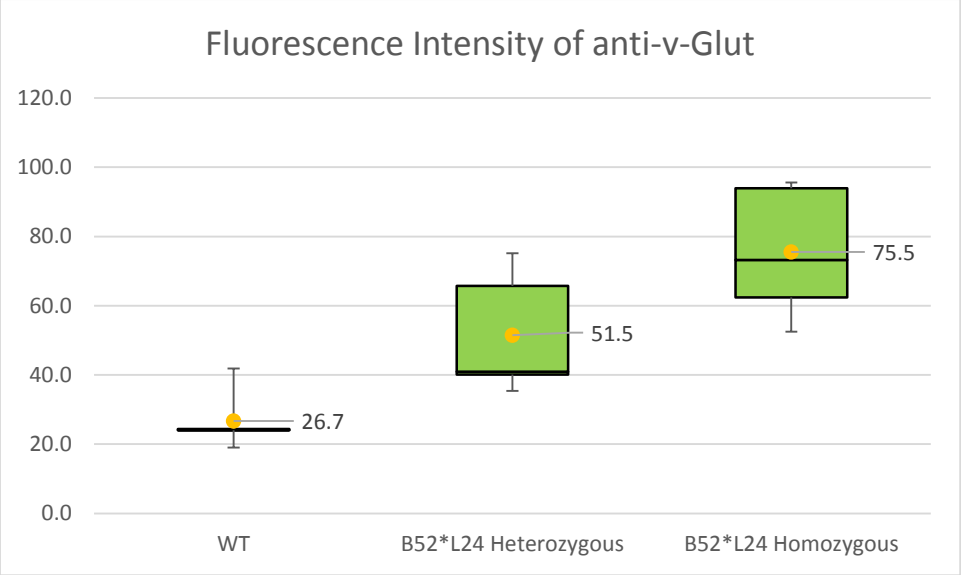

Figure. 5.27b Fluorescence intensity of anti-v-Glut

Yellow dots represent mean value of intensity, and the middle line in the green box represents the median value which separates the populations in half (median value overlaps with Q1 in this case). Compared to WT, the level of ChAT is significantly elevated in B52*L24 homozygous mutants (p= 0.0008). The level of ChAT is also higher in B52*L24 homozygous mutants when compared to B52*L24 heterozygous mutants (p= 0.0726). However, the difference is not statistically significant. More samples could be collectd to further confirm the phenotype distrubution for WT and *B52*L24* heterozygous mutants.

5.2.10. *ChAT* splicing defects in *elavGal4/+; ; UAS-BBS/+* embryos

To test if B52 is regulating ChAT mRNA by splicing, total RNAs of overnight egg lays were collected for both *elavGal4* control and *elavGal4/+; ; UAS-BBS*. These RNAs were then reverse transcribed into cDNA for PCR. Intron 2 and intron 4-7 of *ChAT* were chosen as targets. Forward and reverse primers were designed to cover the flanking sequences (i.e. the exons) of both intron regions (Fig. 5.28). All PCR conditions including concentration of template cDNA were kept the same between the two samples.

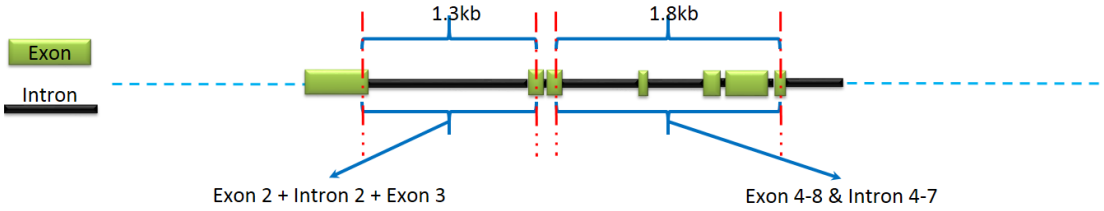

Figure. 5.28. Schematic view of *ChAT* mRNA and primers for intron 2 and intron 4-7

The first pair of primers cover the whole sequence of intron 2 plus small regions of exon 2 and exon 3. The second pair of primers cover from the end part of exon 4 up to the beginning part of exon 8. The total size of intron 2 is 1.1kb and the combined size of intron 4 to 7 is 0.4kb.

The presence of the 1.3kb and 1.8kb fragments, respectively, in the PCR products of *elavGal4/+; ; UAS-BBS* indicates the corresponding intron was not efficiently spliced, as compared to *elavGal4* control, where only the short fragments – the spliced isoforms was amplified (Fig. 5.29).

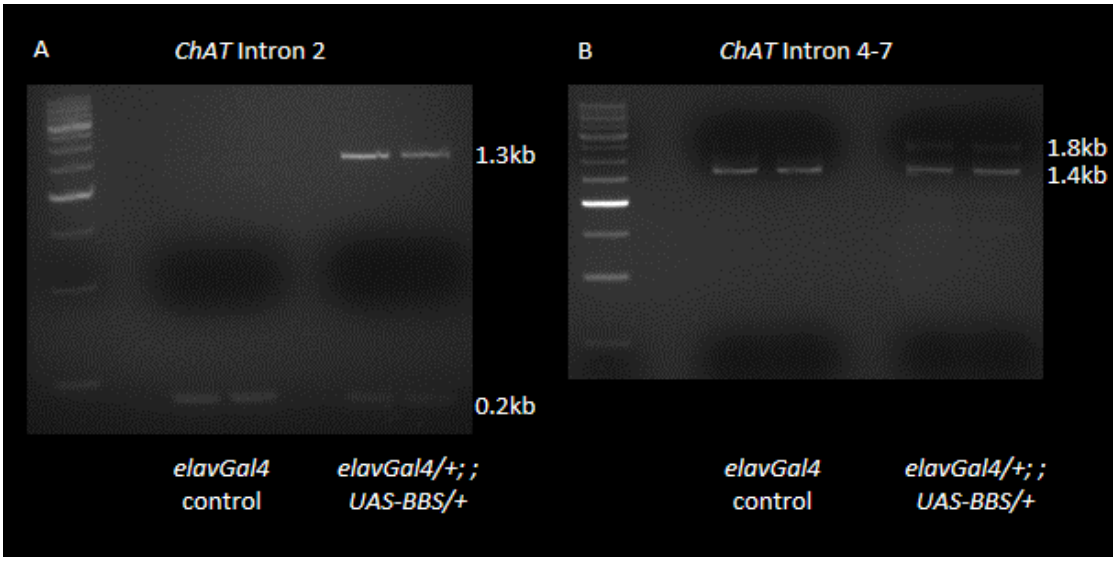

Figure. 5.29 PCR of ChAT intron 2 and intron 4-7 from embryonic RNA

250bp DNA ladder (A*) ChAT* intron 2. The spliced isoform is 0.2kb in length and is present in both *elavGal4* control and *elavGal4/+; ; UAS-BBS*, whereas the unspliced 1.3kb isoform is only present in *elavGal4/+; ; UAS-BBS*. (B) *ChAT* intron 4-7. The spliced isoform is 1.4kb in length and is present in both *elavGal4* control and *elavGal4/+; ; UAS-BBS*. A small amount of the unspliced 1.8kb isoform is also present in *elavGal4/+; ; UAS-BBS*.

5.2.11. *ChAT* splicing defects in embryos homozygous mutant for the B52 Line 24 at larval stages

Since the homozygous mutant of *B52*L24* had shown a very strong phenotype in the level of ChAT in 36hrs larval brain, the splicing of *ChAT* mRNA was examined. After extracting total RNA separately from *B52*L24* homozygous mutants and *B52*L24* heterozygous control, the same reverse transcription process was followed to create cDNA template for PCR. The same pairs of primers for intron 2 and intron 4-7 of *ChAT* were used to perform the PCR. All PCR conditions including concentration of template cDNA were kept the same between the two samples.

A large amount of the unspliced 1.3kb isoform of intron 2 is detected in the homozygous mutant. The spliced 0.2kb isoforms cannot be amplified in both heterozygous and homozygous mutants. For intron 4-7, there both the spliced and unspliced isoforms appear to be elevated in the homozygous mutant (Fig. 5.30).

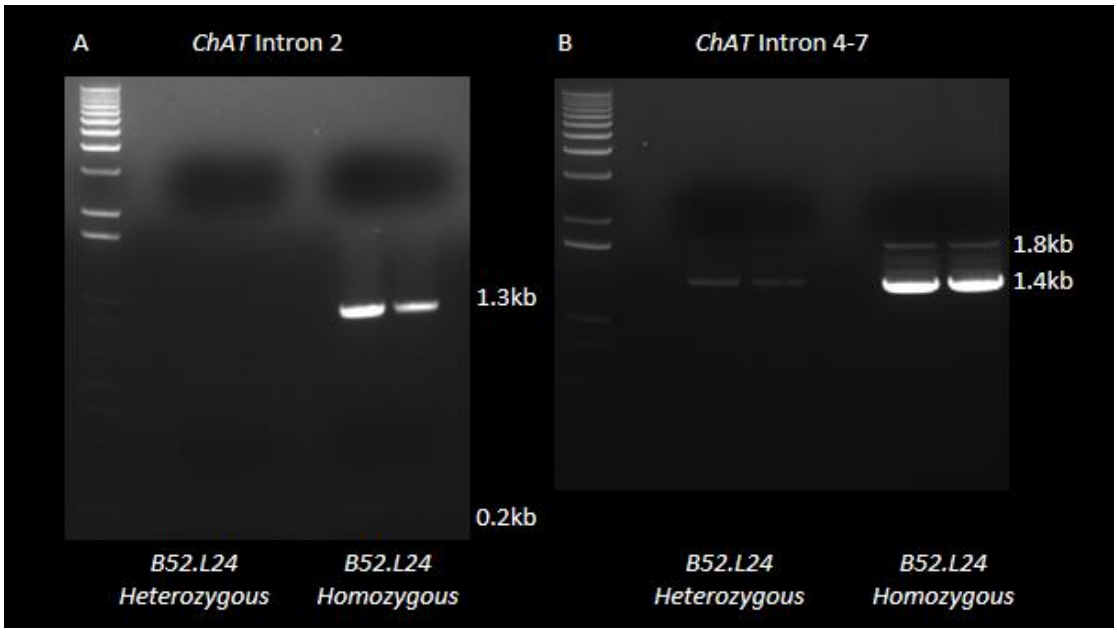

Figure. 5.30 PCR of *ChAT* intron 2 and intron 4-7 from larval RNA

1kb plus DNA ladder. (A) *ChAT* intron 2. Only the 1.3kb unspliced isoform is detected in the homozygous mutant. (B) *ChAT* intron 4-7. The overall level of *ChAT* is substantially higher in the homozygous mutant animals, including both the spliced 1.4kb and unspliced 1.8kb isoforms.

5.2.12. Sequencing of unspliced *ChAT* isoforms

To confirm that the longer fragment detected in the gel was indeed the unspliced isoform of *ChAT*, the corresponding fragments were sent for sequencing. The sequencing results are illustrated below. Alignment of the sequence with the unspliced *ChAT* intron 2 and intron 4-7, respectively, indicates the longer fragments seen on the gel were the unplisced isoforms of *ChAT*.

In general, the sequencing results show that both intron 2 and intron 4-7 of *ChAT* from *B52*L24* have the same sequences as the ones from the fly database, despite a few missing or mismatched nucleotides in the both intron regions between the sequencing results and the database (marked in red colour below). This might simply be the cause of sequencing errors. However, given the locations of some mismatched nucleotides is relatively far away from the M13F or M13R primer sites (the closest is more than 200bp away), this could indicate the splicing mechanism is affected in a way that B52 regulates *ChAT* mRNA splicing to a level beyond simple activation or inhibition. There is a chance that the accuracy of RNA polymerisation, or the subunits of the spliceosome might be affected as a result of *B52* null mutation. This could be confirmed by repeating the sequencing.

The unspliced *ChAT* introns were translated to amino acid sequences in all six reading frames using EMBOSS Transeq (http://www.ebi.ac.uk/Tools/st/emboss_transeq/). The translation was first run starting from the upstream exon (exon2-intron2-exon3), but a stop codon was present as soon as the reading reached to the end of exon1. Therefore, all of the six reading frames were considered because we could not know exactly what happened at the splicing sites. The splicing factor might bypass 1, 2 or 3 nucleotides, or even mistook the previous sequence (i.e. -3, -2 or -1 nucleotides) and therefore resulting in complete change of the reading frame.

Only Intron 4 with reading frame 5 and intron 6 with reading frame 2 were able to be translated into amino acid without being disrupted by the stop codons. Despite that, the most likely situation is that transcription stops at a premature stop codon in the unspliced inton. However, it has been shown *in vitro* that the active site of ChAT involves arginine^{452} in rat [283] and histidine^{426} in *Drosophila* [284]. The length of ChAT-α and ChAT-β isoforms are 721 amino acid (aa) and 714aa (refer to Fig. 5.0 for ChAT protein alignment), respectively, in *Drosophila*. This indicates the ChAT antibody targets the ChAT protein close to amino acid 426, in fact way after intron 2. This suggests that despite the presents of the second intron the translation process still produces the active site domain of ChAT. This implies that translation may start at a novel initiation site within the second intron leading to a N-terminal truncation of the enzyme.

Since the ChAT antibody was still able to detect the corresponding peptide because all the amino acid sequence still remained intact and the only change was that more sequences being added as a result of defects in splicing, this leads to the speculation that the deficiency or down-regulation of B52 somehow makes the translation process bypass the stop codons, possibly caused by mislocating or being unable to resolve the 3D structure of the RNA sequences. For example, the presence of RNA hairpin, a structure commonly formed during intron splicing, could cause the sequence not accessible to the splicing factor, and therefore false signalling the translation process to continue by picking up nearby sequences instead, which ultimately leads to bypassing of the stop codons. As indicated by the gel and sequencing results shown above, the introns are still present. This suggests the splicing (or nucleotide cutting) process is not successful and explains the translation of RNA sequences into amino acids.

The active site of ChAT is present in the normal coding regions (exons) and therefore is not likely to be interrupted. Assuming the sequences nearby the introns were translated instead of the introns themselves, the emerging amino acids sequence should exhibit similar properties as those would in the ChAT protein in its wild type conditions. Therefore, the active site is likely to

remain the same conformation, and allows interaction with the ChAT antibody, or even endogenous B52 protein.

Figure. 5.31 Alignment of unspliced *ChAT* intron 2 region with corresponding ChAT gene region from the database

The sequences obtained from sequencing results for unspliced *ChAT* intron 2 which were used for alignment with the intron 2 region from *ChAT* gene in the database. Primers used for amplifying the intron 2 regions are also listed in the bottom of this section, plus the corresponding gene region of *ChAT* in the database. Nucleotides labelled in red indicating mismatch, intron 2 is highlighted with cyan background. The alignment result is presented in blue and red coloured sequences.

Sequencing result of region amplified by Fwd-Cha Intron 2 and Rev-Cha Intron 2

XXXX = Primers XXXX = ChAT Intron 2 (partial Intron 2 in sequencing results)

*** = missing nucleotide XXX = mismatch

>Unspliced_ChAT_int2_M13F_RC (sequence downstream of M13F in the transformation product – reverse complement)

NNGNGNNNNNNNNNNNNNTNNNTGANNNNNNNNNNNNNNNTNNNNNNNNNGNNNNNNANNNNNTTNGTNNNN
NNNAANGNNAANTAANNNNGGGNTTNNTATGNNANNNGAGNNNGGGTAGNTNCNAGCANNCNANCNGCGNNCANN
NNNNNNNNAAAAANCNAANNTTTTNNAAAANNNNNNCCCCNNNAAACNNNCAAGGCCCCCANCCNNCCCNNNTNNNC
CTNTACACCCCCATACTCACCTGGAAAAAAA*GCACAGCAGCCACAGTAACAACCCCCGAAAAGCAGAGTTAGACATCTAAA
TTGTAAACCGATGTATGACAGGGGAACCCCCCCAGAAAAAAAGGCAAGTGACAAGAGACTAGGTATTCGGATATAACAAA
AGTTTCAATGGCTTTGAAAACGGAGAACACGACGTATGCGGAAGTCAACGACATGCTGATACCTCGTCGTTTCGTTGCTAAG
TGGAAATTTGTGTTTTCGCAGCAGGTAAATCAAGGTCGATGGATACATTTAAATATGAAATTGCAGTCAGAAATCCTGCATT
CAAAACCAGCTGTTTTGGCCATCCGGCAATCGATTGAATTGCAGACCTCGAAACACAACGATTTTCCCACTTGGGAACTCCTA
GAGAAAATTCTCTCAATTAAAGTTTCCGTGCGAGGGTGGAAAGCAGAAAACGGAAAAGGCAAAAATGTCAAGGAGCGGAGT
ACAATGTCAGATTCAAGCCATTCCATTTCTTTTTCTATTTTTTTTTCTTTTTTTGATTTGAAATTTGGCTCCCCAGGGCATAAAGT
TTTTGTACGAGTATTGCTGGTGGCAGGACAAGGCAACTTTCCATTTGACGCTCGATATTGTCATGCATACAAATGAGGAAAT
GGGGGGGGCATTTCCCGGAAAAGCCGGGCAATGTCAAGTGTGGAAGAGAAATAAAATTAAATTTGCAGCACCACGCAGCT
TACTAACCCCATTGAGAACCCTTTGTCCTGATTCCGTTCTTGCAGACTCTACCCAAGGTGCCCGTTCCAGCACTGGATGAAAC
GATGGCCGACTACATCCGCGCCCTGGAACCGATTACCACGCCGGCGCAGCTCGAGCGGACCAAGGAGCTGATCAGGCAGTT
CTCGGCTCCCCAGGGAATCGGAGCG**CGGCTGCATCAGTATCTGCTG**AAGGGCGAATTCTGCAGATATCCATCACACTGGCG
GCCGCTCGAGCATGCATCTAGAGGGCCCAATCGCCCTNNNNNNNNNNN

>WT_ChAT_int2

CCAAAGAAATGGCTCTCAACGGCCGAGTCTGTGGACGAGTTTGGATTCCCTGACGTGAGTAAAATTGATTAAACCATTTCG
AATTCGCCTCCCCATTTCCAGCAAATATTTGCCCTAGGGCTAAACTCGACTGTTACTTGAATAATTCAAAGACAAACACTCGCT
CAGACGACAGACTAATCCTGTTTGTTATAATTACAAATGCAAATAACGAGGGCTTTTGTATGGCAACAGGAGCTCGGGTAGC
TCCTGGCAACCAACCTGCGTGCAAACAAACCGGAAAAACCAACCTTTTCAAAACACAACCCCCCAACGCCCAAGCCCCACCA
CCCGCTACCCTCTACACCCCCATACTCACCTGGAAAAAAAAGCACAGCAGCCACAGTAACAACCCCCGAAAAGCAGAGTTAG
ACATCTAAATTGTAAACCGATGGATGACAGGGGAACCCCCCCAGAAAAAAAGGCAAGTGACAAGAGACTAGGTATTCGGA

TATAACAAAAGTTTCAATGGCTTTGAAAACGGAGAACACGACGTATGCGGAAGTCAACGACATGCTTATACCTCGTCGTTTC
GTTGCTAAGTGGAAATCTGTGTTTTCGCAGCAGGTAAATCAAGGTCGATGGATACATTTAAATATGAAATTGCAGTCAGTAA
TCCTGCATTCAAAACCAGCTGTTTTGGCCATCCGGCAATCGATTGAATTGCAGACCTCGAAACACAACGATTTTCCCACTTGG
GAACTCCTAGAGAAAACCTCTCAATTAAAGTTTCCGTGCGAGGGTGGAAAGCAGAAAACGGAAAAGGCAAAAATGTCAAG
GAGCGGAGTACAATGTCAGATTCAAGCCATTCCATTTCTTTTTCTATTTTTTTTTCTTTTTTTGATTTGAAATTTGGCTCCCCAG
GGCATAAAGTTTTTGTACGAGTATTGCTGGTGGCAGGACAAGGCAACTTTCCATTTGACGCTCGATATTGTCATGCATACAA
ATGAGGAAATGGGGGGGCATTTCCCGGAAAAGCCGGGCAATGTCAAGTGTGGAAGAGAAATAAAATTAAATTTGCAGCAC
CACGCAGCTTACTAACCCCATCGAGAACCCTTTGTCCTGACTCCGTTCTTGCAGACTCTACCCAAGGTGCCCGTTCCAGCACT
GGATGAAACGATGGCCGACTATATCCGCGCCCTGGAACCGATTACCACGCCGGCGCAGCTCGAGCGGACCAAGGAGCTGA
TCAGGCAGTTCTCGGCTCCCCAGGGAATCGGAGCG**CGGCTGCATCAGTATCTGCTG**

>Unspliced_ChAT_int2_M13R (sequence upstream of M13R in the transformation product)
NNNNNNNNNNNNNNNNTATAGAATACTCAAGCTATGCATCAAGCTTGGTACCGAGCTCGGATCCACTAGTAACGGCCGC
CAGTGTGCTGGAATTCGCCCTT**CCAAAGAAATGGCTCTCAACG**GCCGAGTCTGTGGACGAGTTTGGATTCCCTGACGTGAG
TAAAATTGATTAAACCATTTCGAATTCGCCTCCCCATTTCCAGCAAATATTTGCCCTAGGGCTAAACTCGACTGTTACTTGAAT
AATTCAAAGACAAACACTCGCTCAGACGACAGACTAATCCTGTTTGTTATAATTACAAATGCAAATAACGAGGGCTTTTGTAT
GGCAACAGGAGCTCGGGTAGCTCCTAGCAACCAACCTGCGTGCAAACAAACCGGAAAAACCAACCTTTTCAAAACACAACC
CCCCCAAACGCTCAAGCCCCACCACCCTCTACCCTCTACACCCCCATACTCACCTGGAAAAAAA*GCACAGCAGCCACAGTAA
CAACCCCCGAAAAGCAGAGTTAGACATCTAAATTGTAAACCGATGTATGACAGGGGAACCCCCCCAGAAAAAAAGGCAAGT
GACAAGAGACTAGGTATTCGGATATAACAAAAGTTTCAATGGCTTTGAAAACGGAGAACACGACGTATGCGGAAGTCAACG
ACATGCTGATACCTCGTCGTTTCGTTGCTAAGTGGAAATTTGTGTTTTCGCAGCAGGTAAATCAAGGTCGATGGATACATTTA
AATATGAAATTGCAGTCAGAAATCCTGCATTCAAAACCAGCTGTTTTGGCCATCCGGCAATCGATTGAATTGCAGACCTCGA
AACACAACGATTTTCCCACTTGGGAACTCCTAGAGAAAATCTCTCAATTAAAGTTTCCGTGCGAGGGTGGAAAGCAGAAAAC
GGAAAAGGCAAAAATGTCAAGGAGCGGAGTACAATGTCAGATTCAAGCCATTCCATTTCTTTTTCTATTTTTTTTTCTTTTTTT
GATTTGAAATTTGGCTCCCNAGGGCATAAAGTTTTTGTACGAGTATTGCTGGTGGNNGGANNNGCAACTTTNNATTTGACG
CTCGATNTGTCATGCATACAANTGANNANGGGGGGGCATTNNNNAAANNNGGNANNTCAGNGNNNNANAANNAANNA
NNNCAGNNCCNCNCANCTNACTACNNNNNNNNNNNNNNNNNNATCNNNCNNCNANNNNNNNCNNNNNNNNNNTNC
NNN

>Fwd-ChAT-int2

CCAAAGAAATGGCTCTCAACG

>Rev-ChAT-int2_RC

CGGCTGCATCAGTATCTGCTG

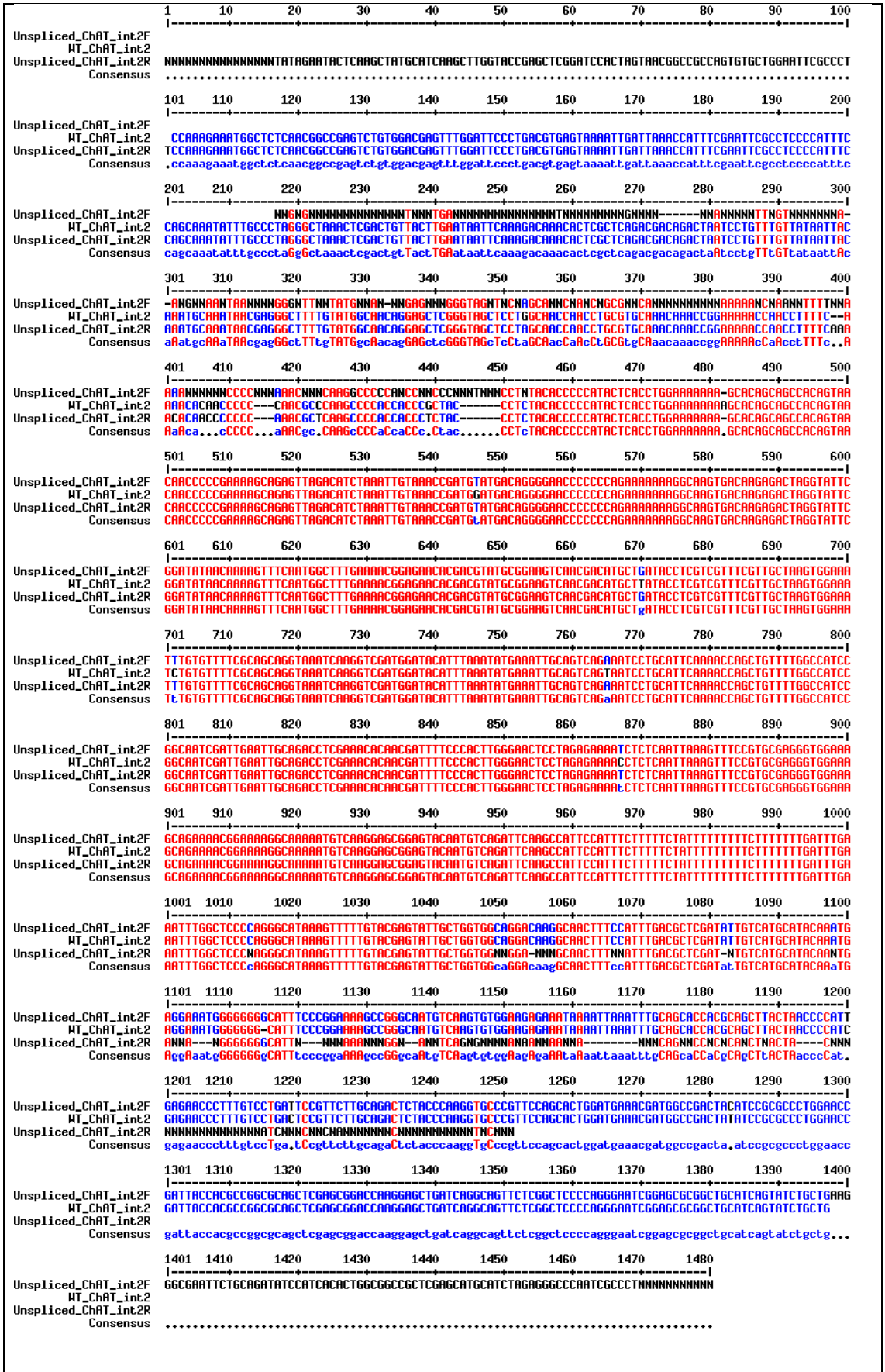
Unspliced_ChAT_int2F
WT_ChAT_int2
Unspliced_ChAT_int2R
Consensus

Figure. 5.32 Alignment of the unspliced *ChAT* intron 4-7 region with the corresponding ChAT gene region from the database

The sequences obtained from sequencing results for unspliced *ChAT* intron 4-7 were used for alignment with the intron 4-7 region from *ChAT* gene in the database. Primers used for amplifying the intron 4-7 regions are also listed in the bottom of this section, plus the corresponding gene region of *ChAT* in the database. Nucleotides labelled in red indicating mismatch, introns 4 to 7 are highlighted with cyan background. The alignment result is presented in blue and red coloured sequences.

Sequencing result of region amplified by Fwd-Cha Intron 4-7 and Rev-Cha Intron 4-7

Primers = **XXXX** ChAT Intron 4-7 = XXXX

*** = missing nucleotide XXX = mismatch

>Unspliced_ChAT_int4-5_M13F (sequence downstream of M13F in the transformation product)

Only Intron 4 and incomplete Intron 5 of *Chat* are covered by this sequence

GNNNNNNNNNNNNAGGGCGATTGGGCCCTCTAGATGCATGCTCGAGCGGCCGCCAGTGTGATGGATATCTGCAGAATTC
GCCCTT**GCAGGACTCGCAGTTCCTGCC**GTCGCGGGAGCGACTGAACGACGAGGATCGCCATGTGGTGGTTATTTGCCGCAA
CCAAATGTATTGCGTCGTGCTGCAGGCTAGCGATCGTGGAAAGTTGTCAGAGAGTGAGATCGCCTCACAGATCCTCTATGTG
CTCAGTGATGCTCCCTGTCTGCCAGCTAAACCAGTGCCGGTGGGTCTGCTGACCGCTGAACCGAGGAGCACGTGGGCACGG
GACCGGGAAATGCTTCAGGAGGACGAACGCAATCAACGCAATCTGGAGCTCATCGAGACGGCACAGGTGGTCCTCTGTCTG
GACGAACCGTTGGCTGGGAACTTTAATGCGCGCGGTTTTACGGGTGCCACGCCCACAGTTCATCGGGCGGGGGATCGGGA
CGAGACGAACATGGCCCACGAGATGATCCACGGCGGAGGCAGCGAATACAACTCCGGAAATCGCTGGTTTGACAAGACCA
TGCAGGTAATGCAACTTTAACTTCCTTAATTAATTGATTTTTTTTTTAAATAACTAACCCAACTTTCAGCTCATTATTTGCACCG
ATGGAACCTGGGGCCTTTGCTATGAGCACTCCTGTTCCGAAGGCATTGCTGTTGTCCAGCTGCTGGAGAAGATCTACAAAAA
AATCGAGGAGCACCCGGACGAGGATAACGGTCTACCGCAACACCACTTGCCACCACCGGAGCGTCTGGAGTGGCATGTGG
GTCCGCAATTGCAATTGCGCTTTGCCCAAGCCTCCAAGAGTGTGGACAAATGCATCGATGACCTGGACTTCTATGTGTACCG
CTACCAGAGTTACGGAAAGACCTTTATCAAATCGTGCCAGGTCAGTCCGGATGTGTACATTCAACTGGCCCTGCAACTGGCT
CACTACAAGCTGTACGGACGTCTGGNGGNNACCTACGAAAGTGCGTCCACTCGACGATTTCTGCACGTAAGTATACCGGCA
TCTTTNCNGGAAATNNNATCCNNNANTNNNATTTNNNNTGNNNTTTCATCGNNNNCNNGNNNNNANNCNTTTCNGGNN
NCNNANACNGCATCNNNNNGNNNNNNNNNNNNNNNNNGCNNNGCNNNNNNNNNNNNNNANNNNCAACGNNCNN
NNNNANNANNNNNNTTNNNNNNN

>WT_ChAT_int4-7

GCAGGACTCGCAGTTCCTGCCGTCGCGGGAGCGACTGAACGACGAGGATCGCCATGTGGTGGTTATTTGCCGCAACCAAAT
GTATTGCGTCGTGCTGCAGGCTAGCGATCGTGGAAAGTTGTCGGAGAGTGAGATCGCCTCACAGATCCTCTATGTGCTCAGT
GATGCTCCCTGTCTGCCAGCTAAACCAGTGCCGGTGGGTCTGCTGACCGCTGAGCCGAGGAGCACGTGGGCACGGGACCG
GGAAATGCTTCAGGAGGACGAACGCAATCAACGCAATCTGGAGCTCATCGAGACGGCACAGGTGGTCCTCTGTCTGGACGA
ACCGCTGGCTGGGAACTTTAATGCGCGCGGTTTTACGGGTGCCACGCCCACAGTTCATCGGGCGGGGGATCGGGACGAGA
CGAACATGGCCCATGAGATGATCCACGGCGGAGGCAGCGAGTACAATTCCGGAAATCGCTGGTTTGACAAGACCATGCAG

GTAATGCAACTTTAACTTCCTTAATTAATTGAATTTTTTTAAAAATAACTAACCTATCTTTCAGCTCATTATTTGCACCGATGGA
ACCTGGGGCCTTTGCTATGAGCACTCCTGTTCCGAAGGCATTGCTGTTGTCCAGCTGCTGGAGAAGATCTACAAAAAAATCG
AGGAGCACCCGGACGAGGATAACGGTCTACCGCAACACCACTTGCCACCACCGGAGCGTCTGGAGTGGCATGTGGGTCCG
CAATTGCAATTGCGCTTTGCCCAAGCCTCCAAGAGTGTGGACAAATGCATCGATGACCTGGACTTCTATGTGTACCGCTACC
AGAGTTACGGAAAGACCTTTATCAAATCGTGCCAGGTCAGTCCGGATGTGTACATTCAACTGGCCCTGCAACTGGCTCACTA
CAAGCTGTACGGACGTCTGGTGGCCACCTACGAAAGTGCGTCCACTCGACGATTTCTGCACGTAAGTATACCGGCATCTTTA
CAGGAAATGTTGATCCTTAATTTAAGATTTTAATCTGTCGGTTTCATCGTCTCTGTATAATTCCATTTCCAGGGTCGCGTAGAC
TGCATCAGAGCGGCCAGCACGGAGGCATTGGAGTGGGCCAAGGCCATGTGCCAGGGTGAGGGTGCAAACGTGCCCCTGG
AGAGCGATCGCGAGGATGAGGAGGAGTCGCGAAAGGTCAAGTTTAGCATTTACAGTGTGGGTATTCCAGCGTAAAGCCAC
CACTGTGAAAATAGTAACTTATCTTTGCCCCGCAACCAACAGAAGGATCATCTCCGGGAGCTTTTCCGGTGCGCCGTCGCCC
GCCAGACTGAGGTGATGGTGAAGAACATCCTGGGCAATGGCATCGACATCCCGCTGCTGGGCCTGCGAGAGGCCAGTATA
GAGGTCACCGGCGAGATGCACGAGCTGTTCAAAGACGAGTCCTACATCATCTCGCAGTGCTTCCTGCTCTCCACCAGTCAGG
TAGTAATTGGCCCACAGGTCTTCGCTAATAAGCACCACTCTGCACTCTATCACCTCTGCACCACCTAATCAATTCTTGCACCAC
AGCACCACTGAGCACAAATCAGCTGCACAAAAGTAGGTATCGGCTAGAATGAAGATATCTTCAGGACTTGGCATACATGTTA
TTGGAATCGTCATAATGATCTTATTGATATACCATTCAGGTGGCCTGCTCTACGGACAGCTTCATGGGATACGGACCGGTAA
CGCCACGTGGTTATGGC**TGCTCCTACAATCCGCATCCG**

>Unspliced_ChAT_int5-7_M13R_RC (sequence upstream of M13R in the transformation product – reverse complement)

Only Intron 5, 6 and 7 of Chat are covered by this sequence

NCNNNNNNNNNNNNTNNNNNNNNNNNNNNNNNNNNNGNNAANNTNTNNNAAAATNGANGNNNNNNNNNGNGATN
NNGTNNNCGNNNNNNNNNCNNNCGAGNNTCNGNNNNNNNTGNGGNTCNNCNNTNNNNGCGCTTNGCCNAAGCNNC
NANGAGTGTGGACNAATGCATCGATGACNTGGACTTCTATGTGTACCGCTACCAGAGTTACGGAAAGACCTTTATCAAATC
GTNCCAGGTCAGTCCGGGATGTGTACATTCAACTGGCCCNGCAACTGGCTCACTACAAGCTGTACGGACGTCTGGTGGCCA
CCTACGAAAGTGCGTCCACTCGACGATTTCTGCACGTAAGTATACCGGCATCTTTACAGGAAATGTTGATCCTTAATTTAAGA
TTTTAATCTGTCGGTTTCATCGTCTCTGTATAATTCCATTTCCAGGGTCGCGTAGACTGCATCAGAGCGGCCAGCACGGAGGC
ATTGGAGTGGGCCAAGGCCATGTGCCAGGGTGAAGGTGCAAACGTGCCCCTGGAGAGCGATCGCGAGGATGAGGAGGAG
TCGCGAAAGGTCAAGTTTAGCATTTACAGTGTGGGTATTCCAGCGTAAAGCCACCACTTTGAAAAGAGTAACTTATCTTTGC
CCCGCAACCAACAGAAGGATCATCTCCGTGAGCTTTTCCGGTGCGCCGTCGCCCGCCAGACTGAGGTGATGGTGAAGAACA
TCCTGGGCAATGGCATCGACATCCCGCTGCTGGGCCTGCGAGAGGCCAGTATAGAGGTCACCGGCGAGATGCACGAGCTG
TTCAAAGACGAGTCCTACATCATCTCGCAGTGCTTCCTGCTCTCCACCAGTCAGGTAGTAATTGGCCCACAGGTCTTCGCTAA
TAAGCACCACTCTGCACTCTATCACCTCTGCACCACCTAATCAATTCTTGCACCACAGCACCACTGAGCACAAATCAGCTGCA
CAAAAGTAGGTATCGGCTAGAATGAAGATATCTTCAGGACTTGGCGCACATTTTTTTGGGATCGTTATAATGCTCTTCTTGAT
ATACCATTCAGGTGGCCTGCTCTACGGACAGCTTCATGGGATACGGACCGGTAACGCCACGTGGTTATGGC**TGCTCCTACAA**
TCCGCATCCGAAGGGCGAATTCCAGCACACTGGCGGCCGTTACTAGTGGATCCGAGCTCGGTACCAAGCTTGATGCATAGC
TTGAGTATTCTATANNNNNNANNANNNNNNN

>Fwd-ChAT-int4-7

GCAGGACTCGCAGTTCCTGCC

>Rev-ChAT-int4-7_RC

TGCTCCTACAATCCGCATCCG

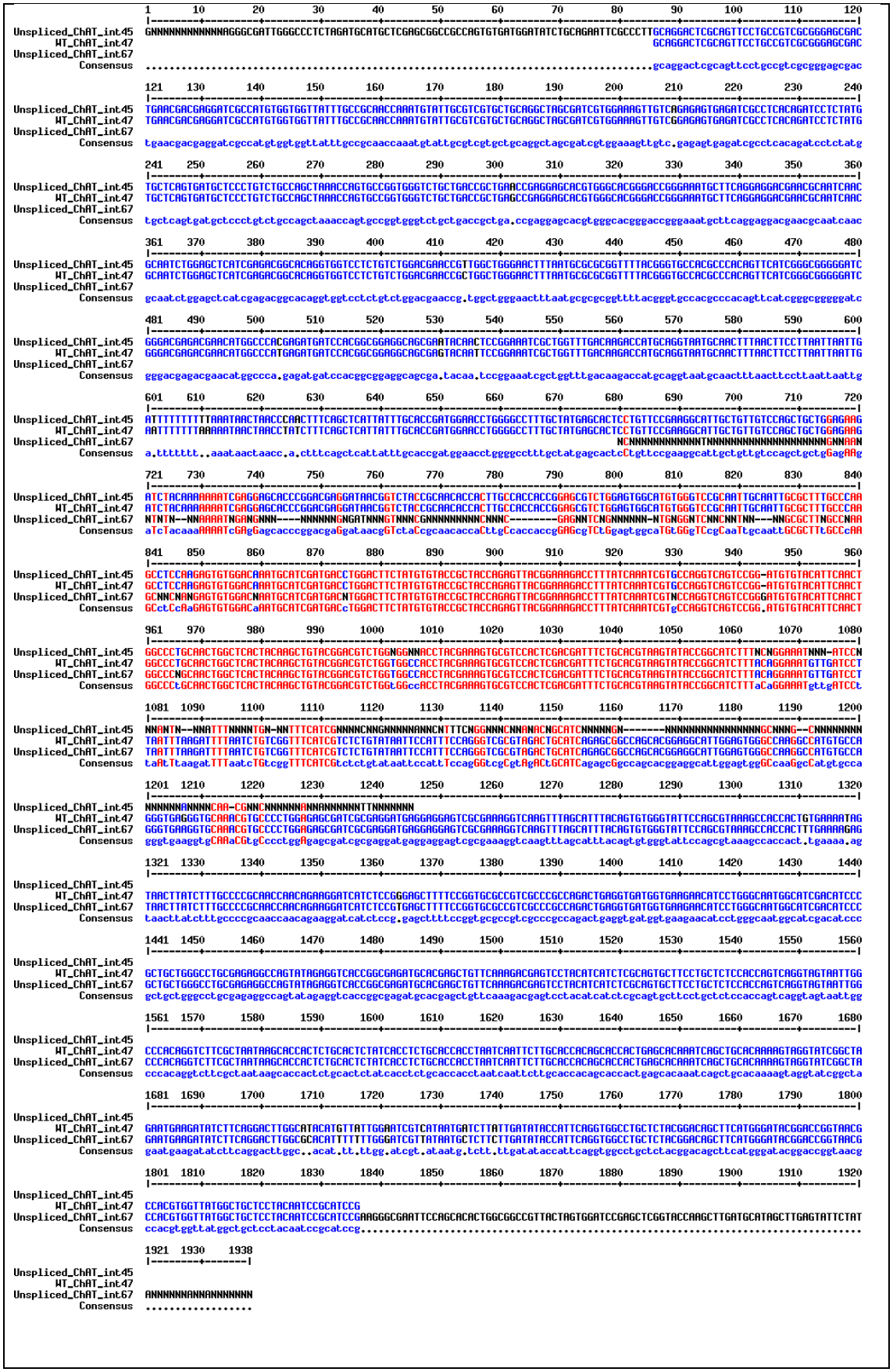

5.3. Discussion

5.3.1. Elevation of ChAT protein level and mis-splicing of ChAT mRNA in the B52 loss of function mutants

Study of ChAT in *Drosophila* dates back to decades ago. ACh is an excitatory neurotransmitter in *Drosophila* and other insects [285, 286]. The release of ACh in the eye is needed by *Drosophila* for executing light avoidance [287]. Constant expression of *ChAT* is needed in *Drosophila* cholinergic neurons for the synthesis of both ACh and vesicular ACh transporter (VAChT), where the *VAChT* gene is nested within the first intron of *ChAT* [288]. Other studies have also pointed out the strong correlation between ChAT and VAChT [289].

Although in this study there is no direct indication of VAChT activity in response to the level of B52, the elevation of ChAT revealed by anti-ChAT staining may well be accompanied by the up-regulation of VAChT in B52 loss of function mutants (*elavGal4/+; ; UAS-BBS/+*, *Gal4^{V2h}/+; ; UAS-B52-TRiP-RNAi/+*, *B52*L24* homozygous mutant). Splicing of the first intron of *ChAT* can be examined to determine whether B52 is also responsible for regulating the correct splicing of *VAChT*.

Overall, elevation of ChAT has been observed whenever expression or activity of B52 is reduced, in several different fly lines (*elavGal4/+; ; UAS-BBS/+*, *Gal4^{V2h}/+; ; UAS-B52-TRiP-RNAi/+*, *B52*L24* homozygous mutant). Also, reduction of ChAT levels is observed when *B52* is overexpressed in all neurons (*elavGal4/+; ; UAS-GFP-B52/+*). Table 5.1 at the end of this chapter summaries levels of different neurotransmitters expressed in the corresponding fly lines relative to the control, where B52 levels are different. In addition, accumulation of unspliced ChAT mRNA has been detected in both *elavGal4/+; ; UAS-BBS/+* and *B52*L24* homozygous mutant. These results strongly suggest B52 mediates splicing of *ChAT*.

5.3.2. Elevation of v-Glut protein level in B52 loss of function mutants

As indicated by the letter "v (vesicular)" in its name, the excitatory neurotransmitter glutamate is loaded into vesicles and then transported to synaptic sites. Widespread expression of v-Glut is found in the neuropil, the site of interneuronal/motoneuronal synapses in *Drosophila* brain and nerve cord [290]. Also, v-Glut has been identified as a major neurotransmitter for motor neurons.

Overexpression of v-Glut causes increases in the size of synaptic vesicle, and subsequent increase of glutamate content per synaptic vesicle. However, this increase of v-Glut plus the glutamate transported does not induce excessive synaptic excitation. Current model suggests uptake of glutamate provides feedback which limits the total release of glutamate, regardless of the increase in the volume of v-Glut [291]. Therefore, behavioural changes observed in larvae (Chapter 6) may not be associated with the level of v-Glut.

A clear indication of the association between v-Glut and B52 levels is seen between *B52^L24* homozygous and heterozygous lines at 24hrs post hatching, where v-Glut is significantly elevated in the homozygous mutants in response to the depletion of B52 protein (Fig. 5.21a). Overexpression of *B52* in all neurons (*elavGal4/+; ; UAS-GFP-B52/+*) also leads to slight reduction of v-Glut. There are also situations where level of v-Glut is not affected by B52 level, such as in elavGal4/+; ; *UAS-GFP-B52*/+ and $Gal4^{V2h}$/+; ; UAS-B52-TRiP-RNAi/+, compared to the corresponding controls, but in most cases, reduction of B52 level results in elevated v-Glut level. A direct way to test whether B52 is responsible for regulating v-Glut is to test the splicing condition of the RNA of the latter in B52 mutation background.

5.3.3. Reduction of B52 levels cause different effects on 5-HT levels

5-HT, or serotonin, is an important neurotransmitter involved in the regulation of a variety of behaviours, such as learning and memory, and circadian entrainment, in *Drosophila* [292, 293].

Reduction of 5-HT in the brain has been associated with insomnia [294], and other neurological disorders, including autism and Alzheimer [295, 296].

In this study, the level of 5-HT follows the same pattern as ChAT in response to B52 level, despite there is only one case (*UAS-BBS/+; elavGal4/+*) where the difference in 5-HT level is statistically significant (Fig. 5.4a) between the mutant lines and the corresponding controls. It is therefore unlikely that the differences in 5-HT levels play a major role in causing behaviour changes in hatching embryos or larvae.

5.3.4. GABA and TH

GABA is a major inhibitory neurotransmitter in the *Drosophila* CNS. GABA has been shown to regulate synaptic transmission [297], circadian sleep/wake cycle [298], olfactory learning [299] and response to mechanical stimulus [300], where reduction of GABA, or its receptor Rdl, often leads to impairment of the corresponding biological pathways.

Levels of GABA relative to B52 have shown inconsistency. In *UAS-BBS/+; elavGal4/+* and *$Gal4^{V2h}$/+; ; UAS-B52-TRiP-RNAi/+*, GABA levels are elevated and reduced, respectively, although both lines have reduced B52 activity. However, in *B52*L24* line, levels of GABA between the heterozygotes and homozygous mutants are not different from one another. These results suggest B52 probably has no regulatory effect over GABA, and the difference in levels of GABA observed in *UAS-BBS/+; elavGal4/+* and *$Gal4^{V2h}$/+; ; UAS-B52-TRiP-RNAi/+* relative to the corresponding control lines are likely to be caused by difference in the magnitude of antibody penetration.

TH is responsible for the synthesis of dopamine. Like 5-HT and GABA, dopamine is involved in regulating sleep and circadian rhythm [301, 302].

It appears that the results regarding TH levels are inconsistent with changes in B52 levels, as shown in *$Gal4^{V2h}$/+; ; UAS-B52-TRiP-RNAi/+* (Fig. 5.18a) and *$Gal4^{V2h}$/+; ; UAS-GFP-B52/+* (Fig.

5.13a). However, in *B52*L24* homozygous mutants, the level of TH was less compared to the heterozygous mutants. Because both up-regulation and down-regulation of B52 resulted in the same reduction of TH, B52 may not be linked with the levels of TH.

5.3.5. Levels of neurotransmitters relative to B52 level

In most cases, reduction of B52 level did not result in any change in levels of neurotransmitters, as seen in *Gal4^{V2h}/+; ; UAS-B52-TRiP-RNAi/+* (72hrs), and *19H09Gal4, UAS-myrm::RFP/UAS-BBS* (84hrs). Also over-expression of B52 did not induce any change as well, as seen in Gal4^{V2h}/+; ; *UAS-GFP-B52*/+ (72hrs) and *19H09Gal4, UAS-myrm::RFP/UAS-B52-GFP* (84hrs). More samples are needed to confirm the phenotypes of ChAT in various cases, such as in *UAS-BBS/+; elavGal4/+* (24hrs) and *p{lacW}B52* homozygous (24hrs). The only confirmed cases are reduction of 5-HT in *UAS-BBS/+; elavGal4/+* (24hrs) compared to the elavGla4 (III) control, and the elevation of ChAT in *B52*L24* homozygous (24hrs and 48hrs) and v-Glut in *B52*L24* homozygous (24hrs) compared to the corresponding *B52*L24* heterozygous control (24hr or 48hrs).

To sum up, in some cases, the exact consequences of changing in B52 level towards neurotransmitter levels could not be defined due to large variance in samples collected. The best way is to collect more samples in order to achieve a normalised distribution, where the mean and median values of the intensity become close enough.

Table 5.1 Levels of neurotransmitters in corresponding fly lines relative to the control

	Elevated(↑) or Reduced(↓)	**No Difference**	**Need Further Confirmation**
UAS-BBS/+; elavGal4/+ (24hrs)	5-HT (↓)	v-Glut	ChAT; GABA
p{lacW}B52 homozygous (24hrs)		5-HT	ChAT
elavGal4/+; ; *UAS-GFP-B52*/+ (48hrs)		ChAT; v-Glut	
Gal4^{V2h}/+; ; *UAS-GFP-B52*/+ (72hrs)		All	
Gal4^{V2h}/+; ; UAS-B52-TRiP-RNAi/+ (72hrs)		ChAT; v-Glut	GABA;5-HT;TH
19H09Gal4, UAS-myrm::RFP/UAS-BBS (84hrs)		ChAT; v-Glut	
19H09Gal4, UAS-myrm::RFP/*UAS-B52-GFP* (84hrs)		ChAT	v-Glut
B52*L24 homozygous (24hrs)	ChAT(↑); v-Glut(↑)	GABA	5-HT; TH
B52*L24 homozygous (36hrs)	ChAT(↑)		v-Glut

All = ChAT, v-Glut, GABA, 5-HT and TH

Chapter 6 B52 and larval locomotion and body features

6.1. Introduction

It takes around 19hrs to 24hrs at 25°C for *Drosophila* embryos to hatch into larvae from egg laying. This is followed by 3 days (or instars, each lasts 24hrs at 25°C) of larval form before they enter pupation. After one or two days they turn into adult flies, which normally will stay alive for about two to three weeks.

The earliest sign of movement occurs 4 hours before hatching [303]. This is followed by disorganised muscle contractions (also known as episodic activity) for a period of up to 3.5 hours. During this time, embryonic movement starts to develop into a more recognisable pattern. The first complete coordinated motor output, which involves left and right side synchronisation and propagation of muscle contraction in a peristaltic wave along the body axis of embryo, takes place 2 hours before hatching, or 15 minutes before tracheal filling [303]. During this 18.5-20.5 hours after egg lay period, embryos also show an increase in response to strokes applied to the anterior segment of the body [304]. Also, with increasing maturity, embryos develops the ability to right themselves when turned upside down [304].

Since motor neurons are not capable of firing action potentials until 17 hours after egg lay [305], all the movements made before this point are myogenic in origin. Blocking of evoked synaptic transmission in all neurons (*elav-Gal4*) by inducing tetanus toxin expression does not affect the occurrence of these premature movements [304]. Removing of either presynaptic terminals by expressing the cell death gene *grim* in all motorneurons, or loss of the glutamate receptor, the receptor for the major motorneuronal neurotransmitter, also do not block these myogenic activities [304]. Blocking of sensory input by expressing tetanus toxin in sensory neurons (*P0164-Gal4*) does not disrupt the transition from myogenic to synchronised muscle contractions [304].

It has been shown that all presynaptic input to the embryonic motorneurons is mediated by ACh [306]. Blocking of cholinergic neurons by expressing tetanus toxin using the *Cha-Gal4* driver [307] results in the absence of bursting activity, which is the rapid, unorganised and vigorous movement of the hatching embryo, indicating bursting activity is controlled by the central network [304]. Upon the occurrence of the first bursting, generation of movements is largely promoted by the constant input of synaptic transmission.

Blocking of synaptic transmission in all neurons (*elav-Gal4*) by manipulating the expression of the temperature sensitive vesicle recycling protein Shibire [308] for 2hrs (105 minutes before tracheal filling to 15 minutes after tracheal filling) and 1hr (45 minutes before tracheal filling to 15 minutes after tracheal filling) results in delays in the occurrence of the first complete movement for 55 minutes and 31 minutes, respectively [303]. This indicates certain level of neuronal activity needs to be achieved in order to generate mature and coordinated neuronal network.

It has previously been shown that in embryos lacking all sensory input, motor episodic activity occurs less frequently and the onset of first coordinated muscle movement is delayed by 1hr [304]. In contrast, elevation in sensory activity, induced by light impulses to sensory neurons (*PO163-Gal4*) expressing the light sensitive channel protein ChR2 [309, 310], leads to more frequent episodic activity and early occurrence of coordinated muscle movement [303]. These results altogether suggest the frequency of episodic activity generated by the immature neuronal network is correlated with the magnitude of sensory input.

In my study, the muscle movement during the period from tracheal filling to hatching was examined. Movements of these hatching larvae are divided into two types: short contractions and long contractions. Short contractions are equivalent to the premature or uncoordinated movements as described by Crisp et al. (2008). They typically last for less than 10 seconds. On the other hand, long contractions are the matured and coordinated form of muscle movement

and usually last much longer than short contractions. The whole hatching process was recorded with under the microscope. The intensity of light projected to the embryos was set at minimum level which was just enough for the camera to recognise the subject. Time interval between each capture was set at 5 second for a recording period of 2 hours or more using HCImage. The temperature of the room for the recording was set to be 20°C.

There was significant difference in the frequency of episodic movements generated in *UAS-BBS/+; elav-Gal4/+* embryos compared to controls. Also, when compared to their heterozygous counterparts, the movement at 36 hours post hatching of *B52*L24* homozygous mutant larvae was severely impaired.

6.2. Results

6.2.1. Antagonising B52 activity with BBS driven by elavGal4 in neurons causes abnormal muscle contractions during larval hatching

Four different lines were used for the hatching test, including wild type (n=3), *elavGal4* (on III) control (n=6), *elavGal4/UAS-B52-RNAi* (101740) (n=5) and *UAS-BBS/+; elavGal4/+* (n=5). Trachea filled embryos were glued on a coverslip, kept in a dark room with temperature set at 20°C. The light used for time lapse recording was set to minimum. The time interval between each capture were set to 5 seconds.

During the first 2 hours after tracheal filling, *UAS-BBS/+; elavGal4/+* animals made three times more short contractions ($p<0.001$) than *elavGal4* (III) control and the wild type larvae. No significant differences in muscle movements were observed between any other two groups. Although the standard error bars for short contractions of *elvaGal4* controls and *elavGal4/UAS-B52-RNAi* (101740) embryos do not overlap with each other, the p value of a t-test is 0.0728 between the two groups, and therefore not statistically significant.

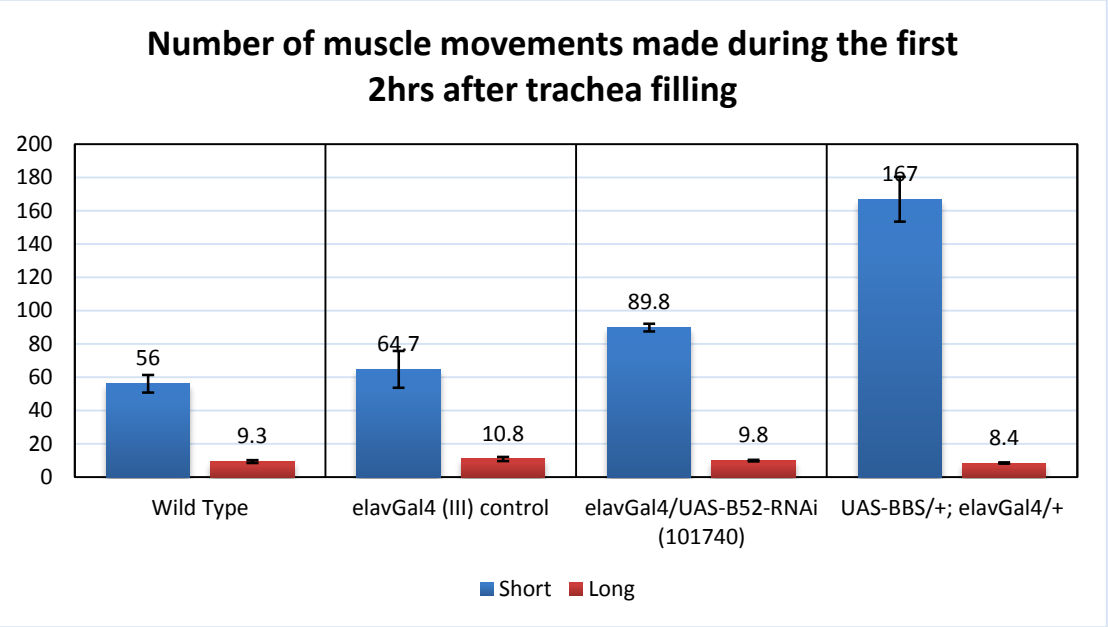

Figure 6.1 Muscle movements made during the first 2hrs after tracheal filling.

The average number of muscle movements made by wild type and *elvaGal4* (III) control are 56 and 64.7 times, respectively. Both of them made significantly less short contractions than *UAS-BBS/+; elavGal4/+*, which topped at 167 times. *elavGal4/UAS-B52-RNAi* (101740) made about 40% more short contractions than *elavGal4* (III) control, but the difference is not statistically significant. The lowest number of long contractions was made by *UAS-BBS/+; elavGal4/+* at 8.4 times, and the highest was made by *elvaGal4* (III) control at 10.8 times. Regardless of an increment of 2.4 times, the difference is not statistically significant between them. Sample sizes for each genotype are n= 3, 6, 5 and 5 for WT, *elvaGal4* (III) control, *elavGal4/UAS-B52-RNAi and UAS-BBS/+; elavGal4/+*, respectively.

6.2.2. Overexpression of B52 with elavGal4 in neurons causes even more severe abnormal muscle contractions during larval hatching

Three different lines were used for the hatching test, including *elavGal4* (on X) control (n=38), *elavGal4/+; ; UAS-BBS/+* (n=37) and *elavGal4/+; ; UAS-GFP-B52/+* (n=13). Comparisons were made with wild type data.

During the first 2 hours after tracheal filling, both *elavGal4* (X) control and *elavGal4/+; ; UAS-BBS/+* made less than half the number of short contractions ($p<0.001$) than the wild type. In addition, the number of long contractions ($p<0.001$) made by *elavGal4/+; ; UAS-BBS/+* was also significantly less than the wild type. Between *elavGal4* (X) control and *elavGal4/+; ; UAS-BBS/+*, there were significant differences in the number of times for both short ($p<0.001$) and long contractions ($p<0.001$) made, respectively. Compared *elavGal4* (X) control to, *elavGal4/+; ; UAS-GFP-B52/+,* double the number of short contractions ($p<0.001$) were made by the former. Also, only half amount of long contractions ($p<0.001$) were made by *elavGal4/+; ; UAS-GFP-B52/+* compared the wild type. The difference in long contractions made is also statistically significant ($p<0.05$) between *elavGal4/+; ; UAS-GFP-B52/+* and *elavGal4* (X) controls.

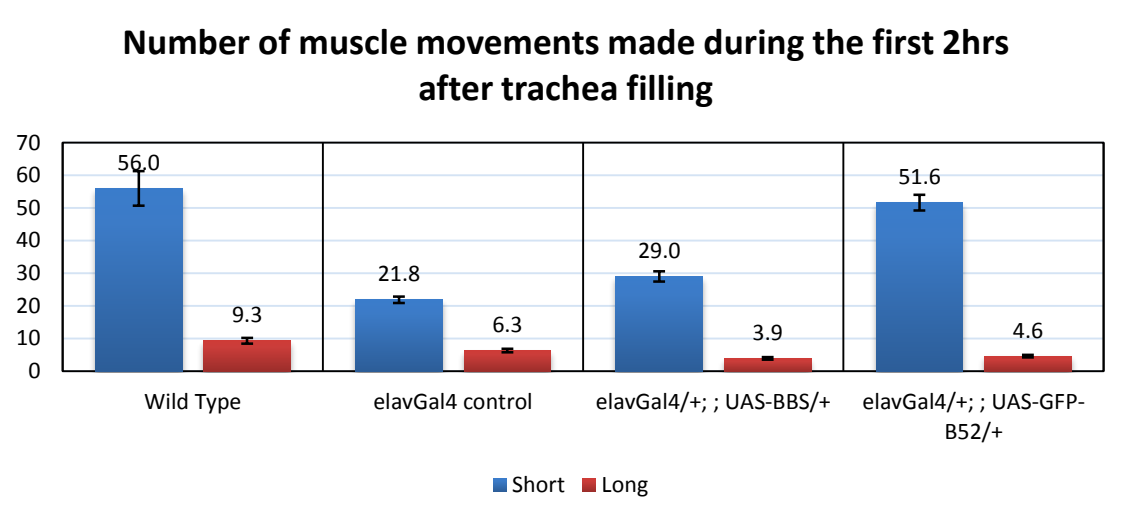

Figure 6.2 Muscle movements made during the first 2hrs after tracheal filling.

The *elvaGal4* (X) line makes much less movements than the wild type in general, with *elavGal4* (X) control and *elavGal4/+; ; UAS-BBS/+* making only about half the amount of short contractions as the wild type. With a difference of 7.2 times, numbers of short contractions made between *elavGal4* (X) control and *elavGal4/+; ; UAS-BBS/+* are significantly different from each other. The number of short contractions made by *elavGal4/+; ; UAS-GFP-B52/+* is close to the wild type, showing no significant difference. Difference in numbers of long contractions is statistically significant between (1) *elavGal4/+; ; UAS-BBS/+* and *elavGal4* (X) control, (2) *elavGal4/+; ; UAS-GFP-B52/+* and *elavGal4* (X) control, and (3) *elavGal4/+; ;*

UAS-GFP-B52/+ and the wild type. Sample sizes for each genotype are n= 3, 38, 37 and 13 for WT, *elvaGal4* (X) control, *elavGal4/+; ; UAS-BBS/+ and elavGal4/+; ; UAS-GFP-B52*, respectively.

6.2.3. Mutation of B52 does not cause severe defects of muscle contractions during larval hatching

Heterozygotes (n=20) and homozygous mutants (n=15) of *B52*L24* were used for the hatching test. Comparisons were made with the previous wild type data.

Unexpectedly, there was no significant difference in the amount of muscle contractions made between the heterozygous and homozygous *B52*L24* during the first 2 hours after trachea filling. However, both mutants displayed significant differences from wild type in terms of both short ($p<0.05$) and long contractions ($p<0.05$) made.

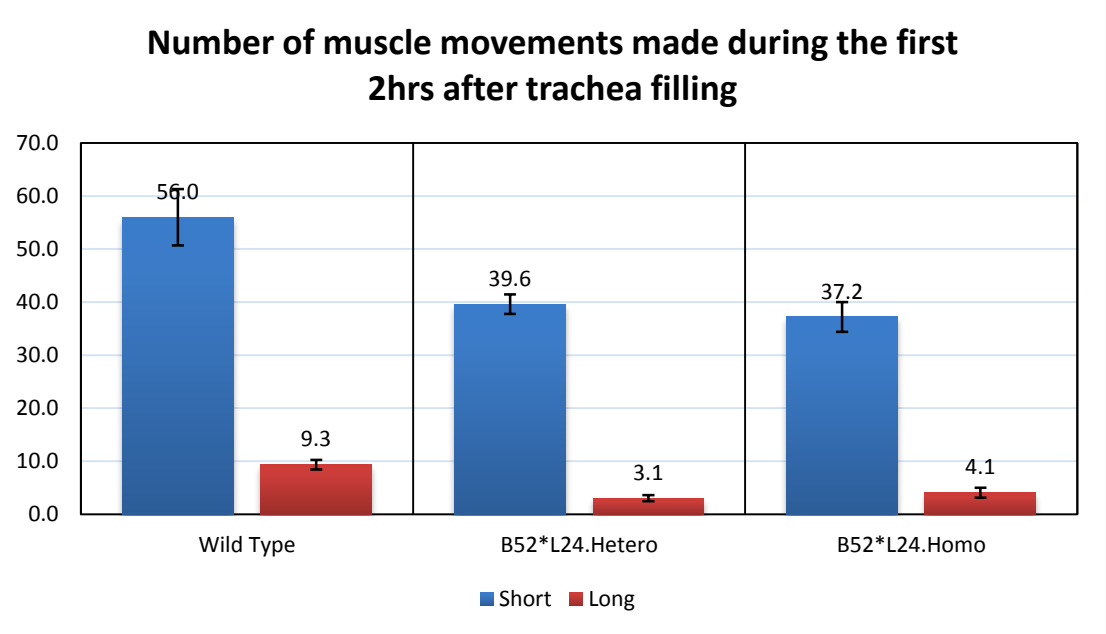

Figure 6.3 Muscle movements made during the first 2hrs after tracheal filling.

The differences in both short and long contractions made between *B52*L24* homozygous and heterozygous mutants are not significant. Both mutants made around 30% less short contractions and

less than half the amount of long contractions made by the wild type. Sample sizes for each genotype are n= 3, 20 and 15 for WT, *B52*L24* heterozygous mutants and *B52*L24* homozygous mutants, respectively.

6.2.4. Mutation of B52 causes dramatic defects in growth and locomotion in 36hrs old larvae

Considering that the reason *B52*L24* homozygous and heterozygous mutants exhibited very similar behaviour patterns might be due to maternal contribution of *B52* RNA, which was still enough to translate into B52 protein until later embryonic stages, an additional larval locomotion test was performed using 36hrs larvae.

The 36hrs post hatching larva of *B52*L24* homozygous mutant had the same body size as a 24hrs post hatching larva, and no active movement was observed at all. To make sure the larva was still alive, a gentle force was applied to the larva with the brush. Water was applied in another experiment to justify that the 36hrs post hatching *B52*L24* homozygous mutant larva was still alive. On the other hand, the heterozygous control larva was moving around actively through the whole time.

6.2.5. Time required for hatching from trachea filling (elavGal4 on X)

The amount of time required for different lines of larvae to hatch was also recorded. The tested subjects were *elavGal4* control (n=38), *elavGal4/+; ; UAS-BBS/+* (n=37) and *elavGal4/+; ; UAS-GFP-B52/+* (n=13). The starting point was set to be at the time when trachea were filled.

Compared to *elavGal4* control, Both *elavGal4/+; ; UAS-BBS/+* ($p<0.05$) and *elavGal4/+; ; UAS-GFP-B52/+* ($p<0.05$) took on average 1 hour longer to hatch.

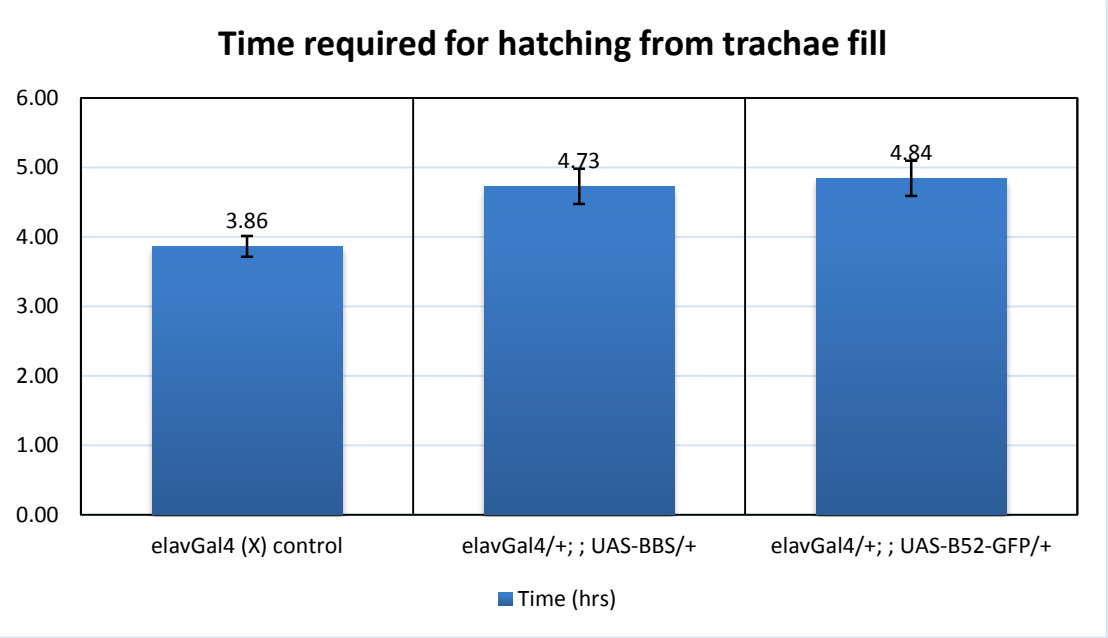

Figure 6.4 Time required for hatching from tracheal filling.

Both elavGal4/+; ; UAS-BBS/+ and elavGal4/+; ; *UAS-GFP-B52*/+ took around one hour longer for hatching, compared to elavGal4 (X) control, and this is statistically significant. Sample sizes for each genotype are n= 38, 37 and 13 for *elvaGal4* (X) control, *elavGal4/+; ; UAS-BBS/+ and elavGal4/+; ; UAS-GFP-B52*, respectively.

6.2.6. Growth defects in B52*L24 homozygous mutant animals

As mentioned in Chapter 5, in 36hrs post hatching larvae, the size of the ventral nerve cord (VNC) in *B52*L24* homozygous mutant appears to be shorter than those in the wild type and *B52*L24* heterozygous mutant. The width (widest section) of the VNC of each genotype is therefore measured with Zen, the program that comes with Zeiss LSM710. The width of VNC in *B52*L24* homozygous mutant is significantly different from those in the wild type and *B52*L24* heterozygous mutant ($p<0.001$ for both t-test analyses).

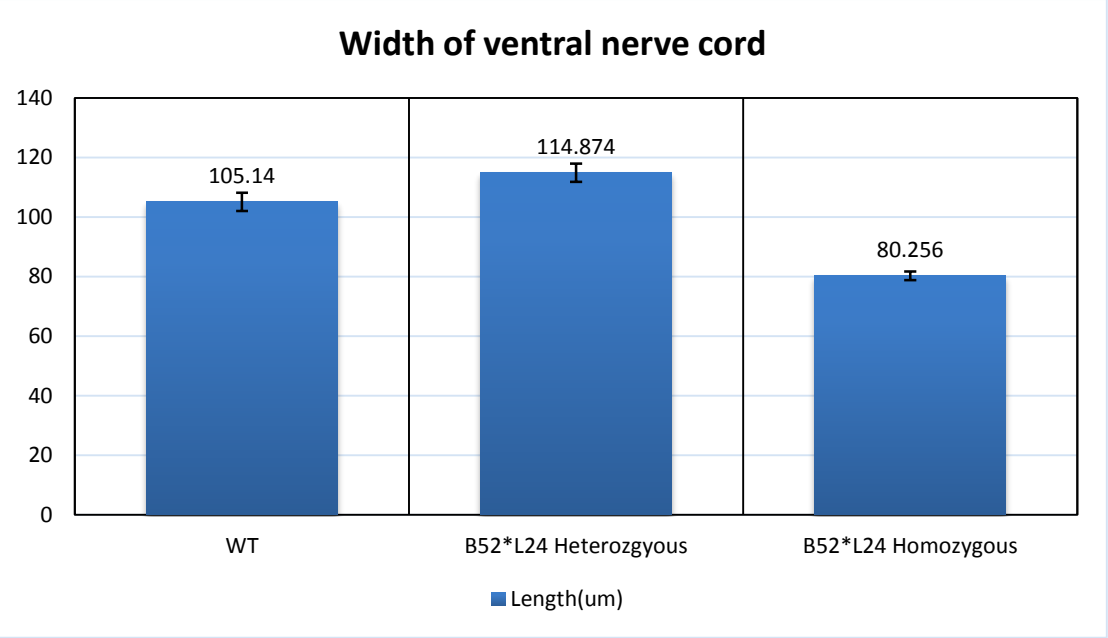

Figure 6.5 Width of ventral nerve cords in stage 17 embryos.

The width of the VNC in *B52*L24* homozygous mutant is around 24% to 30% less than that in the wild type and *B52*L24* heterozygous mutant, respectively. The differences are statistically significant. Sample sizes for each genotype are n= 5, 5 and 5 for WT, *B52*L24* heterozygous mutants and *B52*L24* homozygous mutants, respectively.

6.3. Summary of neurotransmitter and behavioural phenotypes

6.3.1. ChAT is essential for the correct locomotion of larval and B52 is responsible for splicing of ChAT mRNA

The above results suggest the increase in short contractions is always coupled with a decrease in long contractions. This can be justified by the maturity of the neuronal network, since short contractions usually represent uncoordinated movements, whereas the presence of long contractions means a more matured neuronal network. The hatching test results suggest the increase in short contraction, and therefore decrease in long contraction, are caused by reduced B52 level in the embryonic central nervous system (CNS). Also, reduction in B52 level leads to

delayed embryo hatching, possibly due to hindered maturation of the neuronal network, since B52 is involved in regulating the level of neurotransmitters through ChAT and v-Glut.

It seems the locations of *elavGal4* inserted in the genome is affecting the behaviour of the embryos, with *elavGal4* (III) behaves more similar to the wild type, while *elavGal4* (X) being only half active as the wild type, in terms of short contractions made. The insertion of *elavGal4* on X chromosome seems to cause unwanted disruption of the endogenous process. Since the insertion is on the X chromosome, this could mean the associated defect is likely to be sex-specific. The consequences of the insertion cannot be balanced by the second X chromosome since its complementary pair is the Y chromosome. However, it was impossible to tell the sex of hatching embryos when the recording was made, and therefore the phenotypes cannot be separated from one another.

Increase in short contractions was not expected in *elavGal4/+; ; UAS-GFP-B52/+*, because no obvious changes in ChAT or v-Glut level were detected compared to *elavGal4/+* (X) control. It is hard to tell whether this is real or simply an artefact, since this is the only line analysed for muscle movement with elevated B52 level. However, if this movement "defect" is reproducible in *elavGal4/+; ; UAS-GFP-B52/+*, the fact that overexpression of B52 brings the *elavGal4* (X) phenotype back to the wild type may indicate B52 somehow compensates the side effect induced by *elavGal4* insertion on the X chromosome.

In all tests done with *elavGal4* lines (III and X) and *B52*L24* line, levels of both ChAT and v-Glut are elevated in response to reduced B52 activity. The only exception is seen in 36hrs post hatching larval brain of *B52*L24* heterozygotes, where the level of ChAT is lower than that in *B52*L24* homozygous mutant as expected, but the level of v-Glut is the same when compared to *B52*L24* homozygous mutant. On the other hand, in 36hrs post hatching larval brain, ChAT level in *B52*L24* heterozygotes is the same as the wild type, which is expected at first place.

However, the level of v-Glut in *B52*L24* heterozygotes is higher than that in the wild type in 36hrs post hatching larval brain.

It is interesting to know that while the expression level of v-Glut might be different during the time of embryo hatching, which is deduced from the difference in v-Glut level in 24hrs post hatching larval brain of *B52*L24* heterozygous and homozygous mutants, the hatching embryos behave similarly to one another. In contrast, by 36hrs after hatching, both *B52*L24* heterozygous and homozygous mutants have the same level of v-Glut in the brain, but behave completely different from each other. These all together suggest the main contributory factor of difference in behaviour has something to do with the level of ChAT in 36hrs post hatching larval brain, and also v-Glut may not have that strong effect on regulating muscle contractions during embryo hatching.

From the comparisons made between *B52*L24* heterozygous and homozygous mutants, we have the following facts: (1) there is no strong difference in muscle movements during embryo hatching between the two lines; (2) the main difference in neurotransmitter level presents in 36hrs post hatching larval brain where ChAT is significantly elevated (levels of v-Glut are the same) as a result of the complete missing of B52 in *B52*L24* homozygous mutant (level of ChAT is only slightly higher in *B52*L24* homozygous mutant by 24hrs post hatching); (3) 36hrs post hatching larvae of *B52*L24* homozygous mutants are completely motionless, while larvae of *B52*L24* heterozygous mutants show no sign of impairment in movement; (4) unspliced ChAT mRNA is detected only in *B52*L24* homozygous mutants (24hrs post hatching larval brain). All these together suggest the synthesis of Ach mediated by ChAT is critical for the normal movement of larvae, and splicing of ChAT mRNA is in turn regulated by B52.

The underlying cause for the complete motionless of 36hrs post hatching *B52^L24* homozygous mutant larvae could be the accumulation of excessive amount of excitation signals, which results in paralysis of the muscle. This is likely to happen due to the accumulation of acetylcholine (ACh)

and the presence of its receptors. There are mainly two categories of ACh receptors, namely nicotine acetylcholine receptor (nAChR) and muscarinic acetylcholine receptor (mAChR). nAChR is a neurotransmitter-gated ion channel. This channel is found to be present in large quantity at the nerve-muscle synapse, mediating fast chemical transmission of signals in response to ACh [311]. On the other hand, mAChR is found to couple with G proteins, which in turn mediate potassium channels that are capable of causing hyperpolarisation of the plasma membrane in excitable cells [312].

As a result, overloading of excitation signals caused by the up-regulation of ChAT, and consequently prolonged exposure to its synthesis product ACh, eventually triggers the loss of sensation in the muscle, which renders the *B52^L24* homozygous mutant larvae unable to move freely. This is similar to the connection between neurological defects seen in schizophrenia patients and the abnormally high level of 5-HT [313].

As shown in the videos, 36hrs post hatching larvae of *B52^L24* homozygous mutant were able to react by performing weak muscle movement when mechanically stimulated with paint brush or submerged in water. However, the interval between each movement was relatively long compared to its heterozygous counterpart. This indicates that the larva itself was able to manage its movement once for a while possibly by clearing out the accumulated ACh and restoring the electric potential built up in the cell membrane. Nevertheless, the self-regulatory mechanism was not sufficient to overcome the dramatic effect caused by ChAT overexpression. As a result, these larvae were not able to search for food and feed themselves, and eventually ended up dying.

6.3.2. v-Glut is more sensitive to the regulation of B52

According to the comparisons made among the wild type, *B52*L24* heterozygous and homozygous mutants, v-Glut is significantly elevated when B52 level is reduced to half, but no further increase of v-Glut occurs when B52 protein is completely gone. This, in contrary to the

relationship between B52 and ChAT, whose expression level is only increased dramatically when all B52 protein is gone, suggests v-Glut is more sensitive to B52 activity in compare to ChAT. This gives a reason why B52 is more needed, and therefore has higher expression in dMP2 than in vMP2. The presence of B52 is important for the strict control of v-Glut, which is specifically expressed by dMP2 motorneuron, whereas in vMP2 interneuron, the requirement of B52 by ChAT appears to be less demanding.

6.3.3. B52 splicing target ecdysone receptor is a primary target that contributes to the defects in development of larval body and VNC sizes

In addition to the small size of its VNC, it has also been shown in the video that the body size of 36hrs post hatching larvae homozygous mutant for *B52*L24* maintained the size of 24hrs post hatching larvae. The underlying causes for the small sizes of body and VNC in those 36hrs post hatching *B52^L24* homozygous mutant larvae, together with defects in larval locomotion could potentially be attributed to the misregulation of ecdysone receptor (EcR). As indicated by genomic SELEX, the EcR encoding transcript is a potential RNA splicing target of B52 ([219, 234]).

According to FlyBase, EcR has been reported to have a total of six transcripts. Studies of the EcR have been focusing on three protein isoforms: EcR-A, EcR-B1, and EcR-B2 [314, 315]. Mutations that inactivate EcR-B1 and EcR-B2 cause defects in larval molting, for example the transition from 1st instar larva to 2nd instar larva [316]. Mutations that inactivate EcR-B1 block ecdysone responses and prevents metamorphosis. Moreover, mutations of all three EcR protein isoforms are embryonic lethal [317].

Because mutations of all EcR proteins (or EcR common-domain mutants, i.e. the gene sequence that presents in all transcripts is mutated) cause early death at embryonic stages, a mutation construct using heat shock to induce EcR-B2 expression every 12 hours to sustain the life of the embryo in order to reach further developmental stages was used to study the impact of EcR in

larval stages [314]. It has been shown that expression of EcR-B2 during embryogenesis in EcR mutants can allow such mutant animals to develop to the first instar larval stage and to have normal appearance and movement until the end of the first instar. If no further heat pulses are given, they arrest as first instar larvae and die after one or two days [314]. Furthermore, most rescued larvae arrest with mouth parts and posterior spiracles like those of the first instar larvae. The authors grouped the EcR mutants into 3 stages: stage 1, during which larvae actively crawl and constantly move mouthparts; stage 2, during which larvae become stationary and cease movement of mouthparts, if stimulated with a needle, they resume crawling and mouthpart movements; and stage 3, which is basically on the verge of death where larvae generate no response to stimulations, and cease dorsal medial abdominal contraction [314].

The phenotypes described for EcR mutant greatly resembles what has been observed in *B52^L24* homozygous mutants, where the body features of the larva were arrested at 24hrs post hatching, or the end of 1st instar, and within another 12hrs, the larvae stopped moving but were still able to generate weak response to stimulations, followed eventual death shortly afterwards. This suggests EcR a likely RNA splicing target of B52, and the mutation in B52 is ultimately responsible for the defects seen in larval development.

6.4. Discussion

Network formation can be altered in response to neurotransmission. Acetylcholine (ACh) mediated neurotransmission is essential for the formation of behaviour patterns such as limb movement in mouse [318]. In *ChAT* mutant mice, an increased amount of muscle nerve branching, hyperinnervation and perinatal death are observed [319, 320]. ACh is known to be necessary for shaping the early episodic activity into organised muscle movement in embryonic chick and mouse [321, 322]. Deprivation of ACh during embryogenesis alters the pattern of these spontaneous locomotion. In these *ChAT* mutants, coordination of right-left is abnormal [318].

In *C.elegans*, non-lethal mutation of vesicle acetylcholine transporter (VAChT) leads to uncoordinated movements [323, 324]. In this study, there was an increase in uncoordinated movements (Chapter 6) in *B52* dominant negative mutant (*UAS-BBS/+; elavGal4/+*), which might corresponds to the above mentioned elevation of ChAT. In *VAChT* homozygous mutant created by Kitamoto et al., 1st instar larvae are relatively inactive compared to heterozygous mutants [325]. This observation resembles the 36hrs post-hatching larvae of *B52*L24* homozygous mutants.

In this study, antagonising of B52 activity by inducing *BBS* leads to an increase of uncoordinated larval movement as well as delayed hatching, as seen in *UAS-BBS/+; elavGal4/+*. Larval behaviour is not significantly affected by the lack of B52 activity in *B52*L24* homozygous mutant at 24hrs post-hatching. This might be caused by the maternal contribution which provides the last available B52, enough to cover the 1st instar larval stage. As development goes on, severe impairment of larval movement has occurred which results in complete motionless of the larvae at 36hrs post-hatching, shortly before the death of the larvae. From one point, mis-regulation of *ChAT*, which is caused by the lack of B52, and subsequent disruption of ACh synthesis may be the cause of abnormal larval movement and death.

In addition to the above findings, study of *islet* (*isl*) has revealed a possible connection between embryo hatching and other neurotransmitters. Islet is required by *Drosophila* in axon pathfinding and targeting, and mutation of *isl* causes loss of dopamine and serotonin synthesis [271]. Restoring of Islet function by introducing *UAS-isl* using *elavGal4* rescued neurotransmitter specification in tyrosine hydroxylase- (TH), serotonin- and DDC-expressing neurons. However, expression of TH or serotonin was not completely restored in all segments, and these embryos failed to hatch [271]. This suggests expression of TH and serotonin is also essential for embryo hatching. In my experiment, levels of both TH and serotonin did not show significant difference between the mutants (including *elavGal4/+; UAS-BBS/+* and *B52*L24* homozygous mutant) and

the corresponding controls. Therefore, the possible effect of TH and serotonin over the muscle movement defects during embryo hatching can be excluded. This, once again, supports the notion that mis-regualtion of ChAT is the primary cause of movement defects.

Chapter 7 Impact of the Results

This study started with single cell transcriptome analysis, compared the gene expression profile between the two sibling cells vMP2 and dMP2. The *B52* gene was selected due to its strong over-expression (45-times) in the dMP2 cell. Down-regulation of the splicing factor B52 in dMP2 cell causes overshooting of its posterior axon. Also, *B52^L24* homozygous mutants larvae, generated in this study, which are devoid of *B52* mRNA in the brain exhibit impairment in larval movements 36hrs post hatching. The defects in larval locomotion are attributed to the elevation of acertylcholine levels caused by the aberrant splicing of the *ChAT* gene, which correlates with the reduction of B52 level. Further analysis of *ChAT* splicing conditions in *B52^L24* homozygous mutants and also when *B52* is down-regulated through sequestration (*elavGal4/+; ; UAS-BBS/+*) revealed that the lack of B52 causes the presence of an unspliced *ChAT* RNA isoform.

7.1. B52 is involved in axonal pathfinding, neurotransmitter regulation and larval locomotion

It has been shown in this study that manipulation of B52 level does not interfere dramatically with the development of the nervous system in early stage *Drosophila* embryos. For example, the morphology and identity of different groups of neurons, including neuroblasts and all differentiated neurons, were not affected simply because B52 activity was antagonised. Regardless of that, overshooting of posterior axon in the dMP2 cell was observed when B52 activity was reduced (Fig 3.2a). This can possibly attribute to the mis-regulation of *lola*, a potential B52 splicing target identified by both genomic SELEX and microarry [219, 234]. *lola* has a total of 19 splice variants, whose presence affects a range of tissues and cells such as gonad, imaginal discs, or dorsal cell layer of the central nervous system (CNS) in the embryo [244]. Interestingly, *lola* itself encodes a transcription factor regulating a group of targets, including

axon guiding molecules DSCAM and Frazzled [247]. Mutations in *lola* have been reported to cause defects in axon growth and guidance. Specifically, breaks in the longitudinal axons have been observed in *lola* mutants, and pioneer axon MP fails to orient towards its fasciculation target [326]. In a different study, Lola has been shown to have strong correlation with an axon guiding molecule Slit, where ectopic expression of *lola* leads to ectopic expression of *slit* [257]. Slit is a midline repellent signalling molecule which prevents longitudinal axon from crossing the midline.

As the single cell transcriptome analysis indicates, B52 is expressed in a much higher level in dMP2 cell compared to that in its sibling vMP2 cell. The difference in expression levels of B52 may contribute to the different functions each of the two sibling cells were assigned for by the time they differentiate from the mother MP2 cell. The differentiation is a necessary step to ensure the generation of cells with novel properties compared to its precursors through genetic rearrangement, which in this case results in the rise of the vMP2 interneuron which projects axon anteriorly and expressing ACh, and also the dMP2 motor neuron, which projects axon posteriorly and expressing glutamate. The roles of these two sibling cells have become completely distinct from each other by the time they are separated. For example, even though the axons of both cells function as pioneers to guide other longitudinal axons, each of them is programmed to interact and fasciculate with different target axons. Also, later in the larval stage, vMP2 and dMP2 are likely to have opposite or totally independent effects on larval locomotion, where one functions as an inhibitor to suppress the generation of certain movement, and the other facilitates the conduction of a particular movement, based on the fact they innervate different targets and express different neurotransmitters. Neuronal processes like these are all, to a certain degree, regulated by genetic components, especially during early developmental stages where environmental factors only play a minimum role. From the available gene pool of the vMP2 and dMP2 cells, *B52* turns out to be one of the leading factors contributing to their difference in cell fate because the expression levels of this gene have been shown to be

significantly different between vMP2 and dMP2, and this difference in *B52* expression levels in turn contributes to the distinct functions and properties of the corresponding cells. Also, B52 is likely to be needed by more than the genes examined in this study, such as the ones identified by genomic SELEX and microarray [219, 234]. The high level of B52 in dMP2 may well be required by those target genes.

It is evident that the selection of neurotransmitter by specific cells can have great impact on the subsequent regulation of larval movement. For example, the choice between excitatory and inhibitory neurotransmitter can results in completely opposite outcomes when either of them is taking the dominant effect. From the intensity analysis for ChAT and v-Glut levels in 36hrs post hatching larval brain devoid of B52 RNA (*B52^L24* homozygous mutants), it seems that the correlation between B52 level and Chat level is reciprocal (i.e. the increase of one leads to a decrease of the other and vice versa), whereas the relationship between B52 and v-Glut reaches a limit at a relatively early point when the v-Glut level is saturated regardless of further decreases in B52 level, as seen between 24hrs and 36hrs post hatching *B52^L24* homozygous mutants (i.e. a hyperbola curve where v-Glut level saturates at a point where reduction of B52 level does not induce any further change of v-Glut level). In these *B52^L24* homozygous mutants, the expression level of *ChAT* is strongly elevated as compared to the control *B52^L24* heterozygotes, where the *B52* level is only reduced to half of the wild type situation due to defects in splicing of *ChAT* mRNA (Fig. 5.21A and 5.26A). As a result, the accumulation of excessive *ChAT* leads to constant synthesis of ACh, which subsequently causes hyper-polarisation of the cell membrane due to the presence of highly sensitive ACh receptors, which also happen to be in large quantity [311]. This ultimately leads to over-excitation and paralysis of the larval muscle, and therefore explains the cease of movement, while at the same time the ability to generate weak response to stimuli, seen in 36hrs post hatching larvae devoid of *B52* RNA.

In late embryonic and larval stages, muscles movements start to emerge, reflecting the need of neurotransmitters to regulate neuronal processes. On the other hand, in early developmental stages, during which the fundamental infrastructure of the nervous system is still being built, the presence of neurotransmitters may not seem to have that much of an impact. However, mis-regulation of these neurotransmitters is still likely to cause deleterious effects in the nervous system.

For example, an important part of neuronal circuit formation is the process of seeking synaptic partner by each neuron, during which a molecular dance is performed by each participating neuron to check if a potential target is actually the right candidate. This often involves the communication between the pre- and post-synaptic sites. Normally, an exchange of moderate amount of chemical information, in the form of signaling molecules such as neurotransmitters, is enough to tell whether or not the neuron on the other end is the programed target, and therefore prolonged exposure to signaling molecules is usually avoided and apparently is not favoured by nature.

Interestingly, overexpression of ChAT has been shown to be beneficial in several cases. For example, overexpression of cardiac ChAT prevented cardiac remodeling and improved survival after myocardial infarction (commonly known as heart attack) or acute ischemia–reperfusion injury (tissue damage caused by lack of blood supply) through these pleiotropic effects of ACh [327]. However, in a normal setting, the accumulation of neurotransmitter can cause deleterious effects, such as in the case of GABA accumulation as a result of ischemic brain injury, which contributes to the pathogenesis of a stroke in patients [328]. In a non-medical setting, the absence of ACh or ChAT in mouse results in smaller, less well connected nerve terminals at the neuromuscular [319] and the total number of axons are doubled [320], meaning that they fail to locate their targets efficiently. The increase in the number of axons is attributed primarily to

neuromuscular paralysis, which is caused by the lack of regulatory neurotransmitter ACh in this case.

However, in a situation where signals are constantly fired between two neurons, an inevitable outcome is the hyper-polarisation of the cell membrane. This may trigger various downstream effects according to the chemicals released and cells being targeted, having the potential of initiating large scale cascade effects of multiple pathways. The likely result will be the cell losing control of maintaining its components, and eventually collapse and get destroyed by apoptosis, provided the surrounding non-neuronal cells are not affected.

As discussed in greater details in Chapter 6, ecdysone receptor (EcR) is highly likely to be the target of the B52 splicing factor, which is responsible for the arrest of both the larval body and ventral nerve cord (VNC) sizes at 1st instar. It has been shown EcR is an essential factor for larval molting, i.e. the transition of 1st instar larva to 2nd instar larva, which involves growth in body size and hardening of cuticles for example [314]. *EcR* mutants highly resemble the 36hrs post hatching *B52^L24* homozygous mutants. They normally appear to be complete motionless for both their body and mouthparts, but still retain the ability to generate weak response to stimuli, and eventual die due to lack of feeding or the ability to move around and search for food.

Overall, this study has shown that first, the level of ChAT is correlated with the locomotion defects seen in larvae devoid of B52 RNA, and secondly, B52 is responsible for the splicing of *ChAT* mRNA. Two primary potential splicing targets of B52, *lola* and *EcR*, should be tested to further confirm the phenotypes associated with *B52* down-regulation and *B52* mutation.

References

1. Campos-Ortega JA: **Mechanisms of early neurogenesis in Drosophila melanogaster**. *Journal of neurobiology* 1993, **24**(10):1305-1327.
2. Ohno S: **Intercellular junctions and cellular polarity: the PAR-aPKC complex, a conserved core cassette playing fundamental roles in cell polarity**. *Current opinion in cell biology* 2001, **13**(5):641-648.
3. Wodarz A: **Establishing cell polarity in development**. *Nature cell biology* 2002, **4**(2):E39-44.
4. Schober M, Schaefer M, Knoblich JA: **Bazooka recruits Inscuteable to orient asymmetric cell divisions in Drosophila neuroblasts**. *Nature* 1999, **402**(6761):548-551.
5. Wodarz A, Ramrath A, Kuchinke U, Knust E: **Bazooka provides an apical cue for Inscuteable localization in Drosophila neuroblasts**. *Nature* 1999, **402**(6761):544-547.
6. Wodarz A: **Tumor suppressors: linking cell polarity and growth control**. *Current biology : CB* 2000, **10**(17):R624-626.
7. Petronczki M, Knoblich JA: **DmPAR-6 directs epithelial polarity and asymmetric cell division of neuroblasts in Drosophila**. *Nature cell biology* 2001, **3**(1):43-49.
8. Kaltschmidt JA, Davidson CM, Brown NH, Brand AH: **Rotation and asymmetry of the mitotic spindle direct asymmetric cell division in the developing central nervous system**. *Nature cell biology* 2000, **2**(1):7-12.
9. Muller HA, Wieschaus E: **armadillo, bazooka, and stardust are critical for early stages in formation of the zonula adherens and maintenance of the polarized blastoderm epithelium in Drosophila**. *The Journal of cell biology* 1996, **134**(1):149-163.
10. Kuchinke U, Grawe F, Knust E: **Control of spindle orientation in Drosophila by the Par-3-related PDZ-domain protein Bazooka**. *Current biology : CB* 1998, **8**(25):1357-1365.
11. Kraut R, Chia W, Jan LY, Jan YN, Knoblich JA: **Role of inscuteable in orienting asymmetric cell divisions in Drosophila**. *Nature* 1996, **383**(6595):50-55.
12. Parmentier ML, Woods D, Greig S, Phan PG, Radovic A, Bryant P, O'Kane CJ: **Rapsynoid/partner of inscuteable controls asymmetric division of larval neuroblasts in Drosophila**. *The Journal of neuroscience : the official journal of the Society for Neuroscience* 2000, **20**(14):RC84.
13. Schaefer M, Petronczki M, Dorner D, Forte M, Knoblich JA: **Heterotrimeric G proteins direct two modes of asymmetric cell division in the Drosophila nervous system**. *Cell* 2001, **107**(2):183-194.
14. Schaefer M, Shevchenko A, Knoblich JA: **A protein complex containing Inscuteable and the Galpha-binding protein Pins orients asymmetric cell divisions in Drosophila**. *Current biology : CB* 2000, **10**(7):353-362.
15. Yu F, Morin X, Cai Y, Yang X, Chia W: **Analysis of partner of inscuteable, a novel player of Drosophila asymmetric divisions, reveals two distinct steps in inscuteable apical localization**. *Cell* 2000, **100**(4):399-409.
16. Ohshiro T, Yagami T, Zhang C, Matsuzaki F: **Role of cortical tumour-suppressor proteins in asymmetric division of Drosophila neuroblast**. *Nature* 2000, **408**(6812):593-596.
17. Peng CY, Manning L, Albertson R, Doe CQ: **The tumour-suppressor genes lgl and dlg regulate basal protein targeting in Drosophila neuroblasts**. *Nature* 2000, **408**(6812):596-600.
18. Albertson R, Doe CQ: **Dlg, Scrib and Lgl regulate neuroblast cell size and mitotic spindle asymmetry**. *Nature cell biology* 2003, **5**(2):166-170.
19. Lamoureux P, Altun-Gultekin ZF, Lin C, Wagner JA, Heidemann SR: **Rac is required for growth cone function but not neurite assembly**. *Journal of cell science* 1997, **110 (Pt 5)**:635-641.

20. Forscher P, Smith SJ: **Actions of cytochalasins on the organization of actin filaments and microtubules in a neuronal growth cone**. *The Journal of cell biology* 1988, **107**(4):1505-1516.
21. Tanaka E, Sabry J: **Making the connection: cytoskeletal rearrangements during growth cone guidance**. *Cell* 1995, **83**(2):171-176.
22. Mitchison TJ, Cramer LP: **Actin-based cell motility and cell locomotion**. *Cell* 1996, **84**(3):371-379.
23. Steketee MB, Tosney KW: **Three functionally distinct adhesions in filopodia: shaft adhesions control lamellar extension**. *The Journal of neuroscience : the official journal of the Society for Neuroscience* 2002, **22**(18):8071-8083.
24. Lin CH, Forscher P: **Growth cone advance is inversely proportional to retrograde F-actin flow**. *Neuron* 1995, **14**(4):763-771.
25. Schmidt A, Hall MN: **Signaling to the actin cytoskeleton**. *Annual review of cell and developmental biology* 1998, **14**:305-338.
26. Mueller BK: **Growth cone guidance: first steps towards a deeper understanding**. *Annual review of neuroscience* 1999, **22**:351-388.
27. Braga VM: **Cell-cell adhesion and signalling**. *Current opinion in cell biology* 2002, **14**(5):546-556.
28. Patel BN, Van Vactor DL: **Axon guidance: the cytoplasmic tail**. *Current opinion in cell biology* 2002, **14**(2):221-229.
29. Wills Z, Marr L, Zinn K, Goodman CS, Van Vactor D: **Profilin and the Abl tyrosine kinase are required for motor axon outgrowth in the Drosophila embryo**. *Neuron* 1999, **22**(2):291-299.
30. Lu M, Witke W, Kwiatkowski DJ, Kosik KS: **Delayed retraction of filopodia in gelsolin null mice**. *The Journal of cell biology* 1997, **138**(6):1279-1287.
31. Meberg PJ, Ono S, Minamide LS, Takahashi M, Bamburg JR: **Actin depolymerizing factor and cofilin phosphorylation dynamics: response to signals that regulate neurite extension**. *Cell motility and the cytoskeleton* 1998, **39**(2):172-190.
32. Conde C, Caceres A: **Microtubule assembly, organization and dynamics in axons and dendrites**. *Nature reviews Neuroscience* 2009, **10**(5):319-332.
33. Dent EW, Gertler FB: **Cytoskeletal dynamics and transport in growth cone motility and axon guidance**. *Neuron* 2003, **40**(2):209-227.
34. Lowery LA, Van Vactor D: **The trip of the tip: understanding the growth cone machinery**. *Nature reviews Molecular cell biology* 2009, **10**(5):332-343.
35. Kabir N, Schaefer AW, Nakhost A, Sossin WS, Forscher P: **Protein kinase C activation promotes microtubule advance in neuronal growth cones by increasing average microtubule growth lifetimes**. *The Journal of cell biology* 2001, **152**(5):1033-1044.
36. Zakharenko S, Popov S: **Dynamics of axonal microtubules regulate the topology of new membrane insertion into the growing neurites**. *The Journal of cell biology* 1998, **143**(4):1077-1086.
37. Fukata Y, Itoh TJ, Kimura T, Menager C, Nishimura T, Shiromizu T, Watanabe H, Inagaki N, Iwamatsu A, Hotani H *et al*: **CRMP-2 binds to tubulin heterodimers to promote microtubule assembly**. *Nature cell biology* 2002, **4**(8):583-591.
38. Liu CW, Lee G, Jay DG: **Tau is required for neurite outgrowth and growth cone motility of chick sensory neurons**. *Cell motility and the cytoskeleton* 1999, **43**(3):232-242.
39. Ahmad FJ, Echeverri CJ, Vallee RB, Baas PW: **Cytoplasmic dynein and dynactin are required for the transport of microtubules into the axon**. *The Journal of cell biology* 1998, **140**(2):391-401.
40. Harada A, Teng J, Takei Y, Oguchi K, Hirokawa N: **MAP2 is required for dendrite elongation, PKA anchoring in dendrites, and proper PKA signal transduction**. *The Journal of cell biology* 2002, **158**(3):541-549.

41. Shaw G, Bray D: **Movement and extension of isolated growth cones**. *Experimental cell research* 1977, **104**(1):55-62.
42. Gould RM, Connell F, Spivack W: **Phospholipid metabolism in mouse sciatic nerve in vivo**. *Journal of neurochemistry* 1987, **48**(3):853-859.
43. Gould RM, Holshek J, Silverman W, Spivack WD: **Localization of phospholipid synthesis to Schwann cells and axons**. *Journal of neurochemistry* 1987, **48**(4):1121-1131.
44. Vance JE, Pan D, Vance DE, Campenot RB: **Biosynthesis of membrane lipids in rat axons**. *The Journal of cell biology* 1991, **115**(4):1061-1068.
45. Verhage M, Maia AS, Plomp JJ, Brussaard AB, Heeroma JH, Vermeer H, Toonen RF, Hammer RE, van den Berg TK, Missler M *et al*: **Synaptic assembly of the brain in the absence of neurotransmitter secretion**. *Science* 2000, **287**(5454):864-869.
46. Posse de Chaves E, Vance DE, Campenot RB, Vance JE: **Alkylphosphocholines inhibit choline uptake and phosphatidylcholine biosynthesis in rat sympathetic neurons and impair axonal extension**. *The Biochemical journal* 1995, **312 (Pt 2)**:411-417.
47. de Chaves EI, Rusinol AE, Vance DE, Campenot RB, Vance JE: **Role of lipoproteins in the delivery of lipids to axons during axonal regeneration**. *The Journal of biological chemistry* 1997, **272**(49):30766-30773.
48. Vance JE, Pan D, Campenot RB, Bussiere M, Vance DE: **Evidence that the major membrane lipids, except cholesterol, are made in axons of cultured rat sympathetic neurons**. *Journal of neurochemistry* 1994, **62**(1):329-337.
49. Posse De Chaves EI, Vance DE, Campenot RB, Kiss RS, Vance JE: **Uptake of lipoproteins for axonal growth of sympathetic neurons**. *The Journal of biological chemistry* 2000, **275**(26):19883-19890.
50. Tennyson VM: **The fine structure of the axon and growth cone of the dorsal root neuroblast of the rabbit embryo**. *The Journal of cell biology* 1970, **44**(1):62-79.
51. Bassell GJ, Zhang H, Byrd AL, Femino AM, Singer RH, Taneja KL, Lifshitz LM, Herman IM, Kosik KS: **Sorting of beta-actin mRNA and protein to neurites and growth cones in culture**. *The Journal of neuroscience : the official journal of the Society for Neuroscience* 1998, **18**(1):251-265.
52. Koenig E, Martin R, Titmus M, Sotelo-Silveira JR: **Cryptic peripheral ribosomal domains distributed intermittently along mammalian myelinated axons**. *The Journal of neuroscience : the official journal of the Society for Neuroscience* 2000, **20**(22):8390-8400.
53. Seeger M, Tear G, Ferres-Marco D, Goodman CS: **Mutations affecting growth cone guidance in Drosophila: genes necessary for guidance toward or away from the midline**. *Neuron* 1993, **10**(3):409-426.
54. Battye R, Stevens A, Jacobs JR: **Axon repulsion from the midline of the Drosophila CNS requires slit function**. *Development* 1999, **126**(11):2475-2481.
55. Kidd T, Bland KS, Goodman CS: **Slit is the midline repellent for the robo receptor in Drosophila**. *Cell* 1999, **96**(6):785-794.
56. Spitzweck B, Brankatschk M, Dickson BJ: **Distinct protein domains and expression patterns confer divergent axon guidance functions for Drosophila Robo receptors**. *Cell* 2010, **140**(3):409-420.
57. Harris R, Sabatelli LM, Seeger MA: **Guidance cues at the Drosophila CNS midline: identification and characterization of two Drosophila Netrin/UNC-6 homologs**. *Neuron* 1996, **17**(2):217-228.
58. Kolodziej PA, Timpe LC, Mitchell KJ, Fried SR, Goodman CS, Jan LY, Jan YN: **frazzled encodes a Drosophila member of the DCC immunoglobulin subfamily and is required for CNS and motor axon guidance**. *Cell* 1996, **87**(2):197-204.

59. Mitchell KJ, Doyle JL, Serafini T, Kennedy TE, Tessier-Lavigne M, Goodman CS, Dickson BJ: **Genetic analysis of Netrin genes in Drosophila: Netrins guide CNS commissural axons and peripheral motor axons**. *Neuron* 1996, **17**(2):203-215.
60. Tear G, Harris R, Sutaria S, Kilomanski K, Goodman CS, Seeger MA: **commissureless controls growth cone guidance across the CNS midline in Drosophila and encodes a novel membrane protein**. *Neuron* 1996, **16**(3):501-514.
61. Keleman K, Rajagopalan S, Cleppien D, Teis D, Paiha K, Huber LA, Technau GM, Dickson BJ: **Comm sorts robo to control axon guidance at the Drosophila midline**. *Cell* 2002, **110**(4):415-427.
62. Sabatier C, Plump AS, Le M, Brose K, Tamada A, Murakami F, Lee EY, Tessier-Lavigne M: **The divergent Robo family protein rig-1/Robo3 is a negative regulator of slit responsiveness required for midline crossing by commissural axons**. *Cell* 2004, **117**(2):157-169.
63. Chen Z, Gore BB, Long H, Ma L, Tessier-Lavigne M: **Alternative splicing of the Robo3 axon guidance receptor governs the midline switch from attraction to repulsion**. *Neuron* 2008, **58**(3):325-332.
64. Shirasaki R, Katsumata R, Murakami F: **Change in chemoattractant responsiveness of developing axons at an intermediate target**. *Science* 1998, **279**(5347):105-107.
65. Lyuksyutova AI, Lu CC, Milanesio N, King LA, Guo N, Wang Y, Nathans J, Tessier-Lavigne M, Zou Y: **Anterior-posterior guidance of commissural axons by Wnt-frizzled signaling**. *Science* 2003, **302**(5652):1984-1988.
66. Stein E, Tessier-Lavigne M: **Hierarchical organization of guidance receptors: silencing of netrin attraction by slit through a Robo/DCC receptor complex**. *Science* 2001, **291**(5510):1928-1938.
67. Parra LM, Zou Y: **Sonic hedgehog induces response of commissural axons to Semaphorin repulsion during midline crossing**. *Nature neuroscience* 2010, **13**(1):29-35.
68. Kidd T, Brose K, Mitchell KJ, Fetter RD, Tessier-Lavigne M, Goodman CS, Tear G: **Roundabout controls axon crossing of the CNS midline and defines a novel subfamily of evolutionarily conserved guidance receptors**. *Cell* 1998, **92**(2):205-215.
69. Yoshikawa S, McKinnon RD, Kokel M, Thomas JB: **Wnt-mediated axon guidance via the Drosophila Derailed receptor**. *Nature* 2003, **422**(6932):583-588.
70. Bonkowsky JL, Yoshikawa S, O'Keefe DD, Scully AL, Thomas JB: **Axon routing across the midline controlled by the Drosophila Derailed receptor**. *Nature* 1999, **402**(6761):540-544.
71. Bourikas D, Pekarik V, Baeriswyl T, Grunditz A, Sadhu R, Nardo M, Stoeckli ET: **Sonic hedgehog guides commissural axons along the longitudinal axis of the spinal cord**. *Nature neuroscience* 2005, **8**(3):297-304.
72. Hiramoto M, Hiromi Y: **ROBO directs axon crossing of segmental boundaries by suppressing responsiveness to relocalized Netrin**. *Nat Neurosci* 2006, **9**(1):58-66.
73. Ogawa S, Tank DW, Menon R, Ellermann JM, Kim SG, Merkle H, Ugurbil K: **Intrinsic signal changes accompanying sensory stimulation: functional brain mapping with magnetic resonance imaging**. *Proceedings of the National Academy of Sciences of the United States of America* 1992, **89**(13):5951-5955.
74. Ogawa S, Lee TM, Nayak AS, Glynn P: **Oxygenation-sensitive contrast in magnetic resonance image of rodent brain at high magnetic fields**. *Magnetic resonance in medicine : official journal of the Society of Magnetic Resonance in Medicine / Society of Magnetic Resonance in Medicine* 1990, **14**(1):68-78.
75. Binder JR, Frost JA, Hammeke TA, Cox RW, Rao SM, Prieto T: **Human brain language areas identified by functional magnetic resonance imaging**. *The Journal of neuroscience : the official journal of the Society for Neuroscience* 1997, **17**(1):353-362.

76. Yamahachi H, Marik SA, McManus JN, Denk W, Gilbert CD: **Rapid axonal sprouting and pruning accompany functional reorganization in primary visual cortex**. *Neuron* 2009, **64**(5):719-729.
77. O'Leary DD, Bicknese AR, De Carlos JA, Heffner CD, Koester SE, Kutka LJ, Terashima T: **Target selection by cortical axons: alternative mechanisms to establish axonal connections in the developing brain**. *Cold Spring Harbor symposia on quantitative biology* 1990, **55**:453-468.
78. Nakamura H, O'Leary DD: **Inaccuracies in initial growth and arborization of chick retinotectal axons followed by course corrections and axon remodeling to develop topographic order**. *The Journal of neuroscience : the official journal of the Society for Neuroscience* 1989, **9**(11):3776-3795.
79. Simon DK, O'Leary DD: **Development of topographic order in the mammalian retinocollicular projection**. *The Journal of neuroscience : the official journal of the Society for Neuroscience* 1992, **12**(4):1212-1232.
80. Zhao Z, Ma L: **Regulation of axonal development by natriuretic peptide hormones**. *Proceedings of the National Academy of Sciences of the United States of America* 2009, **106**(42):18016-18021.
81. Zhao Z, Wang Z, Gu Y, Feil R, Hofmann F, Ma L: **Regulate axon branching by the cyclic GMP pathway via inhibition of glycogen synthase kinase 3 in dorsal root ganglion sensory neurons**. *The Journal of neuroscience : the official journal of the Society for Neuroscience* 2009, **29**(5):1350-1360.
82. Ma L, Tessier-Lavigne M: **Dual branch-promoting and branch-repelling actions of Slit/Robo signaling on peripheral and central branches of developing sensory axons**. *The Journal of neuroscience : the official journal of the Society for Neuroscience* 2007, **27**(25):6843-6851.
83. Kennedy TE, Tessier-Lavigne M: **Guidance and induction of branch formation in developing axons by target-derived diffusible factors**. *Current opinion in neurobiology* 1995, **5**(1):83-90.
84. Bentley CA, Lee KF: **p75 is important for axon growth and schwann cell migration during development**. *The Journal of neuroscience : the official journal of the Society for Neuroscience* 2000, **20**(20):7706-7715.
85. Patel TD, Jackman A, Rice FL, Kucera J, Snider WD: **Development of sensory neurons in the absence of NGF/TrkA signaling in vivo**. *Neuron* 2000, **25**(2):345-357.
86. Glebova NO, Ginty DD: **Heterogeneous requirement of NGF for sympathetic target innervation in vivo**. *The Journal of neuroscience : the official journal of the Society for Neuroscience* 2004, **24**(3):743-751.
87. Krylova O, Herreros J, Cleverley KE, Ehler E, Henriquez JP, Hughes SM, Salinas PC: **WNT-3, expressed by motoneurons, regulates terminal arborization of neurotrophin-3-responsive spinal sensory neurons**. *Neuron* 2002, **35**(6):1043-1056.
88. Heffner CD, Lumsden AG, O'Leary DD: **Target control of collateral extension and directional axon growth in the mammalian brain**. *Science* 1990, **247**(4939):217-220.
89. Sato M, Lopez-Mascaraque L, Heffner CD, O'Leary DD: **Action of a diffusible target-derived chemoattractant on cortical axon branch induction and directed growth**. *Neuron* 1994, **13**(4):791-803.
90. Mirnics K, Koerber HR: **Prenatal development of rat primary afferent fibers: II. Central projections**. *The Journal of comparative neurology* 1995, **355**(4):601-614.
91. Ozaki S, Snider WD: **Initial trajectories of sensory axons toward laminar targets in the developing mouse spinal cord**. *The Journal of comparative neurology* 1997, **380**(2):215-229.

92. Wang KH, Brose K, Arnott D, Kidd T, Goodman CS, Henzel W, Tessier-Lavigne M: **Biochemical purification of a mammalian slit protein as a positive regulator of sensory axon elongation and branching**. *Cell* 1999, **96**(6):771-784.
93. Dent EW, Barnes AM, Tang F, Kalil K: **Netrin-1 and semaphorin 3A promote or inhibit cortical axon branching, respectively, by reorganization of the cytoskeleton**. *The Journal of neuroscience : the official journal of the Society for Neuroscience* 2004, **24**(12):3002-3012.
94. Hutchins BI, Kalil K: **Differential outgrowth of axons and their branches is regulated by localized calcium transients**. *The Journal of neuroscience : the official journal of the Society for Neuroscience* 2008, **28**(1):143-153.
95. Tang F, Kalil K: **Netrin-1 induces axon branching in developing cortical neurons by frequency-dependent calcium signaling pathways**. *The Journal of neuroscience : the official journal of the Society for Neuroscience* 2005, **25**(28):6702-6715.
96. Yates PA, Roskies AL, McLaughlin T, O'Leary DD: **Topographic-specific axon branching controlled by ephrin-As is the critical event in retinotectal map development**. *The Journal of neuroscience : the official journal of the Society for Neuroscience* 2001, **21**(21):8548-8563.
97. Luo L, O'Leary DD: **Axon retraction and degeneration in development and disease**. *Annual review of neuroscience* 2005, **28**:127-156.
98. O'Leary DD, Koester SE: **Development of projection neuron types, axon pathways, and patterned connections of the mammalian cortex**. *Neuron* 1993, **10**(6):991-1006.
99. McLaughlin T, Torborg CL, Feller MB, O'Leary DD: **Retinotopic map refinement requires spontaneous retinal waves during a brief critical period of development**. *Neuron* 2003, **40**(6):1147-1160.
100. Vanderhaeghen P, Cheng HJ: **Guidance molecules in axon pruning and cell death**. *Cold Spring Harbor perspectives in biology* 2010, **2**(6):a001859.
101. Yeo SY, Miyashita T, Fricke C, Little MH, Yamada T, Kuwada JY, Huh TL, Chien CB, Okamoto H: **Involvement of Islet-2 in the Slit signaling for axonal branching and defasciculation of the sensory neurons in embryonic zebrafish**. *Mechanisms of development* 2004, **121**(4):315-324.
102. Kitsukawa T, Shimizu M, Sanbo M, Hirata T, Taniguchi M, Bekku Y, Yagi T, Fujisawa H: **Neuropilin-semaphorin III/D-mediated chemorepulsive signals play a crucial role in peripheral nerve projection in mice**. *Neuron* 1997, **19**(5):995-1005.
103. Taniguchi M, Yuasa S, Fujisawa H, Naruse I, Saga S, Mishina M, Yagi T: **Disruption of semaphorin III/D gene causes severe abnormality in peripheral nerve projection**. *Neuron* 1997, **19**(3):519-530.
104. Gu C, Rodriguez ER, Reimert DV, Shu T, Fritzsch B, Richards LJ, Kolodkin AL, Ginty DD: **Neuropilin-1 conveys semaphorin and VEGF signaling during neural and cardiovascular development**. *Developmental cell* 2003, **5**(1):45-57.
105. Yaron A, Huang PH, Cheng HJ, Tessier-Lavigne M: **Differential requirement for Plexin-A3 and -A4 in mediating responses of sensory and sympathetic neurons to distinct class 3 Semaphorins**. *Neuron* 2005, **45**(4):513-523.
106. Sagasti A, Guido MR, Raible DW, Schier AF: **Repulsive interactions shape the morphologies and functional arrangement of zebrafish peripheral sensory arbors**. *Current biology : CB* 2005, **15**(9):804-814.
107. Horton AC, Ehlers MD: **Dual modes of endoplasmic reticulum-to-Golgi transport in dendrites revealed by live-cell imaging**. *The Journal of neuroscience : the official journal of the Society for Neuroscience* 2003, **23**(15):6188-6199.
108. Horton AC, Racz B, Monson EE, Lin AL, Weinberg RJ, Ehlers MD: **Polarized secretory trafficking directs cargo for asymmetric dendrite growth and morphogenesis**. *Neuron* 2005, **48**(5):757-771.

109. Ye B, Zhang Y, Song W, Younger SH, Jan LY, Jan YN: **Growing dendrites and axons differ in their reliance on the secretory pathway**. *Cell* 2007, **130**(4):717-729.
110. Jefferis GS, Marin EC, Stocker RF, Luo L: **Target neuron prespecification in the olfactory map of Drosophila**. *Nature* 2001, **414**(6860):204-208.
111. Kelsch W, Mosley CP, Lin CW, Lois C: **Distinct mammalian precursors are committed to generate neurons with defined dendritic projection patterns**. *PLoS biology* 2007, **5**(11):e300.
112. Komiyama T, Johnson WA, Luo L, Jefferis GS: **From lineage to wiring specificity. POU domain transcription factors control precise connections of Drosophila olfactory projection neurons**. *Cell* 2003, **112**(2):157-167.
113. Komiyama T, Luo L: **Intrinsic control of precise dendritic targeting by an ensemble of transcription factors**. *Current biology : CB* 2007, **17**(3):278-285.
114. Komiyama T, Sweeney LB, Schuldiner O, Garcia KC, Luo L: **Graded expression of semaphorin-1a cell-autonomously directs dendritic targeting of olfactory projection neurons**. *Cell* 2007, **128**(2):399-410.
115. Furrer MP, Vasenkova I, Kamiyama D, Rosado Y, Chiba A: **Slit and Robo control the development of dendrites in Drosophila CNS**. *Development* 2007, **134**(21):3795-3804.
116. Furrer MP, Kim S, Wolf B, Chiba A: **Robo and Frazzled/DCC mediate dendritic guidance at the CNS midline**. *Nature neuroscience* 2003, **6**(3):223-230.
117. Suli A, Mortimer N, Shepherd I, Chien CB: **Netrin/DCC signaling controls contralateral dendrites of octavolateralis efferent neurons**. *The Journal of neuroscience : the official journal of the Society for Neuroscience* 2006, **26**(51):13328-13337.
118. Zhu H, Luo L: **Diverse functions of N-cadherin in dendritic and axonal terminal arborization of olfactory projection neurons**. *Neuron* 2004, **42**(1):63-75.
119. Garner CC, Kindler S, Gundelfinger ED: **Molecular determinants of presynaptic active zones**. *Current opinion in neurobiology* 2000, **10**(3):321-327.
120. Dresbach T, Qualmann B, Kessels MM, Garner CC, Gundelfinger ED: **The presynaptic cytomatrix of brain synapses**. *Cellular and molecular life sciences : CMLS* 2001, **58**(1):94-116.
121. Garner CC, Zhai RG, Gundelfinger ED, Ziv NE: **Molecular mechanisms of CNS synaptogenesis**. *Trends in neurosciences* 2002, **25**(5):243-251.
122. Sheng M: **Molecular organization of the postsynaptic specialization**. *Proceedings of the National Academy of Sciences of the United States of America* 2001, **98**(13):7058-7061.
123. Kanno Y, Loewenstein WR: **Low-Resistance Coupling between Gland Cells. Some Observations on Intercellular Contact Membranes and Intercellular Space**. *Nature* 1964, **201**:194-195.
124. Lawrence TS, Beers WH, Gilula NB: **Transmission of hormonal stimulation by cell-to-cell communication**. *Nature* 1978, **272**(5653):501-506.
125. Suudhof TC: **Neurotransmitter release**. *Handbook of experimental pharmacology* 2008(184):1-21.
126. Ullian EM, Christopherson KS, Barres BA: **Role for glia in synaptogenesis**. *Glia* 2004, **47**(3):209-216.
127. Umemori H, Linhoff MW, Ornitz DM, Sanes JR: **FGF22 and its close relatives are presynaptic organizing molecules in the mammalian brain**. *Cell* 2004, **118**(2):257-270.
128. Scheiffele P: **Cell-cell signaling during synapse formation in the CNS**. *Annual review of neuroscience* 2003, **26**:485-508.
129. Hall AC, Lucas FR, Salinas PC: **Axonal remodeling and synaptic differentiation in the cerebellum is regulated by WNT-7a signaling**. *Cell* 2000, **100**(5):525-535.
130. Nagler K, Mauch DH, Pfrieger FW: **Glia-derived signals induce synapse formation in neurones of the rat central nervous system**. *The Journal of physiology* 2001, **533**(Pt 3):665-679.

131. Pfrieger FW, Barres BA: **New views on synapse-glia interactions**. *Current opinion in neurobiology* 1996, **6**(5):615-621.
132. Pfrieger FW, Barres BA: **Synaptic efficacy enhanced by glial cells in vitro**. *Science* 1997, **277**(5332):1684-1687.
133. Ullian EM, Sapperstein SK, Christopherson KS, Barres BA: **Control of synapse number by glia**. *Science* 2001, **291**(5504):657-661.
134. Mauch DH, Nagler K, Schumacher S, Goritz C, Muller EC, Otto A, Pfrieger FW: **CNS synaptogenesis promoted by glia-derived cholesterol**. *Science* 2001, **294**(5545):1354-1357.
135. Benson DL, Colman DR, Huntley GW: **Molecules, maps and synapse specificity**. *Nature reviews Neuroscience* 2001, **2**(12):899-909.
136. Takai Y, Shimizu K, Ohtsuka T: **The roles of cadherins and nectins in interneuronal synapse formation**. *Current opinion in neurobiology* 2003, **13**(5):520-526.
137. Benson DL, Tanaka H: **N-cadherin redistribution during synaptogenesis in hippocampal neurons**. *The Journal of neuroscience : the official journal of the Society for Neuroscience* 1998, **18**(17):6892-6904.
138. Inoue A, Sanes JR: **Lamina-specific connectivity in the brain: regulation by N-cadherin, neurotrophins, and glycoconjugates**. *Science* 1997, **276**(5317):1428-1431.
139. Lee CH, Herman T, Clandinin TR, Lee R, Zipursky SL: **N-cadherin regulates target specificity in the Drosophila visual system**. *Neuron* 2001, **30**(2):437-450.
140. Wu Q, Maniatis T: **A striking organization of a large family of human neural cadherin-like cell adhesion genes**. *Cell* 1999, **97**(6):779-790.
141. Sugino H, Hamada S, Yasuda R, Tuji A, Matsuda Y, Fujita M, Yagi T: **Genomic organization of the family of CNR cadherin genes in mice and humans**. *Genomics* 2000, **63**(1):75-87.
142. Lee RC, Clandinin TR, Lee CH, Chen PL, Meinertzhagen IA, Zipursky SL: **The protocadherin Flamingo is required for axon target selection in the Drosophila visual system**. *Nature neuroscience* 2003, **6**(6):557-563.
143. Wang X, Weiner JA, Levi S, Craig AM, Bradley A, Sanes JR: **Gamma protocadherins are required for survival of spinal interneurons**. *Neuron* 2002, **36**(5):843-854.
144. Biederer T, Sara Y, Mozhayeva M, Atasoy D, Liu X, Kavalali ET, Sudhof TC: **SynCAM, a synaptic adhesion molecule that drives synapse assembly**. *Science* 2002, **297**(5586):1525-1531.
145. Dalva MB, Takasu MA, Lin MZ, Shamah SM, Hu L, Gale NW, Greenberg ME: **EphB receptors interact with NMDA receptors and regulate excitatory synapse formation**. *Cell* 2000, **103**(6):945-956.
146. O'Brien RJ, Xu D, Petralia RS, Steward O, Huganir RL, Worley P: **Synaptic clustering of AMPA receptors by the extracellular immediate-early gene product Narp**. *Neuron* 1999, **23**(2):309-323.
147. Scheiffele P, Fan J, Choih J, Fetter R, Serafini T: **Neuroligin expressed in nonneuronal cells triggers presynaptic development in contacting axons**. *Cell* 2000, **101**(6):657-669.
148. O'Brien R, Xu D, Mi R, Tang X, Hopf C, Worley P: **Synaptically targeted narp plays an essential role in the aggregation of AMPA receptors at excitatory synapses in cultured spinal neurons**. *The Journal of neuroscience : the official journal of the Society for Neuroscience* 2002, **22**(11):4487-4498.
149. Mi R, Tang X, Sutter R, Xu D, Worley P, O'Brien RJ: **Differing mechanisms for glutamate receptor aggregation on dendritic spines and shafts in cultured hippocampal neurons**. *The Journal of neuroscience : the official journal of the Society for Neuroscience* 2002, **22**(17):7606-7616.
150. Murai KK, Nguyen LN, Irie F, Yamaguchi Y, Pasquale EB: **Control of hippocampal dendritic spine morphology through ephrin-A3/EphA4 signaling**. *Nature neuroscience* 2003, **6**(2):153-160.

151. Penzes P, Beeser A, Chernoff J, Schiller MR, Eipper BA, Mains RE, Huganir RL: **Rapid induction of dendritic spine morphogenesis by trans-synaptic ephrinB-EphB receptor activation of the Rho-GEF kalirin**. *Neuron* 2003, **37**(2):263-274.
152. Henkemeyer M, Itkis OS, Ngo M, Hickmott PW, Ethell IM: **Multiple EphB receptor tyrosine kinases shape dendritic spines in the hippocampus**. *The Journal of cell biology* 2003, **163**(6):1313-1326.
153. Dean C, Scholl FG, Choih J, DeMaria S, Berger J, Isacoff E, Scheiffele P: **Neurexin mediates the assembly of presynaptic terminals**. *Nature neuroscience* 2003, **6**(7):708-716.
154. Rudenko G, Nguyen T, Chelliah Y, Sudhof TC, Deisenhofer J: **The structure of the ligand-binding domain of neurexin Ibeta: regulation of LNS domain function by alternative splicing**. *Cell* 1999, **99**(1):93-101.
155. Sanes JR, Lichtman JW: **Development of the vertebrate neuromuscular junction**. *Annual review of neuroscience* 1999, **22**:389-442.
156. Graf ER, Zhang X, Jin SX, Linhoff MW, Craig AM: **Neurexins induce differentiation of GABA and glutamate postsynaptic specializations via neuroligins**. *Cell* 2004, **119**(7):1013-1026.
157. Shingai T, Ikeda W, Kakunaga S, Morimoto K, Takekuni K, Itoh S, Satoh K, Takeuchi M, Imai T, Monden M *et al*: **Implications of nectin-like molecule-2/IGSF4/RA175/SgIGSF/TSLC1/SynCAM1 in cell-cell adhesion and transmembrane protein localization in epithelial cells**. *The Journal of biological chemistry* 2003, **278**(37):35421-35427.
158. Takao-Rikitsu E, Mochida S, Inoue E, Deguchi-Tawarada M, Inoue M, Ohtsuka T, Takai Y: **Physical and functional interaction of the active zone proteins, CAST, RIM1, and Bassoon, in neurotransmitter release**. *The Journal of cell biology* 2004, **164**(2):301-311.
159. Ziv NE, Garner CC: **Cellular and molecular mechanisms of presynaptic assembly**. *Nature reviews Neuroscience* 2004, **5**(5):385-399.
160. Bresler T, Shapira M, Boeckers T, Dresbach T, Futter M, Garner CC, Rosenblum K, Gundelfinger ED, Ziv NE: **Postsynaptic density assembly is fundamentally different from presynaptic active zone assembly**. *The Journal of neuroscience : the official journal of the Society for Neuroscience* 2004, **24**(6):1507-1520.
161. Sans N, Petralia RS, Wang YX, Blahos J, 2nd, Hell JW, Wenthold RJ: **A developmental change in NMDA receptor-associated proteins at hippocampal synapses**. *The Journal of neuroscience : the official journal of the Society for Neuroscience* 2000, **20**(3):1260-1271.
162. Bresler T, Ramati Y, Zamorano PL, Zhai R, Garner CC, Ziv NE: **The dynamics of SAP90/PSD-95 recruitment to new synaptic junctions**. *Molecular and cellular neurosciences* 2001, **18**(2):149-167.
163. Friedman HV, Bresler T, Garner CC, Ziv NE: **Assembly of new individual excitatory synapses: time course and temporal order of synaptic molecule recruitment**. *Neuron* 2000, **27**(1):57-69.
164. Okabe S, Urushido T, Konno D, Okado H, Sobue K: **Rapid redistribution of the postsynaptic density protein PSD-Zip45 (Homer 1c) and its differential regulation by NMDA receptors and calcium channels**. *The Journal of neuroscience : the official journal of the Society for Neuroscience* 2001, **21**(24):9561-9571.
165. Marrs GS, Green SH, Dailey ME: **Rapid formation and remodeling of postsynaptic densities in developing dendrites**. *Nature neuroscience* 2001, **4**(10):1006-1013.
166. Prange O, Murphy TH: **Modular transport of postsynaptic density-95 clusters and association with stable spine precursors during early development of cortical neurons**. *The Journal of neuroscience : the official journal of the Society for Neuroscience* 2001, **21**(23):9325-9333.

167. Washbourne P, Bennett JE, McAllister AK: **Rapid recruitment of NMDA receptor transport packets to nascent synapses**. *Nature neuroscience* 2002, **5**(8):751-759.
168. Borgdorff AJ, Choquet D: **Regulation of AMPA receptor lateral movements**. *Nature* 2002, **417**(6889):649-653.
169. Passafaro M, Piech V, Sheng M: **Subunit-specific temporal and spatial patterns of AMPA receptor exocytosis in hippocampal neurons**. *Nature neuroscience* 2001, **4**(9):917-926.
170. Shen K, Meyer T: **Dynamic control of CaMKII translocation and localization in hippocampal neurons by NMDA receptor stimulation**. *Science* 1999, **284**(5411):162-166.
171. Steward O, Schuman EM: **Protein synthesis at synaptic sites on dendrites**. *Annual review of neuroscience* 2001, **24**:299-325.
172. Ju W, Morishita W, Tsui J, Gaietta G, Deerinck TJ, Adams SR, Garner CC, Tsien RY, Ellisman MH, Malenka RC: **Activity-dependent regulation of dendritic synthesis and trafficking of AMPA receptors**. *Nature neuroscience* 2004, **7**(3):244-253.
173. Bockers TM, Segger-Junius M, Iglauer P, Bockmann J, Gundelfinger ED, Kreutz MR, Richter D, Kindler S, Kreienkamp HJ: **Differential expression and dendritic transcript localization of Shank family members: identification of a dendritic targeting element in the 3' untranslated region of Shank1 mRNA**. *Molecular and cellular neurosciences* 2004, **26**(1):182-190.
174. Harris KM, Stevens JK: **Dendritic spines of CA 1 pyramidal cells in the rat hippocampus: serial electron microscopy with reference to their biophysical characteristics**. *The Journal of neuroscience : the official journal of the Society for Neuroscience* 1989, **9**(8):2982-2997.
175. Pierce JP, Mendell LM: **Quantitative ultrastructure of Ia boutons in the ventral horn: scaling and positional relationships**. *The Journal of neuroscience : the official journal of the Society for Neuroscience* 1993, **13**(11):4748-4763.
176. Schikorski T, Stevens CF: **Quantitative ultrastructural analysis of hippocampal excitatory synapses**. *The Journal of neuroscience : the official journal of the Society for Neuroscience* 1997, **17**(15):5858-5867.
177. Hering H, Sheng M: **Dendritic spines: structure, dynamics and regulation**. *Nature reviews Neuroscience* 2001, **2**(12):880-888.
178. Tashiro A, Yuste R: **Structure and molecular organization of dendritic spines**. *Histology and histopathology* 2003, **18**(2):617-634.
179. Bolshakov VY, Siegelbaum SA: **Regulation of hippocampal transmitter release during development and long-term potentiation**. *Science* 1995, **269**(5231):1730-1734.
180. Chavis P, Westbrook G: **Integrins mediate functional pre- and postsynaptic maturation at a hippocampal synapse**. *Nature* 2001, **411**(6835):317-321.
181. Matsuzaki M, Ellis-Davies GC, Nemoto T, Miyashita Y, Iino M, Kasai H: **Dendritic spine geometry is critical for AMPA receptor expression in hippocampal CA1 pyramidal neurons**. *Nature neuroscience* 2001, **4**(11):1086-1092.
182. Nusser Z, Lujan R, Laube G, Roberts JD, Molnar E, Somogyi P: **Cell type and pathway dependence of synaptic AMPA receptor number and variability in the hippocampus**. *Neuron* 1998, **21**(3):545-559.
183. Takumi Y, Ramirez-Leon V, Laake P, Rinvik E, Ottersen OP: **Different modes of expression of AMPA and NMDA receptors in hippocampal synapses**. *Nature neuroscience* 1999, **2**(7):618-624.
184. Choi S, Klingauf J, Tsien RW: **Postfusional regulation of cleft glutamate concentration during LTP at 'silent synapses'**. *Nature neuroscience* 2000, **3**(4):330-336.
185. Renger JJ, Egles C, Liu G: **A developmental switch in neurotransmitter flux enhances synaptic efficacy by affecting AMPA receptor activation**. *Neuron* 2001, **29**(2):469-484.

186. Schmidt JT, Fleming MR, Leu B: **Presynaptic protein kinase C controls maturation and branch dynamics of developing retinotectal arbors: possible role in activity-driven sharpening**. *Journal of neurobiology* 2004, **58**(3):328-340.
187. Trachtenberg JT, Chen BE, Knott GW, Feng G, Sanes JR, Welker E, Svoboda K: **Long-term in vivo imaging of experience-dependent synaptic plasticity in adult cortex**. *Nature* 2002, **420**(6917):788-794.
188. Wong WT, Wong RO: **Changing specificity of neurotransmitter regulation of rapid dendritic remodeling during synaptogenesis**. *Nature neuroscience* 2001, **4**(4):351-352.
189. Hua JY, Smith SJ: **Neural activity and the dynamics of central nervous system development**. *Nature neuroscience* 2004, **7**(4):327-332.
190. Alsina B, Vu T, Cohen-Cory S: **Visualizing synapse formation in arborizing optic axons in vivo: dynamics and modulation by BDNF**. *Nature neuroscience* 2001, **4**(11):1093-1101.
191. Hashimoto K, Kano M: **Functional differentiation of multiple climbing fiber inputs during synapse elimination in the developing cerebellum**. *Neuron* 2003, **38**(5):785-796.
192. Lichtman JW, Colman H: **Synapse elimination and indelible memory**. *Neuron* 2000, **25**(2):269-278.
193. Knott GW, Quairiaux C, Genoud C, Welker E: **Formation of dendritic spines with GABAergic synapses induced by whisker stimulation in adult mice**. *Neuron* 2002, **34**(2):265-273.
194. Chen CC, Wu JK, Lin HW, Pai TP, Fu TF, Wu CL, Tully T, Chiang AS: **Visualizing long-term memory formation in two neurons of the Drosophila brain**. *Science* 2012, **335**(6069):678-685.
195. Allen MJ, Godenschwege TA, Tanouye MA, Phelan P: **Making an escape: development and function of the Drosophila giant fibre system**. *Seminars in cell & developmental biology* 2006, **17**(1):31-41.
196. Thomas JB, Wyman RJ: **Mutations altering synaptic connectivity between identified neurons in Drosophila**. *The Journal of neuroscience : the official journal of the Society for Neuroscience* 1984, **4**(2):530-538.
197. Baird DH, Koto M, Wyman RJ: **Dendritic reduction in Passover, a Drosophila mutant with a defective giant fiber neuronal pathway**. *Journal of neurobiology* 1993, **24**(7):971-984.
198. Filippov V, Filippova M, Duerksen-Hughes PJ: **The early response to DNA damage can lead to activation of alternative splicing activity resulting in CD44 splice pattern changes**. *Cancer research* 2007, **67**(16):7621-7630.
199. Naor D, Sionov RV, Ish-Shalom D: **CD44: structure, function, and association with the malignant process**. *Advances in cancer research* 1997, **71**:241-319.
200. Filippov V, Schmidt EL, Filippova M, Duerksen-Hughes PJ: **Splicing and splice factor SRp55 participate in the response to DNA damage by changing isoform ratios of target genes**. *Gene* 2008, **420**(1):34-41.
201. Tran Q, Coleman TP, Roesser JR: **Human transformer 2beta and SRp55 interact with a calcitonin-specific splice enhancer**. *Biochimica et biophysica acta* 2003, **1625**(2):141-152.
202. Sabate MI, Stolarsky LS, Polak JM, Bloom SR, Varndell IM, Ghatei MA, Evans RM, Rosenfeld MG: **Regulation of neuroendocrine gene expression by alternative RNA processing. Colocalization of calcitonin and calcitonin gene-related peptide in thyroid C-cells**. *The Journal of biological chemistry* 1985, **260**(5):2589-2592.
203. Amara SG, Jonas V, Rosenfeld MG, Ong ES, Evans RM: **Alternative RNA processing in calcitonin gene expression generates mRNAs encoding different polypeptide products**. *Nature* 1982, **298**(5871):240-244.
204. Brain SD, Williams TJ, Tippins JR, Morris HR, MacIntyre I: **Calcitonin gene-related peptide is a potent vasodilator**. *Nature* 1985, **313**(5997):54-56.

205. Mayeda A, Zahler AM, Krainer AR, Roth MB: **Two members of a conserved family of nuclear phosphoproteins are involved in pre-mRNA splicing**. *Proceedings of the National Academy of Sciences of the United States of America* 1992, **89**(4):1301-1304.
206. Zahler AM, Lane WS, Stolk JA, Roth MB: **SR proteins: a conserved family of pre-mRNA splicing factors**. *Genes & development* 1992, **6**(5):837-847.
207. Venables JP, Tazi J, Juge F: **Regulated functional alternative splicing in Drosophila**. *Nucleic acids research* 2012, **40**(1):1-10.
208. Juge F, Fernando C, Fic W, Tazi J: **The SR protein B52/SRp55 is required for DNA topoisomerase I recruitment to chromatin, mRNA release and transcription shutdown**. *PLoS genetics* 2010, **6**(9):e1001124.
209. Kraus ME, Lis JT: **The concentration of B52, an essential splicing factor and regulator of splice site choice in vitro, is critical for Drosophila development**. *Molecular and cellular biology* 1994, **14**(8):5360-5370.
210. Subramaniam V, Bomze HM, Lopez AJ: **Functional differences between Ultrabithorax protein isoforms in Drosophila melanogaster: evidence from elimination, substitution and ectopic expression of specific isoforms**. *Genetics* 1994, **136**(3):979-991.
211. Luo L, Liao YJ, Jan LY, Jan YN: **Distinct morphogenetic functions of similar small GTPases: Drosophila Drac1 is involved in axonal outgrowth and myoblast fusion**. *Genes & development* 1994, **8**(15):1787-1802.
212. Bashaw GJ, Hu H, Nobes CD, Goodman CS: **A novel Dbl family RhoGEF promotes Rho-dependent axon attraction to the central nervous system midline in Drosophila and overcomes Robo repulsion**. *The Journal of cell biology* 2001, **155**(7):1117-1122.
213. Bossing T, Brand AH: **Dephrin, a transmembrane ephrin with a unique structure, prevents interneuronal axons from exiting the Drosophila embryonic CNS**. *Development* 2002, **129**(18):4205-4218.
214. Dittrich R, Bossing T, Gould AP, Technau GM, Urban J: **The differentiation of the serotonergic neurons in the Drosophila ventral nerve cord depends on the combined function of the zinc finger proteins Eagle and Huckebein**. *Development* 1997, **124**(13):2515-2525.
215. Bayraktar OA, Boone JQ, Drummond ML, Doe CQ: **Drosophila type II neuroblast lineages keep Prospero levels low to generate large clones that contribute to the adult brain central complex**. *Neural development* 2010, **5**:26.
216. Bossing T, Barros CS, Brand AH: **Rapid tissue-specific expression assay in living embryos**. *Genesis* 2002, **34**(1-2):123-126.
217. Lee T, Luo L: **Mosaic analysis with a repressible cell marker for studies of gene function in neuronal morphogenesis**. *Neuron* 1999, **22**(3):451-461.
218. Sun Y, Liu L, Ben-Shahar Y, Jacobs JS, Eberl DF, Welsh MJ: **TRPA channels distinguish gravity sensing from hearing in Johnston's organ**. *Proceedings of the National Academy of Sciences of the United States of America* 2009, **106**(32):13606-13611.
219. Gabut M, Dejardin J, Tazi J, Soret J: **The SR family proteins B52 and dASF/SF2 modulate development of the Drosophila visual system by regulating specific RNA targets**. *Mol Cell Biol* 2007, **27**(8):3087-3097.
220. Nicolai LJ, Ramaekers A, Raemaekers T, Drozdzecki A, Mauss AS, Yan J, Landgraf M, Annaert W, Hassan BA: **Genetically encoded dendritic marker sheds light on neuronal connectivity in Drosophila**. *Proceedings of the National Academy of Sciences of the United States of America* 2010, **107**(47):20553-20558.
221. Shi H, Hoffman BE, Lis JT: **RNA aptamers as effective protein antagonists in a multicellular organism**. *Proceedings of the National Academy of Sciences of the United States of America* 1999, **96**(18):10033-10038.
222. Minestrini G, Mathe E, Glover DM: **Domains of the Pavarotti kinesin-like protein that direct its subcellular distribution: effects of mislocalisation on the tubulin and actin**

cytoskeleton during Drosophila oogenesis. *Journal of cell science* 2002, **115**(Pt 4):725-736.
223. Besse F, Pret AM: **Apoptosis-mediated cell death within the ovarian polar cell lineage of Drosophila melanogaster**. *Development* 2003, **130**(5):1017-1027.
224. Morin X, Daneman R, Zavortink M, Chia W: **A protein trap strategy to detect GFP-tagged proteins expressed from their endogenous loci in Drosophila**. *Proceedings of the National Academy of Sciences of the United States of America* 2001, **98**(26):15050-15055.
225. Ring HZ, Lis JT: **The SR protein B52/SRp55 is essential for Drosophila development**. *Molecular and cellular biology* 1994, **14**(11):7499-7506.
226. Bossing T, Udolph G, Doe CQ, Technau GM: **The embryonic central nervous system lineages of Drosophila melanogaster. I. Neuroblast lineages derived from the ventral half of the neuroectoderm**. *Developmental biology* 1996, **179**(1):41-64.
227. Doe CQ: **Molecular markers for identified neuroblasts and ganglion mother cells in the Drosophila central nervous system**. *Development* 1992, **116**(4):855-863.
228. Miguel-Aliaga I, Thor S: **Segment-specific prevention of pioneer neuron apoptosis by cell-autonomous, postmitotic Hox gene activity**. *Development* 2004, **131**(24):6093-6105.
229. Lin DM, Fetter RD, Kopczynski C, Grenningloh G, Goodman CS: **Genetic analysis of Fasciclin II in Drosophila: defasciculation, refasciculation, and altered fasciculation**. *Neuron* 1994, **13**(5):1055-1069.
230. Thomas JB, Bastiani MJ, Bate M, Goodman CS: **From grasshopper to Drosophila: a common plan for neuronal development**. *Nature* 1984, **310**(5974):203-207.
231. Hidalgo A, Brand AH: **Targeted neuronal ablation: the role of pioneer neurons in guidance and fasciculation in the CNS of Drosophila**. *Development* 1997, **124**(17):3253-3262.
232. Fic W, Juge F, Soret J, Tazi J: **Eye development under the control of SRp55/B52-mediated alternative splicing of eyeless**. *PloS one* 2007, **2**(2):e253.
233. Rasheva VI, Knight D, Bozko P, Marsh K, Frolov MV: **Specific role of the SR protein splicing factor B52 in cell cycle control in Drosophila**. *Molecular and cellular biology* 2006, **26**(9):3468-3477.
234. Kim S, Shi H, Lee DK, Lis JT: **Specific SR protein-dependent splicing substrates identified through genomic SELEX**. *Nucleic acids research* 2003, **31**(7):1955-1961.
235. Hoffman BE, Lis JT: **Pre-mRNA splicing by the essential Drosophila protein B52: tissue and target specificity**. *Molecular and cellular biology* 2000, **20**(1):181-186.
236. Brand AH, Perrimon N: **Targeted gene expression as a means of altering cell fates and generating dominant phenotypes**. *Development* 1993, **118**(2):401-415.
237. Xu D, Shi H: **Composite RNA aptamers as functional mimics of proteins**. *Nucleic acids research* 2009, **37**(9):e71.
238. Berger C, Renner S, Luer K, Technau GM: **The commonly used marker ELAV is transiently expressed in neuroblasts and glial cells in the Drosophila embryonic CNS**. *Dev Dyn* 2007, **236**(12):3562-3568.
239. Schmidt H, Rickert C, Bossing T, Vef O, Urban J, Technau GM: **The embryonic central nervous system lineages of Drosophila melanogaster. II. Neuroblast lineages derived from the dorsal part of the neuroectoderm**. *Developmental biology* 1997, **189**(2):186-204.
240. Campbell G, Goring H, Lin T, Spana E, Andersson S, Doe CQ, Tomlinson A: **RK2, a glial-specific homeodomain protein required for embryonic nerve cord condensation and viability in Drosophila**. *Development* 1994, **120**(10):2957-2966.
241. Kristiansen LV, Hortsch M: **Fasciclin II: the NCAM ortholog in Drosophila melanogaster**. *Advances in experimental medicine and biology* 2010, **663**:387-401.

242. Spana EP, Kopczynski C, Goodman CS, Doe CQ: **Asymmetric localization of numb autonomously determines sibling neuron identity in the Drosophila CNS**. *Development* 1995, **121**(11):3489-3494.
243. Giniger E, Jan LY, Jan YN: **Specifying the path of the intersegmental nerve of the Drosophila embryo: a role for Delta and Notch**. *Development* 1993, **117**(2):431-440.
244. Goeke S, Greene EA, Grant PK, Gates MA, Crowner D, Aigaki T, Giniger E: **Alternative splicing of lola generates 19 transcription factors controlling axon guidance in Drosophila**. *Nat Neurosci* 2003, **6**(9):917-924.
245. Madden K, Crowner D, Giniger E: **LOLA has the properties of a master regulator of axon-target interaction for SNb motor axons of Drosophila**. *Dev Biol* 1999, **213**(2):301-313.
246. Spletter ML, Liu J, Su H, Giniger E, Komiyama T, Quake S, Luo L: **Lola regulates Drosophila olfactory projection neuron identity and targeting specificity**. *Neural Dev* 2007, **2**:14.
247. Gates MA, Kannan R, Giniger E: **A genome-wide analysis reveals that the Drosophila transcription factor Lola promotes axon growth in part by suppressing expression of the actin nucleation factor Spire**. *Neural Dev* 2011, **6**:37.
248. Quinlan ME, Heuser JE, Kerkhoff E, Mullins RD: **Drosophila Spire is an actin nucleation factor**. *Nature* 2005, **433**(7024):382-388.
249. Rosales-Nieves AE, Johndrow JE, Keller LC, Magie CR, Pinto-Santini DM, Parkhurst SM: **Coordination of microtubule and microfilament dynamics by Drosophila Rho1, Spire and Cappuccino**. *Nat Cell Biol* 2006, **8**(4):367-376.
250. Schulz JG, Ceulemans H, Caussinus E, Baietti MF, Affolter M, Hassan BA, David G: **Drosophila syndecan regulates tracheal cell migration by stabilizing Robo levels**. *EMBO Rep* 2011, **12**(10):1039-1046.
251. Englund C, Steneberg P, Falileeva L, Xylourgidis N, Samakovlis C: **Attractive and repulsive functions of Slit are mediated by different receptors in the Drosophila trachea**. *Development* 2002, **129**(21):4941-4951.
252. Rhiner C, Gysi S, Frohli E, Hengartner MO, Hajnal A: **Syndecan regulates cell migration and axon guidance in C. elegans**. *Development* 2005, **132**(20):4621-4633.
253. Greenberg L, Hatini V: **Systematic expression and loss-of-function analysis defines spatially restricted requirements for Drosophila RhoGEFs and RhoGAPs in leg morphogenesis**. *Mech Dev* 2011, **128**(1-2):5-17.
254. Billuart P, Winter CG, Maresh A, Zhao X, Luo L: **Regulating axon branch stability: the role of p190 RhoGAP in repressing a retraction signaling pathway**. *Cell* 2001, **107**(2):195-207.
255. Rallis A, Moore C, Ng J: **Signal strength and signal duration define two distinct aspects of JNK-regulated axon stability**. *Dev Biol* 2010, **339**(1):65-77.
256. Guruharsha KG, Rual JF, Zhai B, Mintseris J, Vaidya P, Vaidya N, Beekman C, Wong C, Rhee DY, Cenaj O *et al*: **A protein complex network of Drosophila melanogaster**. *Cell* 2011, **147**(3):690-703.
257. Crowner D, Madden K, Goeke S, Giniger E: **Lola regulates midline crossing of CNS axons in Drosophila**. *Development* 2002, **129**(6):1317-1325.
258. Giniger E: **A role for Abl in Notch signaling**. *Neuron* 1998, **20**(4):667-681.
259. Kuzina I, Song JK, Giniger E: **How Notch establishes longitudinal axon connections between successive segments of the Drosophila CNS**. *Development* 2011, **138**(9):1839-1849.
260. Hiramoto M, Hiromi Y, Giniger E, Hotta Y: **The Drosophila Netrin receptor Frazzled guides axons by controlling Netrin distribution**. *Nature* 2000, **406**(6798):886-889.
261. Shi H, Hoffman BE, Lis JT: **A specific RNA hairpin loop structure binds the RNA recognition motifs of the Drosophila SR protein B52**. *Molecular and cellular biology* 1997, **17**(5):2649-2657.

262. Anderson RL, Jobling P, Gibbins IL: **Development of electrophysiological and morphological diversity in autonomic neurons**. *Journal of neurophysiology* 2001, **86**(3):1237-1251.
263. Treinin M, Gillo B, Liebman L, Chalfie M: **Two functionally dependent acetylcholine subunits are encoded in a single Caenorhabditis elegans operon**. *Proceedings of the National Academy of Sciences of the United States of America* 1998, **95**(26):15492-15495.
264. Alfonso A, Grundahl K, McManus JR, Asbury JM, Rand JB: **Alternative splicing leads to two cholinergic proteins in Caenorhabditis elegans**. *Journal of molecular biology* 1994, **241**(4):627-630.
265. Hobert O, Carrera I, Stefanakis N: **The molecular and gene regulatory signature of a neuron**. *Trends in neurosciences* 2010, **33**(10):435-445.
266. Ladle DR, Pecho-Vrieseling E, Arber S: **Assembly of motor circuits in the spinal cord: driven to function by genetic and experience-dependent mechanisms**. *Neuron* 2007, **56**(2):270-283.
267. Broihier HT, Skeath JB: **Drosophila homeodomain protein dHb9 directs neuronal fate via crossrepressive and cell-nonautonomous mechanisms**. *Neuron* 2002, **35**(1):39-50.
268. Landgraf M, Roy S, Prokop A, VijayRaghavan K, Bate M: **even-skipped determines the dorsal growth of motor axons in Drosophila**. *Neuron* 1999, **22**(1):43-52.
269. Odden JP, Holbrook S, Doe CQ: **Drosophila HB9 is expressed in a subset of motoneurons and interneurons, where it regulates gene expression and axon pathfinding**. *The Journal of neuroscience : the official journal of the Society for Neuroscience* 2002, **22**(21):9143-9149.
270. Thor S, Andersson SG, Tomlinson A, Thomas JB: **A LIM-homeodomain combinatorial code for motor-neuron pathway selection**. *Nature* 1999, **397**(6714):76-80.
271. Thor S, Thomas JB: **The Drosophila islet gene governs axon pathfinding and neurotransmitter identity**. *Neuron* 1997, **18**(3):397-409.
272. Tanabe Y, William C, Jessell TM: **Specification of motor neuron identity by the MNR2 homeodomain protein**. *Cell* 1998, **95**(1):67-80.
273. Cheng L, Arata A, Mizuguchi R, Qian Y, Karunaratne A, Gray PA, Arata S, Shirasawa S, Bouchard M, Luo P *et al*: **Tlx3 and Tlx1 are post-mitotic selector genes determining glutamatergic over GABAergic cell fates**. *Nature neuroscience* 2004, **7**(5):510-517.
274. Cheng L, Samad OA, Xu Y, Mizuguchi R, Luo P, Shirasawa S, Goulding M, Ma Q: **Lbx1 and Tlx3 are opposing switches in determining GABAergic versus glutamatergic transmitter phenotypes**. *Nature neuroscience* 2005, **8**(11):1510-1515.
275. Hutchinson SA, Eisen JS: **Islet1 and Islet2 have equivalent abilities to promote motoneuron formation and to specify motoneuron subtype identity**. *Development* 2006, **133**(11):2137-2147.
276. Borodinsky LN, Root CM, Cronin JA, Sann SB, Gu X, Spitzer NC: **Activity-dependent homeostatic specification of transmitter expression in embryonic neurons**. *Nature* 2004, **429**(6991):523-530.
277. Marek KW, Kurtz LM, Spitzer NC: **cJun integrates calcium activity and tlx3 expression to regulate neurotransmitter specification**. *Nature neuroscience* 2010, **13**(8):944-950.
278. Demarque M, Spitzer NC: **Activity-dependent expression of Lmx1b regulates specification of serotonergic neurons modulating swimming behavior**. *Neuron* 2010, **67**(2):321-334.
279. Yizhar O, Fenno LE, Prigge M, Schneider F, Davidson TJ, O'Shea DJ, Sohal VS, Goshen I, Finkelstein J, Paz JT *et al*: **Neocortical excitation/inhibition balance in information processing and social dysfunction**. *Nature* 2011, **477**(7363):171-178.
280. Oda Y: **Choline acetyltransferase: the structure, distribution and pathologic changes in the central nervous system**. *Pathology international* 1999, **49**(11):921-937.

281. Pahud G, Salem N, van de Goor J, Medilanski J, Pellegrinelli N, Eder-Colli L: **Study of subcellular localization of membrane-bound choline acetyltransferase in Drosophila central nervous system and its association with membranes**. *The European journal of neuroscience* 1998, **10**(5):1644-1653.
282. Matsuo A, Bellier JP, Hisano T, Aimi Y, Yasuhara O, Tooyama I, Saito N, Kimura H: **Rat choline acetyltransferase of the peripheral type differs from that of the common type in intracellular translocation**. *Neurochemistry international* 2005, **46**(5):423-433.
283. Wu D, Hersh LB: **Identification of an active site arginine in rat choline acetyltransferase by alanine scanning mutagenesis**. *The Journal of biological chemistry* 1995, **270**(49):29111-29116.
284. Carbini LA, Hersh LB: **Functional analysis of conserved histidines in choline acetyltransferase by site-directed mutagenesis**. *Journal of neurochemistry* 1993, **61**(1):247-253.
285. Yasuyama K, Salvaterra PM: **Localization of choline acetyltransferase-expressing neurons in Drosophila nervous system**. *Microscopy research and technique* 1999, **45**(2):65-79.
286. Sattelle DB, Jones AK, Sattelle BM, Matsuda K, Reenan R, Biggin PC: **Edit, cut and paste in the nicotinic acetylcholine receptor gene family of Drosophila melanogaster**. *BioEssays : news and reviews in molecular, cellular and developmental biology* 2005, **27**(4):366-376.
287. Keene AC, Mazzoni EO, Zhen J, Younger MA, Yamaguchi S, Blau J, Desplan C, Sprecher SG: **Distinct visual pathways mediate Drosophila larval light avoidance and circadian clock entrainment**. *The Journal of neuroscience : the official journal of the Society for Neuroscience* 2011, **31**(17):6527-6534.
288. Kitamoto T, Wang W, Salvaterra PM: **Structure and organization of the Drosophila cholinergic locus**. *The Journal of biological chemistry* 1998, **273**(5):2706-2713.
289. Salvaterra PM, McCaman RE: **Choline acetyltransferase and acetylcholine levels in Drosophila melanogaster: a study using two temperature-sensitive mutants**. *The Journal of neuroscience : the official journal of the Society for Neuroscience* 1985, **5**(4):903-910.
290. Daniels RW, Collins CA, Gelfand MV, Dant J, Brooks ES, Krantz DE, DiAntonio A: **Increased expression of the Drosophila vesicular glutamate transporter leads to excess glutamate release and a compensatory decrease in quantal content**. *The Journal of neuroscience : the official journal of the Society for Neuroscience* 2004, **24**(46):10466-10474.
291. Moulder KL, Meeks JP, Shute AA, Hamilton CK, de Erausquin G, Mennerick S: **Plastic elimination of functional glutamate release sites by depolarization**. *Neuron* 2004, **42**(3):423-435.
292. Ogren SO, Eriksson TM, Elvander-Tottie E, D'Addario C, Ekstrom JC, Svenningsson P, Meister B, Kehr J, Stiedl O: **The role of 5-HT(1A) receptors in learning and memory**. *Behavioural brain research* 2008, **195**(1):54-77.
293. Yuan Q, Lin F, Zheng X, Sehgal A: **Serotonin modulates circadian entrainment in Drosophila**. *Neuron* 2005, **47**(1):115-127.
294. Yuan Q, Joiner WJ, Sehgal A: **A sleep-promoting role for the Drosophila serotonin receptor 1A**. *Current biology : CB* 2006, **16**(11):1051-1062.
295. Patrick RP, Ames BN: **Vitamin D hormone regulates serotonin synthesis. Part 1: relevance for autism**. *FASEB journal : official publication of the Federation of American Societies for Experimental Biology* 2014.
296. Scholz CJ, Jungwirth S, Danielczyk W, Weber H, Wichart I, Tragl KH, Fischer P, Riederer P, Deckert J, Grunblatt E: **Investigation of association of serotonin transporter and monoamine oxidase-A genes with Alzheimer's disease and depression in the VITA**

study cohort: A 90-month longitudinal study. *American journal of medical genetics Part B, Neuropsychiatric genetics : the official publication of the International Society of Psychiatric Genetics* 2014, **165**(2):184-191.

297. Lee D, Su H, O'Dowd DK: **GABA receptors containing Rdl subunits mediate fast inhibitory synaptic transmission in Drosophila neurons**. *The Journal of neuroscience : the official journal of the Society for Neuroscience* 2003, **23**(11):4625-4634.
298. Chung BY, Kilman VL, Keath JR, Pitman JL, Allada R: **The GABA(A) receptor RDL acts in peptidergic PDF neurons to promote sleep in Drosophila**. *Current biology : CB* 2009, **19**(5):386-390.
299. Liu X, Buchanan ME, Han KA, Davis RL: **The GABAA receptor RDL suppresses the conditioned stimulus pathway for olfactory learning**. *The Journal of neuroscience : the official journal of the Society for Neuroscience* 2009, **29**(5):1573-1579.
300. Hekmat-Scafe DS, Lundy MY, Ranga R, Tanouye MA: **Mutations in the K+/Cl- cotransporter gene kazachoc (kcc) increase seizure susceptibility in Drosophila**. *The Journal of neuroscience : the official journal of the Society for Neuroscience* 2006, **26**(35):8943-8954.
301. Pfeiffenberger C, Allada R: **Cul3 and the BTB adaptor insomniac are key regulators of sleep homeostasis and a dopamine arousal pathway in Drosophila**. *PLoS genetics* 2012, **8**(10):e1003003.
302. Ueno T, Masuda N, Kume S, Kume K: **Dopamine modulates the rest period length without perturbation of its power law distribution in Drosophila melanogaster**. *PloS one* 2012, **7**(2):e32007.
303. Crisp SJ, Evers JF, Bate M: **Endogenous patterns of activity are required for the maturation of a motor network**. *The Journal of neuroscience : the official journal of the Society for Neuroscience* 2011, **31**(29):10445-10450.
304. Crisp S, Evers JF, Fiala A, Bate M: **The development of motor coordination in Drosophila embryos**. *Development* 2008, **135**(22):3707-3717.
305. Baines RA, Bate M: **Electrophysiological development of central neurons in the Drosophila embryo**. *The Journal of neuroscience : the official journal of the Society for Neuroscience* 1998, **18**(12):4673-4683.
306. Baines RA, Uhler JP, Thompson A, Sweeney ST, Bate M: **Altered electrical properties in Drosophila neurons developing without synaptic transmission**. *The Journal of neuroscience : the official journal of the Society for Neuroscience* 2001, **21**(5):1523-1531.
307. Salvaterra PM, Kitamoto T: **Drosophila cholinergic neurons and processes visualized with Gal4/UAS-GFP**. *Brain research Gene expression patterns* 2001, **1**(1):73-82.
308. Kitamoto T: **Conditional modification of behavior in Drosophila by targeted expression of a temperature-sensitive shibire allele in defined neurons**. *Journal of neurobiology* 2001, **47**(2):81-92.
309. Boyden ES, Zhang F, Bamberg E, Nagel G, Deisseroth K: **Millisecond-timescale, genetically targeted optical control of neural activity**. *Nature neuroscience* 2005, **8**(9):1263-1268.
310. Schroll C, Riemensperger T, Bucher D, Ehmer J, Voller T, Erbguth K, Gerber B, Hendel T, Nagel G, Buchner E *et al*: **Light-induced activation of distinct modulatory neurons triggers appetitive or aversive learning in Drosophila larvae**. *Current biology : CB* 2006, **16**(17):1741-1747.
311. Unwin N: **Refined structure of the nicotinic acetylcholine receptor at 4A resolution**. *Journal of molecular biology* 2005, **346**(4):967-989.
312. Ishii M, Kurachi Y: **Muscarinic acetylcholine receptors**. *Current pharmaceutical design* 2006, **12**(28):3573-3581.
313. Wang G, Hu C, Jiang T, Luo J, Hu J, Ling S, Liu M, Xing G: **Overexpression of serotonin receptor and transporter mRNA in blood leukocytes of antipsychotic-free and**

antipsychotic-naive schizophrenic patients: gender differences. *Schizophrenia research* 2010, **121**(1-3):160-171.

314. Li T, Bender M: **A conditional rescue system reveals essential functions for the ecdysone receptor (EcR) gene during molting and metamorphosis in Drosophila**. *Development* 2000, **127**(13):2897-2905.
315. Davis MB, Carney GE, Robertson AE, Bender M: **Phenotypic analysis of EcR-A mutants suggests that EcR isoforms have unique functions during Drosophila development**. *Developmental biology* 2005, **282**(2):385-396.
316. Schubiger M, Wade AA, Carney GE, Truman JW, Bender M: **Drosophila EcR-B ecdysone receptor isoforms are required for larval molting and for neuron remodeling during metamorphosis**. *Development* 1998, **125**(11):2053-2062.
317. Bender M, Imam FB, Talbot WS, Ganetzky B, Hogness DS: **Drosophila ecdysone receptor mutations reveal functional differences among receptor isoforms**. *Cell* 1997, **91**(6):777-788.
318. Myers CP, Lewcock JW, Hanson MG, Gosgnach S, Aimone JB, Gage FH, Lee KF, Landmesser LT, Pfaff SL: **Cholinergic input is required during embryonic development to mediate proper assembly of spinal locomotor circuits**. *Neuron* 2005, **46**(1):37-49.
319. Brandon EP, Lin W, D'Amour KA, Pizzo DP, Dominguez B, Sugiura Y, Thode S, Ko CP, Thal LJ, Gage FH *et al*: **Aberrant patterning of neuromuscular synapses in choline acetyltransferase-deficient mice**. *The Journal of neuroscience : the official journal of the Society for Neuroscience* 2003, **23**(2):539-549.
320. Misgeld T, Burgess RW, Lewis RM, Cunningham JM, Lichtman JW, Sanes JR: **Roles of neurotransmitter in synapse formation: development of neuromuscular junctions lacking choline acetyltransferase**. *Neuron* 2002, **36**(4):635-648.
321. Hanson MG, Landmesser LT: **Characterization of the circuits that generate spontaneous episodes of activity in the early embryonic mouse spinal cord**. *The Journal of neuroscience : the official journal of the Society for Neuroscience* 2003, **23**(2):587-600.
322. Milner LD, Landmesser LT: **Cholinergic and GABAergic inputs drive patterned spontaneous motoneuron activity before target contact**. *The Journal of neuroscience : the official journal of the Society for Neuroscience* 1999, **19**(8):3007-3022.
323. Miller KG, Alfonso A, Nguyen M, Crowell JA, Johnson CD, Rand JB: **A genetic selection for Caenorhabditis elegans synaptic transmission mutants**. *Proceedings of the National Academy of Sciences of the United States of America* 1996, **93**(22):12593-12598.
324. Rand JB, Russell RL: **Choline acetyltransferase-deficient mutants of the nematode Caenorhabditis elegans**. *Genetics* 1984, **106**(2):227-248.
325. Kitamoto T, Xie X, Wu CF, Salvaterra PM: **Isolation and characterization of mutants for the vesicular acetylcholine transporter gene in Drosophila melanogaster**. *Journal of neurobiology* 2000, **42**(2):161-171.
326. Giniger E, Tietje K, Jan LY, Jan YN: **lola encodes a putative transcription factor required for axon growth and guidance in Drosophila**. *Development* 1994, **120**(6):1385-1398.
327. Kakinuma Y, Tsuda M, Okazaki K, Akiyama T, Arikawa M, Noguchi T, Sato T: **Heart-specific overexpression of choline acetyltransferase gene protects murine heart against ischemia through hypoxia-inducible factor-1alpha-related defense mechanisms**. *Journal of the American Heart Association* 2013, **2**(1):e004887.
328. Harvey BK, Airavaara M, Hinzman J, Wires EM, Chiocco MJ, Howard DB, Shen H, Gerhardt G, Hoffer BJ, Wang Y: **Targeted over-expression of glutamate transporter 1 (GLT-1) reduces ischemic brain injury in a rat model of stroke**. *PloS one* 2011, **6**(8):e22135.

Appendix

OPEN ACCESS Freely available online

PLOS ONE

Drosophila Embryos as Model to Assess Cellular and Developmental Toxicity of Multi-Walled Carbon Nanotubes (MWCNT) in Living Organisms

Boyin Liu[1], Eva M. Campo[2], Torsten Bossing[1]*[¤]

1 School of Biological Sciences, University of Bangor, Bangor, United Kingdom, 2 School of Electronic Engineering, University of Bangor, Bangor, United Kingdom

Abstract

Different toxicity tests for carbon nanotubes (CNT) have been developed to assess their impact on human health and on aquatic and terrestrial animal and plant life. We present a new model, the fruit fly *Drosophila* embryo offering the opportunity for rapid, inexpensive and detailed analysis of CNTs toxicity during embryonic development. We show that injected DiI labelled multi-walled carbon nanotubes (MWCNTs) become incorporated into cells in early *Drosophila* embryos, allowing the study of the consequences of cellular uptake of CNTs on cell communication, tissue and organ formation in living embryos. Fluorescently labelled subcellular structures showed that MWCNTs remained cytoplasmic and were excluded from the nucleus. Analysis of developing ectodermal and neural stem cells in MWCNTs injected embryos revealed normal division patterns and differentiation capacity. However, an increase in cell death of ectodermal but not of neural stem cells was observed, indicating stem cell-specific vulnerability to MWCNT exposure. The ease of CNT embryo injections, the possibility of detailed morphological and genomic analysis and the low costs make *Drosophila* embryos a system of choice to assess potential developmental and cellular effects of CNTs and test their use in future CNT based new therapies including drug delivery.

Citation: Liu B, Campo EM, Bossing T (2014) *Drosophila* Embryos as Model to Assess Cellular and Developmental Toxicity of Multi-Walled Carbon Nanotubes (MWCNT) in Living Organisms. PLoS ONE 9(2): e88681. doi:10.1371/journal.pone.0088681

Editor: Shree Ram Singh, National Cancer Institute, United States of America

Received November 20, 2013; **Accepted** January 9, 2014; **Published** February 18, 2014

Funding: Royal Society Research Grant awarded to Torsten Bossing. The funders had no role in study design, data collection and analysis, decision to publish, or preparation of the manuscript.

Competing Interests: The authors have declared that no competing interests exist.

* E-mail: torsten.bossing@plymouth.ac.uk

¤ Current address: School of Biomedical and Healthcare related Sciences, University of Plymouth, Plymouth, United Kingdom

Introduction

The first report of the synthesis of carbon nanotubes (CNTs) two decades ago [1] sparked interest in such diverse fields as electronics, optics, physics, material sciences, medicine and biology. The promise CNTs hold for these fields originates from their unique physical, chemical, electrical and mechanical properties [2]. Consequently, commercial production and applications are increasing and CNTS have a growing presence in our daily lives ([3], see also Woodrow Wilson Nano Inventory). Accumulation of nanoparticles in our environment is still at the detection threshold but the continuous release of particles by production, wear and tear, and waste disposal makes an increased environmental exposure inevitable [4]. In addition, the future use of CNTs in medical applications such as drug delivery, biosensors and surgical scaffolds [5] will increase human contact with CNTs and justifies international efforts for the development and standardisation of existing toxicity tests, as well as of new approaches to test the health impact of CNTs [6].

Environmental concerns and the hazard to human health associated with CNTs have attracted widespread attention [7,8]. CNTs can cause cellular and tissue damage by stimulating inflammation and necrosis due to increased production of reactive oxygen species (ROS) [7,9]. Single walled CNTs tend to be more damaging than multi-walled CNTs (MWCNTs) [10]. The shape, length and the addition of side groups also influence CNT toxicity [7]. An increasing numbers of studies indicate that many of the toxic effects initially reported may be caused by contaminations deposited during CNT production, an observation explaining some of the inconsistencies in previous studies [7,9]. Cell cultures are often the medium of choice for toxicity tests since they offer a fast, low cost and high-throughput approach. Yet, cell culture results vary with cell type and culture conditions [9], and results may not translate directly into the whole organism environment where, in a temporal and spatially controlled fashion, thousands of endogenous proteins and hundreds of different cell types interact with each other. Due to high costs, high throughput toxicity studies on mammals are scarce. It may be advantageous to opt for an alternative way, conducting high throughput studies in lower vertebrates and invertebrates with short generation time and high fecundity, and validate results obtained in these studies in a limited number of rodents. Indeed, zebrafish [11,12,13] and the flatworm *Celegans* [14,15] have been recently used to study the toxicity of CNTs. Both model organisms allow the establishment of basic mechanisms of CNT toxicity by examining viability, fertility, tissue and cellular integrity [16]. They also give an insight into alterations in gene expression changes, which underlie altered organ function [11,15].

Here we present a third simple animal model system towards the study of CNT toxicity, *Drosophila* embryos. Embryos of

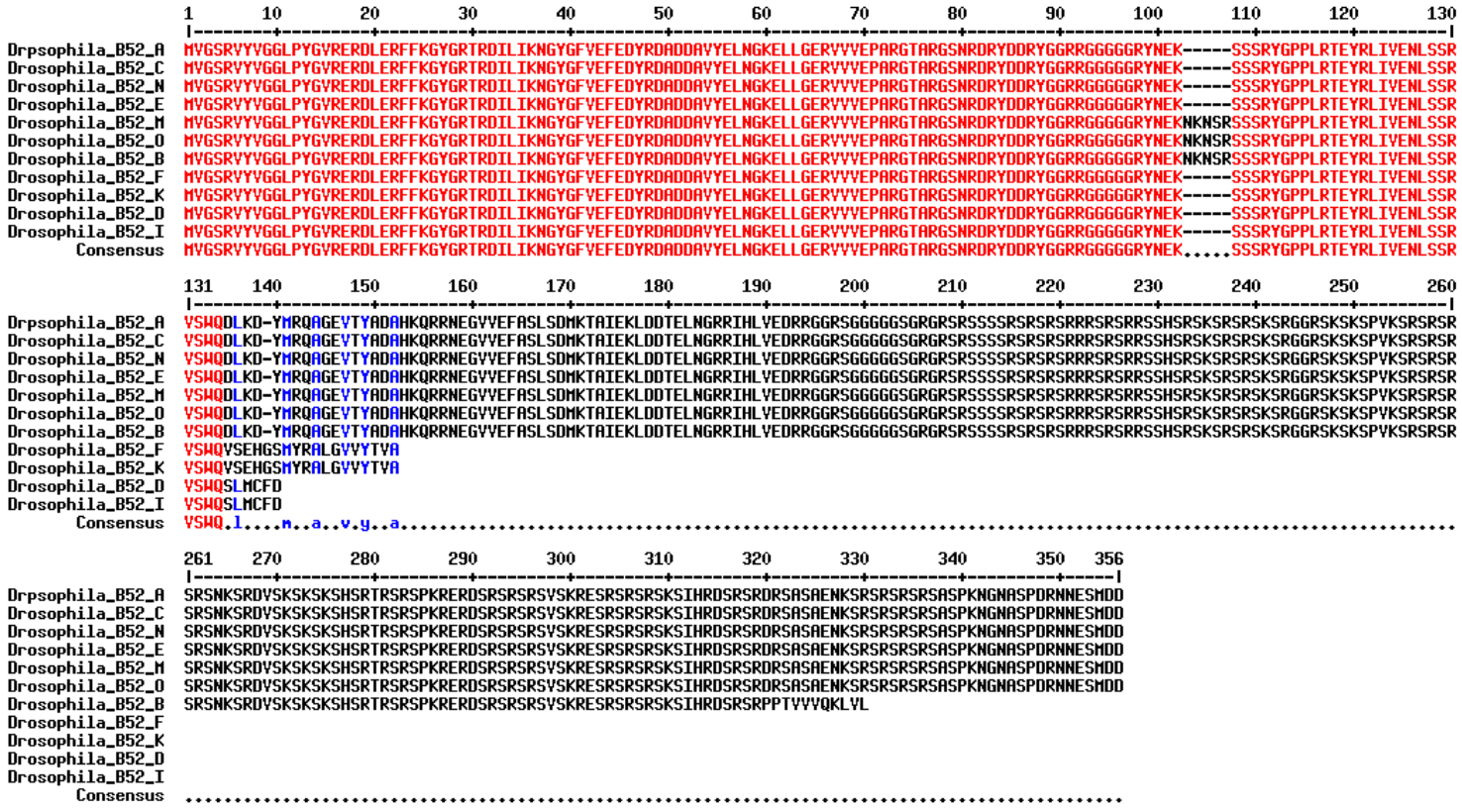

Figure. A1 Alignment of *Drosophila* B52 protein isoforms

Drosophila B52 Isoforms S, K, I and D are the shortest, having sequences about half the length compared to other protein isoforms. Isoforms M, O and B have extra 5 amino acids present in the consensus region. All of them contains at least one RRM (shortest isoforms), 7 of them have long enough sequence to cover a second RRM.